# Molecular cloning, expression, structural and functional characterization of pectate lyase of family 1 polysaccharide lyase (PL1) from *Clostridium thermocellum* ATCC 27405 and its applications in production of immobilized magnetic nanoparticle for bioscouring and pectic oligosaccharides inhibiting colon cancer cells

**PhD Thesis**

***by***

**Soumyadeep Chakraborty**

**March 2015**

**DEPARTMENT OF BIOSCIENCES AND BIOENGINEERING**
**INDIAN INSTITUTE OF TECHNOLOGY GUWAHATI**
**GUWAHATI – 781039, ASSAM, INDIA**


Dedicated to
Sree Ma &
Sree Aurobindo

# Molecular cloning, expression, structural and functional characterization of pectate lyase of family 1 polysaccharide lyase (PL1) from *Clostridium thermocellum* ATCC 27405 and its applications in production of immobilized magnetic nanoparticle for bioscouring and pectic oligosaccharides inhibiting colon cancer cells

***A Thesis***

***Submitted in partial fulfillment of the requirements for the Degree of***

**Doctor of Philosophy**

***by***

**Soumyadeep Chakraborty**

***Under supervision of***

**Professor Arun Goyal**

**March 2015**

**DEPARTMENT OF BIOSCIENCES AND BIOENGINEERING**

**INDIAN INSTITUTE OF TECHNOLOGY GUWAHATI**

**GUWAHATI – 781039, ASSAM, INDIA**

## ACKNOWLEDGEMENTS

*This thesis has been kept on track and been seen through to completion with the support and encouragement of many people including my supervisor, doctoral committee members, my family, my friends and colleagues. I would like to thank all those people who made this thesis possible and an unforgettable experience for me. At the end of my thesis, it is a pleasant task to express my thanks to all those who contributed in many ways and had profound impact in the success of this study deserves special acknowledgment.*

*Firstly from the depth of my heart I express my deep sincere gratitude to the Almighty for the Blessings and strength bestowed upon me to complete this work.*

*At this moment of accomplishment, I am extremely indebted to my thesis supervisor, Professor Arun Goyal, Department of Biotechnology, IIT Guwahati. This work would not have been possible without his guidance, support and encouragement. Under his guidance I successfully overcame many difficulties and learned a lot. I can't forget his how patiently he listened to my problems and provided the necessary instructions. He always used to review my thesis progress, give me valuable suggestions and made corrections numerous times. His unflinching convictions will always inspire me and I hope to continue to work with his noble*

*thoughts. I earnestly thank him for inculcating in me scientific temperament and appreciable work ethics which helped me to achieve this goal.*

*I would also like to express my sincere gratitude to all my doctoral committee members Dr. Debasish Das, Dr. Nitin Chaudhury, Prof. Mohammed Jawed, Dr. Soumen Kumar Maiti for their valuable suggestions and constructive criticism during my progress report presentations that has led to the successful completion of my thesis.*

*I am thankful to Department of Biosciences & Bioengineering and Central Instrumentation Facility (CIF), IITG for providing me instruments for my research work.*

*I would also like to express my sincere gratitude to Prof. M.N. Gupta, Department of Chemistry, IIT Delhi and his PhD student Joyeeta Mukherjee for Circular Dichroism (CD) analysis of my recombinant proteins.*

*I sincerely thank Prof. Pinak Chakrabarti, Department of Biochemistry, Bose Institute, Kolkata, for providing lab facilities and his student Aritrika Pal for teaching me protein crystallization experiments.*

*I would also like to thank the present and previous heads of the Department of Biotechnology, IIT Guwahati, Prof. Arun Goyal and Prof. Venkata. V. Dasu for providing me with the necessary facilities.*

*I am also thankful to my seniors Dr. Shadab Ahamed, Dr. Rishikesh Shukla, Dr. Shraddha Shukla, Dr. T.J.M. Rao, Dr. Saprativ P. Das, Dr. Deeplina*

*Das, Dr. Arabinda Ghosh, A.K. Verma for their help and suggestions. I am immensely thankful to my research group members Damini, Aruna, Arun, Rwivoo, Vikky, Kedar, Ashutosh. I am grateful to all my labmates of Department of Biotechnology for their cooperation and support.*

*I am thankful to my friends Dr. Debayan Dhar, Dr. Mithun Chakraborty, Dr. Manab Adhikari, Dr. Amit Jaiswal, Arghya, Anirban, Mong, Samir, Muthu, Nand kishor, Sudeep, Suradip, Tulsi, Ankita who made my stay at the campus a memorable one by their company and moral support during the tenure of my PhD.*

*I wish to acknowledge the support received from other teaching and non-teaching staff of the Department of Biotechnology, IIT Guwahati.*

*I wish to acknowledge IIT Guwahati for providing financial assistance and experimental facilities and also Department of Biotechnology, Govt. of India, New Delhi for providing me fellowship through its sponsored project.*

*My PhD endeavor would not have been successful without the love, trust, support and blessings of my parents and in-laws. I owe my achievements to my family. I also thank my wife Dipanwita for her constant encouragement and moral support during my PhD period.*

*Soumyadeep Chakraborty*
*March 2015*

# SYNOPSIS

## Introduction

The four major classes of organic molecules in living systems are proteins, lipids, nucleic acids and carbohydrates. Carbohydrates are the most abundant organic molecules found in nature and nearly all organisms synthesize and metabolize carbohydrates. Cellulose, hemicellulose and pectin are the main polysaccharide component in plant cell wall. Pectin is structurally most complex polysaccharide, which constitutes the cell wall by 35% in dicot and monocot, 2-10% in grass and 5% in wood. Pectin acts as a protective material in plants, hence they are commonly found around growing cells, middle lamella and in cell walls of soft parts of plants. Hence pectin plays important role in plant growth and development, defence mechanism, cell-cell adhesion, structural stability of cell wall, regulation of cell permeability and fruit development. The pectic polysaccharides found in plant cell wall are homogalacturonan (HG), rhamnogalacturonan-I (RG-I) and rhamnogalacturonan-II (RG-II). Homogalacturonan (HG) is a widespread linear homopolymer built from chain of 100-200 α-D-galacturonic acid (GalA) residues linked by α-(1,4) glycosidic bonds.

Polysaccharide lyases (PL) (EC 4.2.2.-) belong to a large group of enzymes defined as carbohydrate active enzymes and based on sequence similarities have been classified in 23 families till date (January, 2015), according to CAZy (**C**arbohydrate-**A**ctive en**Zy**mes or CAZymes) database (http://www.cazy.org/Polysaccharide-Lyases.html). The family 1 polysaccharide lyase (PL1) currently contain nearly 99

well characterized sequences where the enzymes so far have shown activities like pectate lyase (EC 4.2.2.2); exo-pectate lyase (EC 4.2.2.9) and pectin lyase (EC 4.2.2.10) (http://www.cazy.org/PL1.html). Pectate lyases of families 1, 2, 3, 9, and 10 catalyse the cleavage of α-(1,4)-glycosidic bond between D-galactopyranosyluronic acid (Gal*p*A) residue in pectate (a low methylesterified form of pectin) by β-elimination and generate Δ4,5 unsaturated Gal*p*A as the product, which exhibits a maximum absorbance at around 235 nm. The enzymatic degradation of polygalacturonan involves two well-known enzymatic mechanisms: i) syn β-elimination found in chondroitin lyase and ii) anti β-elimination in α-(1,4)-polygalacturonan (pectate) lyase resulting in oligomers with Δ4,5 unsaturated residues at the non-reducing end. Pectate lyases are widely distributed among microbial plant pathogens like *Erwinia chrysanthemi* although they have also been found in saprophytic bacteria including the genus *Bacillus* and *Clostridium*. *Clostridium thermocellum* is an anaerobic, saccharolytic and thermophilic bacterium that organizes a consortium of plant cell wall degrading enzymes in a large multienzymatic complex termed the cellulosome. The cellulosome is assembled via the interaction of individual type-I dockerins located at the C-terminal of enzymes into one of the nine cohesins of the scaffoldin subunit, CipA. The majority of glycoside hydrolases that attack cellulose and hemicelluloses are modular enzymes consisting of catalytic modules appended to non-catalytic carbohydrate-binding modules (CBMs). Generally, pectate lyases have a relatively simple structure lacking the CBMs, which is possibly due to the easy accessibility of pectins to biocatalysts. The family 1 polysaccharide lyase (PL1) from *Clostridium thermocellum* under present study contains a family 35 CBM.

Complex carbohydrate hydrolysing enzymes are generally modular. Carbohydrate binding module (CBM) is one of these important modules, which remains associated with the catalytic module. This association of CBMs with the catalytic modules increase its interaction with the substrate, thereby increasing the efficiency of the enzyme. Based on the sequence similarity, CBMs are grouped into 71 families as listed in CAZy database (http://www.cazy.org). Till date family 35 carbohydrate binding module (CBM35) contains 812, 9 and 45 bacterial, archaeal and eukaryotic proteins, respectively and only 12 crystal structures have been solved (http://www.cazy.org/CBM35.html). The 3D structures solved so far of family 35 carbohydrate binding modules have a jelly-roll β-sandwich fold.

**The present work** entitled as "Molecular cloning, expression, structural and functional characterization of pectate lyase of family 1 polysaccharide lyase (PL1) from *Clostridium thermocellum* ATCC 27405 and its applications in production of immobilized magnetic nanoparticle for bioscouring and production of pectic oligosaccharides their effect on colon cancer cells" has been divided into 6 chapters. This study deals with the cloning, expression and purification of a modular carbohydrate-active enzyme of family 1 polysaccharide lyase PL1B-CBM35 (as shown in Fig. 1) and its truncated catalytic module (PL1B) and carbohydrate binding module (CBM35) from *Clostridium thermocellum* ATCC 27405. Biochemical and functional characterization of PL1B-CBM35 and PL1B was extensively carried out to determine its affinity towards different pectic polysaccharides and understand its cleavage pattern. Application of immobilized PL1B on bioscouring of cotton fabric and effect of pectic oligosaccharides on colon cancer cells were studied extensively.

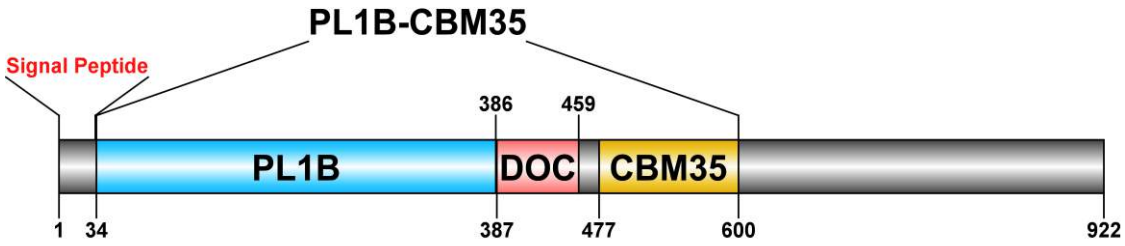


**Fig. 1.** Molecular architecture of modular protein ABN53381.1 from *C. thermocellum* consisting of a 33 aa signal peptide, N-terminal 353 aa family 1 polysaccharide lyase (PL1B), C-terminal 124 aa family 35 carbohydrate binding (CBM35) and sandwich between these modules is a 72 aa type 1 dockerin (DOC) modules.

**Chapter 1** is the General Introduction which embodies the brief review of literature dedicated to the importance of different carbohydrates and their structural features. It mainly focuses on the enzymes having the capability to hydrolyze plant cell-wall pectic polysaccharides. It illustrates sequence-similarity based classification of pectinases and other enzymes hydrolysing uronic acid containing polysaccharides belonging to different polysaccharide lyase (PL) families. It also describes different PLs categorized in to various 'clans' based on fold of proteins or core structural features. This chapter elaborately reviewed family 1 polysaccharide lyase and associated non-catalytic carbohydrate binding module (CBM), especially, CBM35. The chapter reviews about the type of core architecture seen in various family 1 PLs, mainly pectate lyase, exo-pectate lyase and pectin lyase their enzyme activities, substrate specificity, active site and active site residues. Previously characterized recombinant family 1 PLs and family 35 CBM from different bacteria, highlighting their ligand or polysaccharide binding capabilities have been illustrated. A brief review on different pectinase and their mode of action during enzymatic reaction has

been included. A detailed account of applications of pectin degrading enzyme in various industrial processes has also been provided.

Significance of the work has been elaborated in this chapter. Pectinase has found immense interest for its widespread application in various industrial processes. Hence search for an improved variety is always on the go. There are about 134 PL protein sequences from various bacterial source characterized under family 1 polyssacharide lyase in the CAZy database (http://www.cazy.org/PL1_bacteria.html). Cloning of PL1B-CBM35 and its truncated derivatives helped us to overexpress these enzymes, with an improved activity and thermostability which in further course can fulfill the need of modern day food, beverage, textile and oil industries. Functional studies of the catalytic module PL1B helped us to ascertain the cleavage pattern towards pectic polysaccharides, and provided us with the knowledge about its degradation products. Determination of the in-silico structural studies identified the catalytic centre of PL1B and residues involved in catalysis, binding cleft and residues involved in CBM35 for substrate binding was also recognised. Immobilization of PL1B provided it with an improved stability and efficient bioscouring of cotton fabric. Pectic oligosaccharides produced after enzymatic degradation of PL1B can find new avenues in the healthcare industries. Thus cloning and expression of family 1 polysaccharide lyase together with family 35 carbohydrate binding module from *Clostridium thermocellum* in *E.coli* has found a new extent in numerous applications.

**Chapter 2** describes amplification and cloning of the full length gene encoding family 1 polysaccharide lyase PL1B-CBM35 and its truncated derivatives PL1B and CBM35 from the genomic DNA of *Clostridium thermocellum* ATCC

27405 (GenBank Accession No: ABN53381.1). The molecular architecture revealed an N-terminal catalytic family 1 polysaccharide module (PL1B, 1059 bp) followed by C-terminal carbohydrate binding modules (CBM35, 372 bp) sandwiched between these two domains is a type 1 dockerin domain. The PCR amplified fragment of full length gene encoding PL1B-CBM35 showed a band of 1701 bp, whereas, the gene encoding truncated catalytic module (PL1B) and binding module (CBM35), displayed the sizes of 1059 bp and 372 bp, respectively. The PCR amplified fragments were cloned into pGEM-T Easy vector for TA cloning and transformed using *E. coli* (XL10 Gold) competent cells. Positive clones were selected by blue-white colony screening, and plasmid DNA was isolated for restriction digestion. *NheI* and *XhoI* digested plasmid DNA after running on 0.8% agarose gel produced a band of 3 kb for pGEM-T Easy vector and corresponding bands of 1.7 kb, 1 kb and 0.4 kb were produced from the insert fragments of PL1B-CBM35, PL1B and CBM35, respectively. The restriction enzyme digested fragments of PL1B-CBM35, PL1B and CBM35 were ligated with linearized pET-28a(+) vector. The ligated mixture was transformed using *E. coli* (XL10 Gold) competent cells. The positive clones containing recombinant plasmid DNA were screened by restriction enzyme digestion using restriction enzymes, *NheI* and *XhoI*. The restriction enzyme digested products were run on 0.8% agarose gel, where 5.4 kb band was produced for pET-28a(+) vector and corresponding bands of 1.7 kb, 1 kb and 0.4 kb were produced from the insert fragments for genes encoding PL1B-CBM35, PL1B and CBM35, respectively. The positive clones containing recombinant plasmid DNA were transformed into *E. coli* (BL21) competent cells and the recombinant proteins were hyper-expressed. The

purified recombinant proteins displayed a band of approximately, 50 kDa for PL1B-CBM35, 40 kDa for PL1B and a band of 15 kDa for CBM35 on SDS-PAGE. The amount of protein obtained from 100 ml *E.coli* culture of the recombinant proteins PL1B-CBM35, PL1B and CBM35 after Immobilized metal ion affinity chromatography (IMAC) purification were 2.8 mg, 2.1 mg and 1.6 mg, respectively.

**Chapter 3** describes the biochemical and functional characterisation of PL1B-CBM35 and PL1B. PL1B-CBM35 and PL1B showed maximum enzyme activity at optimum pH 9.6 and 9.8, respectively and both were active within the pH range of 8-10. The optimal temperature for both enzymes was 50ºC. PL1B-CBM35 and PL1B were stable over a pH range of 8-10. PL1B-CBM35 was stable in the temperature range of 30-50°C, whereas PL1B was stable in the range of 30-70°C. However PL1B-CBM35 over 60°C and PL1B over 70°C lost significantly the enzyme activity. Both the enzymes showed high activity towards pectic polysaccharides. PL1B-CBM35 and PL1B showed maximum activity 3.7 U/mg and 18.5 U/mg, respectively, with polygalacturonic acid (PGA). These enzymes also showed better activity towards 25% and 55% methyl-esterified citrus pectin than other pectate lyases. Generally, pectate lyase which is specific to non-methylated PGA, displays lower activity towards methylated pectin. But PL1B-CBM35 and PL1B even though displayed highest activity towards PGA also showed around 90-73% activity towards pectin. The kinetic parameters suggested that PL1B is more efficient than PL1B-CBM35 in degrading PGA and other pectic polysaccharides.

The enzyme activity of PL1B-CBM35 increased by nine-fold (0.41 U/mg to 3.70 U/mg) by 0.6 mM $Ca^{2+}$ or 1.2 mM $Mg^{2+}$ and PL1B was increased four-fold by

the same metal ions at same concentrations (4.02 U/mg to 18.5 U/mg), implying that these ions are essential cofactors. Marginal increase in the activities of both enzymes was also observed with $Li^{+}$ and $Mn^{2+}$ ions. However, the enzyme activity was unaffected by lower concentrations of $Ni^{2+}$, $Cu^{2+}$, $Zn^{2+}$ and $Co^{2+}$ ions. The trivalent metal ion, $Al^{3+}$ also showed marginal increase in the activity. The addition of 0.6 mM $Mg^{2+}$ or $Li^{+}$ in presence of 0.6 mM $Ca^{2+}$ ions also increased the 100% (3.7 U/mg) activity in PL1B-CBM35 by 14% (4.2 U/mg) and 12% (4.1 U/mg), respectively. The same metal ions at 0.6 mM of $Mg^{2+}$ or $Li^{+}$ ions to PL1B along with the presence of equimolar $Ca^{2+}$ ions in the reaction mixture increased the 100% (18.5 U/mg) activity of the enzyme by 20% (22.2 U/mg) and 15% (21.3 U/mg), respectively. 1.5 mM EGTA and 1.8 mM EDTA was required to chelate 0.6 mM $CaCl_2$ and completely abolish the activity of both the enzymes. Use of 2-3 times higher concentration of chelating agent suggested that $Ca^{2+}$ ions have a strong affinity towards both these enzymes. The TLC analysis of the hydrolysed products of PGA and citrus pectin by PL1B revealed that unsaturated di- and tri-galacturonate were the main sugars released. The accumulation of both these unsaturated products increased with time and was highest at 60 min of the reaction. The results of TLC analysis clearly suggested that PL1B followed an endolytic cleavage pattern towards its substrate and identified as an endo-pectate lyase. The protein-melting peak of PL1B shifted to higher temperature in the presence of $Ca^{2+}$ ions. This further corroborated the fact that $Ca^{2+}$ ions not only enhances activity but also impart thermal stability to the protein structure.

**Chapter 4** focuses on the structural aspects of PL1B and CBM35. The 3-dimensional structures of endo-pectate lyase (PL1B) of family 1 polysaccharide lyase and family 35 carbohydrate binding module (CBM35) from *Clostridium thermocellum*, were generated by comparative modelling. The secondary structures of PL1B and CBM35 predicted from their amino acid sequence showed that PL1B is composed of <5% α-helices, >35% β-sheets and <60% random coils and CBM35 of <49.2% β-sheets and <50.8% random coils. The predicted secondary structures were verified by CD analyses, where PL1B displayed presence of 2 α-helices (2.06%), 23 β-sheets (40.54%) and 26 random coils (57.4%) and CBM35 contained 2.02% α-helices 11 β-strands (47.3%) and 19 random coils (50.68%). The 3-D structural model of PL1B and CBM35 was predicted by multiple template based homology modelling. The PL1B model showed a right handed parallel β-helix structure, where three parallel β-sheets are linked by loops. However, CBM35 displayed the jelly-roll type β-sandwich fold where the two β-sheets are connected by loops. Conclusively, both PL1B and CBM35 structures were rich in β-sheets and loops. The quality of predicted structure was assessed by Ramachandran plot, where in the PL1B and CBM35 structures, 82.8% and 92.7% amino acid residues, respectively, were found in the most favoured region. Molecular dynamic simulation for 5 ns was carried out to understand the stability and compactness of both the predicted models. The results showed significant changes in PL1B structure in the initial 1.75 ns of simulation, whereas after 2 ns the fluctuations reduced and the overall deflection was less than 0.4 Å. MD results of CBM35 displayed that the changes in the structure are very less and the structure is stabilized after 0.3 ns with deflection less than 0.3 Å. The

significant difference in time for the structures to stabilize was due to the presence of 353 aa residues in PL1B as compared to 124 aa residues in CBM35. PL1B showed highest affinity towards tri-galacturonic acid (TGA) with a binding energy of -6.99 kcal/mol. The key of PL1B residues involved during catalysis were Asp151, Arg209, Asn234, Arg236, Tyr271 and Ser272. Asp151 and Arg209 at the catalytic site were found to be responsible for proton donation and abstraction, respectively during β-elimination. CBM35 displayed highest affinity towards D-galacturonic acid and no affinity for polygalacturonan. The binding energy of CBM35 with D-galacturonic acid was -3.34 kcal/mol. The residues of CBM35 involved in substrate binding were Phe26, Gln28, Asp112, Gly114 and Arg116. The effect of chaotropic agents on PL1B was studied by change in tryptophan fluorescence intensity, which showed that the protein structure unfolds at 6M and 4M concentrations of GuHCl and Urea, respectively. Unfolded fraction of PL1B was less at a lower concentration of chaotropic agent and the apparent free energy change varied linearly with their varying concentrations. It was evident that the PL1B structure is stable and structural deformation occurs only at higher concentration of these chaotropic agents. PL1B structure was destabilized by a lower concentration of urea as compared with GuHCl.

**Chapter 5** describes the immobilization of PL1B on synthesised superparamagnetic ($Fe_3O_4$) nanoparticles (MNPs) and their use in biscouring of cotton fabric. The superparamagnetic nanoparticles (MNPs) were successfully synthesized by chemical coprecipitation from mixture of $FeCl_3.6H_2O$ and $FeCl_2.4H_2O$ salts in the molar ratio 1:2. The X-ray diffraction (XRD) analysis of synthesised MNPs showed series of characteristic peaks at 2.96(220), 2.52(311), 2.09(400), 1.71(422), 1.61(511),

1.47(440) and 1.27(533) which indicated the cubic spinel phase and an average size 20±5 nm. HRTEM analysis displayed that MNPs were not perfectly spherical and SAED analysis confirmed the formation of highly crystalline nanoparticles. A simple protocol for activation and immobilization of recombinant PL1B from *Clostridium thermocellum* on MNPs was developed. MNPs were activated in the presence of EDC hydrochloride (carbodiimide), which facilitated the direct binding of the protein to MNPs. It was observed that at 50 mg/ml concentration of MNPs the binding efficiency of PL1B was 97%, whereas at 70 mg/ml and above concentration of MNPs the binding efficiency was always 100%. The binding of PL1B to MNPs was confirmed by FT-IR spectroscopy studies, where the peak at 1628 $cm^{-1}$ due to N-H bending in bare MNPs was significantly shortened after immobilization of PL1B. This result suggested that the binding was accomplished via the reaction between the amino group on $Fe_3O_4$ nanoparticles and the carboxyl group of the protein after being activated by carbodiimide. The characteristic peak of PL1B at 1418 $cm^{-1}$ due to the C-C stretching in aromatic residues appeared in PL1B immobilized MNPs (PL1B-MNP), suggested the presence of aromatic amino acid residues from PL1B. EDX analysis of immobilized PL1B-MNP showed the presence of Carbon (C), Sulphur (S), Calcium (Ca) and Chloride (Cl) beside Iron (Fe) and Oxygen (O). The presence of carbon and sulphur in the sample suggested that these elements were from the carbon backbone and di-sulphide bonds of PL1B. Saturation magnetization (*M*s) of activated MNPs and immobilized PL1B-MNP were 36 emu/gm and 17 emu/gm, respectively. The reduction in Ms resulted due to encapsulation of MNP by PL1B attached to its surface. Immobilized PL1B-MNP showed slightly higher specific activity of 20.3 and

18.2 U/mg compared to free PL1B of 17.8 and 16.2 U/mg with PGA and citrus pectin, respectively. The immobilized PL1B-MNP could be easily recovered from the reaction mixture with the help of a magnet and reused till 5 cycles, retaining 70% of initial activity at the completion of 5 cycles. The immobilized MNP-PL1B showed enhanced thermostablilty at 80° and 90°C as compared to free PL1B which only showed thermostability till 70°C. The improved thermostability and reusability of immobilized PL1B makes it a good candidate for use in various industrial processes involving high temperature. After bioscouring of coarse cotton fabric with free PL1B the water absorbing time was decreased to 3 min as compared to untreated fabric, which was further reduced to 15 sec only after treatment of the fabric with immobilized PL1B-MNP. Hence efficient pectin removal and improved wettability was displayed by immobilized PL1B-MNP during bioscouring of cotton fabrics. Therefore, this alkaline pectinase upon immobilization can find new avenues in textile industries, providing an economic and environment friendly method as an alternative to chemical bioscouring process.

**Chapter 6** describes the isolation of natural pectin, characterization and effect of pectic oligosaccharide on colon cancer cells. Natural pectin was isolated from waste citrus peels of *Citrus limetta* (Sweet lemon) by acid extraction, yielding 12% powdered pectin. The structure of isolated natural pectin was characterized by NMR spectroscopy and was found to contain 77% methyl-esterification in the polysaccharide chain. Enzymatic treatment of the isolated natural pectin by PL1B produced unsaturated di-galacturonate as the major product, as confirmed by TLC analysis of samples collected at different time intervals between 0 to 60 min. The

commercial PGA and citrus pectin (25% methyl-esterified) were also treated with PL1B to produce unsaturated di- and tri-galacturonate as the major products, as mentioned earlier in Chapter 3. The enzyme degraded products from commercial PGA and citrus pectin when analysed by tandem mass spectroscopy showed molecular mass of 175 Da, 351 Da and 527 Da for unsaturated mono-, di- and tri-galacturonate respectively. Whereas the enzyme degraded products from isolated natural pectin produced methylated unsaturated mono- and di-galacturonate which displayed molecular mass of 191 Da and 383 Da, respectively. These oligosaccharides were then separated by gel filtration using Bio-Gel P2 matrix, where deionized water was used as the mobile phase. The effect of these oligosaccharides at varying concentrations from 0.05 to 0.5 mg/ml was tested on colon cancer cell lines (HT-29) for 3, 6, 12, 24 h. The population of viable cells present after the treatment was measured by MTT assay, where the cell viability is measured by the colorimetric changes. The results showed 53%, 61% and 77% inhibition in the growth of HT-29 cells after treatment for 24 h with 0.5 mg/ml of oligosaccharides, produced after enzymatic reaction of PL1B with PGA, citrus pectin (25% methyl-esterified) and isolated natural pectin, respectively. This result was further verified by observing the changes in the cell morphology upon treatment with these oligosaccharides. Light microscopic images of 0.5 mg/ml oligosaccharides treated HT-29 cells showed disintegrated cell membrane as compared to the untreated cells. A close insight into the HT-29 cells inhibition pattern revealed that methyl-esterified oligosaccharide show relatively higher inhibition of the cell growth as compared with less methyl-esterified oligosaccharides. Pectin being large polymeric compound is difficult to get absorbed by the alimentary

canal hence enzymatic degradation facilitates the production of smaller oligosaccharides which gets easily absorbed by the alimentary canal. Hence, the pectic oligosaccharides can be produced from citrus peels by recombinant endo pectate lyase from *Clostridium thermocellum* on a large scale. The citrus peel which is generally considered as waste can serve as source for a potent healthcare commodity.

## CONTENTS

**Chapter 3. Biochemical and functional characterization, stability studies of PL1B-CBM35, PL1B and binding analysis of CBM35**

# Chapter 1

## General Introduction

### 1. Carbohydrates

The four major classes of organic molecules in living systems are proteins, lipids, nucleic acids and carbohydrates. Carbohydrates are the most abundant organic molecules found in nature and nearly all organisms synthesize and metabolize carbohydrates (Wade, 1999). The term carbohydrate arose from the fact that most simple sugars have the empirical formula $C_nH_{2n}O_n$, where n is $\geq 3$, suggesting that carbon atoms are combined with water. Chemists referred to these compounds as ‘‘hydrates of carbon’’ or ‘‘carbohydrates’’ (Wade, 1999). Glucose is a common monosaccharide that is oxidized to form carbon dioxide and water, providing energy for cellular processes such as protein synthesis, movement and transport. Plants and animals associate abundant glucose molecules together to form large energy-storing molecules like starch and glycogen. However, glucose molecules may be linked to form a variety of other macromolecules. Cellulose is a component of the cell wall in

plants and it is composed of glucose molecules linked together through β-(1,4) glycosidic bonds. The glucose monomers in starch, on the other hand, are linked through α-(1,4) glycosidic bonds and the glycosidic bonds of glycogen are α-(1,4) and α-(1,6) (Wade, 1999). The complex heterogeneity of carbohydrates in living systems is directly related to their unique properties *viz.* the ability of different types and numbers of sugar residues to form glycosidic bonds among them, the structural features of these molecules, the type of anomeric linkage, the position and the absence or presence of branching (Mody *et al*., 1995; Gorelik *et al*., 2001). These structural features provide millions of different possible combinations of carbohydrate structures that are suited for serving their function in nature (Fontes *et al*., 2010); as for example two identical hexose monosaccharide can produce 11 different disaccharides whereas four different hexose monosaccharide can produce around 35,500 unique tetrasaccharides (Sharon *et al*., 1989 and 1993).

**1.1 Structural polysaccharides in plants**

Cellulose, hemicellulose and pectin are the main polysaccharide component in plant cell wall (Mohnen *et al*., 2008). Other polysaccharides which are frequently found are mixed-linkage glucan and lignins. Polysaccharides are macromolecular carbohydrates comprising chain of monosaccharides linked together by glycosidic bonds, formed as a result of condensation reaction (Berg, 2007). The bulk of plant cell wall material is cellulose, a homopolymer of β-(1,4)-glucose which takes on an overall linear shape. Plant cell walls also contain a number of other sugar polymers termed hemicellulose which includes xylan (β-1,4-linked xylose), laminarin (β-1,3-linked glucose), mannan (β-1,4-linked mannose) and lichenan (mixed 1,3-1,4-β-D-glucan) (Scheller *et al*., 2010). The other main structural polysaccharide found within the plant

cell wall are pectins and substituted heteropolysaccharides composed of a α-(1,4)-D-galacturonic acid backbone with rhamnose, galactose and arabinose as side chain substituents (Bayer *et al*., 1998).

### 1.1.1 Cellulose

Cellulose is the polysaccharide that provides structural integrity to plants. About 40% of the plant carbon is bound to cellulose (Demain *et al*., 2005). However, the percentage of cellulose in plant varies depending on the origin. Its occurrence is widespread, from higher plants to primitive organism such as sea-weads, flagellates and bacteria. Other cellulose-containing materials include agriculture residues, water plants, grasses etc. The cellulose is a linear homopolymer consisting of regio- and enantio- selective D-glucopyranose (also known as anhydroglucose) units linked together by β-(1,4)-glycosidic linkage.

### 1.1.2 Hemicellulose

Hemicelluloses are hetero-polysaccharide present in plant cell walls containing β-(1,4)-linked backbones of arabinose, galactose, rhamnose, mannose or xylose (Scheller *et al*., 2010). They commonly occur in the nature as xyloglucans, xylans, arabinoxylans, arabinogalactans, mannans and glucomannans (Schadel *et al*., 2009). Hemicelluloses are known to be synthesized by various glycosyltransferases in Golgi apparatus. Many glycosyltransferases involved in the process of biosynthesis of xyloglucans and mannans are known (Schadel *et al*., 2009). Other hemicelluloses found in primary and secondary walls include xyloglucan, glucuronoxylan, arabinoxylan, glucomannan, and galactomannan (Schadel *et al*., 2009). Xylans are the most abundantly hemicellulose found in plants, which has a backbone of β-(1,4)-linked xylose residues. Xylans are substituted with α-(1,2)-linked glucuronosyl and 4-

*O*-methyl glucuronosyl residues in the secondary wall of dicots (Scheller *et al*., 2010). Glucouronoxylans have β-(1-4)-xylose backbone with 4-*O*-methylglucuronic acid side-chains. Sometimes arabinose and *O*-acetyl side-chains may also be found attached to the main chain. Glucouronoxylans are the major polysaccharide of secondary walls of dicot plants (Urbanowicz *et al*., 2012). Arabinoxylans are composed of β-(1,4) linked D-xylopyranosyl backbone, with one or more α-L-arabinofuranosyl residues substituted at position *O*-2 or *O*-3. On the other hand, in many cases, arabinoxylan also contains hexose or and hexuronic acid substitutions, but as minor constituents (Cosgrove, 1999). Xyloglucans are composed of β-(1,4)-glucose backbone, substituted with α-(1,6)-D-xylose side chains, the xylose residue is often capped by galactose followed by fucose residues (Fry, 1989; Brennan *et al*., 2010). Arabinogalactans of plant cell-wall comprise β-(1,5) or β-(1,6) linked galactan backbone, substituted with α-(1,3) or α-(1,5) linked L-arabinofuranosyl residues in a comb-like or a ramified arrangement (Bhamidi *et al*., 2008). Mannans are homo-polymers containing β-(1,4)-D-mannopyranose backbone that is substituted with galactose in galactomanan or glucose in glucomanan (Cui *et al*., 2009).

### 1.1.3 Lignin

The main building blocks of lignin are the hydroxycinnamyl alcohols (or monolignols) coniferyl alcohol and sinapyl alcohol, with typically minor amounts of p-coumaryl alcohol. Lignins are large groups of aromatic polymers that result from the oxidative combinatorial coupling of 4-hydroxyphenylpropanoids (Boerjan *et al*., 2003; Ralph *et al*., 2004). Lignin is found in all vascular plants, mostly between the cells and also within the cells and in the cell walls. It usually occurs as complex structure bound to the hemicelluloses in wood.

### 1.1.4 Pectin

Pectin is structurally most complex polysaccharides, which constitute the cell wall by 35% of in dicot and monocot, 2-10% in grass and 5% in wood. Pectin acts as a protective material in plants, hence they are commonly found around growing cells, middle lamella, walls of cells in the soft plant parts (Fig. 1.1A) (O'Neill *et al*., 1990; Ridley *et al*., 2001). Pectin is also found in cell walls of gymnosperms, pteridophytes, bryophytes and in charophycean algae (O'Neill *et al*., 2004). The structural complexity of pectin polysaccharides and their reasonably high proportion (one-third) in dry matter of the primary cell walls coupled with presence of cell wall-based pectin modifying enzymes, suggest their involvement in plant growth, morphology and development. Hence pectin has a prevalent role in plant growth and development, defence mechanism, cell-cell adhesion, providing structural stability to cell wall, regulation of cell permeability and fruit development (Ridley *et al*., 2001; Willats *et al*., 2001). Pectin is use as a gelling and stabilizing agent in food and cosmetic industry, pectic polysaccharides have displayed health benefits *viz.* lowering cholesterol, blood glucose level, inhibiting cancer and enhances immunity (Jackson *et al*., 2007; Inngjerdingen *et al*., 2007).

Pectic polysaccharides, abundantly found in the plant primary cell walls and middle lamellae (Fig. 1.1A) are diverse in their structure. The basic unit of the pectic polysaccharide chain is galacturonic acid in non-methylated pectin, while the methyl-esterified galacturonate moieties are present in methylated pectin (Fig. 1.1B). Three pectic polysaccharide domains referred to as galacturonans, are found in plants and have been isolated from primary cell walls (O'Neil *et al*., 1990). These are

homogalacturonan (HG), rhamnogalacturonan-I (RG-I) and rhamnogalacturonan-II (RG-II).

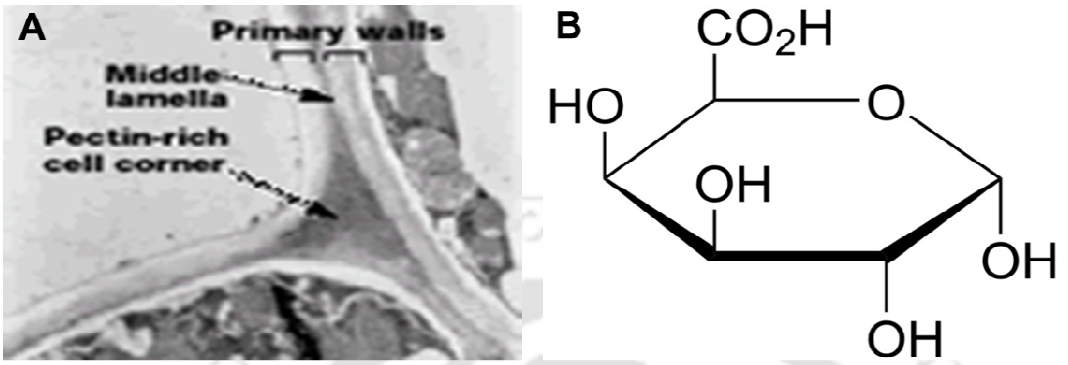


**Fig. 1.1** (A) The space between the two adjacent cell wall is known as middle lamella, which is often filled with pectin rich polysaccharides. (B) Galacturonic acid structure where the C-6 carbon is methyl-esterified in pectin.

### 1.1.4.1 Homogalacturonan

Homogalacturonan (HG) is a widespread linear homopolymer. Its basic structure consists of a chain of α-D-galacturonic acid residues (GalA) linked by α-(1,4) glycosidic bonds (Fig. 1.2) and is thought to contain some 100-200 GalA residues (Zhan *et al*., 1998). HG domains are referred to as the smooth region of pectin (Schols *et al*., 1996). The carboxyl groups at C6 position of galacturonic acid residues in HG is partially methyl-esterified or sometimes *O*-acetylated at *O*-2 or *O*-3 (Ishii, 1995 and 1999). The pattern and degree of methyl-esterification vary from one plant to other and within a given species with developmental stage and location in the cell wall. This means that, plants are capable of synthesizing and eventually modifying pectin molecules for their survival. Highly methyl-esterified pectin molecules are synthesized in the Golgi apparatus and secreted into the plant cell wall where they are subjected to modifications (Ridley *et al*., 2001). De-esterification of HG appears to be a complex regulated process that does not occur uniformly throughout tissues or cell walls (Liberman *et al*., 1999). This can be expected because

different plant tissues have different functions. On the other hand, un-esterified carboxyl groups (negatively charged groups) in adjacent HG molecules may interact in presence of divalent cations like $Mg^{2+}$ or $Ca^{+2}$ forming a salt bridge, this stable gel is important for maintaining the cell walls integrity. HG cross-linked via salt bridges has impact on cell wall mechanical properties and cell wall matrix porosity (Somerville *et al*., 2004). The interaction of HG with divalent ions is favored in the presence of long un-esterified galacturonic acid chains. The amount of methyl groups, acetyl esters and their distribution in the polymer largely determine its chemical properties and its fitness for particular industrial applications.

**1.1.4.2 Rhamnogalacturonan I**

Rhamnogalacturonan-I (RG-I) represents 20-35% of pectic polysaccharides composed of a backbone of a repeating disaccharide -4)-α-D-GalA-(1,2)-α-L-Rhamnose-(1- to which a variety of glycan chains (arabinan and galactan) are attached (Fig. 1.2) (O'Neill *et al*., 1990; Willats *et al*., 2001). The sugar composition of RG-I is highly heterogeneous. Because the rhamnosyl residues (20-80%) are substituted at C-4 with neutral and acidic side chains, RG-I is large and highly variable family of polysaccharides (Albersheim *et al*., 1996). RG-I is known as the hairy region of pectin (Schols *et al*., 1996).

**1.1.4.3 Rhamnogalacturonan II**

Rhamnogalacturonan II (RG-II) constitutes about 10% of the pectic polysaccahrides, with highest degree of structural complexity (O'Neill *et al*., 2004). They have a α-(1,4) linked D-Galacturonic acid (GalA) backbone like HG, substituted with 12 different types of sugars with 20 different linkages in its branches (Fig. 1.2). RG-II in the plant cell wall exists in a dimeric form comprising two separate RG-II

monomers cross linked with each other (O'Neill *et al*., 2004). RG-II interacts covalently with HG and RG-I to build a complex macromolecular pectin network (Matsunaga *et al*., 2004).

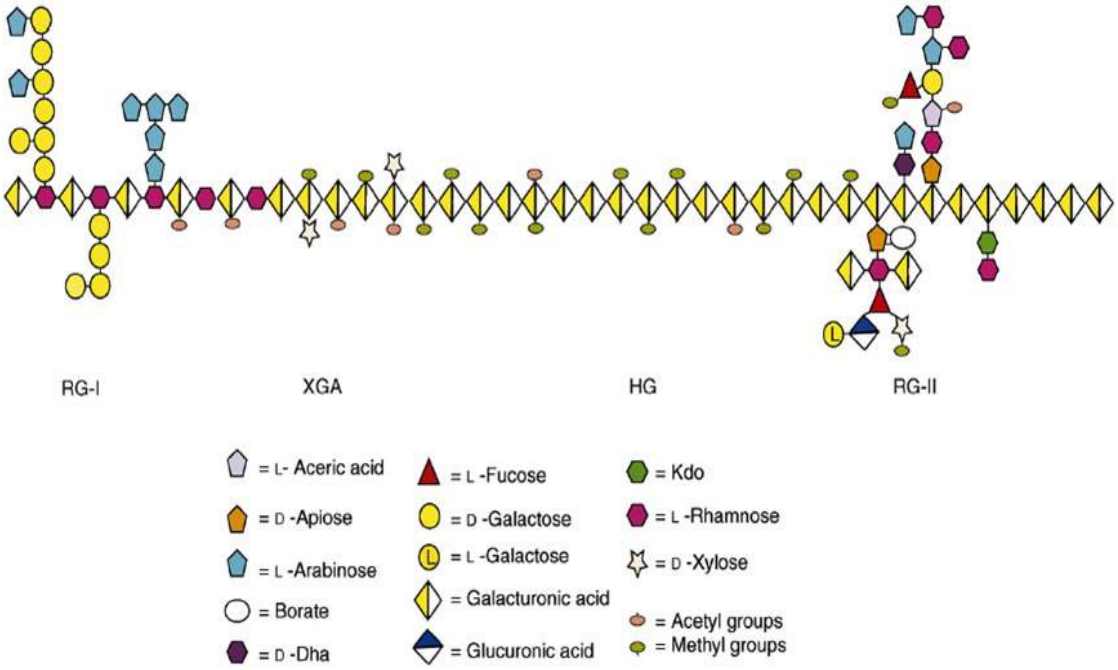


**Fig. 1.2** Schematic representation of complex pectic polysaccharide, where Homogalacturonan (HG), Rhamnogalacturonan I (RGI), Rhamnogalacturonan II (RGII) and Xylogalacturonan (XGA) (adapted from Mohen, 2008).

### 1.2 Carbohydrate-active enzymes

Carbohydrates are dynamic molecules that are constantly synthesized and broken down. There are varieties of enzymes involved in the synthesis as well as breakdown of carbohydrates. Carbohydrate modifying enzymes are divided into four classes: glycoside hydrolases (GHs), glycosyltransferases (GTs), polysaccharide lyases (PLs), and carbohydrate esterases (CEs). The glycosyltransferases (GTs) are mainly involved in the formation of the glycosidic bond or biosynthesis of carbohydrates. The polysaccharide lyases (PLs), carbohydrate esterase (CEs) and glycoside hydrolases (GHs) are concerned with the breakdown of polysaccharides. In

summary, the carbohydrate-active enzymes are grouped into 269 families based on amino acid sequence similarity and are listed in the continually updated carbohydrate-active enzyme (CAZy) database (www.cazy.org) (Cantarel *et al*., 2009). Out of 269 carbohydrate-active enzymes, about 23 families belong to PLs. These 23 PL families contain nearly 1884 species of bacteria, 130 species of archaea and 65 species of eukaryote (www.cazy.org). A close inspection of the genomes listed within the database reveals the fact that 1-3% of the genome of most organisms is devoted to encoding glycosyltransferases (GTs) and glycoside hydrolases (GHs) (www.cazy.org). The information available at CAZy database provide a wealth of gene sequences (many yet to be characterized) to study the structure and function of carbohydrate-active enzymes (Cantarel *et al.*, 2009).

### 1.2.1 Glycosyltransferase

Glycosyltransferase (GT) are enzymes that catalyse the transfer of sugar moiety from activated donor molecule to a specific acceptor molecule, forming a glycosidic bond (Sinnot, 1990). These enzymes utilize 'activated' sugar phosphates as glycosyl donors and catalyze glycosyl group transfer to a nucleophilic group, usually an alcohol (Campbell *et al*., 1997). The product of glycosyl transfer may be an O-, N-, S-, or C-glycoside; the glycoside may be part of a monosaccharide, oligosaccharide or polysaccharide (Lairson *et al*., 2008). As of now, nearly 94 families of GTs have been recognized and are listed in the CAZy database (http://www.cazy.org/GlycosylTransferases.html). There are almost over 8000 gene sequences in GenBank and the crystal structure of 36 GTs has been solved till date (http://www.cazy.org/GlycosylTransferases.html). Many GTs have been reported

from wide range of bacterial population *viz. Acidophilium, Actinoplanes, Bacillus, Clostridium, Gloeobacter, Lactobacillus* etc. (Coutinho *et al*., 2008).

### 1.2.2 Carbohydrate esterase

The carbohydrate esterase (CE) catalyzes the de-O or de-N-acylation of substituted saccharides. Two types of substrates have been considered for carbohydrate esterases: i) those in which the sugar plays the role of the "acid", such as pectin methyl esters for 4-*O*-methyl-glucuronoyl methylesterase from *Schizophyllum commune* (Li *et al*., 2007) and ii) those in which the sugar behaves as the alcohol, such as acetylated xylan for acetyl xylan esterase (family 1 and 2 CEs) from *Clostridium thermocellum* ATCC 27405 (Montanier *et al*., 2009).

### 1.2.3 Glycoside hydrolase

Glycoside hydrolase (GH) are enzymes that catalyze the hydrolysis of the glycosidic linkage of glycosides, leading to the formation of a sugar hemiacetal or hemiketal and the corresponding free aglycone. Glycoside hydrolases are also referred to as glycosidases and sometimes also as glycosyl hydrolases. Glycoside hydrolases can catalyze the hydrolysis of O-, N- and S-linked glycosides. The glycoside hydrolases are group of enzymes that exists in most of the living organisms (Cantarel *et al*., 2009). They hydrolyze the glycosidic linkages between two or more carbohydrates or between a carbohydrate and a non-carbohydrate moiety.

### 1.2.4 Polysaccharide lyase

Polysaccharide lyase (PL) are the enzymes (EC 4.2.2.-) which cleave uronic acid polysaccharides via a β-elimination mechanism to generate an unsaturated hexenuronic acid residue with a new reducing end (Yip *et al*., 2006). PLs have been identified in different organisms ranging from archaea, eubacteria, fungi, algae, plants

and mammals (Sutherland, 1995). The catalytic mechanism involved in cleaving the polygalacturonic chain by PLs is broadly divided in three events. First of all, abstraction of the C-5 proton of the uronic acid by a basic amino acid (arginine, lysine and histidine) side chain, secondly stabilizing the resultant anion into the C-6 carbonyl group by charge delocalization and lastly the cleavage of the α-(1,4)-glycosidic bond, facilitated by proton donation from an acidic amino acid (aspartate and glutamate) at the catalytic center of the enzyme, producing an unsaturated hexenuronan moiety and a reducing end (Yip *et al*., 2004 and 2006). Depending on the monosaccharide composition of the substrate and its conformation in the PL active site, the proton removed from C-5 and the departing oxygen on C-4 may lay either syn or anti to each other (Fig. 1.3). Substrate recognition by PLs is often mediated by the interaction of bivalent cations (often $Ca^{2+}$), or positively charged amino acid side chains, with uronic acid groups in the substrate. This bivalent cation usually stabilizes the transient anion in the reaction pathway (Yip *et al*., 2004). PLs are defined as carbohydrate active enzymes and based on sequence similarities have been classified in 23 families till date (January, 2015), according to CAZy (**C**arbohydrate-**A**ctive en**Zy**mes or CAZymes) database (http://www.cazy.org/Polysaccharide-Lyases.html). Different PLs characterized so far are endo-pectate lyase (EC 4.2.2.2), exo-pectate lyase (EC 4.2.2.9), pectin lyase (EC 4.2.2.11), rhamnogalacturonan lyase (EC 4.2.2.-), alginate lyase (EC 4.2.2.3), chondroitin AC lyase (EC 4.2.2.5), chondroitin ABC lyase (EC 4.2.2.4), heparin lyase (EC 4.2.2.7), heparan lyase (EC 4.2.2.8) and hyaluronate lyase (EC 4.2.2.1).

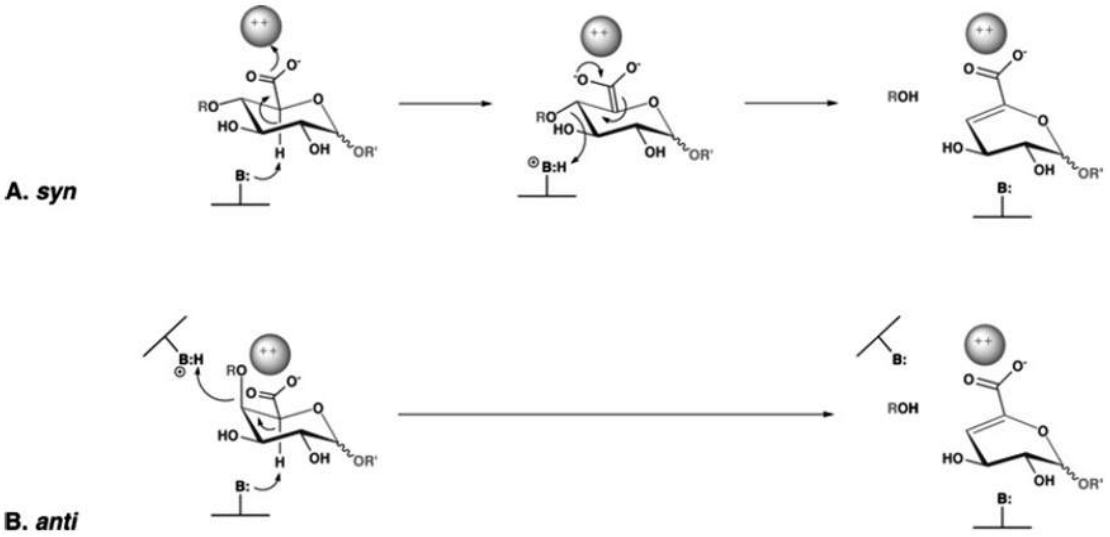


**Fig. 1.3** (A) syn-β-elimination and (B) anti-β-elimination, as in α-(1,4)-linked polysaccharide lyase. In both, polysaccharides are cleaved to produce an 4,5 unsaturated galacturonate moiety at the newly formed non-reducing end of the chain. As the cleavage is caused in the polysaccharide chain, the C-5 proton adjacent to the carbonyl group is abstracted by a basic amino acid at the catalytic centre (B:). Removal of the glycosidic oxygen is facilitated by proton donation from an acidic amino acid residue (B:H). Syn elimination is commonly found in chondroitin lyase, while anti elimination is observed in pectate lyase or pectin lyase (adapted from Lombard *et al*., 2010).

### 1.3 Family 1 polysaccharide lyase

The family 1 polysaccharide lyase (PL1) currently contain nearly 99 well characterized sequences where the enzymes so far have shown activities like endo-pectate lyase (EC 4.2.2.2); exo-pectate lyase (EC 4.2.2.9) and pectin lyase (EC 4.2.2.10) (http://www.cazy.org/PL1.html). Pectate lyases of families 1, 2, 3, 9, and 10 catalyse the cleavage of α-(1,4)-glycosidic bond between D-galacturonic acid residue in pectate (a low methylesterified form of pectin) by β-elimination and generate Δ4,5 unsaturated galacturonates as the product, which exhibits a maximum absorbance at 235 nm ($A_{235}$). The main structural fold found in family 1 polysaccharide lyase is parallel β-helix, where the parallel β-sheets folds into a right handed helix. Three sets

of parallel β-sheets containing of 7 to 10 β-strands are joined together by loops forming a β-helix core. An extended or compound loop in the structure is found which participates in the ligand binding during catalysis. The β-helix structure found in family 1 consists of 10 complete turns as compared to family 3 and 9 both having 8 and 11 turns, respectively (Garron *et al.*, 2010). There are around 15 archaeal, 815 bacterial, 470 eukaryotic and 15 viral sequences present in family 1 polysaccharide lyase. Among which 102 sequences are characterized and 14 crystal structures have been determined till date. Bacterial family 1 polysaccharide lyase has been thoroughly classified from *Bacillus sp*. (25 sequences), *Erwinia sp*. (12 sequences), *Pectobacterium sp*. (7 sequences), *Pseudomonus sp*. (6 sequences), *Streptomyces sp*. (3 sequences), *Xanthomonas sp*. (5 sequences) and *Thermotoga maritima* (1 sequence) (http://www.cazy.org/PL1_characterized.html).

### 1.3.1 Characteristics of family 1 polysaccharide lyase

As mentioned above several family 1 polysaccharide lyases have already being characterized and among them *Bacillus sp*. is the most studied. A thermophilic pectate lyase Pel SWU of 33 kDa, was isolated from *Bacillus sp*. RN1 having stability of pH in the range of 4-10 and optimum temperature 70°C (Sukhumsiirchart *et al*., 2009). It produced unsaturated di- and tri-galacturonate as the major degradation product. Three extracellular pectate lyases Pel-22, Pel-66 and Pel-90 from *Bacillus sp*. were isolated from fermenting cocoa beans (Ouattara *et al*., 2010). All three enzymes showed optimum activity at 60°C and optimum pH were 7.5 for Pel-22 and 8.0 for Pel-66 and Pel-90. These enzymes showed better activity towards methyl-esterified pectin and $Fe^{2+}$ ions were preferred cofactor than $Ca^{2+}$ ions. Another pectate lyase from *Bacillus pumilus* DKS1 with a molecular weight of 35 kDa and working at 60°C

with pH range of 8.5-9.0, showed efficient degumming of ramie fibres (Basu *et al*., 2011). An alkaline pectate lyase (Bsp165PelA) from *Bacillus sp*. N16-5 had a molecular mass of 42 kDa, which showed optimum activity at pH 11 and 50°C. It showed efficient depolymerisation of pectic acid and pectin with a metal ion cofactor (Li *et al*., 2010). Another alkaline pectate lyase Pel-4A from alkaliphilic *Bacillus sp*. P-4-N of 34 kDa, showed stability in the range of pH 5-11.5 in presence of 100 mM NaCl (Kobayashi *et al*., 2000). A thermostable pectate lyase PL47 from *Bacillus sp*. TS47 showed temperature stability and optima at 70°C (Takao *et al*., 2001). Five isoforms of pectate lyase PelA (Tamaki *et al*., 1988; van Gijsegem, 1989), PelB (Keen *et al*., 1986), PelC (Tamaki *et al*., 1988), PelD (van Gijsegem, 1989) and PelE (Keen *et al*., 1986; van Gijsegem *et al*., 1989) was identified from *Erwinia chrysanthemi*. Two pectate lyase of molecular size 68 and 75 kDa were identified in marine Antarctic bacterium *Pseudoalteromonas haloplanktis* strain ANT/505 and both displayed the optimum temperature of 30°C and pH 9-10 (Truong *et al*., 2001). A pectate lyase (Pel) from *Xanthomonas campestris pv*. malvacearum strain B414 was identified with molecular size of 41 kDa (Liao *et al*., 1996). It was evident from multiple sequence analysis that Pel proteins of non-*Erwinia* phytopathogens including *Xanthomonas*, *Pseudomonas* and *Bacillus* constituted a distinct cluster, which showed 20 to 43% amino acid sequence identity to the four established Pel families of *Erwinia*. All of these *Xanthomonas sp*. produced an alkaline Pel and were capable of causing soft-rot in potato tuber slices and green pepper fruits. An endo pectate lyase (EC 4.2.2.2) was cloned and expressed from *Amycolata sp*. produced a molecular size of 30 kDa (Bruhlmann *et al*., 1997). This pectate lyase belongs to pectate lyase superfamily and shared profound sequence similarities with *Erwinia sp*. and *Bacillus*

*sp.* PelS a pectate lyase from *Pseudomonas syringae* had similarity with *E. chrysanthemi* PelE in its substrate preference, ability to catalyse pectic polysaccharides and to macerate potato tuber tissue (Bauer *et al*., 1997). PelA a pectate lyase from *Thermotoga maritima* is a thermostable tetrameric enzyme (Kluskens *et al*., 2003). The enzyme showed its highest activity at an optimum temperature of 90°C and pH 9, with half-life of thermal inactivation of 2 h at 95°C (Yuan *et al*., 2012). PelA displayed an exo-cleaving pattern towards its substrate and produced tri-galacturonate as major product. A low temperature alkaline pectate lyase (PLD) from *Xanthomonas campestris* ACCC 10048 was cloned and expressed as a homogenous protein of 38 kDa. The pH and temperature optimum was 9 and 30°C, respectively. PelD showed highest activity on polygalacturonic acid and enhanced biscouring properties on jute fibres.

### 1.4 Different types of pectin degrading enzymes

#### 1.4.1 Protopectinases

Protopectinases hydrolyse protopectin by reacting with the polygalacturonic acid region or with the polysaccharide chains connecting cell wall constituents. This results in detaching pectic polymers from the plant cell wall with subsequent formation of highly polymerized soluble pectin (Sakai *et al*., 1993; Alkorta *et al*., 1998; Kashyap *et al*., 2001).

#### 1.4.2 Polymethylgalacturonases

Polymethylgalacturonase (PMG) facilitates the hydrolytic cleavage of α-(1,4)-glycosidic bonds in highly esterified pectin, producing 6-methyl-D-galacturonate (Fig. 1.4A) (Jayani *et al*., 2005). They show either endolytic or exolytic mode of cleavage mechanism towards their substrates.

### 1.4.3 Polygalacturonases

Polygalacturonase (PG) hydrolyses the cleavage of α-(1,4)-glycosidic linkages in polygalacturonic acid producing D-galacturonate (Fig. 1.4A). They belong to family 28 of glycoside-hydrolases (http://www.cazy.org/GH28.html). Unlike PMG they also act on their substrates by either endo- or exo- mode. Endo-PG and endo-PMG randomly cleave the substrate, whereas exo-PG and exo-PMG causes hydrolytic cleavage of the substrate producing mono-galacturonate or di-galacturonate (Rombouts and Pilnik, 1980).

### 1.4.4 Pectin methyl esterases

Pectin methyl esterase (PME) (EC 3.1.1.11) is responsible for the deesterification of the methoxyl group at C-6 carbon of the galacturonic acid moiety in pectin (Fig. 1.4B). Major products in this reaction are pectic acid and methanol. The enzyme acts preferentially on a methyl ester group of galacturonate unit next to a non-esterified galacturonate unit. Action of PME on methyl-esterified pectin facilitates polygalacturonases and pectate lyases to cleave the non-esterified polygalacturonan chain. PME belongs to family 8 carbohydrate esterase of the CAZy database (http://www.cazy.org/PL8.html).

### 1.4.5 Pectin acetyl esterases

Pectin acetyl esterase (PAE) (EC 3.1.1.-) hydrolyses the acetyl ester at C-6 carbon of the galacturonic acid moiety of pectin producing pectic acid and acetate (Fig. 1.4B) (Shevchik *et al.*, 1997). PAE belongs to families 12 and 13 of carbohydrate esterase in CAZy database (http://www.cazy.org/PL12.html, http://www.cazy.org/PL13.html).

### 1.4.6 Pectate lyases

Pectate lyase (PL) cleaves the α-(1,4)-glycosidic bond preferentially in polygalacturonic acid producing unsaturated product (Δ-4,5-D-galacturonate) through β-transelimination reaction (Fig. 1.4C). PGL is $Ca^{2+}$ ions dependent and some has an absolute requirement of $Ca^{2+}$ ions for activity (Jayani *et al*., 2005). Pectate lyases are of two types endo-PL (EC 4.2.2.2) that follows a random cleavage pattern towards their substrates always producing more than one unsaturated degradation product, exo-PL (EC 4.2.2.9) catalyze the substrate cleavage from non-reducing end producing a single unsaturated degradation product. They have been classified in polysaccharide lyase families 1, 2, 3, 9 and 10.

### 1.4.7 Pectin lyases

Pectin lyase (PGL) cleaves the α-(1,4)-glycosidic bond in highly esterified pectin. Unsaturated methyl oligogalacturonates are produced as degradation products after the β-transelimination of glycosidic linkages (Fig. 1.4C). PLs do not have an absolute requirement of $Ca^{2+}$ but they are stimulated by this and other cations. Up until now, all described pectin lyases are endo-PGLs (EC 4.2.2.10) (Sinitsyna *et al*., 2007). They have been classified in family 1 polysaccharide lyase (http://www.cazy.org/PL1.html).

### 1.4.8 Rhamnogalacturonan rhamnohydrolases

Rhamnogalacturonan rhamnohydrolase or α-L-rhamnosidase (EC 3.2.1.40) causes the hydrolytic cleavage of β-(1,4) linked rhamnogalacturonan chain at nonreducing end producing rhamnose (Mutter *et al*., 1994). These enzymes are classified into glycoside hydrolase (GH) families 28, 78 and 106

(http://www.cazy.org/GH28.html,http://www.cazy.org/GH78.html,http://www.cazy.org/GH106.html).

### 1.4.9 Rhamnogalcturonan galacturonohydrolases

Rhamnogalcturonan galacturonohydrolase (EC 3.2.1.-) catalyzes hydrolytic cleavage of the β-(1,4) linked rhamnogalacturonan chain at nonreducing end producing mono galacturonate (Mutter *et al*., 1998). It has been classified into glycoside hydrolase family 28 (http://www.cazy.org/GH28.html, http://www.cazy.org/GH28.html).

### 1.4.10 Rhamnogalacturonan hydrolases

Rhamnogalacturonan hydrolase randomly hydrolyses the rhamnogalacturonan chain producing oligogalacturonates (Mutter *et al*., 1998). They have been classified into glycoside hydrolase family 28 and 78 (http://www.cazy.org/GH78.html).

### 1.4.11 Rhamnogalacturonan lyases

Rhamnogalacturonan lyases (EC 4.2.2.-) catalyzes the random transelimination of the α-(1,4)-glycosidic linkage between rhamnose and galcturonate in the rhamnogalacturonan chain. The sugars produced are unsaturated oligogalacturonate at nonreducing end and a second oligogalacturonate containing a rhamnose as a reducing end residue (Mutter *et al*., 1996). These enzymes has been classified into polysaccharide lyase families 4 and 11 (http://www.cazy.org/PL4.html, http://www.cazy.org/PL11.html).

### 1.4.12 Rhamnogalacturonan acetylesterases

Rhamnogalacturonan acetylesterase (EC 3.1.1.-) causes the hydrolytic cleavage of acetyl groups from rhamnogalacturonan chain (Searle *et al*., 1992). It has

been classified into carbohydrate esterase family 12 (http://www.cazy.org/CE12.html).

### 1.4.13 Xylogalacturonan hydrolase

Xylogalacturonan hydrolase or Xylogalacturonase (EC 3.2.1.-) hydrolytically cleaves the α-(1,4)-glycosidic linkages between two galacturonate residues in xylose containing rhamnogalacturonan chain, hence producing xylose-galacturonate dimers (Vlugt-Bergmans *et al*., 2000). These enzymes are classified into glycoside hydrolase family 28 (http://www.cazy.org/GH28.html).

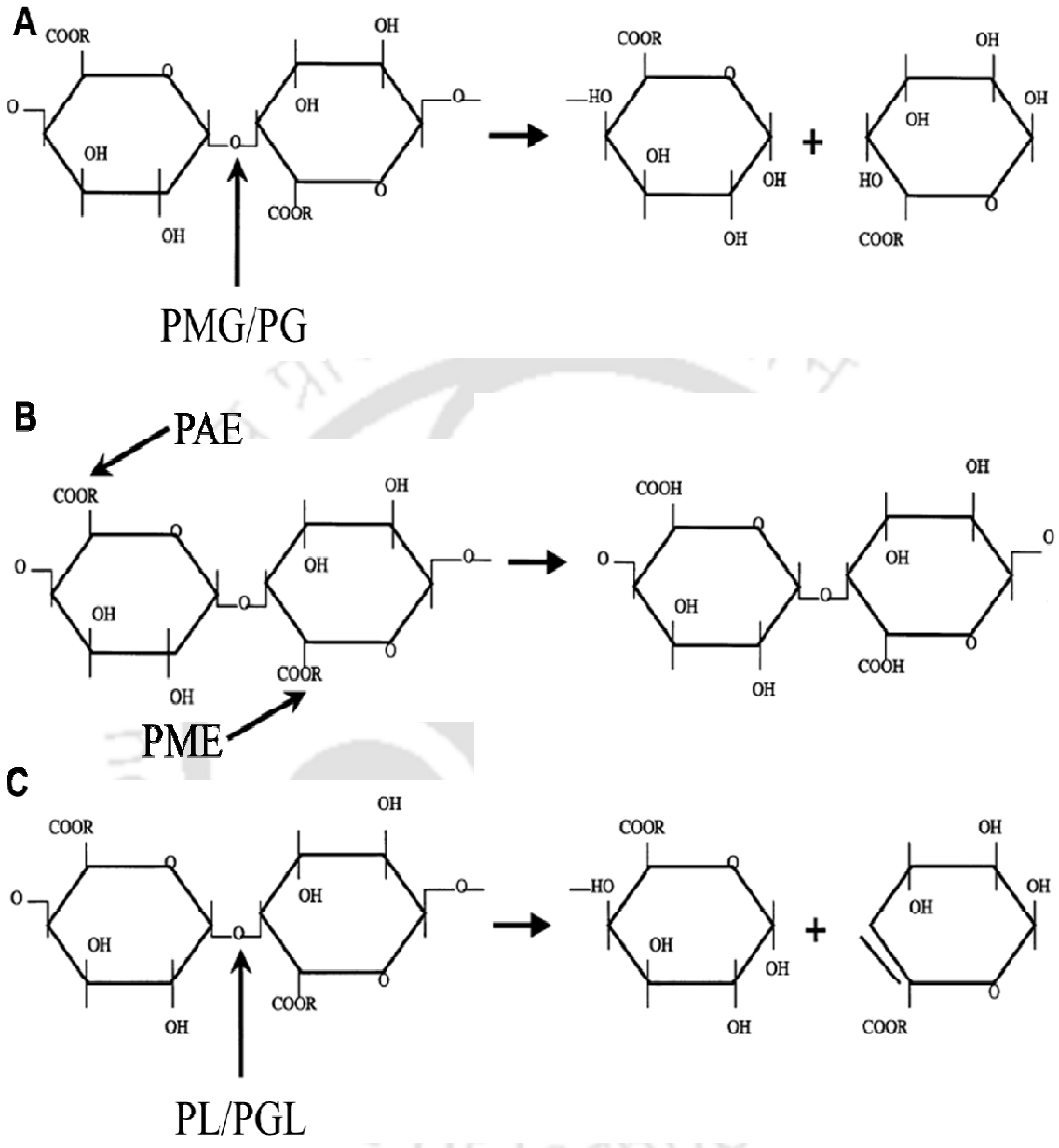


**Fig. 1.4** Various types of pectinases and their mode of action on pectic polysaccharides. (A) R=H for PG (Polygalacturonase) and R=$CH_3$ for PMG (Polymethylgalacturonase), (B) R=$COCH_3$ for PAE (Pectin acetyl esterase) and R=$CH_3$ PME (Pectin methyl esterase) (C) R=H for PL (Pectate lyase) and R=CH3 for PGL (Pectin lyase). Arrow indicates the attack site of the polysaccharide where the pectinase actually cleaves (adapted from Sathyanarayana *et al*., 2003).

## 1.5 Applications of microbial pectinases

Microbial pectinases have found widespread applications in various industrial processes such as food and textile industry, paper making, wastewater treatment, tea and coffee fermentation, citrus oil extraction, plant fiber degumming etc.

### 1.5.1 Food processing

Pectinases are used in extraction and clarification of fruit juice by degradation of pectin and thus decreasing the filtration time (Blanco *et al*., 1999). Pectinases when used in conjunction with enzymes like cellulase, arabinase and xylanase increase the volume of juice during extraction (Gailing *et al*., 2000). Softening of the peel in citrus fruits by pectinases during vaccum infusion process reduces labour and help in recovery of the intact pulp. Pectinases are widely used in pickle processing, preparation of vegetable puree and maceration of soybean for tofu making (Baker *et al*., 1996). During wine manufacturing process addition of pectinases to macerated fruits improves its colour and stability (Revilla *et al*., 2003). Tea fermentation is accelerated in presence of pectinase, whereas coffee fermentation is facilitated by removal of the mucilaginous coat on coffee beans (Carr, 1985).

### 1.5.2 Textile processing

Bioscouring of cotton fabric by pectinase to remove the non-cellulosic material facilitates proper dyeing of the fabric. This environmental friendly process is an alternative to chemical scouring by caustic soda (Hoondal *et al*., 2000).

### 1.5.3 Paper and Pulp making

Pectinases facilitate depolymerization of pectin during paper and pulp making which reduces the cationic demand and pitch deposit on whitewater (Reid *et al*., 2004).

### 1.5.4 Plant fiber degumming

Pectinase in association with xylanase facilitates the degumming of plant fibers which easily releases the intact fibers which is also an economic and eco-friendly process (Kapoor *et al*., 2001).

### 1.5.5 Wastewater treatment

Wastewater released from food processing industries contains pectin. Depolymerization of pectin by pectinases helps in removal of pectinaceous material and further accelerates the activated sludge process (Hoondal *et al*., 2000).

### 1.5.6 Citrus oil extraction

Oil extraction from citrus peels by the action of pectinases reduces the emulsifying properties of pectin, thus facilitating efficient extraction and collection of oil (Scott, 1975).

## 1.6 Cellulosome structure

The cellulosome is a macromolecular complex, whose components interact in a synergistic manner to catalyze the efficient degradation of cellulose (Bayer *et al*., 2007). The cellulosome complex (Fig. 1.5) comprises numerous types of polysaccharide degrading enzymes, which are assembled by virtue of a unique type of scaffolding known as scaffoldin (Bayer *et al*., 2004). The cellulosomal enzymes from *Clostridium thermocellum* range in molecular size from about 40 to 180 kDa (Fontes *et al*., 2010). The realization about the multienzyme complex (cellulosome) of C. *thermocellum* occurred gradually with discoveries of different catalytic and binding domains and dockerins, first in clostridial species and, subsequently in other bacteria and fungi (Doi *et al*., 1994; Belaich *et al*., 1997; Doi *et al*., 2004). Each of the cellulosomal subunit consists of a multiple set of modules, two classes of which

(dockerin domains on the enzymes and cohesin domains on scaffoldin) govern the incorporation of the enzymatic subunits into the cellulosome complex (Bayer *et al*., 1998a and 1998b). The cellulosomal enzymes are usually members of the glycoside hydrolase families of enzymes, which hydrolyze oligosaccharides and polysaccharides (Henrissat, 1991; Fontes *et al*., 2010).

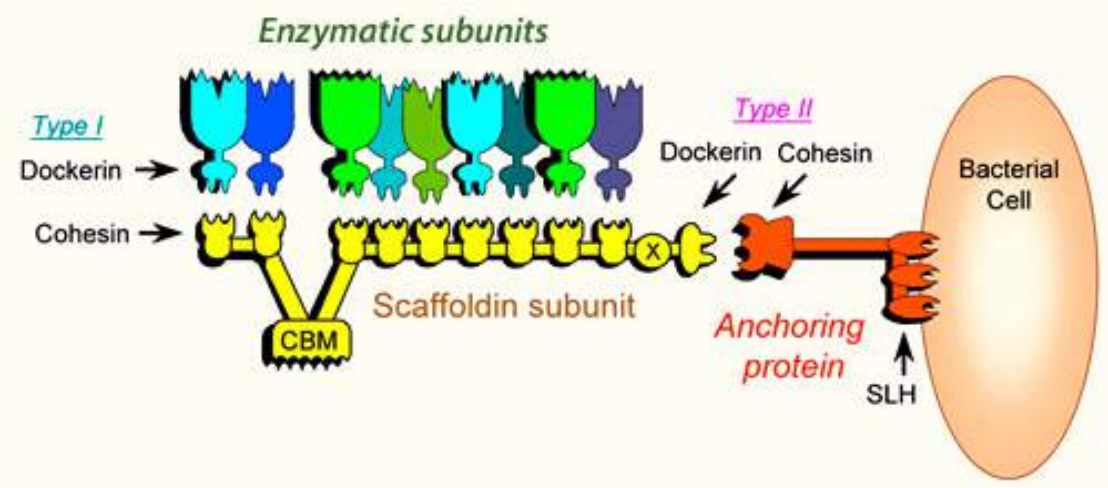


**Fig. 1.5** Structure of Cellulosome from *Clostridium thermocellum*, where multiple enzymatic subunits are attached to a Scaffoldin subunit connected by cohesion dockerin interaction. In the figure CBM is a carbohydrate binding module, X is a module of unknown function and SLH is S-layer homology module or sortase anchorage module (Credit: Cazypedia http://www.cazypedia.org/index.php/Cellulosome).

### 1.7 Carbohydrate binding modules

The carbohydrate binding modules (CBMs) were described earlier as cellulose-binding domains (CBDs) as at that time only cellulose binding domains were known. As more diverse carbohydrate binding ligands were identified for new CBMs, the term CBDs was changed to CBMs. The first identification of a cellulose binding domain was illustrated in 1986 by the proteolytic degradation of a cellulase produced from the fungus *Trichoderma reesei* (Saha, 2003). It was observed that one domain retained the cellulase activity and the other domain had cellulose-binding

capacity (Saha, 2003). Carbohydrate binding modules (CBMs) may be defined as independently folding modules, occurring alongside the carbohydrate-active enzymes. The CBMs are the non-catalytic modules known to help or bring the catalytic modules in close proximity to its substrates and also some CBMs are known to stabilize the structure of catalytic modules and increase its thermal stability (Boraston *et al*., 2004; Henshaw *et al*., 2006; Dvortsov *et al*., 2009). The CBMs may be found to contain up to 200 amino acids and can be found attached as single, double or triple domain in one protein, located at either C- or N-terminal within the parental protein (Shoseyov *et al*., 2006). Based upon amino acid sequence similarity CBMs have been grouped into 71 families till date (March 2015) according to the Carbohydrate Active enZYmes (CAZy) database (http://www.cazy.org/Carbohydrate-Binding-Modules.html).

### 1.7.1 Carbohydrate binding module clans based on fold of their 3-dimensional structures

Currently seven families of folds are reported for CBMs in the CAZy database (Cantarel *et al*. 2008). The seven different folds include the β-sandwich fold, the β-trefoil fold, the oligonucleotide-carbohydrate binding fold (OB), the knottin fold, the hevein fold, the hevein-like fold and a unique fold (http://www.cazy.org/CBM35.html). The most frequent is the jelly-roll β-sandwich fold which is common to plant legume lectins and animal galectins (Boraston *et al*., 2004). Depending on the structural refinement three types of CBM have been identified. Type A CBMs (Fig. 1.6A) can recognize the crystalline polysaccharides, while Type B CBMs (Fig. 1.6B) are classified according to their endo mode of binding internally to the glycan chain (Gilbert *et al*., 2013). Type C CBMs (Fig. 1.6C) are classified by their exo mode of binding either to the side chain or the terminal end

of polysaccharides (Gilbert *et al*., 2013). The family 35 CBM are mainly Type B CBMs (Valenzuela *et al*., 2012), displaying a diverse specificity towards various plant polysaccharides (Tunnicliffe *et al*., 2005). Ligand binding to CBMs creates a conformational change which therefore accommodates the substrate within the binding site (Tunnicliffe *et al*., 2005).

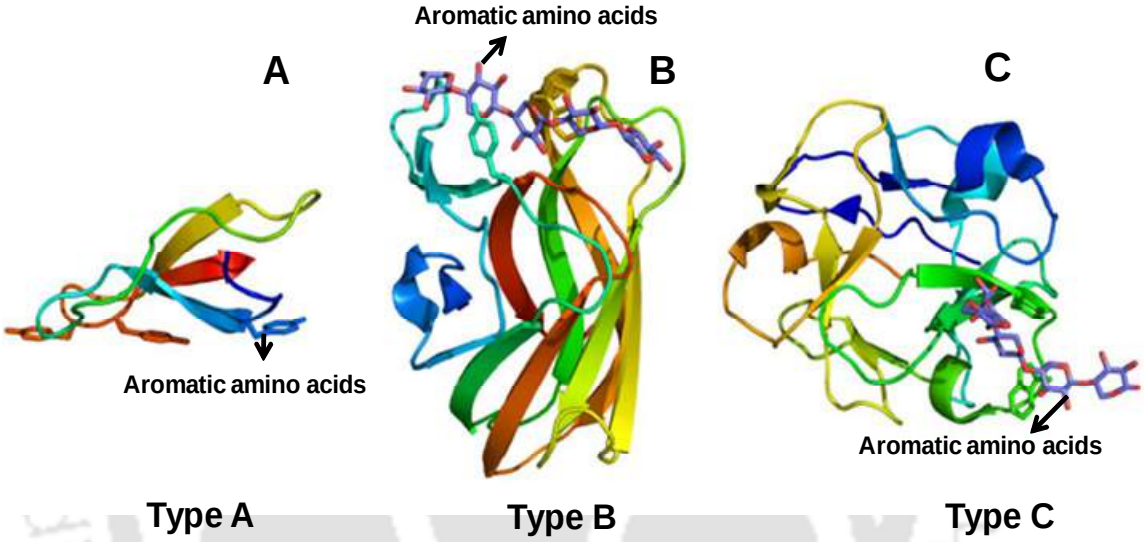


**Fig. 1.6** Three types of binding site architecture and ligand binding in CBMs. Aromatic amino acids involved in binding are shown in stick (A) Type A, cellulose binding *Hj*CBM1 from *Hypocrea jecorina* (PDB code 1CBH), (B) Type B, *Ct*CBM6 from *Clostridium thermocellum* in complex with xylopentaose (PDB code 1UXX), (C) Type C, *Sl*CBM13 from *Streptococcus lividans* in complex with xylopentaose (PDB code 1MC9).

### 1.7.2 Functions of carbohydrate binding modules

Carbohydrate binding modules (CBMs) increase the ability of associated catalytic modules to efficiently degrade the polysaccharide substrates (Fig. 1.7). This occurs through three different roles that CBMs play in polysaccharide breakdown, i) they localize the soluble enzyme to its target substrate (Shoham *et al*., 1999), ii) they are associated with a catalytic domain and contain multiple clefts to attach with substrate, thereby enhancing the catalytic activity (Henshaw *et al*., 2004; Hashimoto *et*

*al*., 2006) iii) The fusion proteins containing a CBM are capable of binding to a cellulose matrix. These fusion proteins can be used in a protein-purification system (Shpigel *et al*., 1998).

The proximity effect describes the binding of the CBM that brings the catalytic module in close proximity (or association) to the substrate and maintains it for a prolonged period. This effect is seen primarily on insoluble substrates such as cellulose and xylan (Tomme *et al*. 1988; Boraston *et al*. 2004).

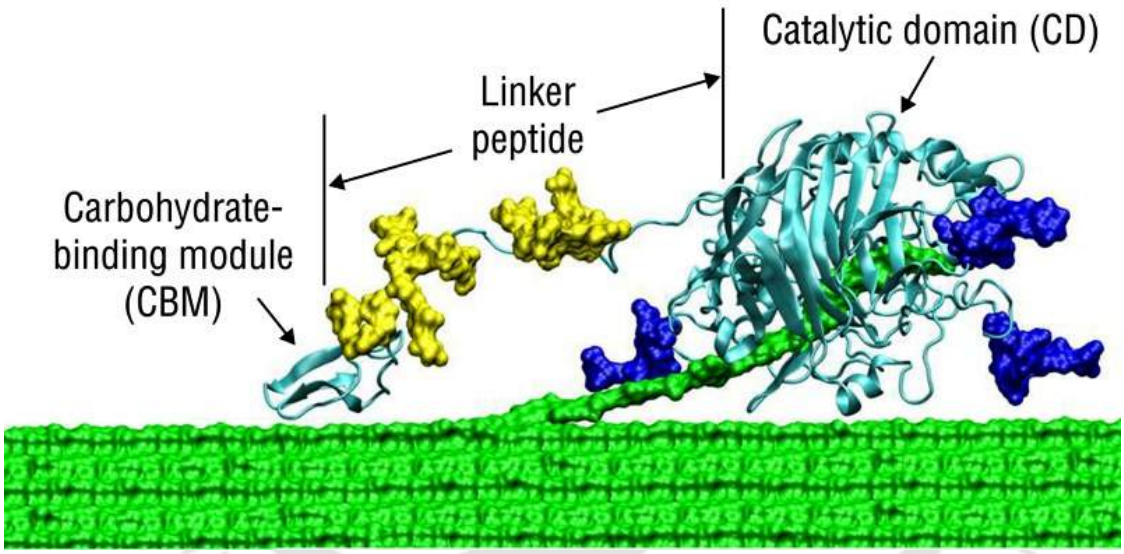


**Fig. 1.7** Diagrammatic representation of cellulosomal enzyme from *T. reesei* consisting of three modules; a carbohydrate-binding molecule (CBM), a linker peptide and a catalytic domain (CD). A single polysaccharide chain from the plant polysaccharide complex (green) while moving through the CD is cleaved into their corresponding sugars. CBM help the enzyme to remain attached on the surface of the polysaccharide complex, thus enhancing its activity. (Credit: NREL, http://www.nrel.gov/continuum/deliberate_science/biofuels.cfm).

### 1.7.3 Applications of carbohydrate binding modules

Three basic features have led to CBMs being perfect candidates for many applications: (i) CBMs are usually independently folding units and therefore can function autonomously in chimeric proteins; (ii) the attachment matrices are abundant

and inexpensive and have excellent chemical and physical properties; and (iii) the binding specificities can be controlled by modifying the structure using tools such as site directed mutagenesis and therefore the right solution can be adopted for a particular problem (Abbott *et al*., 2009).

### 1.7.3.1 Bioprocessing

Bio-specific affinity purification (affinity chromatography) has become one of the most rapidly developing divisions of immobilized affinity ligand technology. Many protein entities have been expressed when fused to CBMs, establishing CBMs as high-capacity purification tags for the isolation of biologically active target peptides at relatively low cost (Bolam *et al*., 2004; Shosheyov *et al*., 2006; Abbott *et al*., 2009). A high-level production of a cellulose binding domain ($CBD_{Cex}$) of cellulase (Cex) from *Cellulomonas fimi* expressed in *E. coli*, served as affinity tag in a novel secretion-affinity fusion system for purification of recombinant exoglucanase (Hasenwinkle *et al*., 1997). Also, a strategy for selecting and characterizing linker peptides for CBM9-tagged fusion proteins expressed in *Escherichia coli* for purification of recombinant proteins was developed (Kavoosi *et al*., 2007).

### 1.7.3.2 Cell immobilization using carbohydrate binding modules

Surface-exposed CBMs can be an efficient means of whole-cell immobilization. Whole-cell immobilization by cellulosic material was first demonstrated when an *E. coli* surface anchored CBM, derived from *Cellulomonas fimi*, was attached to cellulose (Saha, 2000). The cells bound tightly to cellulose at a wide range of pH and the extent of immobilization was dependent on the surface of exposed CBM (Saha, 2000; Numan *et al*., 2006).

#### 1.7.3.3 Bio-engineering of carbohydrate binding modules for different applications

The potential of carbohydrate binding modules (CBMs) for modifying the characteristics of several enzymes has been reported. The basic approach in CBM engineering was to replace or add a CBM in order to improve hydrolytic activity. Addition of a CBM derived from cellobiohydrolase II of *Trichoderma reesei* to *Trichoderma harzianum* chitinase resulted in increased hydrolytic activity of insoluble substrates (Shoseyov *et al*., 2006). The replacement of the CBM of endo-1,4-β-glucanase from *Bacillus subtilis* with the CBM of exoglucanase I (Texl) from *Trichoderma viride* conferred higher binding with enhanced hydrolytic activity on the microcrystalline cellulose (Shoseyov *et al*., 2006). In addition, the hybrid enzyme was more resistant to the tryptic digestion (Shoseyov *et al*., 2006).

### 1.8 The microorganism

*Clostridium thermocellum* is an anaerobic, thermophilic, cellulolytic and ethanologenic, Gram-positive bacterium capable of directly converting cellulose biomass into ethanol (Bayer *et al*., 2000a). The general cellular structure of *C. thermocellum* is similar to most rod-shaped bacteria as shown in Scanning Electron Microscopic images (Fig. 1.8A) (Lamed *et al*., 1987). However, the fibrous and protuberant structures on the cell surface are visible only when the cell is stained with cationized ferritin (CF) and viewed under Transmission electron microscope (Fig. 1.8B). The TEM image of *C. thermocellum* clearly showed fibrous and protuberant structures on the cell surface (Fig. 1.8B). The three major types of labeling: the monolayer (m) of CF particles which envelop the entire cell surface, the fibrous structures (f) which sometimes connect two adjacent cells, and the nodulous

protuberances (p) which appear in large numbers over the entire cell surface (Fig. 1.8B). In tangentially sectioned areas of the cell surface (t), there are indications that the protuberances may be interconnected secondarily by low-lying structures (l) (Fig. 1.8B).

The capability of *Clostridium thermocellum* cellulosomal enzymes to directly convert the cellulose biomass into a usable energy source *viz*. bio-fuel or ethanol makes it useful. However, there are some shortfalls in applying the organism to practical applications due to it having low ethanol yield, at least partially due to branched fermentation pathways that produce acetate, formate and lactate along with ethanol. Recent research has been directed to optimizing the ethanol-producing metabolic pathway in the hopes of creating more efficient biomass conversion (Zhang *et al*., 2005). Biotechnological research has shown that the cellulose degrading bacteria produces a large, complex cellulase system known as the cellulosome which consists about 20 catalytic proteins that are involved in the bacteria's adherence to cellulose, breakdown and regulation of cellulose degradation and the transport of sugar monomers (Bayer *et al*., 2000b; Fontes *et al*., 2010).

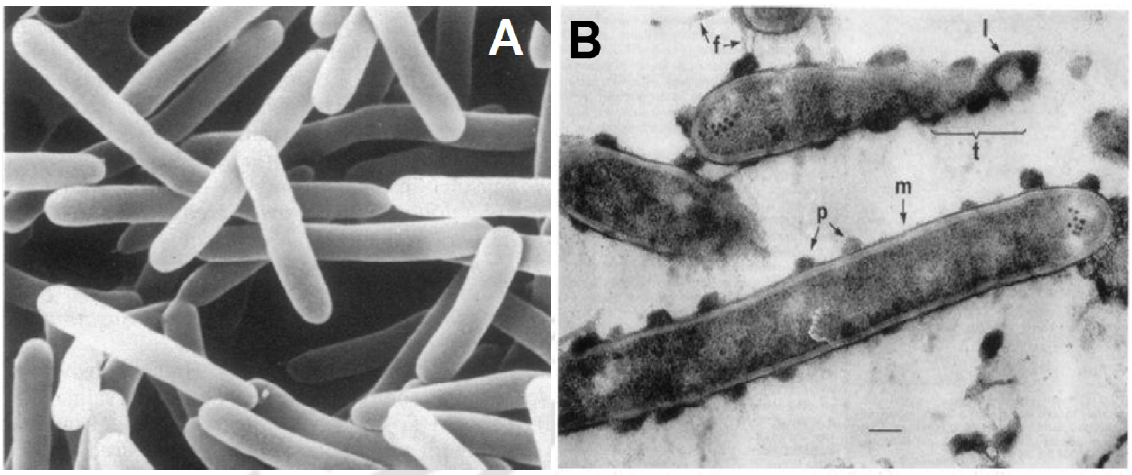


**Fig. 1.8** (A) Scanning electron microscope (SEM) images of *Clostridium thermocellum*, showing normal rod shaped cells (adapted from Lamed *et al*., 1987); (B) Transmission electron microscope (TEM) image of cationized ferritin (CF) stained *Clostridium thermocellum* grown on cellobiose. The three major types of labelling: the monolayer (m) of CF particles enveloping the entire cell surface, the fibrous structures (f) which connecting two adjacent cells and the nodulous protuberances (p) over the entire cell surface. In tangentially sectioned areas of the cell surface (t), there are indications that the protuberances may be interconnected secondarily by low-lying structures (I) (adapted from Bayer and Lamed, 1986).

## 1.9 Objectives of the present study

### 1.9.1 Why study family 1 PLs and associated family 35 CBMs from Clostridium thermocellum

The reason for selecting the family 1 polysaccharide lyase (PL1) and associated family 35 carbohydrate binding modules (CBM35) from *Clostridium thermocellum* are summarized:

1. *Clostridium thermocellum* genome contains a complex cellulosome that possesses a large number of enzymes, capable of degrading different plant polysaccharide.
2. *Clostridium thermocellum* cellulosomal enzyme complex is 50 times more efficient in degrading polysaccharides than any normal enzyme of same kind (Fontes *et al*., 2010).
3. Functional characterization of family 1 polysaccharide lyase (PL1) is important as all the enzymes belonging to family 1 PL may have the same β-elimination mechanism of catalysis but the degradation products will indicate its exo or endo mode during cleavage.
4. Family 1 PLs are generally pectate lyases which are essential for complete degradation of pectic acid and pectin, hence they has can be widely used in removal of pectic polysaccharide during various industrial processes.
5. It is important to determine the role of CBMs in substrate binding if they are altering the activity of the catalytic modules.

This study deals with the cloning, expression and purification of a modular enzyme pectate lyase (PL1B), its associated carbohydrate binding module (CBM35) and the full length module (PL1B-CBM35) from *Clostridium thermocellum* ATCC 27405. Biochemical and functional characterization of PL1B and PL1B-CBM35 will be carried out to determine their affinity towards different pectic polysaccharides and

understand their cleavage pattern. Application of immobilized PL1B on bioscouring of cotton fabric and effect of pectic oligosaccharides on colon cancer cells will be studied.

### 1.9.2 Specific objectives

1. Cloning and expression of family 1 polysaccharide lyase full length module (PL1B-CBM35) and its truncated derivatives (PL1B and CBM35) from *Clostridium thermocellum* genomic DNA
2. Biochemical and functional characterization of full length (PL1B-CBM35) and catalytic module (PL1B), substrate binding analysis of CBM35
3. Homology modeling and ligand docking study of catalytic (PL1B) and binding (CBM35) modules.
4. Immobilization of PL1B on magnetic nanoparticles and its application in bioscouring of cotton fabric
5. Isolation of natural pectin from citrus peels, production, characterization and purification of pectic oligosaccharides produced by enzymatic cleavage of PL1B, and their effect on colon cancer cells

## 1.10 References

Abbott, D.W., Ficko-Blean, E., van Bueren, A.L., Rogowski, A., Cartmell, A., Coutinho, P.M., Henrissat, B., Gilbert, H.J., Boraston, A.B. (2009) Analysis of the structural and functional diversity of plant cell wall specific family 6 carbohydrate binding modules. Biochemistry, 48: 10395–10404.

Albersheim, P., Darvill, A.G., O'Neill, M.A., Schols, H.A., Voragen, A.G.J. (1996) An hypothesis: the same six polysaccharides are components of the primary cell walls of all higher plants. Proceedings of International Symposium on Progress in Biotechnology, Pectins and pectinases, Vol. 14 (eds. Visser, J., Voragen, A.G.J.), pp. 47–53. Elsevier Sciences, Amsterdam, NL.

Alkorta, I., Gabirsu, C., Lhama, M.J., Serra, J.L. (1998) Industrial applications of pectic enzymes: a review. Process Biochemistry, 33: 21–28.

Baker, R.A., Wicker, L. (1996) Current and potential application of enzyme infusion in the food industry. Trends in Food Science and Technology, 7: 279–284.

Basu, S., Roy, A., Ghosh, A., Bera, A., Chattopadhyay, D., Chakrabarti, K. (2011) $Arg^{235}$ is an essential catalytic residue of *Bacillus pumilus* DKS1 pectate lyase to degum ramie fibre. Biodegradation, 22(1):153–161.

Bauer, D.W., Collmer, A. (1997) Molecular cloning, characterization, and mutagenesis of a pel gene from Pseudomonas syringae pv. lachyrmans encoding a member of the Erwinia chrysanthemi pelADE family of pectate lyases. Molecular Plant Microbe and Interaction 10(3): 369–379.

Bayer, E.A., Morag, E., Lamed, R., Yaron, S., Shoham, Y. (1998b) Cellulosome structure: Four-pronged attack using biochemistry, molecular biology, crystallography and bioinformatics, In Carbohydrases from *Trichoderma*

*reesei* and Other Microorganisms, Claeyssens, M., Nerinckx, W., Piens, K. (Eds.), The Royal Society of Chemistry, London, 39–67.

Bayer, E.A., Belaich, J.P., Shoham, Y., Lamed, R. (2004) The cellulosomes: multi-enzyme machines for degradation of plant cell wall polysaccharides. Annual Review in Microbiology, 58: 521–554.

Bayer, E.A., Chanzy, H., Lamed, R., Shoham, Y. (1998) Cellulose, cellulases and cellulosomes. Current Opinion Structural Biology, 8: 548–557.

Bayer, E.A., Lamed, R. Himmel, M.E. (2007) The potential of cellulases and cellulosomes for cellulosic waste management. Current Opinion in Biotechnology, 18: 237–245.

Bayer, E.A., Shoham, Y., Lamed, R. (2000a) Cellulose-decomposing prokaryotes and their enzyme systems. (3rd ed.) Dworkin, M., Falkow, S., Rosenberg, E., Schleifer, K.H., and Stackebrandt, E. (ed.), In The Prokaryotes: An Evolving Electronic Resource for the Microbiological Community, 2: 578–617.

Bayer, E.A., Shoham, Y., Lamed R. (2000b) The cellulosome-an exocellular organelle for degrading plant cell wall polysaccharides. In Doyle, R.J. (ed.). Glycomicrobiology. Kluwer Academic/Plenum Publishers, New York. 387–439.

Belaich, J.P., Tardif, C., Belaich, A., Gaudin, C. (1997) The cellulolytic system of *Clostridium cellulolyticum*, Journal of Biotechnology, 57: 3–14.

Berg, J.M. (2007) In Biochemistry, (6th ed), pp. 310–323. New York: W.H. Freeman.

Bhamidi, S., Scherman, M. S., Rithner, C. D., Prenni, J. E., Chatterjee, D., Khoo, K.-H., McNeil, M. R. (2008) The identification and location of succinyl residues and the characterization of the interior arabinan region allow for a model of the

complete primary structure of *Mycobacterium tuberculosis* Mycolyl Arabinogalactan. Journal of Biological Chemistry, 283(19): 12992–13000.

Blanco, P., Sieiro, C., Villa, T.G. (1999) Production of pectic enzymes in yeasts. FEMS Microbiology Letters, 175: 1–9.

Boerjan, W., Ralph, J., Baucher, M. (2003) Lignin biosynthesis. Annual Review of Plant Biology, 54: 519–546.

Bolam, D.N., Xie, H., Pell, G., Hogg, D., Galbraith, G., Henrissat, B., Gilbert, H.J. (2004) X4 modules represent a new family of carbohydrate-binding modules that display novel properties. Journal of Biological Chemistry, 279: 22953–22963.

Boraston, A.B., Bolam, D.N., Gilbert, H.J., Davies G.J. (2004) Carbohydrate-binding modules: fine-tuning polysaccharide recognition. Biochemical Journal 382: 769–781.

Brennan, M., Harris, P.J. (2011) Distribution of fucosylated xyloglucans among the walls of different cell types in monocotyledons determined by immunofluorescence microscopy. Molecular Plant, 4: 144–56.

Bruhlmann, F., Keen, N.T. (1997) Cloning, sequence and expression of the pel gene from an *Amycolata sp*. Gene, 202(1–2): 45–51.

Campbell, J.A., Davies, G.J., Bulone, V., Henrissat, B. (1997) A classification of nucleotide-diphospho-sugar glycosyltransferases based on amino acid sequence similarities. Biochemical Journal, 326: 929–939.

Cantarel, B.L., Coutinho, P.M., Rancurel, C., Bernard, T., Lombard, V., Henrissat, B. (2009) The Carbohydrate-Active EnZymes database (CAZy): an expert resource for Glycogenomics. Nucleic Acids Res. 37: 233–238.

Cantarel, B.L., Coutinho, P.M., Rancurel, C., Bernard, T., Lombard, V., Henrissat, B. (2009) The Carbohydrate-Active EnZymes database (CAZy): an expert resource for Glycogenomics. Nucleic Acids Research, 37: 233–238.

Carr, J.G. (1985) Tea, coffee and cocoa. In: Wood BJB, editor. Microbiology of fermented foods, vol. 2. London: Elsevier Science Ltd., p. 133–154.

Cosgrove, D.J. (1999) Enzymes and other agents that enhance cell wall extensibility. Annual Review of Plant Physiology and Plant Molecular Biology, 50: 391–417.

Coutinho, P.M., Henrissat, B. (1999) Carbohydrate-active enzymes: an integrated database approach. In "Recent Advances in Carbohydrate Bioengineering", Gilbert HJ, Davies G, Henrissat B, Svensson B. Eds. Cambridge: The Royal Society of Chemistry, 3–12.

Coutinho, P.M., Deleury, E., Davies, G.J., Henrissat, B. (2008) An evolving hierarchical family classification for glycosyltransferases. Journal of Molecular Biology, 328: 307–317.

Cui, S.W., Wang, Q. (2009) Cell wall polysaccharides in cereals: chemical structures and functional properties. Structural Chemistry, 20: 291–297.

Demain, A.L., Newcomb, M., Wu, J.H. (2005) Cellulose, clostridia and ethanol. Microbiology Molecular Biology Review, 69: 124–154.

Doi, R.H., Kosugi, A. (2004) Cellulosome: plant-cell-wall degrading enzyme complexes. Nature Review in Microbiology, 2: 541–551.

Doi, R.H., Goldstein, M., Hashida, S., Park, J.S., Takagi, M. (1994) The *Clostridium cellulovorans* cellulosome. Critical Review in Microbiology, 20: 87–93.

Dvortsov, I.A., Lunina, N.A., Chekanovskaya, L.A., Schwarz, W.H., Zverlov, V.V., Velikodvorskaya, G.A. (2009) Carbohydrate-binding properties of a separately folding protein module from beta-1,3-glucanase Lic16A of *Clostridium thermocellum*. Microbiology, 155: 2442–2449.

Fontes, C.M.G.A., Gilbert, H.J. (2010) Cellulosomes: highly efficient nanomachines designed to deconstruct plant cell wall complex carbohydrates. Annual Review of Biochemistry, 79: 655–681.

Fry, S.C. (1989) The structure and functions of xyloglucan. Journal of Experimental Botany, 40: 1–11.

Gailing, M.F., Guibert, A., Combes, D. (2000) Fractional factorial designs applied to enzymatic sugar beet pulps pressing improvement. Bioprocess Engineering, 22: 69–74.

Garron, M.L., Cygler, M. (2010) Structural and mechanistic classification of uronic acid-containing polysaccharide lyases. Glycobiology, 20(12): 1547–1573.

Gilbert, H.J., Knox, J.P., Boraston, A.B. (2013) Advances in understanding the molecular basis of plant cell wall polysaccharide recognition by carbohydrate binding modules. Current Opinion in Structural Biology, 23: 669–677.

Gorelik E., Galili U., Raz A. (2001) On the role of cell surface carbohydrates and their binding proteins (lectins) in tumor metastasis. Cancer Metastasis Review, 20: 245–77.

Hasenwinkle, D., Jervis, E., Kops, O., Liu, C., Lesnicki, G., Haynes, C.A., Kilburn, D.G. (1997) Very high-level production and export in *Escherichia coli* of a cellulose binding domain for use in a generic secretion-affinity fusion system. Biotechnology Bioengineering, 55: 854-863.

Hashimoto, K., Yoshida, M., Hasumi, K. (2011) Isolation and characterization of CcAbf62A, a GH62 α-L-arabinofuranosidase, from the basidiomycete *Coprinopsis cinerea*. Bioscience Biotechnology and Biochemistry, 75: 342–345.

Henrissat, B. (1991) A classification of glycosyl hydrolases based on amino-acid sequence similarities. Biochemical Journal, 280: 309–316.

Henshaw, J., Horne-Bitschy A., van Bueren, A.L., Money, V.A., Bolam, D.N., Czjzek, M., Ekborg, N.A., Weiner, R.M., Hutcheson, S.W., Davies, G.J., Boraston, A.B., Gilbert, H.J. (2006) Family 6 carbohydrate binding modules in β-agarases display exquisite selectivity for the non-reducing termini of agarose chains. Journal of Biological Chemistry 281: 17099–17107.

Henshaw, J.L., Bolam, D.N., Pires, V.M., Czjzek, M., Henrissat, B., Ferreira, L.M., Fontes, C.M.G.A., Gilbert, H.J. (2004) The family 6 carbohydrate binding module CmCBM6-2 contains two ligand-binding sites with distinct specificities. Journal Biological Chemistry, 279: 21552–21559.

Hoondal, G.S., Tiwari, R.P., Tiwari, R., Dahiya, N., Beg, Q.K. (2000) Microbial alkaline pectinases and their applications: a review. Applied Microbiology and Biotechnology 59: 409–418.

Inngjerdingen, K.T., Patel, T.R., Chen, X., Kenne, L., Allen, S., Morris, G.A., Harding, S.E., Matsumoto, T., Diallo, D., Yamada, H., Michaelsen, T.E., Inngjerdingen. M., Paulsen, B.S. (2007) Immunological and structural properties of a pectic polymer from *Glinus oppositifolius*. Glycobiology, 17: 1299–1310.

Ishii, T. (1995) Pectic polysaccharides from bamboo shoot cell walls. Mokuzai Gakkaishi, 41: 669–676.

Ishii, T. (1999) O-acetylated oligosaccharides from pectins of potato tuber cell walls. Plant Physiology, 113: 1265–1272.

Jackson, C.L., Dreaden, T.M., Theobald, L.K., Tran, N.M., Beal. T.L., Eid, M., Gao M.Y., Shirley, R.B., Stoffel, M.T., Kumar, M.V., Mohnen, D. (2007) Pectin induces apoptosis in human prostate cancer cells: correlation of apoptotic function with pectin structure. Glycobiology, 17: 805–819.

Jayani, R.S., Saxena, S., Gupta, R. (2005) Microbial pectinolytic enzymes: A review. Process Biochemistry, 40: 2931–44.

Kapoor, M., Beg, Q.K., Bhushan, B., Singh, K., Dadich, K.S., Hoondal, G.S. (2001) Application of alkaline and thermostable polygalacturonase from Bacillus sp. MG-cp-2 in degumming of ramie (*Boehmeria nivea*) and sunn hemp (*Crotolaria juncia*) bast fibers. Process Biochemistry, 36: 803–807.

Kashyap, D.R., Vohra, P.K., Tewari, R. (2001) Application of pectinases in the commercial sector: a review. Bioresource Technology, 77: 215–27.

Kavoosi, M., Creagh, A.L., Kilburn, D.G., Haynes, C.A. (2007) Strategy for selecting and characterizing linker peptides for CBM9-tagged fusion proteins expressed in *Escherichia coli*. Biotechnology Bioengineering, 98: 599–610.

Keen, N.T., Tamaki, S. (1986) Structure of two pectate lyase genes from *Erwinia chrysanthemi* EC16 and their high-level expression in *Escherichia coli*. Journal of Bacteriology, 168(2): 595–606.

Kluskens, L.D., van Alebeek, G.J., Voragen, A.G., de Vos, W.M., van der Oost, J. (2003) Molecular and biochemical characterization of the thermoactive family

1 pectate lyase from the hyperthermophilic bacterium *Thermotoga maritima*. Biochemical Journal, 370(2): 651–659.

Kobayashi, T., Hatada, Y., Suzumatsu, A., Saeki, K., Hakamada, Y., Ito, S. (2000) Highly alkaline pectate lyase Pel-4A from alkaliphilic *Bacillus sp.* strain P-4-N: its catalytic properties and deduced amino acid sequence. Extremophiles, 4(6): 377–383.

Lairson, L.L., Henrissat, B., Davies, G.J., Withers, S.G. (2008) Glycosyltransferases: structures, functions, and mechanisms. Annual Review of Biochemistry, 77: 521–555.

Lamed, R., Naimark, J., Morgenstern, E., Bayer, E.A. (1987) Specialized cell surface structures in cellulolytic bacteria. Journal of Bacteriology, 169: 3792–3800.

Li, G., Rao, L., Xue, Y., Zhou, C., Zhang, Y., Ma, Y. (2010) Cloning, expression, and characterization of a highly active alkaline pectate lyase from alkaliphilic *Bacillus sp*. N16-5. Journal of Microbiology and Biotechnology, 20(4): 670–677.

Li, X.L., Spániková, S., de Vries, R.P., Biely, P. (2007) Identification of genes encoding microbial glucuronoyl esterases. FEBS Letters, 581: 4029–4035.

Liao, C.H., Gaffney, T.D., Bradley, S.P., Wong, L.C. (1996) Cloning of a pectate lyase gene from *Xanthomonas campestris pv*. malvacearum and comparison of its sequence relationship with pel genes of soft-rot *Erwinia* and *Pseudomonas*. Molecular Plant Microbe and Interaction, 9(1): 14–21.

Libermans, M., Mutaftschiev, S., Jauneau, A., Vian, B., Catesson, A., Goldberg, R. (1999) Mung bean hypocotyl homogalacturonan: localization, organization and origin. Annals of Botany, London 84: 225–233.

Lombard, V., Bernard, T., Rancurel, C., Brumer, H., Coutinho, P.M., Henrissat, B. (2010) A hierarchical classification of polysaccharide lyases for glycogenomics. Biochemical Journal, 432(3): 437–444.

Matsunaga, T., Ishii, T., Matsumoto, S., Higuchi, M., Darvill, A., Albersheim, P., O'Neill, M.A. (2004) Occurrence of the primary cell wall polysaccharide rhamnogalacturonan II in pteridophytes, lycophytes, and bryophytes. Implication for the evolution of vascular plants. Plant Physiology, 134: 339–351.

Mody, R., Joshi, S., Chaney, W. (1995) Use of lectins as diagnostic and therapeutic tools for cancer. Journal of Pharmacology and Toxicology Methods, 3:1–10.

Mohnen, D., Bar-Peled, M., Somerville, C. (2008) Biosynthesis of Plant Cell Walls. Biomass Recalcitrance, Chapter 5 (eds. Himmel, M.), pp. 94–187. Blackwell Publishing, Oxford.

Montanier, C., Money, V.A., Pires, V.M.R., Flint, J.E., Pinheiro, B.A., Goyal, A., Prates, J.A.M., Izumi, A., Stalbrand, H., Morland, C., Cartmell, A., Kolenova, K., Topakas, E., Dodson, E.J., Bolam, D.N., Davies, G.J., Fontes, C.M.G.A., Gilbert, H.J. (2009) The active site of a carbohydrate esterase displays divergent catalytic and noncatalytic binding functions. PLoS Biology, 31: e71.

Mutter, M., Beldman, G., Schols, H.A., Voragen, A.G.J. (1994) Rhamnogalacturonan α-L-Rhamnopyranohydrolase: a novel enzyme specific for the terminal nonreducing rhamnosyl unit in rhamnogalacturonan regions of pectin. Plant Physiology, 106: 241–50.

Mutter, M., Renard, C.M.G.C., Beldman, G., Schols, H.A., Voragen, A.G.J. (1998) Mode of action of RG-hydrolase and RG-lyase toward rhamnogalacturonan oligomers: characterization of degradation products using RG-rhamnohydrolase and RG-galacturonohydrolase. Carbohydrate Research, 311: 155–64.

Numan, M.T., Bhosle, N.B. (2006) Alpha-L-arabinofuranosidases: the potential applications in biotechnology. Journal of Industrial Microbiology and Biotechnology 33: 247–260.

O'Neill, M., Albersheim, P., Darvill, A. (1990) The pectic polysaccharides of primary cell walls. In: Methods in Plant Biochemistry, Vol. 2. (eds. Dey D.M.), pp: 415–441. Academic Press, London.

O'Neill, M.A., Ishii, T., Albersheim, P., Darvill, A.G. (2004) Rhamnogalacturonan II: structure and function of a borate cross-linked cell wall pectic polysaccharide. Annual Review of Plant Biology, 55: 109–139.

Ouattara, H.G., Reverchon, S., Niamke, S.L., Nasser, W. (2010) Biochemical properties of pectate lyases produced by three different *Bacillus* strains isolated from fermenting cocoa beans and characterization of their cloned genes. Applied and Environmental Microbiology, 76(15): 5214–5220.

Ralph, J., Lapierre, C., Marita, J.M., Kim, H., Lu, F., Hatfield, R.D., Ralph, S., Chapple, C., Franke, R., Hemm, M.R., Van Doorsselaere, J., Sederoff, R.R., O'Malley, D.M., Scott, J.T., MacKay, J.J., Yahiaoui, N., Boudet, A., Pean, M., Pilate, G., Jouanin, L., Boerjan, W. (2004) Elucidation of new structures in lignins of CAD- and COMT-deficient plants by NMR. Phytochemistry, 57: 993–1003.

Reid, I., Richard, M. (2004) Purified pectinase lowers cationic demand in peroxide-bleached mechanical pulp. Enzyme Microbial Technology 34: 499–504.

Revilla, I., Ganzalez-san jose, M.L. (2003) Addition of pectolytic enzymes: an enological practice which improves the chromaticity and stability of red wines. International Journal of Food Science and Technology, 38: 29–36.

Ridley, B.L., O'Neill, M.A., Mohnen, D. (2001) Pectins: structure, biosynthesis, and oligogalacturonide-related signaling. Phytochemistry, 57: 929–967.

Rombouts, F.M., Pilnik, W. (1980) Pectic enzymes. In: Rose AH, Ed. Microbial Enzymes and Bioconversions. Academic Press London, 5: 227–72.

Saha, B.C. (2003) Hemicellulose bioconversion. Journal of Indian Microbiology and Biotechnology, 30: 279–291.

Sakai, T., Sakamoto, T., Hallaert, J., Vandamme, E. (1993) Pectin, pectinase and protopectinase: production, properties and applications. Advances in Applied Microbiology, 39: 213–294.

Sathyanarayana, N.G., Panda, T. (2003) Purification and biochemical properties of microbial pectinases – a review. Process Biochemistry, 38(7): 987–996.

Schadel, C., Blochl, A., Richter, A., Hoch, G. (2009) Short-term dynamics of nonstructural carbohydrates and hemicelluloses in young branches of temperate forest trees during bud break. Tree Physiology, 29: 901–911.

Scheller, H.V., Ulvskov, P. (2010) Hemicellulose. Annual Review Plant Biology, 61: 263–289.

Schols, H.A., and Voragen, A.G.J. (1996) Complex pectins: Structure elucidation using enzymes. In: J. Visser and A.J. Voragen (editors) Pectins and Pectinases, Elsevier Science, Amsterdam. pp 3–19.

Scott, D. (1975) Enzymes, industrial. In: Grayson M, Ekarth D, Othmer K, editors. Encyclopedia of chemical technology. New York: Wiley, p. 173–224.

Searle-Van Leeuwen, M.J.F, Van Den Broek, L.A.M, Schols H.A., Beldman, G., Voragen, A.G.J. (1992) Rhamnogalacturonan acetylesterase: a novel enzyme from *Aspergillus aculeatus*, specific for the deacetylation of hairy (ramified) regions of pectins. Applied Microbiology Biotechnology, 38: 347-9.

Sharon N., Lis, H. (1989) Lectins as cell recognition molecules. Science, 246: 227–234.

Sharon N., Lis, H. (1993) Carbohydrates in cell recognition. Scientific American, 268: 82–89.

Shevchik, V.E., Hugouvieux-Cotte-Pattat, N. (1997) Identification of a bacterial pectin acetyl esterase in *Erwinia chysanthemi* 3937. Molecular Microbiology, 24(6): 1285–1301.

Shoham, Y., Lamed, R., Bayer, E.A. (1999) The cellulosome concept as an efficient microbial strategy for the degradation of insoluble polysaccharides. Trends in Microbiology, 7: 275–281.

Shoseyov, O., Shani, Z., Levy, I. (2006) Carbohydrate binding modules: biochemical properties and novel applications. Microbiology and Molecular Biology Review 70: 283–295.

Shpigel, E., Elias, D., Cohen, I. R., Shoseyov, O. (1998) Production and purification of a recombinant human hsp60 epitope using the cellulose-binding domain in Escherichia coli. Protein Expression and Purification, 14: 185–191.

Sinitsyna, O.A., Fedorova, E.A., Semenova, M.V., Gusakov, A.V., Sokolova, L.M., Bubnova, T.M., Okunev, O.N., Chulkin, A.M., Vavilova, E.A., Vinetsky, Y.P.,

Sinitsyn, A.P. (2007) Isolation and characterization of extracellular pectin lyase from *Penicillium canescens*. Biochemistry (Moscow), 72(5): 565–71.

Sinnott, M.L. (1990) Catalytic mechanisms of enzymatic glycosyl transfer. Chemical Review, 90, 1171–1202.

Somerville, C., Bauer, S., Brininstool, G., Facette, M., Hamann, T., Milne, J.,Osborne, E., Paredez, A., Persson, S., Raab, T., Vorwerk, S., Youngs, H. (2004) Toward a systems approach to understanding plant-cell walls. Science, 306(5705): 2206–22011.

Sukhumsiirchart, W., Kawanishi, S., Deesukon, W., Chansiri, K., Kawasaki, H., Sakamoto, T. (2009) Purification, characterization, and overexpression of thermophilic pectate lyase of *Bacillus sp*. RN1 isolated from a hot spring in Thailand. Bioscience, biotechnology and biochemistry, 73(2): 268–273.

Sutherland, I. W. (1995) Polysaccharide lyases. FEMS Microbiology Review, 16: 323–347.

Takao, M., Nakaniwa, T., Yoshikawa, K., Terashita, T., Sakai, T. (2001) Molecular cloning, DNA sequence, and expression of the gene encoding for thermostable pectate lyase of thermophilic *Bacillus sp*. TS 47. Biosciences Biotechnology Biochemistry 65(2): 322–329.

Tamaki, S.J., Gold, S., Robeson, M., Manulis, S., Keen, N.T. (1988) Structure and organization of the pel genes from *Erwinia chrysanthemi* EC16. Journal of Bacteriology 170(8): 3468–3478.

Tomme, P., Boraston, A., McLean, B., Kormos, J., Creagh, A.L., Sturch, K., Gilkes, N.R., Haynes, C.A., Warren, R.A., Kilburn, D.G. (1998) Characterization and

affinity applications of cellulose-binding domains. Journal of Chromatography B, 715: 283–96.

Truong, L.V., Tuyen, H., Helmke, E., Binh, L.T., Schweder, T. (2001) Cloning of two pectate lyase genes from the marine Antarctic bacterium *Pseudoalteromonas haloplanktis* strain ANT/505 and characterization of the enzymes. Extremophiles, 5(1): 35–44.

Tunnicliffe, R.B., Bolam, D.N., Pell, G., Gilbert, H.J., Williamson, M.P. (2005) Structure of a mannan-specific family 35 carbohydrate binding module: evidence for significant conformational changes upon ligand binding. Journal of Molecular Biology, 347: 287–296.

Urbanowicz, B.R., Peña, M.J., Ratnaparkhe, S., Avci, U., Backe, J., Steet, H.F., Foston, M., Li, H., O'Neill, M.A., Ragauskas, A.J., Darvill, A.G., Wyman, C., Gilbert, H.J., York, W.S. (2012) 4-O-methylation of glucuronic acid in Arabidopsis glucuronoxylan is catalyzed by a domain of unknown function family 579 protein. Proceedings of National Academy Science, USA, 109: 14253–14258.

Valenzuela, S.V., Diaz, P., Pastor, F.I. (2012) Modular glucuronoxylan specific xylanase with a family CBM35 carbohydrate binding module. Applied Environmental Microbiology, 78: 3923–3931.

van Gijsegem, F. (1989) Relationship between the pel genes of the pel ADE cluster in *Erwinia chrysanthemi* strain B374. Molecular Microbiology, 3(10): 1415–1424.

Vlugt-Bergmans, C.J.B., Meeuwsen, P.J.A, Voragen, A.G.J, Van Ooyen, A.J.J. (2000) Endo-xylogalacturonan hydrolase, a novel pectinolytic enzyme. Applied Environmental Microbiology, 66(1): 36–41.

Wade Jr, L.G. (1999) Organic chemistry. Prentice-Hall Inc.

Willats, W.G.T, McCartney, L., Mackie, W., Knox, J.P. (2001) Pectin: cell biology and prospects for functional analysis. Plant Molecular Biology, 47: 9–27.

Yip, V. L., Withers, S. G. (2006) Breakdown of oligosaccharides by the process of elimination. Current Opinion in Chemical Biology, 10: 147–155.

Yip, V.L.Y., Varrot, A., Davies, G.J., Rajan, S.S., Yang, X.J., Thompson, J., Anderson, W.F., Withers, S.G. (2004) An unusual mechanism of glycoside hydrolysis involving redox and elimination steps by a family 4 β-glycosidase from *Thermotoga maritima*. Journal of American Chemical Society, 126: 8354–8355.

Yuan, P., Meng, K., Wang, Y., Luo, H., Shi, P., Huang, H., Tu, T., Yang, P., Yao, B. (2012) A low-temperature-active alkaline pectate lyase from *Xanthomonas campestris* ACCC 10048 with high activity over a wide pH range. Applied Biochemistry and Biotechnology 168(6): 1489–1500.

Zhan, D., Janssen, P., Mort, A.J. (1998) Scarcity or complete lack of single rhamnose residues interspersed within the homogalacturonan regions of citrus pectin. Carbohydrate Research, 308: 373–380.

Zhang, Y.H., Lynd, L.R. (2005) Cellulose utilization by *Clostridium thermocellum*: bioenergetics and hydrolysis product assimilation. Proceedings of National Academy of Science (USA), 102: 7321–7325.

# Chapter 2

## Cloning, expression and purification of family 1 polysaccharide lyase, full length module (PL1B-CBM35), truncated catalytic module (PL1B) and carbohydrate binding module (CBM35) and the from *Clostridium thermocellum* ATCC 27405

### 2.1 Introduction

Plant cell wall lysis carried out by saprophytic and phytopathogenic microbes is essential for the recycling of carbon stored in plant biomass and of intrinsic biotechnological importance. Plant cell walls are composed of a complex network of polysaccharides which are primarily cellulose, hemicelluloses and pectic substances (Carpita *et al*., 1993). Pectins are a highly heterogeneous group of polymers mainly comprising of high quantity of galacturonic acid. Pectins are mainly found in primary cell wall and middle lamella and give shape and firmness to the cell. This recalcitrant carbohydrate is readily soluble in water than cellulose and hemicelluloses, making the cell prone to microbial degradation (Ochiai *et al*., 2010). Polysaccharide lyases (PL) (EC 4.2.2.-) belong to a large group of enzymes defined as carbohydrate-active-enzymes, classified into 23 families (February 2015), according to CAZy (**C**arbohydrate-**A**ctive en**Zy**mes or CAZymes) database

(http://www.cazy.org/Polysaccharide-Lyases.html; Cantarel *et al*., 1999). Based on the analysis of characterized polysaccharide lyases, they have been sub grouped into three levels of the classification: fold, family and subfamily. It has also been found that the sequence based families of polysaccharide lyase are often polyspecific (Lombard *et al*., 2010). Pectate lyases of families 1, 2, 3, 9 and 10 catalyse the β-eliminative cleavage of α(1,4)-glycosidic bond between D-galactopyranosyluronic acid (Gal*p*A) residue in pectate (a low methylesterified form of pectin) resulting in the formation of generate Δ4,5 unsaturated Gal*p*A (Pages *et al*., 2003), which exhibits maximum absorbance at around 235 nm (Jurnak *et al*., 1996). Family 1 polysaccharide lyase (PL1) (http://www.cazy.org/PL1.html) currently contains nearly 99 well characterized sequences showing activities like pectate lyase (EC 4.2.2.2); exo-pectate lyase (EC 4.2.2.9) and pectin lyase (EC 4.2.2.10).

Unlike glycoside hydrolases (GHs), PLs frequently have multi-modular structure in which the catalytic modules are found asociated with other modules such as carbohydrate-binding modules (CBMs) (Boraston *et al*., 2004; Guillen *et al*., 2010). These non-catalytic polysaccharide recognizing modules were initially named as cellulose binding domain (Bayer *et al*., 2000). Later on the term CBM (carbohydrate binding module) evolved reflecting the diversity in ligand specificity of these proteins (Boraston *et al*., 2004; Shoseyov *et al*., 2006). Based on the amino acid sequence similarity, currently there are 71 defined families of CBMs (http://www.cazy.org/Carbohydrate-Binding-Modules.html). They showed profound diversity in ligand binding property. Majority of GHs that attack cellulose and hemicelluloses are modular enzymes consisting of catalytic modules appended to non-catalytic carbohydrate-binding modules (CBMs) (Davis *et al*., 1995). PLs on the

contrary, generally have a relatively simple structure lacking CBMs, which is possibly explained by the accessibility of pectins to soluble biocatalysts (McKie *et al*., 2001). The CBMs are categorized into three types based on their structure and functional similarities: (i) surface binding (type A), (ii) binding with single polysaccharide chain (type B) and (iii) small sugar binding (type C) (van Bueren *et al.*, 2005; Shoseyov *et al*., 2006). Family 35 carbohydrate binding module (CBM35) currently contains 55 characterized sequences which display binding with different polysaccharides like xylan, mannan, mano-oligosaccharides and β-galactan (http://www.cazy.org/CBM35.html). CBM35 is structurally related to other CBMs and belong to the large β-jelly-roll CBM superfamily (Tunnicliffe *et al*., 2005). Analysis of biological role of 4 members of family CBM35 revealed that the biological role of CBM35 is not dictated solely by the substrate specificity of their appended catalytic domains, but they may also recognize the products of pectin hydrolysis (Montanier *et al*., 2009).

In the present study a modular cellulosomal carbohydrate-active enzyme with accession number ABN53381.1 and Uniprot ID A3DHF2 belonging to family 1 polysaccharide lyase (PL1B) from *Clostridium thermocellum* ATCC 27405 were cloned and expressed in *Escherichia coli*. The gene and protein sequence was retrieved from the CAZy database and analyzed by different computational approach which displayed (Fig. 2.1) protein PL1B-CBM35 contains an N-terminal signal peptide followed by a catalytic module (PL1B), a C-terminal carbohydrate-binding module belonging to family 35 (CBM35) and sandwiched between them is a type 1 dockerin module (DOC). These three genes correspond to catalytic domain *pl1b*, binding domain *cbm35* and the full length domain *pl1b-cbm35*. The expressed

proteins were further purified by immobilized metal ion affinity chromatography (IMAC).

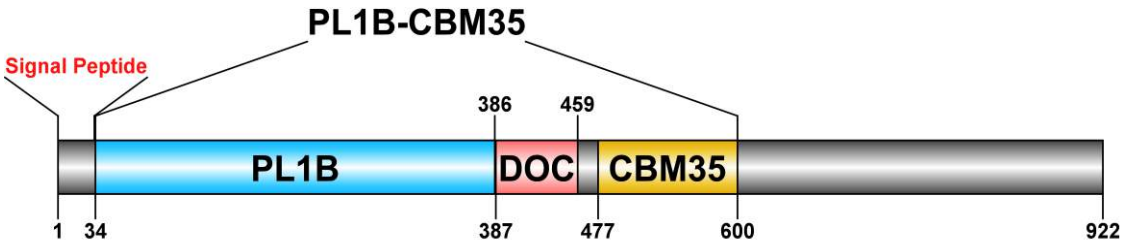


**Fig. 2.1** Molecular architecture of PL1B-CBM35 showing boundaries and designation of different domains.

The molecular architecture of modular protein ABN53381.1 from *C. thermocellum* consisting of a 33 aa signal peptide, N-terminal 353 aa family 1 polysaccharide lyase (PL1B), C-terminal 124 aa family 35 carbohydrate binding (CBM35) and sandwich between these modules is a 72 aa type 1 dockerin (DOC) modules. In the present study the gene encoding PL1B-CBM35 and its truncated derivatives PL1B and CBM35 were cloned. All the proteins expressed in *E. coli* and purified by immobilized metal ion affinity chromatography (IMAC) for further biochemical, functional and structural characterization.

## 2.2 Materials and Methods

### 2.2.1 Chemicals, reagents and kits

The oligonucleotide primers for PCR amplification of PL1B-CBM35, PL1B and CBM35 were procured from Eurofins, India. BIOTAQ DNA polymerase was supplied by Biolone, UK. The dNTPs and $MgCl_2$ were obtained from Sigma-Aldrich Pvt. Ltd., USA. PCR tubes (0.2 ml) were from Axygen, Germany. pGEM-T Easy vector system for TA cloning was purchased from Promega, USA. Restriction enzymes *Nhe*I, and *Xho*I were purchased from Promega, USA. The expression vector pET-28a, were purchased from Novagen, Germany. $T_4$ DNA ligase, 10x ligase buffer were purchased from Promega, USA. RNAse solution (20 mg/ml), glacial acetic acid (99.9 % pure) Trizma base (Tris free base), ethidium bromide, Bradford reagent, nuclease free water (pH 8.0) and components of polyacrylamide gel electrophoresis were obtained from Sigma-Aldrich Pvt. Ltd. USA. The GenElute plasmid miniprep isolation kit and GenElute gel-extraction kit was from Sigma-Aldrich Pvt. Ltd. India. The DNA was run on agarose gel prepared using Agrose, with low EEO from Sigma-Aldrich Pvt. Ltd. India. DNA marker Hyperladder I was purchased from Bioline, UK. Page Ruler protein marker was procured from Fermentas, Germany. Disodium ethylenediamine tetra acetate salts (EDTA), glucose, sodium hydroxide, sodium dodecyl sulphates (SDS), LB medium and SOC medium components were supplied by Himedia, India. The antibiotics, ampicillin and kanamycin were procured from Sigma-Aldrich Pvt. Ltd. USA. SDS-PAGE was performed using Mini-PROTEAN Tetra Cell purchased from Bio-Rad Laboratories (India) Private Limited. The protein staining dye Coomassie Brilliant Blue R250 was procured from Himedia and methanol from Merck, India. The genomic DNA of *Clostridium thermocellum* ATCC

27405 was purchased from Leibniz Institute DSMZ - German Collection of Microorganisms and Cell Cultures.

### 2.2.2 Microorganisms

Commercially available *E. coli* (XL10 Gold) cells were procured from Invitrogen (USA) and *E. coli* BL-21 (DE3) for expression of recombinant proteins were obtained from Novagen, Germany.

### 2.2.3 PCR amplification of PL1B-CBM35, PL1B and CBM35

The gene of interest PL1B-CBM35, PL1B and CBM35 was amplified with designed oligonucleotide primers from the protein sequence ABN53381.1 of *Clostridium thermocellum* ATCC 27405 genomic DNA. The primers contained the restriction enzyme sites of NheI and XhoI as mentioned in Table 2.1. Amplification of each module was done following the schematic representation in Fig. 2.2. Components of 50 µl PCR reaction mixture and the PCR cycles for amplification are detailed in Tables 2.2 and 2.3, respectively. PCR amplification was performed in a thermal cycler (Applied Biosystems, GeneAmp PCR System 9700). The amplicons were run on a 0.8 % (w/v) agarose gel in presence of DNA marker (Hyperladder I) as mentioned in Section 2.2.5.

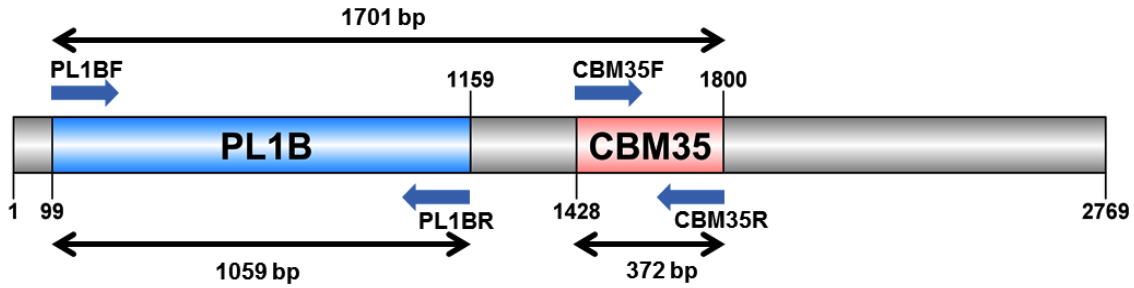


**Fig. 2.2** Schematic representation of PCR amplification of PL1B, CBM35 and PL1B-CBM35 from 2769 bp gene sequence of protein ABN53381.1 of *Clostridium thermocellum*

**Table 2.1** Oligonucleotide primers used for cloning of PL1B, CBM35 and PL1B-CBM35 from *Clostridium thermocellum*, nucleotides shown in bold are the restriction enzyme sites.

| Module | Primer name | Primer sequence |
|---|---|---|
| **PL1B-CBM35** | PL1BF | 5'- ctct**gctagc**gcgccaagctttgaactg -3' |
| | CBM35R | 5'- cgcg**ctcgag**ggcacttacaattactttgtc -3' |
| **PL1B** | PL1BF | 5'- ctct**gctagc**gcgccaagctttgaactg -3' |
| | PL1BR | 5'- cgcg**ctcgag**ctgctgagtatttttcgg -3' |
| **CBM35** | CBM35F | 5'- ctct**gctagc**gaaggtgtggtacacgag -3' |
| | CBM35R | 5'- cgcg**ctcgag**ggcacttacaattactttgtc -3' |

**Table 2.2** PCR reaction setup for amplification of PL1B-CBM35, PL1B and CBM35 from *Clostridium thermocellum.*

| PCR components | Volume (µl) | Final concentration |
|---|---|---|
| 10x reaction buffer | 5.0 | 1x |
| $MgCl_2$ (50 mM) | 2.5 | 1mM |
| dNTP mix (100 mM) | 1.0 | 2 mM |
| Forward primer (15 µM) | 1.5 | 0.45 µM |
| Reverse primer (15 µM) | 1.5 | 0.45 µM |
| Sigma water, pH 8.0 | 37 | -- |
| Genomic DNA (15 µg/ml) | 0.5 | 7.5 ng |
| Taq polymerase (2.5 U/µl) | 1.0 | 2.5 U |
| Total | 50.0 | -- |

**Table 2.3** Conditions for PCR thermal cycles for amplification of PL1B-CBM35, PL1B and CBM35 from *Clostridium thermocellum*.

| Steps | | Time (min) |
|---|---|---|
| I. Denaturation at 94°C | | 4 |
| II. 30 cycles of | i) Denaturation at 94°C | 0.5 |
| | ii) Annealing at 55°C | 1 |
| | iii) Extension at 72°C | 2 |
| III. Final extension at 72°C | | 10 |

### 2.2.4 Agarose gel electrophoresis of PCR amplicons

The PCR amplicons were run on 0.8% agarose gel prepared in 1x TAE buffer. A stock solution of TAE buffer was prepared according to Sambrook and Russell (2001) keeping the concentrations of components to 10x (400 mM Tris-acetate, 10 mM EDTA pH 8.0). The gel was prepared by dissolving agarose (400 mg for 0.8% and 500 mg for 1.0% gel) in 50 ml of 1x TAE buffer by heating in a microwave oven to get a clear solution. Then 5.0 µl of ethidium bromide (5.0 mg/ml) was added when the solution temperature was around 50°C. The solution was mixed well and poured on the casting apparatus, combs were placed and the gel was allowed to solidify. For separating of PCR amplicons, 1x TAE (Tris-acetate-EDTA) buffer was used for preparing of agarose gels and also as an electrophoresis running buffer (Sambrook and Russel, 2001). The DNA sample and DNA loading dye were mixed in 4:1 ratio and the gel run at 60 Volts for 70% migration of the leading dye. The bands were then visualized under UV illumination in a gel documentation system (BioRad XR Gel documentation system).

#### 2.2.4.1 DNA loading dye

The DNA or sample loading dye was prepared by mixing the components mentioned below in Table 2.4. A 5x stock solution of DNA loading dye was prepared and mixed with 4 volumes of DNA to make it to 1x before loading on to agarose gel. The final pH of the DNA loading dye adjusted to pH 8.0.

**Table 2.4** Composition of 5x DNA loading dye.

| Components | Final concentration (5x) |
|---|---|
| Tris-HCl | 50 mM |
| Glycerol | 25% (w/v) |
| EDTA | 5.0 mM |
| Bromophenol blue | 0.2% (w/v) |
| Xylene cyanol | 0.2% (w/v) |

### 2.2.5 Extraction of DNA from agarose gel

The PCR amplified DNA or other plasmid DNA were purified from agarose gel using a kit (Sigma Gel Extraction Kit), following the protocol provided by the manufacturer as discussed in Section 2.2.6.1. The extracted DNAs were eluted in 30 µl elution buffer supplied with the kit (Sigma-Aldrich Pvt. Ltd.).

#### 2.2.5.1 DNA gel extraction protocol

1. 1.5 ml sterile, empty microcentrifuge tubes were weighed and weight noted.
2. The PCR or plasmid DNAs were excised from gel using sharp sterile scalpel and transferred to empty microcentrifuge tubes. The tubes were weighed again and the weight of excised gel was determined by subtracting the empty tube weight.
3. Now, 3 volumes of Gel solubilization solution were added to every 1 volume of gel (100 mg ~ 100 µl).
4. The microcentrifuge tubes containing excised gel were incubated at 50°C for 10 min (or until the gel slice dissolved completely) indicated by the yellow colour of the solution.
5. 1 gel volume of isopropanol was added to this solution for PCR amplicons and to recombinant plasmids to get higher yield of DNA fragments <500 bp and >4 kb.
6. GenElute binding column G was placed in 2 ml collection tube provided with the kit. 500 µl of column preparation solution were added to each column membrane and centrifuged at 16,000 g for 1 min. The flow through was discarded before the next step.

7. The solution containing PCR-amplified or plasmid DNAs (>700 µl) were added to DNA binding columns and centrifuged at 16,000g for 1 min at room temperature discarding the flow through. If the volume was more than 700 µl, the remaining solution was centrifuged similarly and again the flow through was discarded.
8. 700 µl of Wash solution was added to each DNA bound spin column and the mixture centrifuged at 16,000g for 1 min at room temperature, discarding the flow through. The column was given an additional spin of 1 min at 16,000g to completely remove the residual ethanol.
9. Now the column containing bound DNA was placed in a fresh 1.5 ml sterile microcentrifuge tube. 30 µl of DNAse free water (Sigma-Aldrich Pvt. Ltd.) or eluent solution (10 mM Tris-Cl, pH 8.5) was added at the centre of the column. The column was incubated for 2 min at room temperature and centrifuged at 16,000g for 1 min. For efficient recovery of DNA, the elution solution was preheated to 65°C prior to adding it to the membrane. Eluting at 65 °C improves DNA recoveries by 2 to 3-fold.
10. The PCR-amplicons or plasmids DNAs were eluted from GenElute spin columns and collected in 1.5 ml sterile microcentrifuge tube. The PCR-amplicons or other DNAs were stored at -20°C for further use.

### 2.2.6 Preparation of Luria-Bertani (LB) medium

The most commonly used LB medium for growing the recombinant *E. coli* cells was prepared by dissolving the ingredients (Table 2.5) in 800 ml of deionized water. The pH was adjusted to 7.2 and final volume was made up to 1 litre. 100 ml of LB medium were then transferred to each of 250 ml conical flask and autoclaved at

121°C at 15 psi for 20 min. The filter sterilized antibiotics (ampicillin and kanamycin) were added to autoclaved and cooled LB medium prior to inoculation.

**Table 2.5** Composition of Luria-Bertani medium (Sambrook *et al*., 1989).

| Components | Final concentration (%, w/v) |
|---|---|
| Tryptone | 1.0 |
| Yeast extract powder | 0.5 |
| Sodium chloride | 1.0 |

### 2.2.6.1 Preparation of LB-agar medium

LB agar medium was prepared by boiling 2% (w/v) Agar Agar type I in broth medium. The medium was autoclaved as described in Section 2.2.6 cooled to around 50-55°C and appropriate amount of antibiotic was added under laminar air flow. 25 ml of medium supplemented with antibiotics were poured in sterile petri plates and allowed to solidify for 15- 20 min.

### 2.2.7 Preparation of SOC medium

The SOC (super optimal medium with catabolic repression) was prepared using ingredients detailed in Table 2.6. It is a modified SOB medium with addition of glucose (Hanahan, 1983; Deutscher, 2008; Park *et al.*, 2012). Bactotryptone, yeast extract powder and NaCl were autoclaved separately. 1 M stock solutions of KCl, $MgCl_2$, $MgSO_4$ and glucose were filter-sterilized and required quantities added to above solution in the laminar hood to finally make SOC medium.

**Table 2.6** Composition of SOC medium (Sambrook *et al*., 1989).

| Components | Final concentration |
|---|---|
| Bactotryptone | 2.0 (%, w/v) |
| Yeast extract powder | 0.5 (%, w/v) |
| NaCl | 10 mM |
| KCl | 2.5 mM |
| $MgCl_2$ | 10 mM |
| $MgSO_4$ | 10 mM |
| Glucose | 20 mM |

### 2.2.8 Preparation of *E. coli* (XL10 Gold) competent cells

**Day 1**

1. 50 µl of culture of *E. coli* (DH5α) from glycerol stocks were inoculated into 5.0 ml LB medium (Sambrook *et al*., 1989) contained, in test tube and grown overnight at 37ºC and 180 rpm.
2. 0.1 M $CaCl_2$ solution was filter-sterilized by passing through 0.22 µm filter in laminar air flow and kept in refrigerator.

**Day 2**

3. 1.0 ml culture from day 1 was inoculated into 100 ml LB medium kept in 250 ml conical flask and incubated at 37ºC with 180 rpm till cell OD reached 0.4-0.6 at 550 nm.
4. Micro-centrifuge tubes, 50 ml centrifuge tubes (round bottom) and micro tips were autoclaved and kept on ice bath placed in a laminar air flow hood.
5. 40 ml culture was transferred aseptically to round bottom centrifuge tubes.
6. The tubes were centrifuged at 4ºC with 4000g for 10 min.
7. The step was repeated to centrifuge the entire 100 ml culture.

8. The cell pellet was first suspended in 3-4 ml sterile, ice-chilled 0.1 M $CaCl_2$ solution followed by making up the final volume to 20 ml. The suspension in centrifuge tubes was kept on ice for 10 min.
9. The tubes were centrifuged again at 4000g at 4ºC for 10 min.
10. The supernatant was carefully removed and the pellet resuspended in 3.0 ml of sterile ice chilled 0.1 M $CaCl_2$ solution.
11. 200 µl of competent cells were aliquoted into each 1.5 ml microcentrifuge tube containing 10 (%, v/v) glycerol (final concentration) and kept at -80ºC for further use.

### 2.2.9 Cloning of PL1B-CBM35, PL1B and CBM35 amplicons into pGEM-T Easy vector

PCR amplicons of PL1B-CBM35, PL1B and CBM35 after gel extraction was subjected to TA cloning. Detail description of pGEM-T Easy vector construct from Promega, USA is given in section 2.2.6.1. Ligation reaction was setup following the protocol mentioned in section 2.2.6.2.

#### 2.2.9.1 Description of pGEM-T easy vector

The pGEM-T Easy Vector Systems (Fig. 2.3) are convenient systems for the cloning of PCR products. The vectors are prepared upon linearization of pGEM-5Zf(+) vector (GenBank accession no. X65308) with EcoR V, and adding a 3´-terminal thymidine to both the ends. These single 3´-T overhangs at the insertion site greatly improve the efficiency of ligation of a PCR product into the plasmids by preventing recircularization of the vector and providing a compatible overhang for PCR products generated by certain thermostable polymerases. These polymerases often add a single deoxyadenosine, in a template-independent fashion, to the 3´-ends

of the amplified fragments. The high copy number pGEM-T Easy vectors contain T7 and SP6 RNA polymerase promoters flanking a multiple cloning region within the alpha-peptide coding region of the enzyme beta-galactosidase. Hence successful insertion of the PCR amplicons of PL1B-CBM35, PL1B and CBM35, will interrupt the coding sequence of β-galactosidase and the recombinant clones can be identified by colour screening on indicator plates. Clones containing PCR products produce white colonies, whereas blue colonies usually do not contain any clone. Rarely the blue colonies may contain positive clone, which happens when the PCR fragments are cloned in-frame with the lacZ gene.

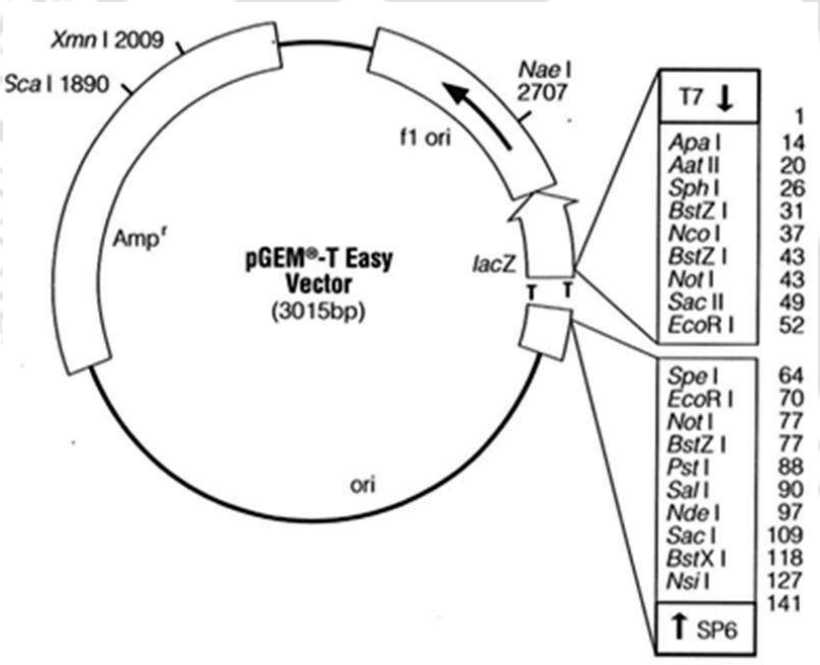


**Fig. 2.3** pGEM-T Easy vector map and sequence reference points

### 2.2.9.2 Ligation of PL1B-CBM35, PL1B and CBM35 PCR amplicons into pGEM-T Easy vector

The gel eluted PCR amplicons of PL1B-CBM35, PL1B and CBM35 were ligated with pGEM-T Easy vector following the components of ligation reaction as mentioned in Table 2.7. Three ligation reactions were setup in 0.5 ml microcentrifuge

tubes and incubated at 16°C overnight to get maximum number of transformants. Again the reactions were setup at an insert: vector molar ratio of 3:1, where the amount of insert required in a reaction is calculated using the following formula (Engler *et al*., 1982),

$$\frac{\text{amount of vector(ng)} \times \text{size of insert(kb)}}{\text{size of vector (kb)}} \times \text{insert :vector molar ratio} = \text{amount of insert (ng)}$$

$$\frac{25\ (\text{ng}) \times 1.701\ (\text{kb})}{3.015\ (\text{kb})} \times \frac{3}{1} = 42.5\ \text{ng}$$

$$\frac{25\ (\text{ng}) \times 1.059\ (\text{kb})}{3.015\ (\text{kb})} \times \frac{3}{1} = 26.5\ \text{ng}$$

$$\frac{25\ (\text{ng}) \times 0.372\ (\text{kb})}{3.015\ (\text{kb})} \times \frac{3}{1} = 9.3\ \text{ng}$$

**Table 2.7** Components for ligation reaction setup for TA cloning PCR amplicons.

| **Reaction components** | **PL1B-CBM35 (µl)** | **PL1B (µl)** | **CBM35 (µl)** |
|---|---|---|---|
| 2X Rapid Ligation Buffer | 5 | 5 | 5 |
| pGEM®-T Easy Vector (50ng) | 0.5 (25ng) | 0.5 (25ng) | 0.5 (25ng) |
| PCR product | 3 (42.5ng) | 2 (26.5ng) | 0.5 (9.3ng) |
| T4 DNA Ligase (3 units/µl) | 1 | 1 | 1 |
| Nuclease-free water | 0.5 | 1.5 | 3 |

### 2.2.9.3 Transformation of ligated products after TA cloning

The *E. coli* (XL10 Gold) competent cells were transformed with TA clone plasmid DNAs of PL1B, CBM35 and PL1B-CBM35. Preparation of *E.coli* competent cell preparation has described in Section 2.2.7. The step-wise transformation protocol is described below:

1. The microcentrifuge tube containing competent cell (200 µl) was taken out from -80°C and kept on ice for 5 min, followed by addition of 10 µl of ligation mixture (the mixture was given a very short spin prior to use).
2. The tube was gently tapped 4-5 times and kept on ice for 30 min.
3. The cells were given a heat shock at 42°C for 40s.
4. The cells were immediately transferred to ice for 2-3 min.
5. 800 µl of super optimal medium with catabolite repression (SOC) (Hanahan, 1983; Sambrook *et al*., 1989; shown in Section 2.2.7) was added to the transformed cells (previously incubated at 37°C).
6. The transformed cells were incubated at 37°C in a shaking incubator at 220 rpm for 1h.
7. The cells were harvested by centrifugation at 2000g at 25°C for 5 min.
8. 800 µl supernatant was discarded and the cell pellet resuspended in remaining 200 µl supernatant.
9. The 200 µl cells were spread plated on LB agar plates as described in Section 2.2.6.1 supplemented with antibiotics ampicillin, IPTG (Isopropyl β-D-1-thiogalactopyranoside) and X-Gal (5-bromo-4-chloro-3-indolyl-β-D-galactoside) at a final concentration of 100 µg/ml, 0.5 mM and 80 µg/ml, respectively.

10. The LB agar plates were incubated overnight at 37°C.

11. The transformation efficiency was calculated using the following formula,

$$\text{Transformation efficiency} = \frac{\text{No. of colonies on LB plate x 1000}}{\text{Amount of insert (ng)}} = \text{cfu/µg}$$

The 10 µl ligation mixture was added to 200 µl E. coli (XL10 Gold) competent cells, following the above transformation protocol. The transformed cells were spread on LB agar plates supplemented with ampicillin, IPTG and X-Gal and incubated overnight at 37ºC.

**2.2.9.4 Screening of positive TA clones of PL1B-CBM35, PL1B and CBM35**

Positive TA clones are identified by the process of blue white screening. Overnight grown plates were observed for blue white colonies. White colonies containing the positive clones were picked up in a laminar air flow and grown overnight in 5 ml LB media supplemented with ampicillin (100 µg/ml). The positive TA clones produce white colonies are unable to produce β-galactosidase because of the interrupted *lacZ* gene induced by the presence of the insert DNA. In absence of β-galactosidase the cells cannot degrade X-Gal and produce blue colour colonies.

**2.2.9.5 Isolation of plasmid DNA from positive colonies by TELT method**

Plasmid DNA was isolated from fully grown *E.coli* (XL10 Gold) cells which were picked up from the LB plates after transformation of the ligated TA cloned products of PL1B, CBM35 and PL1B-CBM35. TELT method as described below was employed for isolation of plasmid.

1. Cells from overnight grown 5 ml LB media were centrifuged in a 1.5 ml microcentrifuge tube at 14,000g for 5 min.

2. The supernatant was periodically removed by aspiration and the process repeated until a thick cell pellet is obtained.
3. The cell pellet was resuspend in 100 µl TELT buffer, composition as mentioned in Table 2.8.
4. 100 µl of 25:24:1 phenol/chloroform/isoamyl alcohol was added to the above suspended cell pellet.
5. To mix it was vortexed for 15 sec.
6. The suspension in the microcentrifuge tube was centrifuged at 14,000g for 10 min at room temperature.
7. Supernatant transferred to a fresh microcentrifuge tube and 200 µl of 95 (% v/v) erthanol was added. It was then mixed gently and incubated at room temperature for 15 min.
8. The mix was centrifuged at 14,000g for 5 min discarding the supernatant.
9. The white pellet containing the plasmid DNA was air dried for complete removal of ethanol.
10. The DNA pellet was resuspended in 20 µl Tris-EDTA buffer or Nuclease free water.

**Table 2.8** Composition of TELT buffer for plasmid isolation

| Components | Final Concentration |
|---|---|
| Tris-HCl pH 8.0 | 50 mM |
| EDTA | 62.5 mM |
| Lithium chloride | 2.5 M |
| Triton X-100 | 4 (%w/v) |

### 2.2.9.6 Screening of recombinant plasmid DNAs for identification of positive TA clones by restriction digestion

15 µl of recombinant plasmid DNA from positive TA clones of PL1B-CBM35, PL1B and CBM35 which was isolated by TELT method as described in Section 2.2.9.5, were taken in a fresh sterile microcentrifuge tube for restriction enzyme digestion analysis. The recombinant plasmid DNA of each of the above mentioned derivatives was digested with restriction enzymes, *Nhe*I and *Xho*I, to check for positive clones following a 30 µl reaction mixture set up as mentioned in Table 2.9. The reaction mixtures for each recombinant derivative were incubated at 37ºC in a water bath for 90 min. The digested products were run on 0.8% agarose gel as described in Section 2.2.4. The digested vector and the respective insert DNA of above mentioned recombinant derivatives were visualized by placing the gel under UV transilluminator. The digested fragments of expected size were taken as positive TA clones. Glycerol stocks of *E. coli* (XL 10 Gold) cells containing the positive TA clones of each of the above mentioned derivatives were prepared in glycerol (20-25% v/v) and stored at -80°C.

**Table 2.8** Restriction enzyme digestion set up of recombinant DNA.

| **Digestion set up** | **1x (µl)** |
|---|---|
| 10x buffer | 3.0 |
| DNAse free water | 10.0 |
| Recombinant plasmid DNA (approx. 75 ng) | 15.0 |
| *Nhe*I (10 U/µl) | 1.0 |
| *Xho*I (10 U/µl ) | 1.0 |
| Total | 30.0 |

### 2.2.10 Cloning of restriction digestion products of PL1B-CBM35, PL1B and CBM35 containing plasmids to pET-28a(+) vector

The pET-28a(+) vector is commonly used for cloning and expression of recombinant proteins in *E. coli*. It is a modified form of pBR322 with a strong T7 promoter system originally developed by Studier and colleagues (Studier and Moffatt, 1986; Studier *et al.*, 1990). Although this system is extremely powerful, it is also possible to control expression levels simply by manipulating the concentration of inducer. The desired genes to be cloned in pET plasmids are under the influence of strong bacteriophage T7 transcription and the expression is induced by T7 RNA polymerase in the host cell. An additional advantage with pET system is its ability to maintain target genes transcriptionally silent in the uninduced state. The $His_6$-Tag is useful and easy to purify recombinant protein in a single step by making use of affinity chromatography. The pET-28a(+) vector is incorporated with an N-terminal $His_6$-Tag/thrombin/T7-Tag configuration in addition to an optional C-terminal $His_6$-Tag sequence (Fig. 2.4). The thrombin tag can be used to remove the $His_6$-Tag, during structural and western blotting detection of the recombinant protein. The location of His-Tag, T7 coding sequence, T7 terminator, kanamycin coding region and f1 origin are depicted in the Fig. 2.4.

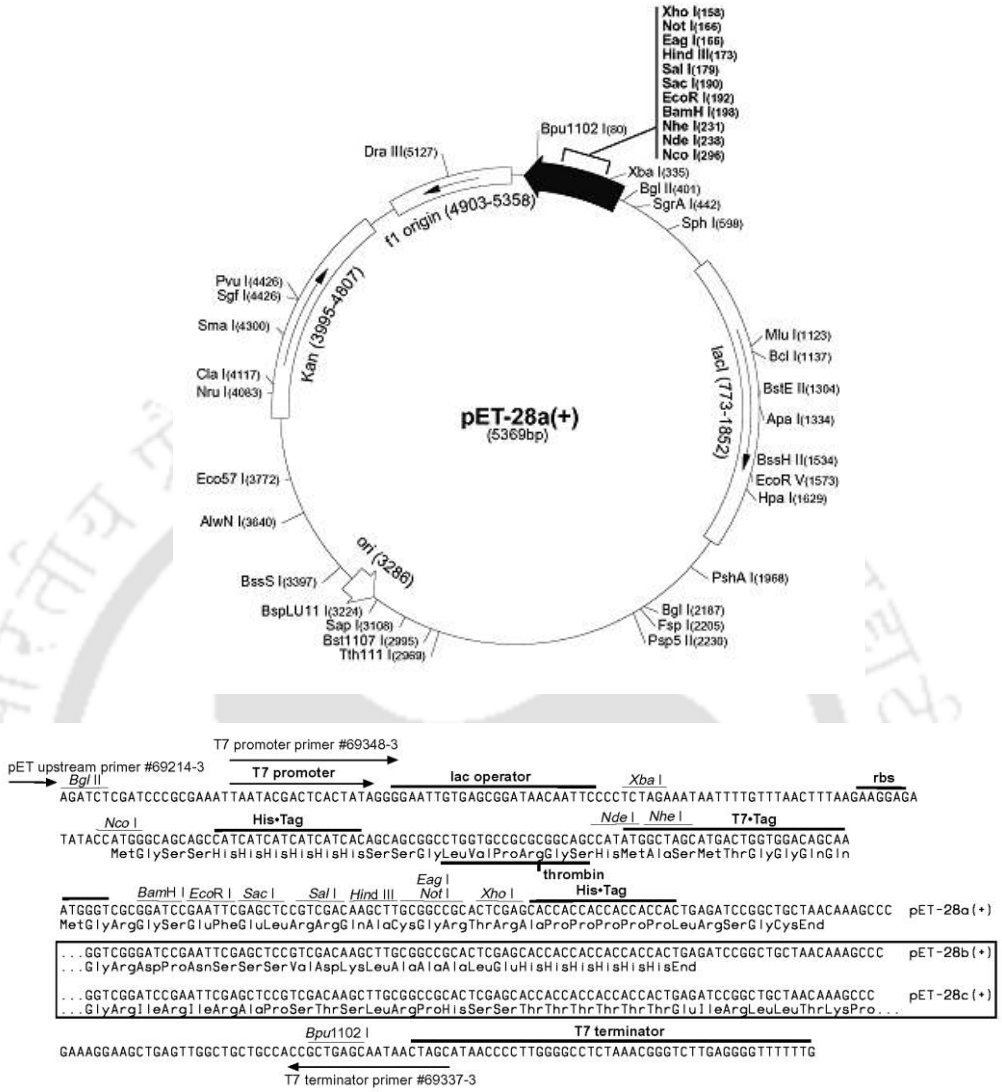


**Fig. 2.4** Restriction map of the pET-28a(+) expression vector showing multiple cloning site (158-203 bp), restriction enzyme sites, N-terminal $His_6$-Tag coding sequence (270-287 bp), C-terminal $His_6$-Tag coding sequence (140-157 bp), T7 promoter (370-386), T7 terminator (26-72 bp), pBR322 origin (3286 bp), kanamycin marker (3995-4807 bp) and a f1 origin (4903-5358). *Nhe*I cuts at 231 and *Xho*I at 158.

The pET-28a(+) vector was digested with *Nhe*I-*Xho*I to prepare them for cloning of PCR amplified fragments of PL1B-CBM35, PL1B and CBM35. A stock solution (100 ng/µl) was prepared from the supplied stock of 10 µg for each of the above vectors using DNAse free water (pH 8.0). The restriction enzyme digestions of pET vectors were then carried out as described below (Table 2.9). The digestion

mixtures were incubated at 37°C in a water bath for 90 min. The *Nhe*I-*Xho*I digested pET vectors were purified from agarose gel as described in Section 2.2.5.

#### 2.2.10.1 Ligation of PL1B-CBM35, PL1B and CBM35 inserts to pET-28a(+) vector

The *Nhe*I-*Xho*I digested fragnments of PL1B-CBM35, PL1B and CBM35 from TA clones in Section 2.2.9.6 were cloned into pET-28a(+) vector, which were also digested with same restriction enzymes as described in Section 2.2.10. Three ligation reactions were setup using the reaction components mentioned in Table 2.9 and incubated at 16°C overnight to get maximum number of transformants. Again the reactions were setup at an insert: vector molar ratio of 3:1, where the amount of insert is calculated as mentioned below.

$$\frac{50\ (\text{ng}) \times 1.701\ (\text{kb})}{5.369\ (\text{kb})} \times \frac{3}{1} = 47.5\ \text{ng}$$

$$\frac{50\ (\text{ng}) \times 1.059\ (\text{kb})}{5.369\ (\text{kb})} \times \frac{3}{1} = 29.6\ \text{ng}$$

$$\frac{50\ (\text{ng}) \times 0.372\ (\text{kb})}{5.369\ (\text{kb})} \times \frac{3}{1} = 10.4\ \text{ng}$$

**Table 2.9** Components for ligation reaction setup for PL1B, CBM35 and PL1B-CBM35 inserts from TA clone into pET-28a (+) expression vector

| Reaction components | PL1B-CBM35 (µl) | PL1B (µl) | CBM35 (µl) |
|---|---|---|---|
| 10X Rapid Ligation Buffer | 2 | 2 | 2 |
| pET-28a (+) Vector (100ng) | 0.5 (50 ng) | 0.5 (50 ng) | 0.5 (50 ng) |
| TA clone digested product | 2.5 (47.5 ng) | 1 (29.6 ng) | 1.5 (10.4ng) |
| T4 DNA Ligase (3 units/µl) | 1 | 1 | 1 |
| Nuclease-free water | 4 | 5.5 | 5 |

#### 2.2.10.2 Transformation of ligated products after cloning into pET-28a(+)

The *E. coli* (XL10 Gold) competent cells were transformed with pET-28a(+) ligated plasmid DNAs of PL1B-CBM35, PL1B and CBM35, after overnight ligation. Transformation protocol was followed as mentioned in Section 2.2.9.3. The transformed XL 10 Gold cells were plated on LB plates supplemented with kanamycin (50 µg/ml) and grown overnight at 37°C, 180rpm.

#### 2.2.10.3 Isolation of plasmid DNA from pET-28a(+) ligation products containing colonies by miniprep kit

Overnight incubated plates were observed for colonies. Colonies preferably from the centre of the plate were randomly picked in a laminar air flow and grown overnight in 5 ml LB medium supplemented with kanamycin (50 µg/ml). The plasmid DNA from this 5 ml culture was isolated by miniprep kit (Sigma-Aldrich) following the protocol mentioned in Section 2.2.10.3.1.

#### 2.2.10.3.1 Plasmid isolation protocol by miniprep kit

1. 1.5 ml from each of the grown recombinant culture were taken and transferred to 1.5 ml microcentrifuge tube aseptically.
2. The cells were then centrifuged at 14,000g for 1 min and the process was repeated twice with another 1.5 ml of grown culture.
3. The resulting cell pellets of each recombinant derivative were suspended in 200 µl resuspension solution and vortexed. RNAse in final concentration of 20 µg/ml was added to the re-suspension solution prior to use.
4. 200 µl of lysis solution was added to each tube and the tubes were inverted gently 5-6 times to ensure mixing and allowed to stand for 2-5 min.

5. 350 µl of neutralization solution was added to the mixture and the tubes were inverted again for 4–6 times to mix properly.
6. The mixture was centrifuged at 16,000g for 10 min.
7. The DNA binding columns were prepared or activated by adding 500 µl of column preparation solution to binding column and centrifuging at 14,000g for 1 min. The flow through accumulated in collection tube was discarded.
8. The clear lysate was then transferred to activate DNA binding column, centrifuged at 14,000g for 1 min and the flow through in the collection tube was discarded again.
9. The plasmid DNAs bound to column were washed with wash solution and spun at 14,000g for 1 min. The flow through was discarded and the column was given another 1 min spin at 14,000g for removing the wash solution completely.
10. The DNA binding column was transferred to a fresh sterile microcentrifuge tube and 25 µl of TE buffer solution or DNAse free water was added at the centre of binding column. The microcentrifuge tube was allowed to stand for 10 min at room temperature and then plasmid DNA was eluted by centrifugation at 14,000g for 1 min. The plasmid DNA then got collected in the sterile microcentrifuge tube.
11. The eluted plasmid DNAs in sterile microcentrifuge tube were stored at -20°C.

#### 2.2.10.4 Screening of recombinant plasmid DNAs for positive pET-28a(+) clones by restriction digestion

15 µl of recombinant plasmid DNA from pET-28a(+) clones of PL1B-CBM35, PL1B and CBM35 that was isolated in the last step, was taken in a fresh sterile microcentrifuge tube for restriction enzyme digestion analysis. The recombinant plasmid DNA of each of the above mentioned derivatives was digested with restriction enzymes, *Nhe*I and *Xho*I, to check for positive clones following a 30 µl reaction mixture set up as mentioned in Table 2.8. The digestion reaction protocols and identification of digested products were done following the methods mentioned in Section 2.2.9.6.

### 2.2.11 Preparation of competent *E. coli* BL-21 cells

The competent *E. coli* BL-21 (DE3) cells were prepared by calcium chloride method following the protocol as discussed in Section 2.2.8. Finally, 10% (v/v) glycerol (final concentration) was added to competent cells and 200 µl aliquots were made in sterile microcentrifuge tubes and stored at -80°C for further use.

### 2.2.12 Transformation of recombinant plasmids containing genes encoding PL1B-CBM35, PL1B and CBM35 using *E. coli* (BL21) cells for expression

10 µl of from each of the recombinant plasmid of positive pET-28a(+) clones isolated in Section 2.2.10.3 were used for transformation of 200 µl *E. coli* (BL-21) for hyper-expression of PL1B-CBM35 and PL1B, CBM35 following the transformation protocol described in Section 2.2.9.3. The transformed XL 10 Gold cells were plated on LB agar plates supplemented with kanamycin (50 µg/ml) and grown overnight at 37°C.

### 2.2.13 Hyper-expression of recombinant PL1B, CBM35 and PL1B-CBM35

The overnight grown plates were observed and colonies, preferably from the centre of the plate were randomly picked within a laminar air flow and grown in 5 ml LB media supplemented with kanamycin (50 µg/ml) at 37°C and 180 rpm. The cells were grown till mid-exponential phase or till cell O.D. reached $A_{550} \approx 0.6$ (Taylor *et al*., 2005). 1 ml of this culture, containing uninduced cells was used for sample preparation for SDS-PAGE analysis and stored for glycerol stock prepration. The remaining 4 ml culture was then induced with 1 mM IPTG for hyper-expression of recombinant proteins and further incubated for 24h at 24ºC, 180 rpm. Expression of recombinant proteins in each colony was analysed after running the uninduced and induced cultures separately on SDS-PAGE (Section 2.2.14). Comparing their expression level, the colonies containing each recombinant plasmid were selected for glycerol preparation and stored at -80°C for further use.

### 2.2.14 Sodium dodecyl sulphate-Polyacrylamide gel electrophoresis (SDS-PAGE) analysis of recombinant proteins

The recombinant proteins were separated on SDS-PAGE gel on the basis of their respective molecular size. PAGE was used to separate components of a protein mixture based on their size (Laemmli, 1970; Sambrook *et al*., 1989). Analysis of expression and purification of PL1B and PL1B-CBM35 was done in 10.5% SDS-PAGE, whereas CBM35 was analysed in 12.5% SDS-PAGE prepared by ingredients mentioned in Table 2.10 and 2.11.

**Table 2.10** Composition of SDS-PAGE components for preparation of resolving gel.

| Components | 10.5% gel volume (mL) | 12.5% gel volume (mL) |
|---|---|---|
| Acrylamide solution (30%,w/v) | 3.5 | 4.2 |
| Deionized water | 1.2 | 0.5 |
| SDS (10%,w/v) | 1.0 | 1.0 |
| Glycerol (50%,v/v) | 1.0 | 1.0 |
| 1.5 M Tris-HCl (pH 8.8) | 3.3 | 3.3 |
| APS (10%,w/v) | 0.1 | 0.1 |
| TEMED | 0.01 | 0.01 |

**Table 2.11** Composition of SDS-PAGE components for preparation of stacking gel.

| Components | 4% gel volume (mL) |
|---|---|
| Acrylamide solution (30%,w/v) | 0.7 |
| Deionized water | 2.8 |
| SDS (10%,w/v) | 0.5 |
| 0.5 M Tris-HCl (pH 6.8) | 1.0 |
| APS (10%,w/v) | 0.05 |
| TEMED | 0.005 |

Every SDS-PAGE was run in 1x Tris-Glycine (pH 8.3-8.5) running buffer at constant voltage of 50 to 100 V. The expressed and purified protein samples were viewed after staining the gel with staining soultion containing Coomassie Brilliant Blue (CBB) R-250 dye prepared by dissolving (0.25% w/v) in 50 ml deionized water, 40 ml methanol and 10 ml glacial acetic acid. The gels were destained by immersing the gel in destaining solution containing 50 ml deionized water, 40 ml methanol and 10 ml glacial acetic acid with gentle rocking and periodic change of buffer, until the protein bands became clearly visible.

### 2.2.15 Purification of recombinant proteins PL1B-CBM35, PL1B and CBM35

The *E. coli* BL-21(DE3) cells harbouring recombinant plasmids were grown in 100 ml LB medium supplemented with kanamycin (50 µg/ml) in 250 ml flask. The recombinant proteins containing a $His_6$-tag at the N-terminal were purified through a single step purification method based on immobilized metal-ion affinity chromatography (IMAC) Section 2.2.15.1. His-tag purification of these recombinant proteins was done in 1.0 ml sepharose columns (GE Healthcare, HiTrap chelating HP). The compositions of binding as well as elution buffers used for affinity column purification are mentioned Table 2.12.

**Table 2.12** Composition of buffers required for purification recombinant proteins by affinity purification (IMAC).

| Buffers | Composition |
|---|---|
| Equilibration buffer | 50 mM Tris-HCl, pH 8.0<br>300 mM NaCl, 70 mM Imidazole |
| Elution buffer | 50 mM Tris-HCl, pH 8.0<br>300 mM NaCl, 500 mM Imidazole |
| Cleaning buffer | 50 mM Tris-HCl, pH 8.0<br>500 mM NaCl, 50 mM EDTA |

#### 2.2.15.1 IMAC purification protocol for recombinant PL1B-CBM35, PL1B and CBM35

1. The bacterial cells (100 ml culture) were harvested by centrifugation at 10,000g at 4°C. The cell pellets were re-suspended in 5 ml of 50 mM Tris-HCl buffer pH 8.0.
2. The cells were sonicated on ice for 15 min (10s on and 15s off pulse; with 33% amplitude) and centrifuged at 12,000g at 4ºC for 30 min to get the crude cell free extract.

3. The cell free extract was passed through a 0.22 µm filter membrane before loading into HiTrap chelating HP column which was pre-washed with 5 volumes of filtered and degassed water to remove the alcohol.
4. Column was charged using 2.0 ml of 0.1 M $NiSO_4$ solution and the unbound nickel was washed away with 2-5 volumes of water.
5. Then the column was equilibrated with 5-10 volumes of equilibration buffer (Table 2.2.15.1).
6. The filtered cell free extract of recombinant protein was loaded on to the column at a flow rate of 1 ml/min.
7. The column was then washed with 50-60 column volumes of equilibration buffer to remove the unbound proteins.
8. The retained proteins of interest were then eluted with elution buffer under a gradient of 0-100% imidazole concentration and 1 ml fractions were collected (Carvalho *et al.*, 2004; Taylor *et al.*, 2005).
9. The column was cleaned using cleaning buffer as mentioned in Table 2.2.17, washed with 2-5 volumes of water and incubated in 1N NaOH at 4°C for 2h. The column was then washed with 10-20 volumes of water to remove NaOH, and finally stored in 20% (v/v) ethanol at 4°C.

The purified recombinant protein PL1B-CBM35 and PL1B was dialyzed against 50 mM Tris-HCl buffer, pH 8.6 with 100 mM NaCl, and CBM35 was dialyzed against 50 mM Tris-HCl, buffer pH 8.0 with 100 mM NaCl. The purity and molecular mass of recombinant proteins were verified by SDS-PAGE as described in Section 2.2.14.

### 2.2.16 Protein concentration determination of purified recombinant proteins

The concentration of purified protein was determined from their corresponding absorbance at 280 nm using the formula mentioned below (Layne, 1957; Stoscheck, 1990). Reading was taken after proper dilution of the sample in spectrophotometer (Cary 100, Varian) having a path length of 1 cm. The molar extinction co-efficient being 67,645 $M^{-1}cm^{-1}$ for PL1B-CBM35, 44,725 $M^{-1}cm^{-1}$ for PL1B and 16,960 $M^{-1}cm^{-1}$ for CBM35 and, respectively.

$$\text{Concentration of protein (mg/ml)} = \frac{\text{Absorbance at 280 nm x Dilution factor}}{\text{Extinction coefficient x Path length x 1000}}$$

## 2.3 Results and Discussion

### 2.3.1 PCR amplification of family 1 polysaccharide lyase PL1B-CBM35, PL1B and CBM35

Inspection of a modular protein sequence PL1B-CBM35 with accession number ABN53381.1 from *C. thermocellum* revealed that they contained a module PL1B, putatively expressing lyase activity and another module CBM35 which putatively expressed carbohydrate binding activity (Fig. 2.1). This protein sequence was associated with type I dockerin (DOC), which is the signature module of the cellulosomal proteins. Analysis of the deduced amino acid sequence of the three enzymes revealed characteristic N-terminal signal sequences with putative cleavage sites located between Ala-33/Ala-34 (Fig. 2.1) suggesting that the proteins were exported into the extracellular space. PL1B-CBM35, PL1B and CBM35 were amplified from genomic DNA of *Clostridium thermocellum* ATCC 27405 strain using the conditions as mentioned in Section 2.2.3 and detected on 0.8% agarose gel and shown in figure 2.5 below. The PCR products were purified from gel using gel extraction kit as mentioned in Section 2.2.5 and stored at -20°C for subsequent TA cloning.

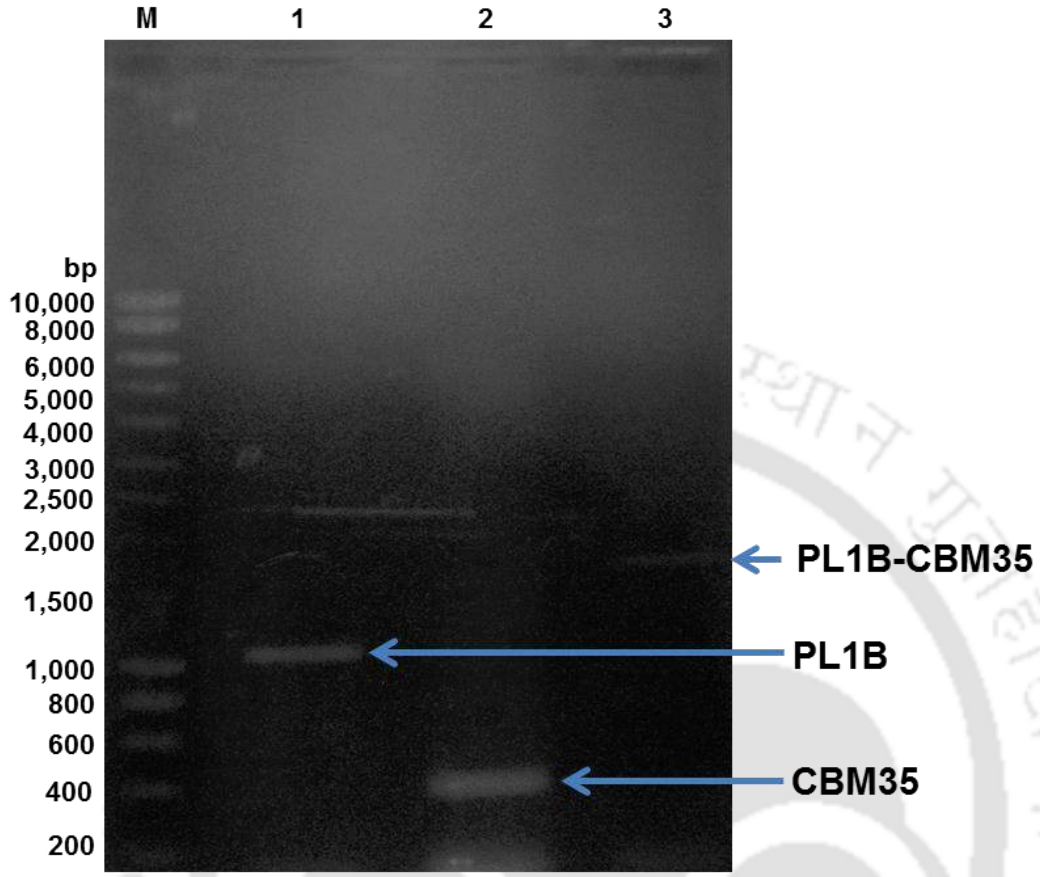


**Fig. 2.5** 0.8% agarose gel showing PCR amplification of PL1B (lane 1), CBM35 (lane 2) and PL1B-CBM35 (lane 3) around 1059 bp, 372 bp and 1701 bp respectively.

### 2.3.2 TA cloning of PL1B-CBM35, PL1B and CBM35

The PCR amplified products of PL1B-CBM35, PL1B and CBM35 with 3'-A overhangs was ligated to pGEM-T Easy vector following the method described in Section 2.2.9.2. The ligated products were transformed into *E.coli* (XL 10 Gold) competent cells and positive clones were selected by blue-white colony selection as described in Section 2.2.9.3. The transformation efficiency of *E.coli* (XL 10 Gold) competent cells after transformation of the ligated products is mentioned in Table 2.13.

**Table 2.13** Transformation efficiency of *E.coli* (XL10 Gold) competent cells

| Clone | insert DNA (ng) | No. of colonies | Transformation Efficiency (cfu/µg) |
|---|---|---|---|
| +ve control | 1.0 | 198 | $9.8\times10^4$ |
| pGEM-T+PL1B-CBM35 | 1.8 | 125 | $3.5\times10^4$ |
| pGEM-T+PL1B | 2.0 | 179 | $4.5\times10^4$ |
| pGEM-T+CBM35 | 1.5 | 152 | $5.0\times10^4$ |

#### 2.3.2.1 Plasmid isolation of TA cloned plasmid DNA of PL1B-CBM35, PL1B and CBM35

Plasmid DNA from positive colonies after TA cloning was isolated by TELT method mentioned in Section 2.2.9.5. The isolated plasmids are visualized after running in 0.8% agarose gel. Positive clones were confirmed after restriction digestion of this isolated plasmid DNA.

#### 2.3.2.2 Restriction digestion of isolated plasmid DNA for confirmation of TA clone

The isolated TA clone plasmid DNA was digested with *Nhe*I and *Xho*I restriction enzymes to confirm and prepare the insert DNA of PL1B-CBM35, PL1B and CBM35 for further cloning into pET-28a (+) expression vector. The plasmid DNA after restriction digestion was run on 0.8% agarose gel. *NheI* and *XhoI* digested fragments of PL1B-CBM35 (Fig 2.6A; Lane 2, 3), PL1B (Fig 2.6B; Lane 2) and CBM35 (Fig 2.6C; Lane 2) was visualized on agarose gel around 1.7 kb, 1 kb and 0.4 kb respectively. pGEM-T Easy vector was visualized at around 3 kb after restriction digestion. The digested fragments of PL1B-CBM35, PL1B and CBM35 were gel eluted and prepared for their cloning into pET-28a (+) vector. The expression vector was also linearized after restriction digestion by *NheI* and *XhoI*, and used for ligation with the insert.

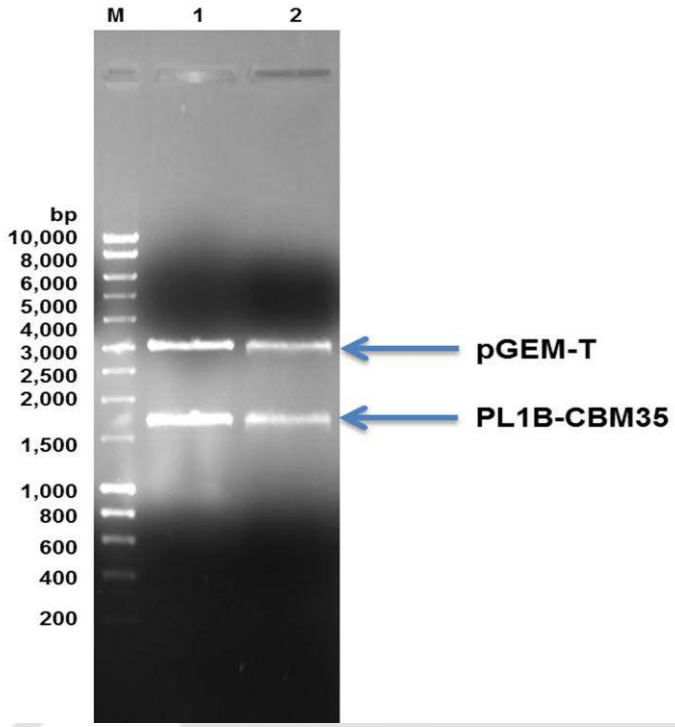


**Fig. 2.6A** Agarose gel (0.8%) showing *Nhe*I-*Xho*I digested TA clone plasmid DNA. Lane 1: DNA marker (Hyper ladder I, Bioline), Lane 2: 1.7 kb PL1B-CBM35 insert fragment and 3 kb pGEM-T Easy vector.

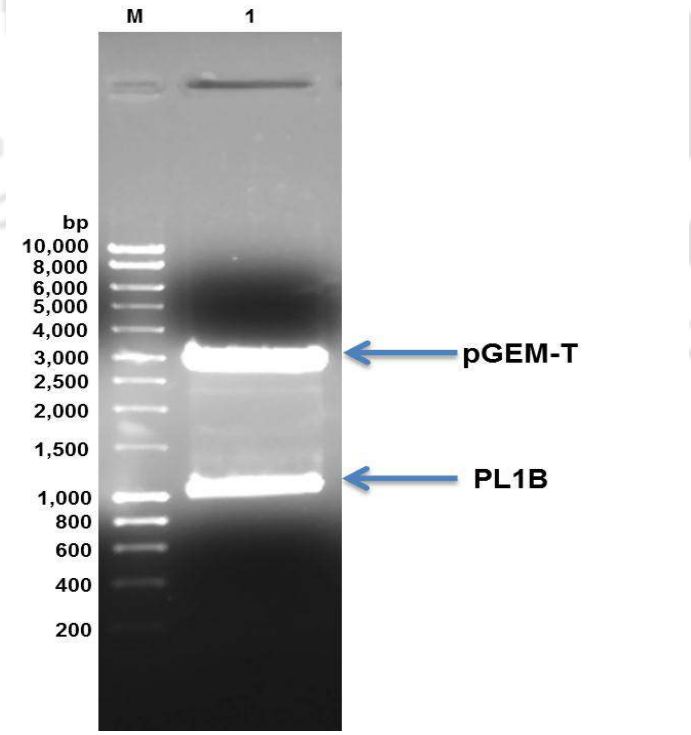


**Fig. 2.6B** Agarose gel (0.8%) showing *Nhe*I-*Xho*I digested TA clone plasmid DNA. Lane 1: DNA marker (Hyper ladder I, Bioline), Lane 2 and 3: 1 kb PL1B insert fragment and 3 kb pGEM-T Easy vector.

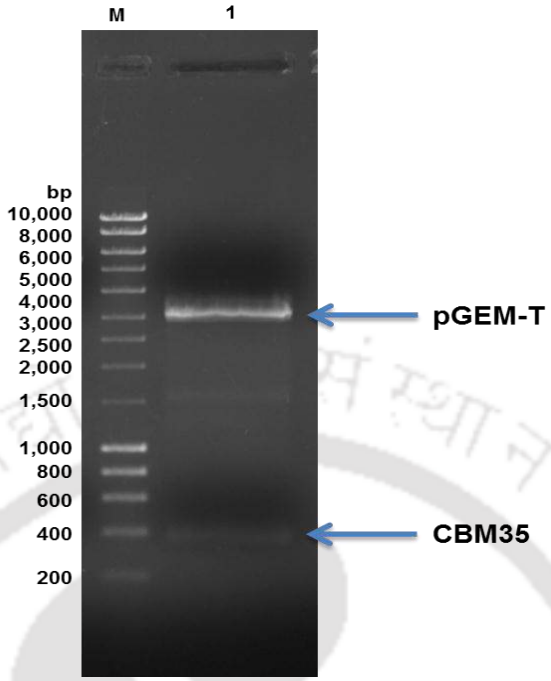


**Fig. 2.6C** Agarose gel (0.8%) showing *Nhe*I-*Xho*I digested TA clone plasmid DNA. Lane 1: DNA marker (Hyper ladder I, Bioline), Lane 2: 0.4 kb CBM35 fragment and 3 kb, pGEM-T Easy vector.

### 2.3.3 Cloning of PL1B-CBM35, PL1B and CBM35 into pET-28a (+) vector

The restriction enzyme digested fragments of PL1B, PL1B-CBM35 and CBM35 were ligated with the linearized fragments of pET-28a(+) vector following the protocol mentioned in Section 2.2.10.1. The ligation product was transformed into *E. coli* (XL10 Gold) competent cells and grown overnight on LB agar plates grown at 37°C under stationary condition. The transformation efficiency of *E. coli* (XL 10 Gold) competent cells after transformation of the ligated products is mentioned in Table 2.13.

**Table 2.13** Transformation efficiency of *E. coli* (XL10 Gold) competent cells.

| Clone | insert DNA (ng) | No. of colonies | Transformation Efficiency (cfu/µg) |
|---|---|---|---|
| +ve control | 1.0 | 186 | $3.7\times10^4$ |
| pET28a+PL1B-CBM35 | 1.6 | 174 | $2.2\times10^4$ |
| pET28a+PL1B | 1.2 | 204 | $3.4\times10^4$ |
| pET28a+CBM35 | 2.0 | 109 | $1.1\times10^4$ |

### 2.3.3.1 Isolation of recombinant plasmid DNA

Plasmid DNA from grown colonies after cloning into pET-28a(+) was isolated using Plasmid miniprep kit following the protocol mentioned in Section 2.2.13.3.1. The isolated plasmids were visualized after running in 0.8% agarose gel. Positive clones were confirmed after restriction digestion of this isolated plasmid DNA.

### 2.3.3.2 Restriction digestion of isolated plasmid DNA for confirmation of positive clone

The isolated plasmid DNA was digested with *Nhe*I and *Xho*I restriction enzymes for confirming the positive clones. The plasmid DNA after restriction digestion was run on 0.8% agarose gel. *NheI* and *XhoI* digested fragments of PL1B-CBM35 (Fig 2.7A; Lane 2), PL1B (Fig 2.7B; Lane 2) and CBM35 (Fig 2.7C; Lane 3) were visualized on agarose gel around 1.7 kb, 1 kb and 0.4 kb respectively. pET-28a (+) vector was visualized at around 5.4 kb after restriction digestion.

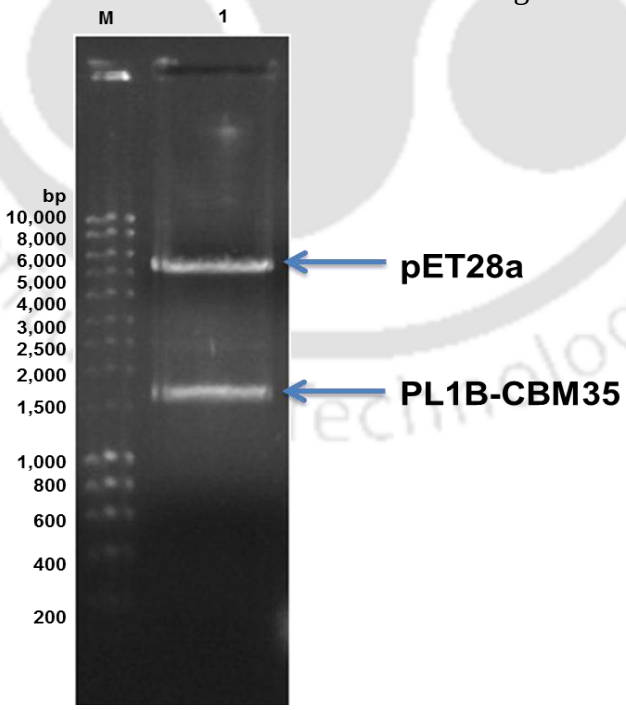


**Fig. 2.7A** Agarose gel (0.8%) showing *Nhe*I-*Xho*I digested pET-28a clone plasmid DNA. Lane 1: DNA marker (Hyper ladder I, Bioline), Lane 2: 1.7 kb PL1B-CBM35 insert fragment and 5.4 kb pET-28a (+) vector.

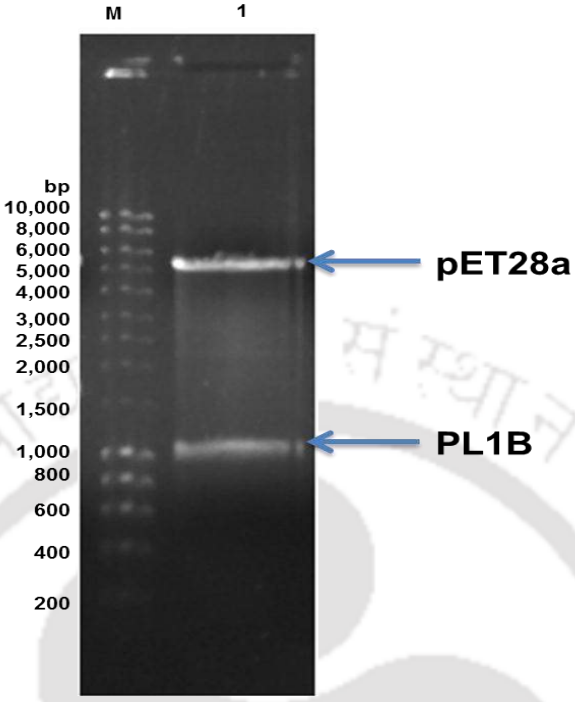


**Fig. 2.7B** Agarose gel (0.8%) showing *Nhe*I-*Xho*I digested TA clone plasmid DNA. Lane 1: DNA marker (Hyper ladder I, Bioline), Lane 2: 1 kb PL1B insert fragment and 5.4 kb pET-28a (+) vector.

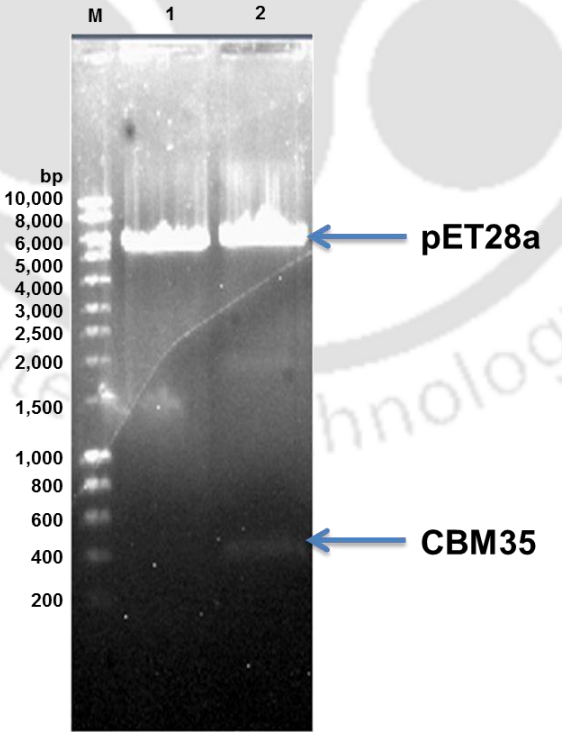


**Fig. 2.7C** Agarose gel (0.8%) showing *Nhe*I-*Xho*I digested TA clone plasmid DNA. Lane 1: DNA marker (Hyper ladder I, Bioline), Lane 3: 0.4 kb CBM35 fragment and 5.4 kb pET-28a (+) vector.

### 2.3.4 Hyper-expression analysis and purification of recombinant proteins

The *E. coli* (BL-21) competent cells were transformed with positive clones of pET-28a (+) cloned plasmid DNA of PL1B-CBM35, PL1B and CBM35. The colonies were picked randomly and grown in 5 ml LB medium supplemented with kanamycin (50 µg/ml) as described in Section 2.2.13. The cells were induced for hyperexpression of protein at mid exponential stage as described in Section 2.2.13. Hyper-expression of protein was analyzed on SDS-PAGE by loading uninduced as well as the induced cells of recombinant protein on adjacent wells, as depicted in Fig. 2.8A to Fig. 2.8C. The hyper-expression of PL1B-CBM35 in Fig. 2.8A (lane 2), PL1B is shown in Fig. 2.8B (lane 2), and the expression of CBM35 is displayed in Fig. 2.8C (lane 2).

The hyper-expressed recombinant proteins were purified by immobilized metal ion affinity chromatography as described in Section 2.2.15 and then dialyzed for removal of imidazole and salt. Fig. 2.8A and Fig. 2.8B show SDS-PAGE (10.5%) analysis of expression and purification of PL1B and PL1B-CBM35, respectively. The purified PL1B-CBM35 (Fig. 2.8A, lane 6) and PL1B (Fig. 2.8B, lane 6) showed band of molecular size 50 kDa and 40 kDa, respectively. The CBM35 was also hyper-expressed and checked for homogenous bands of purified proteins on SDS-PAGE (12.5%). The purified CBM35 showed molecular size of 15 kDa (Fig. 2.8C, lane 6).

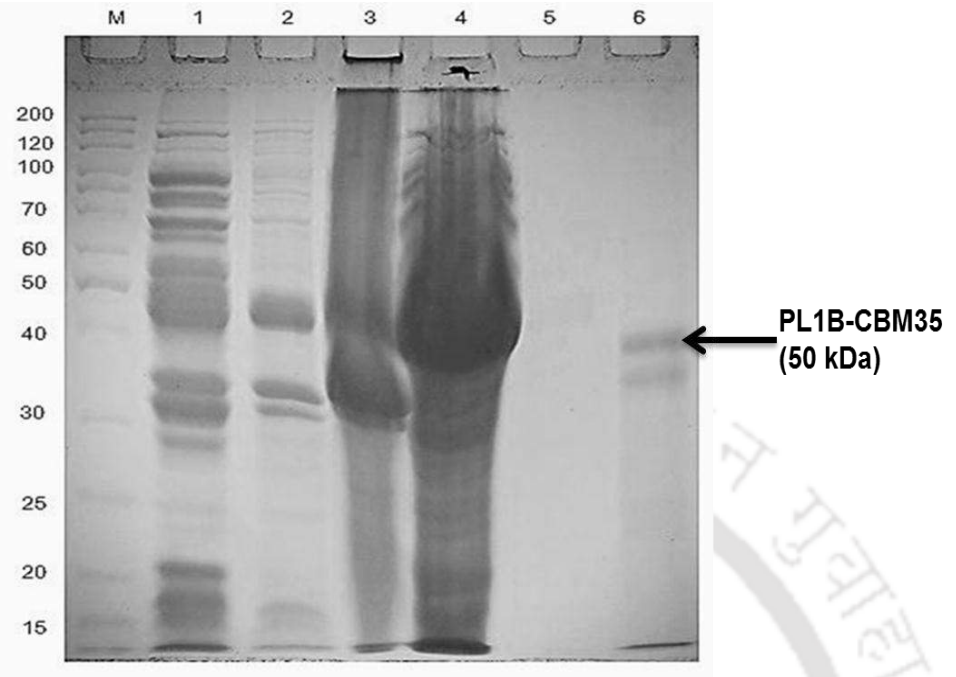


**Fig. 2.8A** SDS-PAGE (10.5%) gel showing expression and purification of recombinant PL1B-CBM35 in *E. coli* BL-21 cells, Lane M: Page Ruler marker (Fermentas), Lane 1: Uninduced cells, Lane 2: Induced cells, Lane 3: Cell pellet (cell debris after sonication), Lane 4: Cell free extract, Lane 5: Last column wash, Lane 6: Purified dialyzed PL1B (50 kDa approx.).

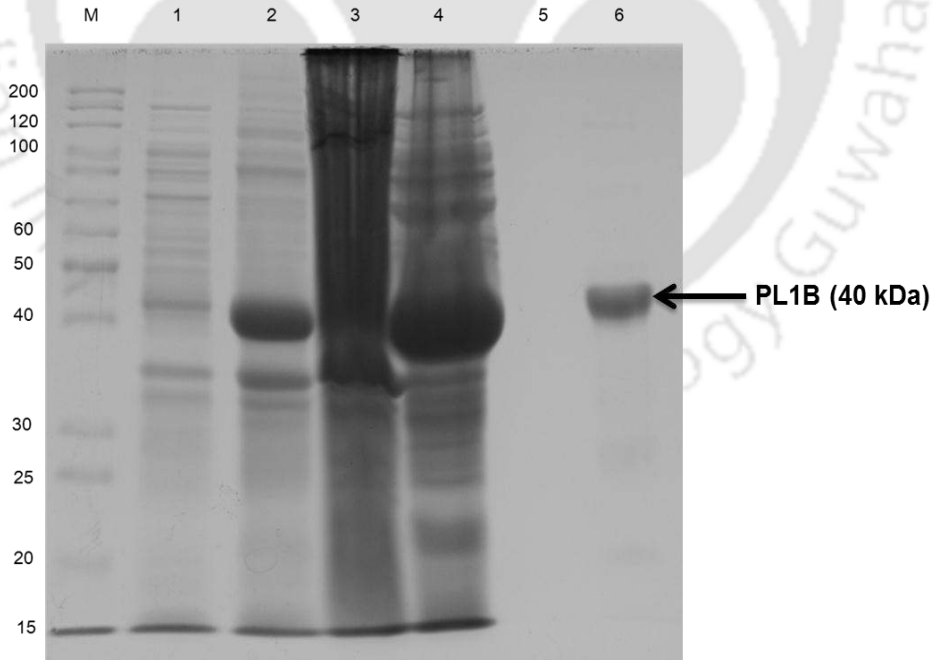


**Fig. 2.8B** SDS-PAGE (10.5%) gel showing expression and purification of PL1B in *E. coli* BL-21 cells, Lane M: Page Ruler marker (Fermentas), Lane 1: Uninduced cells, Lane 2: Induced cells, Lane 3: Cell pellet (cell debris after sonication), Lane 4: Cell free extract, Lane 5: Last column wash, Lane 6: Purified dialyzed PL1B (40 kDa approx.).

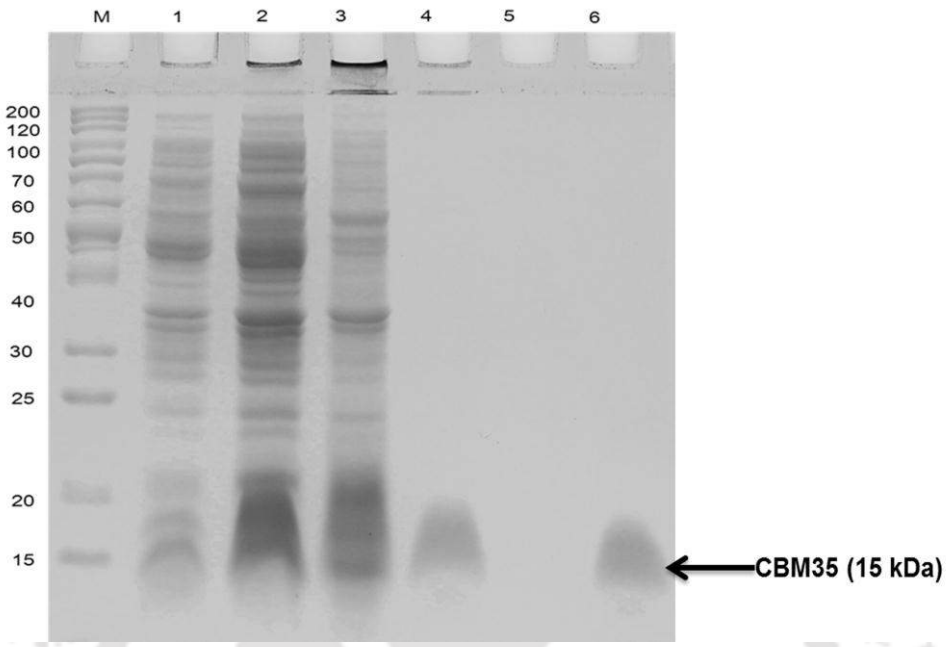


**Fig. 2.8C** SDS-PAGE (12.5%) gel showing expression and purification of recombinant protein CBM35 in *E. coli* BL-21 cells, Lane M: Page Ruler marker (Fermentas), Lane 1: Uninduced CBM35 cells, Lane 2: Induced CBM35 cells, Lane 3: Cell pellet (cell debris after sonication), Lane 4: Cell free extract, Lane 5: Last column wash, Lane 6: Purified dialyzed CBM35 (15 kDa approx.).

### 2.3.5 Protein estimation of expressed and purified recombinant derivatives

The amount of purified recombinant proteins obtained from 100 ml of grown cultures was calculated using the formula mentioned in Section 2.2.16 and is listed in Table 2.14. The concentrations of recombinant proteins purified after HiTrap column and after dialysis against respective buffers were in the range of 1.4-0.8 mg/ml (Table 2.14). The total amount of recombinant enzymes present in eluted 2 ml of was 2.1mg (PL1B-CBM35), 2.8 mg (PL1B), and 1.6 mg (CBM35) as displayed in Table 2.3.3.

**Table 2.14** Amount of purified recombinant proteins obtained from 100 ml cultures.

| Recombinant protein | Protein concentration (mg/ml) | Volume of purified protein (ml) | Total amount of purified protein (mg) |
|---|---|---|---|
| PL1B-CBM35 | 1.05±0.13 | 2.0 | 2.10±0.13 |
| PL1B | 1.40±0.15 | 2.0 | 2.80±0.15 |
| CBM35 | 0.80±0.05 | 2.0 | 1.60±0.05 |

## 2.4 Conclusions

Family 1 polysaccharide lyase (PL1) PL1B-CBM35 and its truncated derivatives PL1B and CBM35 were cloned from the genomic DNA of *Clostridium thermocellum* ATCC 27405 (GenBank Accession No: ABN53381.1). The molecular architecture revealed an N-terminal catalytic family 1 polysaccharide module (PL1B, 1059 bp) followed by C-terminal carbohydrate binding modules (CBM35, 372 bp) sandwiched between these two domains is a type 1 dockerin domain. The PCR amplified fragment of full length gene encoding PL1B-CBM35 showed a band of 1701 bp, whereas, the gene encoding truncated catalytic module (PL1B) and binding module (CBM35), displayed the sizes of 1059 bp and 372 bp, respectively. The PCR amplified fragments were cloned into pGEM-T Easy vector for TA cloning and transformed using E. coli (XL10 Gold) competent cells. Positive clones were selected by blue-white colony screening, and plasmid DNA was isolated for restriction digestion. NheI and XhoI digested plasmid DNA after running on 0.8% agarose gel produced a band of 3 kb for pGEM-T Easy vector and corresponding bands of 1.7 kb, 1 kb and 0.4 kb were produced from the insert fragments of PL1B-CBM35, PL1B and CBM35, respectively. The restriction enzyme digested fragments of PL1B-CBM35, PL1B and CBM35 were ligated with linearized pET-28a(+) vector. The ligated mixture was transformed using E. coli (XL10 Gold) competent cells. The positive clones containing recombinant plasmid DNA were screened by restriction enzyme digestion using restriction enzymes, NheI and XhoI. The restriction enzyme digested products were run on 0.8% agarose gel, where 5.4 kb band was produced for pET-28a(+) vector and corresponding bands of 1.7 kb, 1 kb and 0.4 kb were produced from the insert fragments for genes encoding PL1B-CBM35, PL1B and CBM35,

respectively. The positive clones containing recombinant plasmid DNA were transformed into E. coli (BL21) competent cells and the recombinant proteins were hyper-expressed. The purified recombinant proteins displayed a band of approximately, 50 kDa for PL1B-CBM35, 40 kDa for PL1B and a band of 15 kDa for CBM35 on SDS-PAGE. The amount of protein obtained from 100 ml E.coli culture of the recombinant proteins PL1B, PL1B-CBM35 and CBM35 after Immobilized metal ion affinity chromatography (IMAC) purification were 2.1 mg, 2.8 mg and 1.6 mg, respectively.

## 2.5 References

Bayer, E.A., Shoham, Y. Lamed, R. (2000) Cellulose-decomposing prokaryotes and their enzyme systems. In (3rd ed.) Dworkin, M., Falkow, S., Rosenberg, E., Schleifer, K.H., and Stackebrandt, E. (ed.), The Prokaryotes: An Evolving Electronic Resource for the Microbiological Community. 2: 578–617.

Boraston, A.B., Bolam, D.N., Gilbert, H.J., Davies, G.J. (2004) Carbohydrate-binding modules: fine-tuning polysaccharide recognition. Biochemical Journal, 382: 769–781.

Cantarel, B.L., Coutinho, P.M., Rancurel, C., Bernard, T., Lombard, V., Henrissat, B. (1999) The Carbohydrate-Active EnZymes database (CAZy): an expert resource for Glycogenomics. Nucleic Acids Research, 37: D 233–238.

Carpita, N.C., Gibeaut, D.M. (1993) Structural models of primary cell walls in flowering plants: consistency of molecular structure with the physical properties of the walls during growth. Plant Journal, 3: 1–30.

Davis, G., Henrissat, B. (1995) Structures and mechanisms of glycosyl hydrolases. Structures, 3: 853–859.

Deutscher, J. (2008) The mechanisms of carbon catabolite repression in bacteria. Current Opinion in Microbiology, 11: 87–93.

Engler, M.J., Richardson, D.C. (1982) DNA ligases. In P.D. Boyer (ed.), *The Enzymes*. Academic Press, San Diego. 15: 3–30.

Guillen, D., Sanchez, S. Rodriguez-Sanoja, R. (2010) Carbohydrate-binding domains: multiplicity of biological roles. Applied Microbiology and Biotechnology, 85: 1241–1249.

Hanahan, D. (1983) Studies on transformation of *Escherichia coli* with plasmids. Journal of Molecular Biology, 166: 557–580.

Jurnak, F., Kita, N., Garrett, M., Heffron, S. E., Scavetta, R., Boyd, C., Keen, N. (1996) Functional implications of the three-dimensional structures of pectate lyases. In Pectin and Pectinases, vol. 14, pp. 295–308. Edited by J. Visser and A .G. J. Voragen. Amsterdam: Elsevier.

Layne, E. (1957) Spectrophotometric and Turbidimetric Methods for Measuring Proteins. Methods in Enzymology 3: 447-455.

Lombard, V., Bernard, T., Rancurel, C., Brumer, H., Coutinho, P.M., Henrissat, B. (2010) A hierarchical classification of polysaccharide lyases for glycogenomics. Biochemical Journal, 432: 437-444

McKie, V.A., Vincken, J.P., Voragen, A.G.J., Van Den Broek, L., Stimson, E., Gilbert, H.J. (2001) A new family of rhamnogalacturonan lyases contains an enzyme that binds to cellulose. Biochemical Journal, 355: 167–177.

Montanier, C., van Bueren, A.L., Dumon, C., Flint, J.E., Correia, M.A., Prates, J.A., Firbank, S.J., Lewis, R.J., Grondin, G.G., Ghinet, M.G., Gloster, T.M., Herve, C., Knox, J.P., Talbot, B.G., Turkenburg, J.P., Kerovuo, J., Brezezinski, R., Fontes, C.M.G.A., Davies, G.J., Boraston, A.B., Gilbert, H.J. (2009) Evidence that family 35 carbohydrate binding modules display conserved specificity but divergent function. Proceedings of National Academy of Science (USA), 106(9): 3065–3070.

Ochiai, A., Itoh, T., Maruyama, Y., Kawamata, A., Mikami, B., Hashimoto, W., Murata, K. (2007) A novel structural fold in polysaccharide lyases: *Bacillus*

*subtilis* family 11 rhamnogalacturonan lyase yesw with an eight-bladed β-propeller. Journal of Biological Chemistry, 282: 37134–37145.

Pages, S., Valette, O., Abdou, L., Belaich, A., Belaich, J.P. (2003) A rhamnogalacturonan lyase in the *Clostridium cellulolyticum* cellulosome. Journal of Bacteriology, 16: 4727–4733.

Park, J.M., Vinuselvi, P., Lee, S.K. (2012) The mechanism of sugar-mediated catabolite repression of the propionate catabolic genes in *Escherichia coli*. Gene, 504: 116–121.

Sambrook, J., Russel, D.W. (2001) In (3rd ed.) *Molecular Cloning: A Laboratory Manual,* Vol. 1. Cold Spring Harbor Laboratory Press, Woodbury, New York.

Sambrook, J., Fritsch, E.F., Maniatis, T. (1989) In (2nd ed.) *Molecular Cloning: A Laboratory Manual,* Vol. 1. Plainview, Cold Spring Harbor Laboratory Press, Woodbury, New York.

Shoseyov, O., Shani, Z., Levy, I. (2006) Carbohydrate binding modules: biochemical properties and novel applications. Microbiology and Molecular Biology Review, 70: 283–295.

Stoscheck, C.M. (1990) Quantitation of Protein. Methods in Enzymology, 182: 50–69.

Studier, F.W., Moffatt, B.A. (1986) Use of bacteriophage T7 RNA polymerase to direct selective high-level expression of cloned genes. Journal of Molecular Biology, 189: 113–130.

Studier, F.W., Rosenberg, A.H., Dunn, J.J., Dubendorff, J.W. (1990) Use of T7 RNA polymerase to direct expression of cloned genes. Methods Enzymology, 185: 60–89.

Tunnicliffe, R.B., Bolam, D.N., Pell, G., Gilbert, H.J., William, M.P. (2005) Structure of a mannan-specific family 35 carbohydrate-binding module: evidence for significant conformational changes upon ligand binding. Journal of Molecular Biology, 347(2): 287–296.

van Bueren, A.L., Morland, C., Gilbert, H.J., Boraston, A.B. (2005) Family 6 carbohydrate binding modules recognize the non-reducing end of β-1,3-linked glcans by presenting a unique ligand binding surface. Journal of Biological Chemistry, 280: 530–537.

# Chapter 3

## Biochemical and functional characterization, stability studies of PL1B-CBM35, PL1B and binding analysis of CBM35

### 3.1 Introduction

Plant cell wall degradation carried out by saprophytic and phytopathogenic microbes is essential for the recycling of carbon stored in plant biomass which is of intrinsic biotechnological importance. Plant cell walls are composed of a complex network of polysaccharides, primarily cellulose, hemicelluloses and pectic substances (Carpita *et al*., 1993). The middle lamella of plant cell wall is composed of pectinaceous intercellular materials such as Pectic acid and Pectin. These components provide rigidity and act as a cementing material between two adjacent cells which are present there in the form of calcium pectate or magnesium pectate. The relative molecular masses of pectic substances range from 25 to 360 kDa. Pectic substances account for 0.5–4.0% of the fresh weight of plant material (Kashyap *et al*., 2001). Pectic acid is composed of galacturonic acid backbone which is hydrophilic and

readily soluble. Pectic polysaccharides can also form salt bridges with $Mg^{2+}$ and $Ca^{2+}$ ions to form insoluble gels. The carboxylic group of galacturonic acid are weak acid and usually exists in negatively charged or uncharged state depending on their protonation (Rastogi, 1998). Pectin is the methylated ester of polygalacturonic acid, which consists of chains of 300 to 1000 galacturonic acid units joined with α-1,4 linkages (Gibbons *et al*., 2002). This recalcitrant carbohydrate is more soluble in water than cellulose and hemicellulose, suggesting that it constitutes the initial target for plant associated microbial attack (Ochiai *et al*., 2007). Pectins are divided into three polysaccharides i.e., homogalacturonan (HG), rhamnogalacturonan type-I (RG-I) and rhamnogalacturonan type-II (RG-II). HG is present as a linear backbone, while RG-I and RG-II are branched carbohydrates (Darvill *et al*., 1978). Due to the structural complexity, pectin degradation requires the concerted action of several enzymes. The enzymatic degradation of polygalacturonan involves two well-known enzymatic mechanisms: i) hydrolysis by glycoside hydrolases (GH) that cleave glycoside bonds in the polysaccharide and ii) β-elimination reactions carried out by polysaccharide lyases resulting in oligomers with Δ4,5 unsaturated residues at the non-reducing end (Linhardt *et al*., 1986; Davis *et al*., 1995). Pectate lyases are widely distributed among microbial plant pathogens like *Erwinia sp*. (Hugouvieux-Cotte-Pattat *et al*., 1996; Pissavin *et al*., 1996; Shevchik *et al*., 1997) although they have also been found in saprophytic bacteria including the genus *Bacillus sp.* (Soriano *et al*., 2006; Sukhumsiirchart *et al*., 2009) and *Clostridium sp.* (Pages *et al*., 2003). *Clostridium thermocellum* is an anaerobic, saccharolytic and thermophilic bacterium that organizes a consortium of plant cell wall degrading enzymes in a large multienzymatic complex termed the cellulosome (Bayer *et al*., 1983; Lamed *et al*.,

1983). The cellulosome is assembled via the interaction of individual type-I dockerins located at the C-terminus of enzymes into one of the nine cohesins of the scaffoldin subunit, CipA (Lamed *et al*., 1983). The majority of glycoside hydrolases that attack cellulose and hemicelluloses are modular enzymes consisting of catalytic modules appended to non-catalytic carbohydrate binding modules (CBMs) (Davis *et al*., 1995). Pectinases on the contrary generally have a relatively simple structure lacking CBMs, which is possibly explained by the accessibility of pectins to soluble biocatalysts (McKie *et al*., 2001).

Biochemical and functional characterization of PL1B-CBM35 and PL1B is essential to understand the mechanism of catalysis and to determine their substrate specificity. In the present study the full length module PL1B-CBM35 and truncated catalytic module PL1B were investigated and functionally characterized. The enzyme activities of PL1B-CBM35 and PL1B against various pectic polysaccharides and other carbohydrates were determined. The specific activity and kinetic parameters of both these enzymes were compared to explore the influence of CBMs on the enzyme activity. Structural stability of catalytic module PL1B under the influence of varying temperatures and chaotropic agents was studied. Binding analysis of CBM35 was carried out to determine its affinity towards various polysaccharides.

## 3.2 Materials and Methods

### 3.2.1 Substrates and reagents

Polygalacturonic acid (PGA) from citrus, rhamnogalacturonan from soyabean (RGAS) and potato (RGAP), pectic galactans from potato (PGP) and lupin (PGL), wheat arabinoxylan, pustulan, crudlan, mannan, galactomannan were purchased from Megazyme International, Ireland. Pectins from citrus fruits (with varying degrees of methyl-esterification, PC) and apple (PA), oat spelt xylan, birchwood xylan, carboxy methylcellulose (CMC), carboxy ethylcellulose (CEC) were purchased from Sigma Chemical Co., USA. Trizma (Tris base), glycine, sodium hydroxide, ethylene glycol-bis(2-aminoethylether)-N,N,N′,N′-tetraacetic acid (EGTA) were procured from Sigma-Aldrich Pvt. Ltd., USA. Disodium 2-[2-carboxylatomethyl-(carboxymethyl)-amino]-ethyl-(carboxymethyl)-amino] acetate (disodium EDTA) and salts of metal ions *viz.* $Ca^{2+}$, $Mg^{2+}$, $Ni^{2+}$, $Zn^{2+}$, $Mn^{2+}$, $Cu^{2+}$, $Co^{2+}$, $Al^{3+}$ and $Li^{+}$ were procured from Himedia Laboratories Pvt. Ltd., India. Butanol, ethanol, acetic acid, sulphuric acid and α–naphthol were purchased from Merck Limited, India. Readymade silica coated aluminium TLC plates obtained from Merck, Germany.

### 3.2.2 Enzyme activity assay

Initially the enzyme activity of PL1B-CBM35 and PL1B was determined against different substrates, in a reaction mixture containing 0.1% (w/v) of substrate dissolved in 50 mM Tris-HCl buffer (pH 7) containing 1 mM $CaCl_2$ at 50ºC for 30 min. Later on assays of PL1B-CBM35 and PL1B was carried out by incubating 10 µl (14 µg) of enzyme with 0.1% (w/v) of substrate in 50 mM Glycine-NaOH buffer containing 0.6 mM $CaCl_2$ for 15 min under the optimized condition of pH, temperature and $CaCl_2$ concentration. The reactions were stopped by incubation on

ice for 10 min and centrifuged at 13,000g for 5 min. The supernatant containing the released unsaturated oligogalacturonates was measured by spectrophotometer (Cary 100 Bio Varian). The molar extinction coefficient used for the unsaturated oligogalacturonates released at 235 nm ($A_{235}$), was 4,600 $M^{-1}cm^{-1}$ (Hasegawa *et al*., 1966). 1 Unit of enzyme was defined as the amount of enzyme that forms 1 µmole of 4,5-unsaturated oligogalacturonates per minute, under the described assay conditions.

**3.2.2.1 Calculation of enzyme activity**

The activity of the enzyme was expressed as U/ml and the specific activity as U/mg of protein. 1 Unit of enzyme was defined as the amount of enzyme that forms 1 µmole of 4,5-unsaturated oligogalacturonates per minute. The enzyme activities of PL1B-CBM35 and PL1B were calculated as described below,

$$\text{Enzyme activity (U/ml)} = \frac{\Delta A_{235} \times 1000}{\varepsilon \times t \times v}$$

Where,

$\Delta A_{235}$ = Absorbance of unsaturated oligogalacturonates

ε = Molar extinction of unsaturated oligogalacturonates at $A_{235}$, 4,600 $M^{-1}cm^{-1}$

t = Time of reaction in min

v = Total volume of reaction in ml

$$\text{Specific activity (U/mg)} = \frac{\text{Enzyme activity (U/ml)}}{\text{Concentration of protein used (mg/ml)}}$$

### 3.2.3 Substrate specificity of PL1B-CBM35 and PL1B

Recombinant PL1B-CBM35 and PL1B was assayed against several polysaccharides, to determine their substrate specificity. According to several reports of family 1 polysaccharide lyase it has been found that these enzymes showed activity on pectic polysaccharides. Hence the major substrates were polygalacturonic acid, pectin, rhamnogalacturonan, pectic galactans and lupins. Initially the activity of PL1B-CBM35 and PL1B was determined in a 1 ml reaction volume containing 0.1% (w/v) of substrate dissolved in 50 mM Tris-HCl buffer (pH 7), 1 mM $CaCl_2$ and 0.7 mg/ml enzyme at 50 ° C for 30 min. Finally the substrate specificity was determined following the optimized conditions of pH, temperature and $CaCl_2$ concentration. The enzyme activity and specific activity was calculated by using the formula mentioned in Section 3.2.2.1.

### 3.2.4 Determination of optimum pH of PL1B-CBM35 and PL1B

The optimum pH of PL1B-CBM35 and PL1B was determined after performing enzyme assay in a wide range of pH using three different buffers. Activity of PL1B-CBM35 and PL1B at different pH values was determined by incubating the enzymes with 0.1% (w/v) Polygalacturonic acid (PGA) at 50°C using following buffers: 50 mM Tris-HCl (pH 7.0-9.0), 50 mM Glycine-NaOH (pH 9.0-11) and 50 mM $Na_2HPO_4$-NaOH (11-12), and the absorbance was measured at $A_{235}$ nm to calculate the specific activity as mentioned earlier in Section 3.2.2.1.

### 3.2.5 Determination of optimum temperature of PL1B-CBM35 and PL1B

The optimized pH and optimized concentration of $CaCl_2$ was used for determination of optimum temperature. PL1B-CBM35 and PL1B activity was determined by performing the enzyme assay in the temperature range, 10-100°C.

Each enzyme reaction of 1 ml was prepared by dissolving 0.1% (w/v) PGA in 50 mM Glycine-NaOH buffer 9.6 for PL1B-CBM35 and pH 9.8 for PL1B, containing 0.6 mM $CaCl_2$. Specific activity at different temperatures was determined from amount of unsaturated oligogalacturonates produced at $A_{235}$nm as mentioned earlier in Section 3.2.2.1.

### 3.2.6 Determination of pH stability of PL1B-CBM35 and PL1B

The pH stability was determined after incubating 20 µl (1.4 mg/ml) of both the enzymes in 80 µl 50 mM of different buffers of pH ranging from 7-12. Each enzyme was incubated at 24°C for 30 and 60 min. The residual activity of this incubated PL1B-CBM35 and PL1B was determined after performing assay in 1 ml reaction volume with 0.1% (w/v) PGA dissolved in 50 mM Glycine-NaOH buffer of 9.6 for PL1B-CBM35 and pH 9.8 for PL1B, containing 0.6 mM $CaCl_2$. The specific activity for both the enzymes was calculated as mentioned earlier in Section 3.2.2.1.

### 3.2.7 Determination of temperature stability of PL1B-CBM35 and PL1B

20 µl each of PL1B-CBM35 (1.4 mg/ml) and PL1B (1.4 mg/ml) was incubated in 80 µl 50 mM Tris-HCl pH 8.6 (optimized stable pH), at different temperature ranging from 30 to 100°C. Each enzyme was incubated for 30 and 60 min. The residual activity was determined after performing assay in 1 ml reaction volume with 0.1% (w/v) PGA dissolved in 50 mM Glycine-NaOH buffer of 9.6 for PL1B-CBM35 and pH 9.8 for PL1B, containing 0.6 mM $CaCl_2$. The specific activity for both the enzymes was calculated as mentioned earlier in Section 3.2.2.1.

### 3.2.8 Determination of kinetic parameters of PL1B-CBM35 and PL1B

The kinetic parameters of PL1B-CBM35 and PL1B were determined under optimized condition of pH, temperature and $CaCl_2$ concentration. 20 µl of PL1B-

CBM35 (1.4 mg/ml) and PL1B (1.4 mg/ml) was incubated in 1 mL of reaction volume containing 50 mM Glycine-NaOH pH 9.6 (PL1B-CBM35) and pH 9.8 (PL1B), 0.6 mM $CaCl_2$ and varying concentrations of PGA (0.01 to 0.5%, w/v). The reaction mixture was incubated at 50ºC and released unsaturated product was monitored spectophotometrically at $A_{235}$. The specific activity was calculated as mentioned earlier in Section 3.2.2.1. $k_{cat}$ and $K_m$ were determined using the Michaelis-Menten plot and Lineweaver-Burk plot, where average molecular weight of PGA was approximately, 25,000 g/mole (White *et al*., 1999). All the reactions were carried out in triplicate and results were reported as mean±SD.

### 3.2.9 Effect of metal ions on activity of PL1B-CBM35 and PL1B

The effects of different metal ions on the activity of PL1B-CBM35 and PL1B (1.4 mg/ml) were determined using 1 ml reaction mixture, containing 0.1% (w/v) PGA in 50 mM Glycine-NaOH buffer pH 9.6 (PL1B-CBM35) and pH 9.8 (PL1B) with varying low molar concentrations of respective metal salts. All reactions were incubated for 15 min at 50ºC. The effects of metals ion on the activity of PL1B-CBM35 and PL1B was studied using varying concentration of corresponding salts of metal ions *viz.* $CaCl_2$ (0.2–1.5 mM), $MgCl_2$ (0.2–2.2 mM), $MnCl_2$ (0.2–2 mM), $CuCl_2$ (0.2–2 mM), $CoCl_2$ (0.2–2 mM), $ZnSO_4$ (0.2–1.6 mM), $NiSO_4$ (0.2–1.6 mM), LiCl (0.2–2 mM) and $AlCl_3$ (0.2–2 mM).

### 3.2.10 Effect of metal ions on activity of PL1B-CBM35 and PL1B in presence of $CaCl_2$

PL1B-CBM35 (1.4 mg/ml) and PL1B (1.4 mg/ml) were treated with equimolar amount of different metal ions *viz.* $CaCl_2$, $MgCl_2$, $MnCl_2$, $CuCl_2$, $CoCl_2$, $ZnSO_4$, $NiSO_4$, LiCl, $AlCl_3$ in presence of 0.6 mM $CaCl_2$. Enzyme assay was

performed in 1 ml reaction mixture containing 0.1% (w/v) PGA in 50 mM Glycine-NaOH pH 9.6 (PL1B-CBM35) and pH 9.8 (PL1B), containing 0.6 mM $CaCl_2$ and 0.6 mM salt of respective metal ions. The enzyme activity was determined to find the effect of metal ions in the presence of 0.6 mM $CaCl_2$. The specific activity for both the enzymes was calculated as mentioned earlier in Section 3.2.2.1.

### 3.2.11 Effect of EGTA and EDTA on PL1B-CBM35 and PL1B in presence of $CaCl_2$

1 ml reaction mixture of PL1B-CBM35 or PL1B contained 0.6 mM $CaCl_2$ (optimized concentration), which was treated using varying concentration of EGTA (0.2-1.5 mM) and EDTA (0.2-2 mM). Enzyme assay was performed in 50 mM Glycine-NaOH buffer pH 9.6 (PL1B-CBM35) and pH 9.8 (PL1B) at 50°C. The unsaturated oligogalacturonates produced were determined at $A_{235}$ and the specific activity was calculated as mentioned earlier in Section 3.2.2.1.

### 3.2.12 Analysis of PL1B hydrolyzed products from substrates by TLC

10 µl of PL1B (1.4 mg/ml) was incubated in 1 ml reaction mixture containing 0.1% (w/v) PGA or citrus pectin (25% methyl-esterified). The reaction was carried out in 50 mM Glycine-NaOH buffer pH 9.8 at 50°C for different time intervals from 0 to 60 min. After reaction the enzyme was deactivated by keeping on ice for 5 min and the sample was treated with equal volume of ethanol to precipitate un-hydrolyzed polysaccharide and protein. The samples were centrifuged at 14,000g for 15 min and the supernatant was collected in a fresh micro-centrifuge tube. Ethanol was removed and samples were concentrated to 500 µl by heating at 50°C. 1 µl of sample was then loaded on the TLC plate (readymade silica coated aluminum TLC plates obtained from Merck, Germany) for running the hydrolyzed products under a solvent system

containing butan-1-ol/water/acetic acid in the ratio of 5:3:2 (Lojkwoska *et al*., 1995). The spots on TLC plates were visualized by a solution containing 0.5% (w/v) α-naphthol and 5% (v/v) sulphuric acid in ethanol (Cote *et al*., 2005), after heating at 95°C for 10 min in hot air oven. Standard oligogalacturonides like D-galacturonic acid (S1), di-galacturonic acid (S2) and tri-galacturonic acid (S3) (procured from Sigma Chem. Co., USA) were used to analyze the degradation product formed from different substrates upon enzymatic treatment.

### 3.2.13 Protein-melting study of PL1B

The protein melting curves of PL1B was generated by subjecting recombinant proteins to varying temperatures and thereafter measuring the change in the absorbance at 280 nm ($A_{280}$) by a UV-Visible spectrophotometer (Varian, Carry 100-Bio) following the method of Dvortsov *et al*. (2009). The purified PL1B was dialyzed against 50 mM Tris-HCl pH 8.6. Now 10 µl (1.4 mg/ml) of the dialyzed enzyme was used in a 1 ml solution containing 50 mM Tris-HCl pH 8.6, and the absorbance at 280 nm was measured with varying temperatures from 25 to 95°C using a peltier temperature controller. Similar experiment was carried out; with the addition of 0.6 mM $CaCl_2$ in the 1 ml solution with varying temperatures. A curve of relative absorbance versus temperature was plotted to display the melting profile of recombinant PL1B.

### 3.2.14 Structural stability of PL1B in presence of chaotropic agents

The structural stability of PL1B was monitored in presence of chaotropic agents like guanidine hydrochloride (GuHCl) or urea, under an isothermal condition by fluorescence studies. 100 µl reaction was setup using 10 µl (1.4 mg/ml) PL1B in 50 mM Tris-HCl buffer, pH 8.6 with varying concentrations of GuHCl or urea (0.2-8

M). The above solutions were incubated at room temperature for 4 h. The fluorescence spectrum of PL1B at each concentration of GuHCl or Urea was recorded on spectrofluorometer (Fluoromax 4, Jobin) after 10 times dilution of the reaction mixture. The tryptophan residues of the samples were excited at a wavelength of 295 nm and the emission spectrum was recorded in the wavelength range, 310-400 nm. The loss in structural integrity of PL1B was monitored by the shifting of the emission spectrum peak to a higher wavelength. A control sample (buffer and chaotropic agent) without PL1B was used for each concentration of the chaotropic agent. The apparent Gibbs free energy for denaturation was calculated from the relationship between fraction of denatured protein and free energy change, as described by Ahmad *et al*. 1992.

### 3.2.15 Quantitative binding analysis of CBM35 against polysaccharides

#### 3.2.15.1 Preparation of native-PAGE with soluble substrates

Binding of CBM35 to polysaccharides was evaluated by affinity electrophoresis following the protocol of Tomme *et al*., (2000) on native-PAGE in absence and presence of varying amount of polysaccharide. The native gel was prepared using stock solutions *viz.* 30% (w/v) acrylamide, 1.0 % (w/v) polysaccharide, 1M Tris-HCl (pH 8.8), 50% (v/v) glycerol, 10% (w/v) ammonium per sulfate and TEMED as described for SDS-PAGE in Chapter 2, Section 2.2.14. The only difference in native-PAGE was the absence of SDS in resolving gel. So, 7.5% resolving (native) gel was prepared following the protocol described in Chapter 2, Section 2.2.14 without SDS. 1.0% (w/v) stock solution of polysaccharides (*viz*. D-galacturonic acid, unsaturated pectic oligosaccharides, polygalacturonic acid, methyl-esterified citrus pectin, rhamnogalacturonan) were made by dissolving in

sterile deionized water until a clear solution was obtained. Thereafter, necessary amount of substrate solution (from the stock) was added to the resolving gel prior to the polymerization. The remaining components of native-PAGE, described above were added and the gel was polymerized. Bovine serum albumin (BSA) (10 µg) was loaded on the gels as an internal standard for reference. Electrophoresis was carried out at 4°C in a Mini PROTEAN Tetra pack (Bio-Rad, USA) at a constant current of 10 mA. The gels were stained with Coomassie Brilliant Blue R250 (Sigma) for identification of qualitative binding of the CBMs 7.5% native-PAGE. Quantitative analysis of substrate binding was assessed by measuring the migration distance of CBM35 for calculating the equilibrium association constant ($K_a$). Relative mobility for CBM35 was calculated as the migration distance of native protein divided by the migration distance of bromophenol blue dye front.

**3.2.15.2 Preparation of native-PAGE running buffer**

The native-PAGE buffer was prepared using components as described in Table 3.1. The native-PAGE running buffer did not contain SDS as a component unlike SDS-PAGE running buffer but the final pH was same (pH 8.3). A 5x stock of running buffer was prepared and diluted to 1x before use (Table 3.1).

**Table 3.1** Composition of 5x native-PAGE running buffer.

| Components | Final concentration (5x buffer) |
|---|---|
| Tris base | 0.125 M |
| Glycine | 1.25 M |

### 3.2.15.3 Preparation of sample buffer

A 5x sample loading buffer was prepared by dissolving the components maintaining the concentration of components as described in Table 3.2 and pH of the buffer was adjusted to 6.8. The components were dissolved in the order as mentioned in Table 3.2 to make 5x sample buffer. However, the final concentration while loading to a native-PAGE gel was always kept to 1x by mixing 4 volumes of sample (protein) with 1 volume of 5x sample buffer.

**Table 3.2** Composition of 5x sample loading buffer (Laemmli, 1970).

| Components | Final concentration (5x buffer) |
|---|---|
| Tris-HCl (pH 6.8) | 62.5 mM |
| Glycerol | 20.0 (%,v/v) |
| Bromophenol Blue | 0.025 (%, w/v) |

## 3.3 Results and Discussion

### 3.3.1 Substrate specificity of PL1B-CBM35 and PL1B

The enzyme activity of PL1B-CBM35 and PL1B was determined under the optimized conditions as described in Section 3.2.2. The activity of full length module PL1B-CBM35 and truncated catalytic module PL1B with various polysaccharides are reported in Table 3.3. Both the enzymes showed activity mainly towards pectic polysaccharides where highest activity was observed with polygalacturonic acid and citrus pectin (25% methyl-esterified). Negligible activity was observed towards other xylan and mannan based polysaccharides, this is because both PL1B-CBM35 and PL1B recognizes the galacturonic acid moiety and subsequently cleaves those polysaccharides made of polygalacturonic acid chains. Hence both this enzymes showed lesser activity to other polysaccharides in comparison with pectic polysaccharides. Both PL1B-CBM35 and PL1B showed highest activity with PGA rather than citrus pectin, and the activity was even lesser with citrus pectins with higher degree of methyl-esterification. This striking fact infers that both PL1B-CBM35 and PL1B are a pectate lyases rather than pectin lyases. But in comparison with other reported pectate lyases (Pissavin *et al*., 1998; Shevchik *et al*., 1999; Hatada *et al*., 2001) both these enzymes displayed significantly higher activity with 55% and 85% methyl-esterified citrus pectin. Similar high activity of pectate lyase on pectins with high degree of methyl-esterification has been previously reported only from *Bacillus subtillis* (Soriano *et al*., 2006). The enzymes that degrade the backbones of pectic substances utilize two distinct cleavage mechanisms, the hydrolysis or the β-elimination. The method used to evaluate the activity of PL1B-CBM35 and PL1B provide evidence that these enzymes are lyases, as they catalyse the β-eliminative

cleavage of glycosidic bonds with the production of Δ4,5 unsaturated oligogalacturonates, which can be followed spectrophotometrically at absorbance of 235 nm.

**Table 3.3** Activity of PL1B-CBM35 and PL1B towards different polysaccharides.

| Substrates (% w/v) | Specific Activity [a]PL1B-CBM35 (U/mg) | Specific Activity [b]PL1B (U/mg) |
|---|---|---|
| Polygalacturonic Acid | 3.70±0.18 | 18.50±0.23 |
| Citrus pectin (25% methyl-esterified) | 3.36±0.33 | 16.80±0.11 |
| Citrus pectin (55% methyl-esterified) | 2.70±0.12 | 13.50±0.17 |
| Citrus pectin (85% methyl-esterified) | 1.18±0.20 | 5.92±0.10 |
| Apple pectin | 1.77±0.14 | 8.88±0.21 |
| Pectic galactan (Lupin) | 0.89±0.08 | 4.44±0.11 |
| Pectic galactan (Potato) | 0.67±0.11 | 3.35±0.10 |
| Rhamnogalactouronan (Potato) | 0.05±0.04 | 0.25±0.08 |
| Rhamnogalactouronan (Soyabean) | 0.04±0.07 | 0.20±0.06 |
| Arabinoxylan (Wheat) | 0.01±0.03 | 0.01±0.03 |
| Pustulan | ND | ND |
| Mannan | 0.01±0.05 | 0.02±0.04 |
| Carob galactomannan | 0.01±0.02 | 0.02±0.03 |
| Crudlan | ND | ND |
| Oat spelt xylan | 0.01±0.02 | 0.05±0.03 |
| Birchwood xylan | 0.01±0.03 | 0.06±0.04 |
| Carboxy methyl cellulose | ND | ND |
| Carboxy ethylcellulose | ND | ND |

*All the assays were performed at 50°C using 50 mM Glycine-NaOH buffer for [a]PL1B-CBM35 (pH 9.6) and [a]PL1B (pH 9.8), with 0.6 mM $CaCl_2$.*

*The assays were performed in triplicates. The reaction conditions for measuring concentration of unsaturated oligogalacturonates and enzyme activity calculations are described in the Section 3.2.2.1.*

ND = *No activity detected.*

### 3.3.2 Optimum pH for activity of PL1B-CBM35 and PL1B

The effect of pH on the activity of the recombinant PL1B-CBM35 and PL1B was determined using PGA as substrate. The results showed that both these enzymes were active under alkaline conditions. Both PL1B-CBM35 and PL1B were active within pH range (8-10) displaying highest activity at pH 9.6 and 9.8, respectively (Fig. 3.1). Similar results were also reported for pectate lyase (PelA) activity from *Bacillus sp*. which showed optimum pH of 10 (Soriano *et al*., 2006). Hence both PL1B and PL1B-CBM35 can be called alkaline pectate lyases, unlike other pectate lyases such as PelA from *T. maritima* which showed optimum pH at 9.0 (Kluskens *et al*., 2003), Pel 15H from *Bacillus sp*. KSM-P15 which showed pH at 11.5 (Ogawa *et al*., 2000).

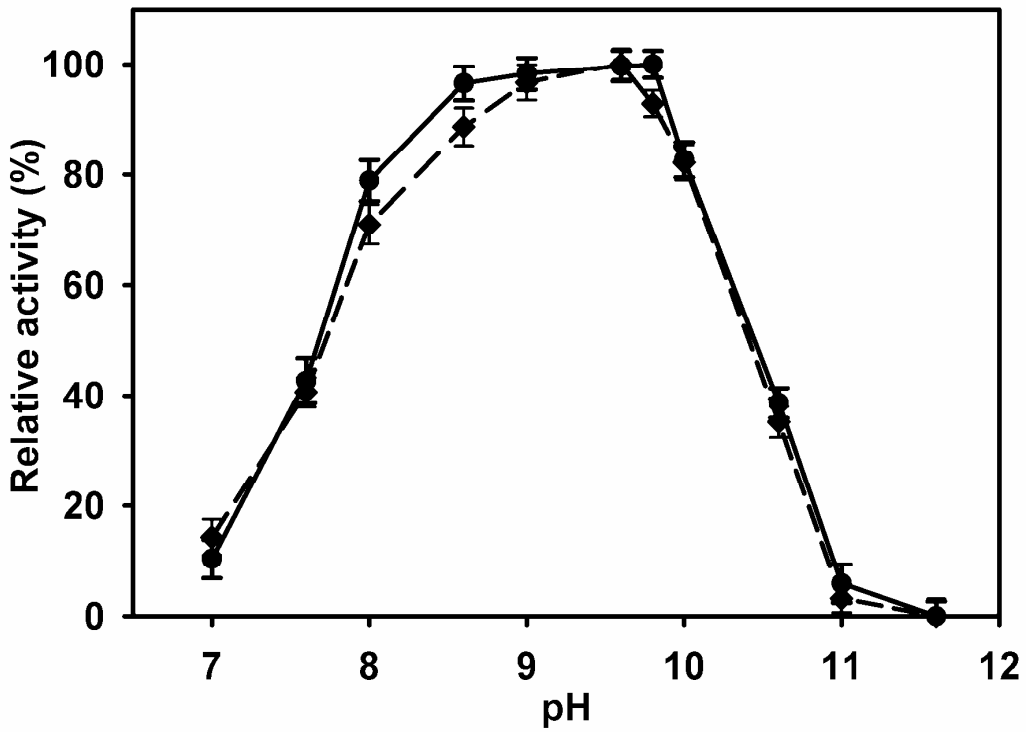


**Fig. 3.1** Optimum of pH for the activity of PL1B-CBM35 (---) and PL1B (—).

### 3.3.3 Optimum temperature for activity of PL1B-CBM35 and PL1B

The optimum temperature for the activity of PL1B-CBM35 and PL1B was determined after performing assay with PGA under varying temperatures 10 to100°C. The optimum temperature for both PL1B-CBM35 and PL1B (Fig. 3.2) was found to be 50ºC which was expected because these enzymes originated from a thermophilic bacterium. Whereas a rapid decrease of activity was seen above 70°C and 80°C for PL1B-CBM35 and PL1B respectively. Thermosatble pectate lyases reported earlier showed optimum temperature of 95°C for PelA from *Thermotoga maritima* (Kluskens *et al*., 2003) and pectate lyase from a UV mutant of *Bacillus tequilensis* SV11 showed optimum temperature of 60°C (Chiliveri *et al*., 2014).

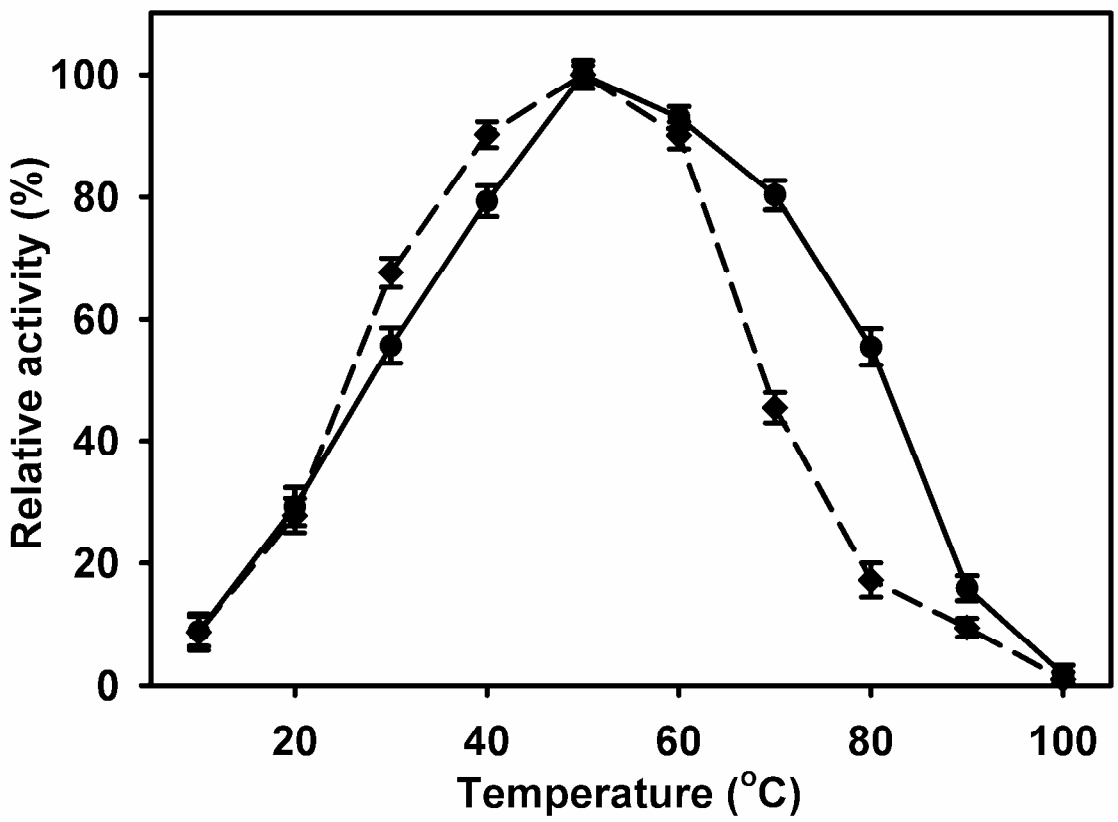


**Fig. 3.2** Optimum temperature for activity of PL1B-CBM35 (---) and PL1B (—).

### 3.3.4 pH stability of PL1B-CBM35 and PL1B

Both PL1B-CBM35 and PL1B were found to be stable in the pH range of 8-10 (Fig. 3.3), and most stable at pH 8.6. The pH stability of an enzyme depends on two factors, i) type of enzyme and direct involvement of ionic groups in the catalytic mechanism and ii) participation of charged groups in the stabilization of the protein structure (Branden *et al*., 1991). Enzyme catalysis occurs by interaction of ionic groups from amino acid side chains at the active centre of the enzyme. These ionic groups get protonated during catalysis to carry out a successful reaction. As the pH deviates from the optimum pH value the protonation state of ionic groups involved may alter and hinders proper catalysis of the substrate, thus resulting in a lower activity. Both PL1B-CBM35 and PL1B showed stability as well as optima within the pH range of 8-10 retaining more than 80% residual activity within this range.

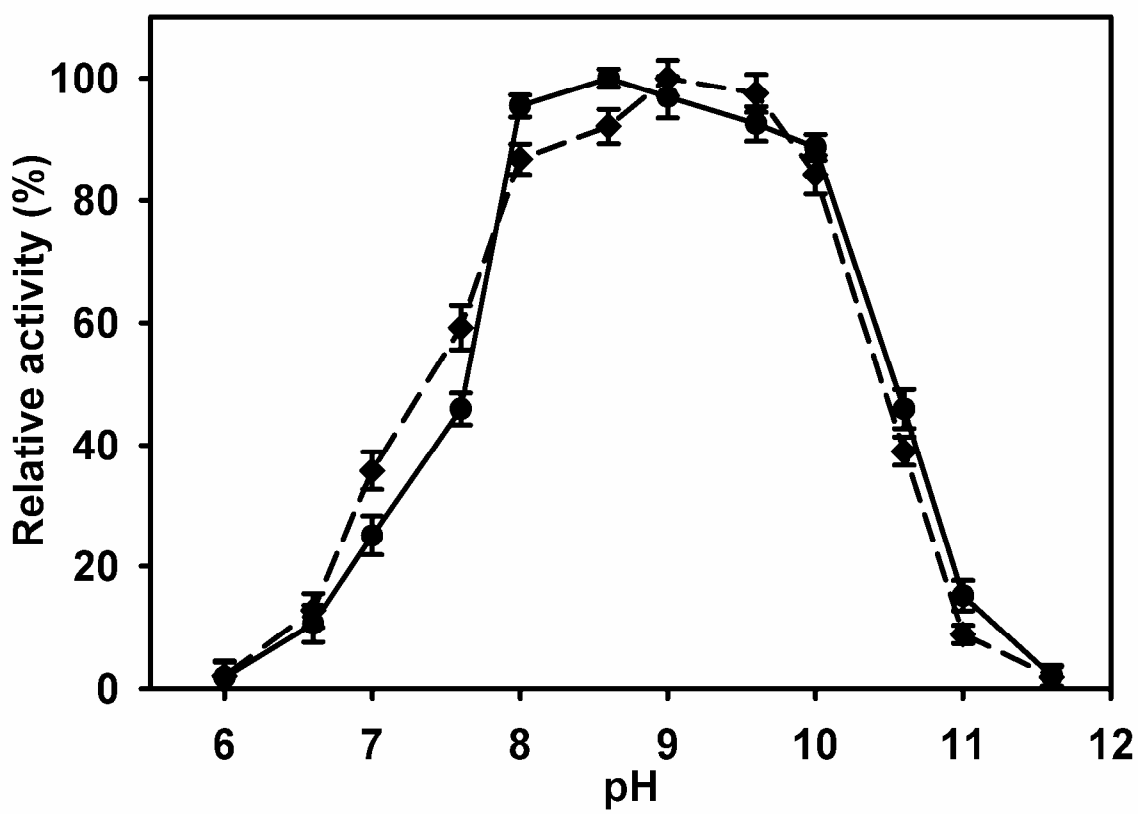


**Fig. 3.3** pH stability for the activity of PL1B-CBM35 (---) and PL1B (—).

### 3.3.5 Temperature stability of PL1B-CBM35 and PL1B

PL1B-CBM35 was stable in temperature range of 30-50°C, whereas PL1B was found to be stable in temperature range of 30-70°C (Fig. 3.3.4). However, at higher temperature more than 60°C for PL1B-CBM35 and 70°C for PL1B, there was a sharp decrease in the residual activity suggesting significant decrease in the enzyme stability (Fig. 3.4). The most accepted explanation loss of enzyme activity at high temperature is the opening or uncoiling of the protein architecture, which results in decreased stability and consequently lowering the activity (Branden *et al*., 1991; Creighton, 1992). The opening of protein tertiary structure changes the conformation of protein architecture that directly affects the velocity of enzyme catalyzed reaction.

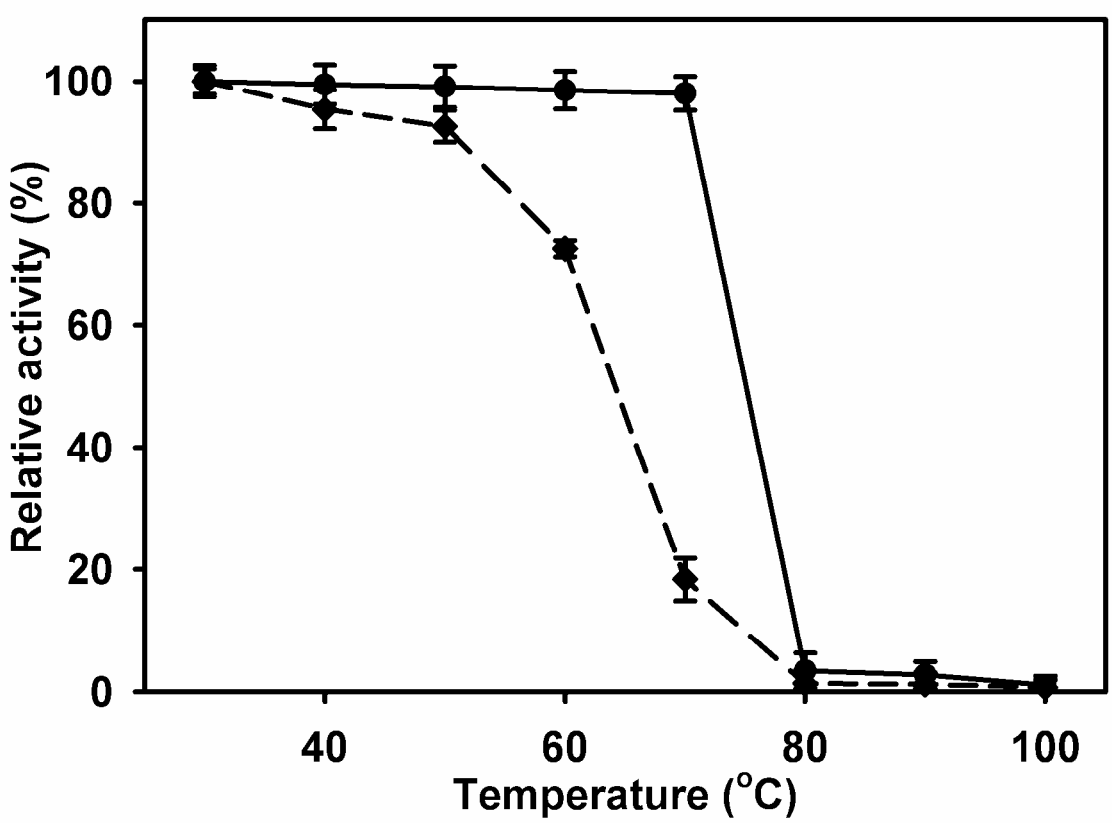


**Fig 3.4** Temperature stability for the activity of PL1B-CBM35 (---) and PL1B (—).

### 3.3.6 Kinetic parameters of PL1B-CBM35 and PL1B

Kinetic parameters of both PL1B-CBM35 and PL1B were determined against PGA and are presented in Table 3.4. The data revealed that PL1B-CBM35 and PL1B, showed turnover number values ($k_{cat}$) of 0.35 and 1.76 $min^{-1}$, respectively. The catalytic efficiency ($k_{cat}/K_m$) values exhibited by PL1B-CBM35 and PL1B were 12.5 and 62 $mM^{-1}min^{-1}$, respectively, revealing that PL1B exhibit higher catalytic efficiency on PGA than PL1B-CBM35.

**Table 3.4** Kinetic parameters of PL1B-CBM35 and PL1B with Polygalacturonic acid (PGA) from citrus. One unit of enzymatic activity (U) was defined as the amount of enzyme in mg that produces 1 mmol/L of unsaturated product per minute**.**

| Enzyme | Substrate | $k_{cat}$ ($min^{-1}$) | $K_m$ (mM) | $k_{cat}/K_m$ ($mM^{-1}$ $min^{-1}$) |
|---|---|---|---|---|
| **PL1B-CBM35** | **PGA** (citrus) | 0.35±0.04 | 0.0278±0.003 | 12.5±0.52 |
| **PL1B** | **PGA** (citrus) | 1.76±0.05 | 0.0286±0.002 | 62.0±0.43 |

*All experiments were performed in triplicate following the method mentioned in Section 3.2.8.*

### 3.3.7 Effect of metal ions on the activity of PL1B-CBM35 and PL1B

The enzymes PL1B-CBM35 and PL1B showed an exclusive requirement of $Ca^{2+}$ ions to achieve their maximum activity. PL1B-CBM35 and PL1B showed only 11% and 22% of their maximum activity in the absence of 0.6 mM $Ca^{2+}$ ions, respectively (Fig. 3.5A). The optimum $Ca^{2+}$ ions concentration required to achieve 100% pectinolytic relative activity were 0.6 mM for both PL1B-CBM35 and PL1B. It is also known that pectate lyases require $Ca^{2+}$ for *in vitro* activity and they presumably utilize the abundant $Ca^{2+}$ in the plant cell wall for *in vivo* activity (Barres *et al*., 1994; Herron *et al*., 2003). In presence of 1.2 mM $Mg^{2+}$ ion concentration both PL1B-CBM35 and PL1B showed around 98% and 97% pectinolytic activity respectively (Fig. 3.5.B). Hence, $Mg^{2+}$ ions proved to be almost equally effective as $Ca^{2+}$ ions in

enhancing the activity of these enzymes. PL1B-CBM35 and PL1B activity in presence of 1.2 mM $Mn^{2+}$ ions was 55% and 50%, respectively (Fig. 3.5C) as compared to the control. A marginal increase in the activity of PL1B-CBM35 and PL1B was observed in presence of $Ni^{2+}$ ions (39% and 50%; Fig. 3.5D), $Cu^{2+}$ ions (24% and 34%; Fig. 3.5E), $Zn^{2+}$ (18% and 29%; Fig. 3.5F), $Co^{2+}$ ions (20% and 25%; Fig. 3.5G). Trivalent cations showed enhancement of activity of PL1B-CBM35 and PL1B to 40% and 45% respectively by 0.8 mM $Al^{3+}$ ions (Fig. 3.5H). 1 mM $Li^{+}$ also enhanced the activity of both the enzymes (50% and 55%; Fig. 3.5I). The maximum activities of PL1B-CBM35 and PL1B achieved at respective concentration of metal ions are enlisted in Table 3.5.

**Table 3.5** Effect of metal ions on the activity of PL1B-CBM35 and PL1B**.**

| Metal ion | Concentration of salt (mM) | Relative activity (%) | |
|---|---|---|---|
| | | PL1B-CBM35 | PL1B |
| Control | -- | 11 | 22 |
| $Ca^{2+}$ ($CaCl_2$) | 0.6 | 100 | 100 |
| $Mg^{2+}$ ($MgCl_2$) | 1.2 | 98 | 97 |
| $Mn^{2+}$ ($MnCl_2$) | 1.2 | 55 | 50 |
| $Ni^{2+}$ ($NiSO_4$) | 1.2 | 39 | 50 |
| $Cu^{2+}$ ($CuCl_2$) | 1.0 | 24 | 34 |
| $Zn^{2+}$ ($ZnSO_4$) | 0.6 | 18 | 29 |
| $Co^{2+}$ ($CoCl_2$) | 1.2 | 20 | 25 |
| $Al^{3+}$ ($AlCl_3$) | 0.8 | 40 | 45 |
| $Li^{+}$ (LiCl) | 1.0 | 50 | 55 |

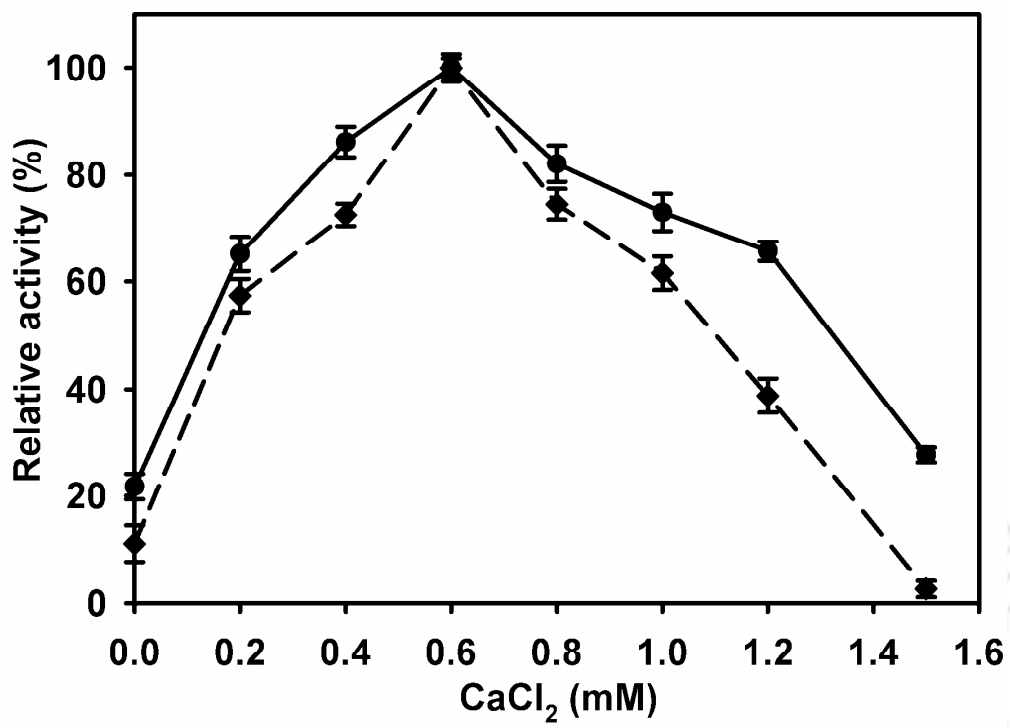


**Fig. 3.5A** Effect of $CaCl_2$ on enzyme activity of PL1B-CBM35 (---) and PL1B (—) from *Clostridium thermocellum*.

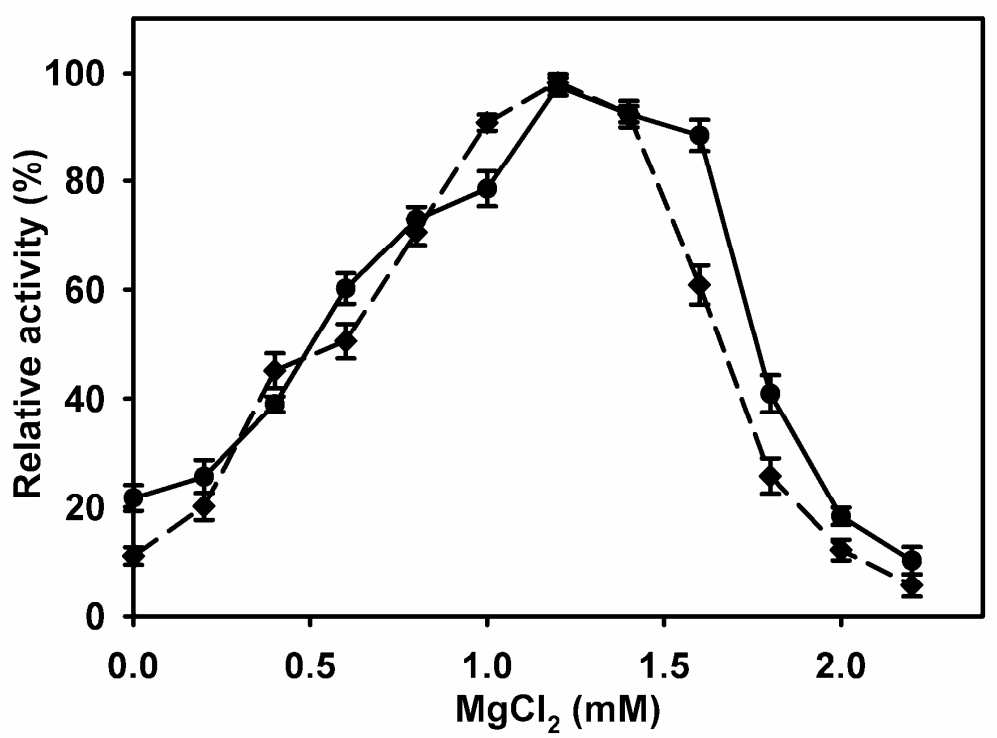


**Fig. 3.5B** Effect of $MgCl_2$ on enzyme activity of PL1B-CBM35 (---) and PL1B (—) from *Clostridium thermocellum*.

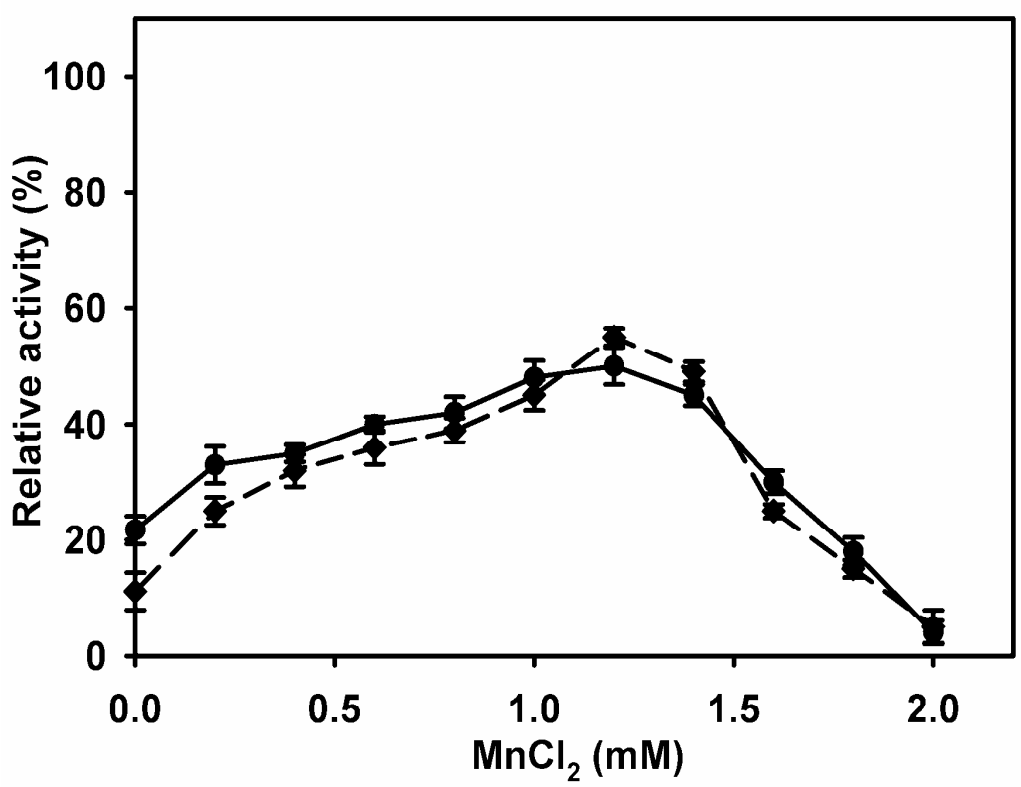


**Fig. 3.5C** Effect of $MnCl_2$ on enzyme activity of PL1B-CBM35 (---) and PL1B (—) from *Clostridium thermocellum*.

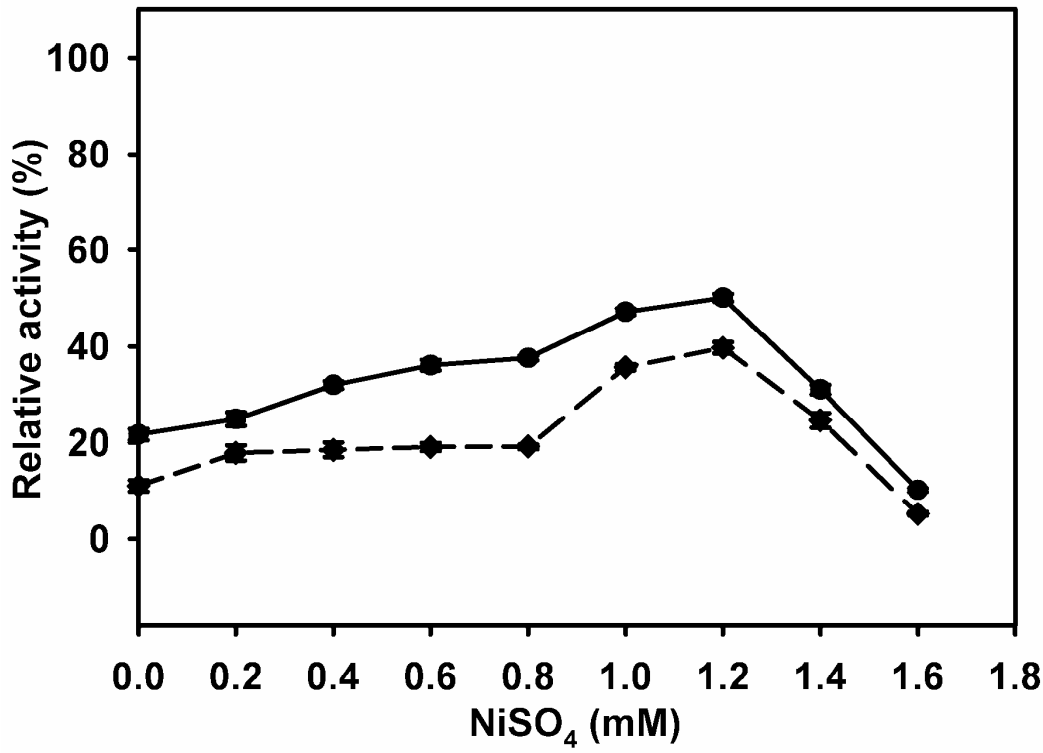


**Fig. 3.5D** Effect of $NiSO_4$ on enzyme activity of PL1B-CBM35 (---) and PL1B (—) from *Clostridium thermocellum*.

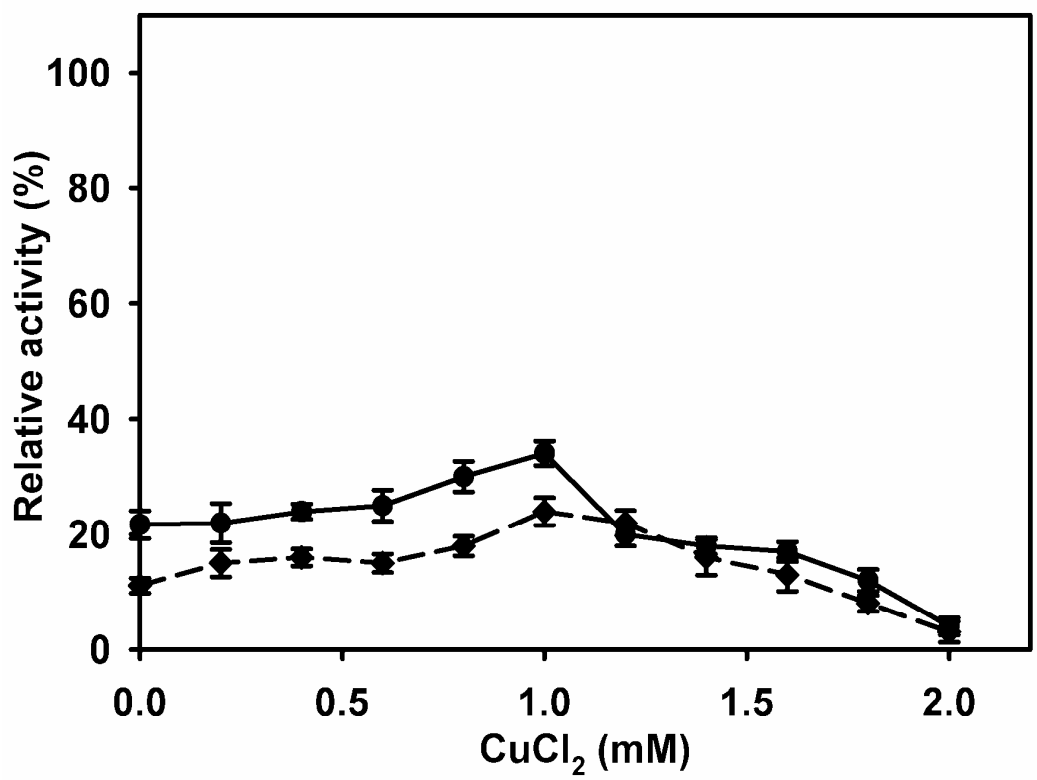


**Fig. 3.5E** Effect of $CuCl_2$ on enzyme activity of PL1B-CBM35 (---) and PL1B (—) from *Clostridium thermocellum.*

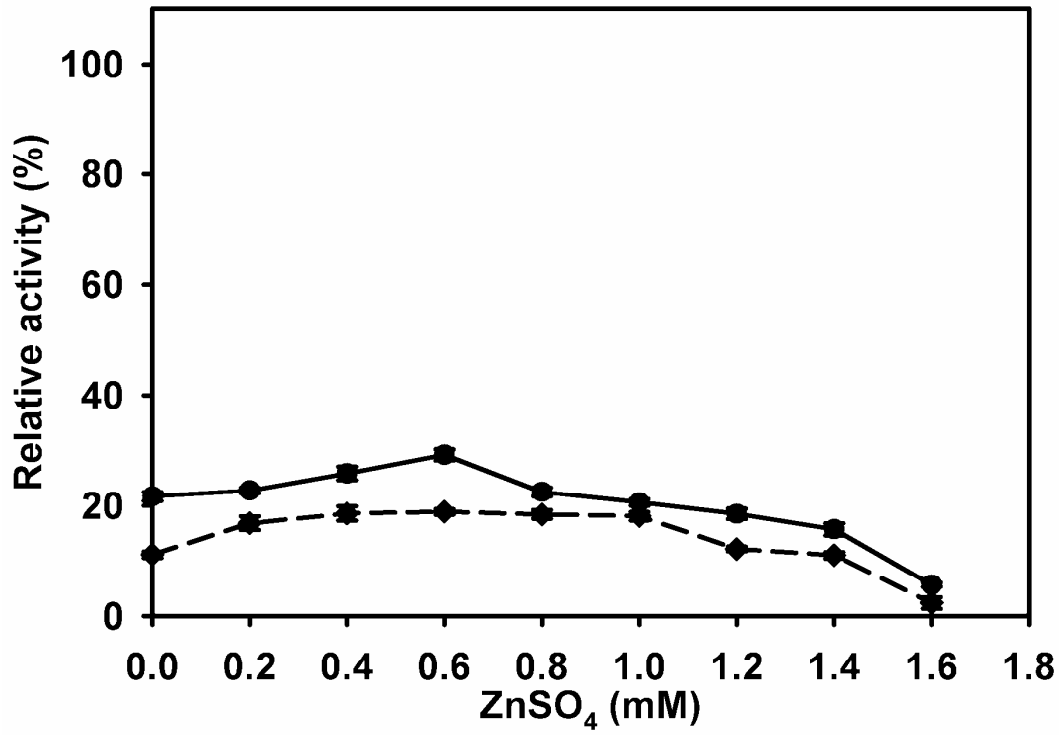


**Fig. 3.5F** Effect of $ZnSO_4$ on enzyme activity of PL1B-CBM35 (---) and PL1B (—) from *Clostridium thermocellum.*

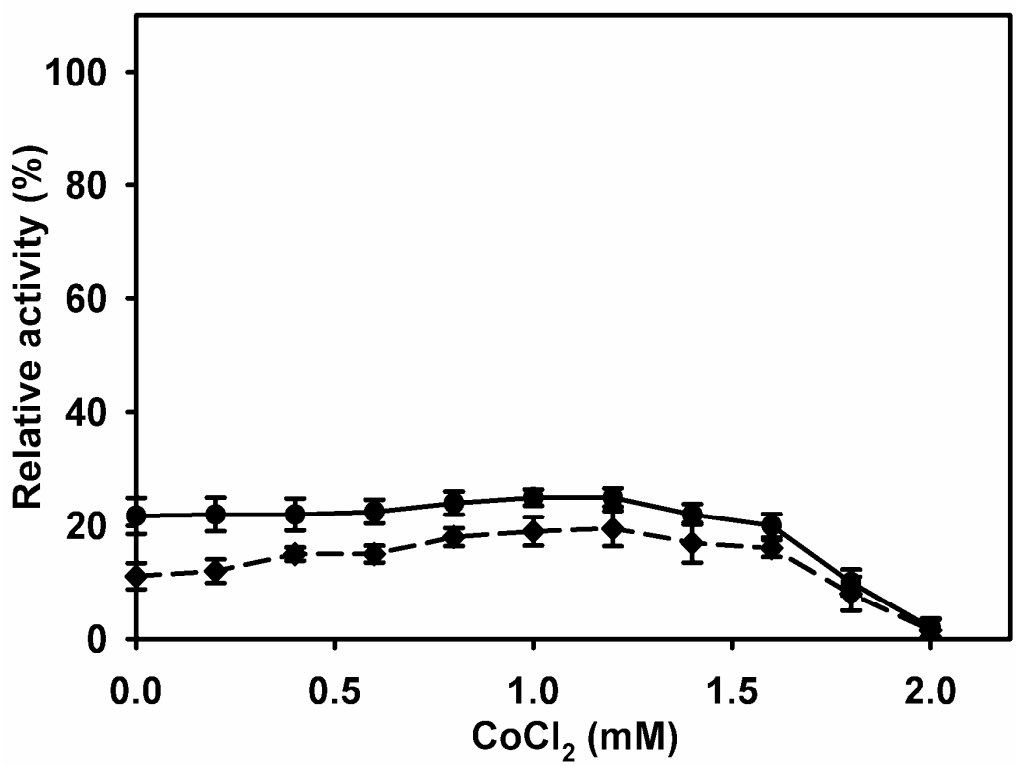


**Fig. 3.5G** Effect of $CoCl_2$ on enzyme activity of PL1B-CBM35 (---) and PL1B (—) from *Clostridium thermocellum.*

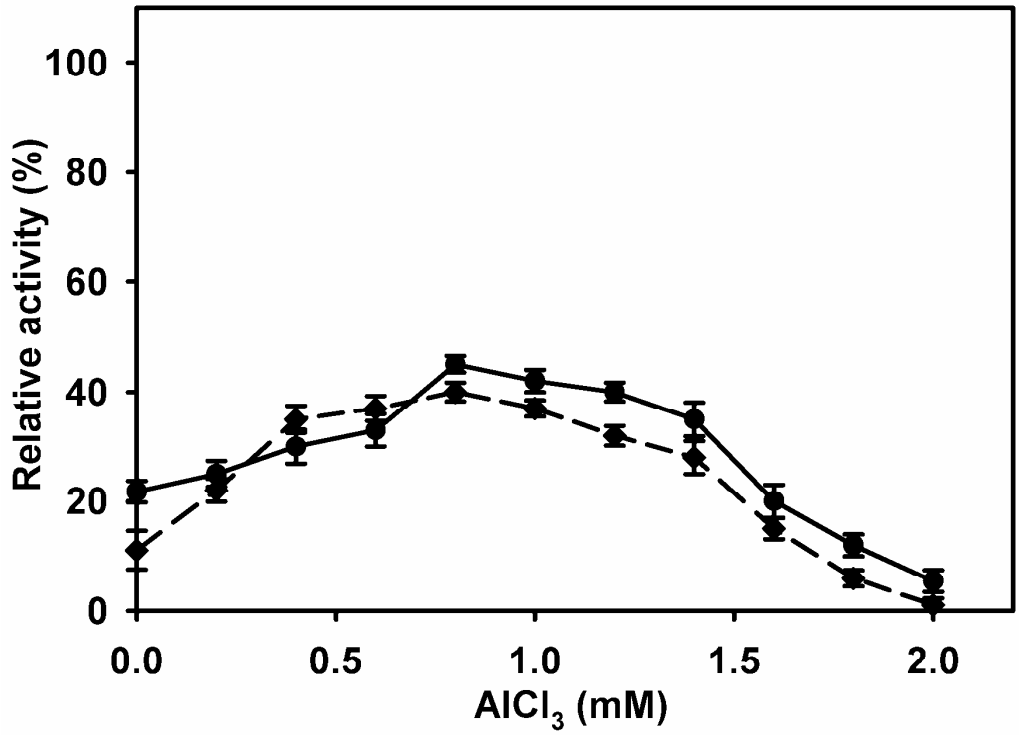


**Fig. 3.5H** Effect of $AlCl_3$ on enzyme activity of PL1B-CBM35 (---) and PL1B (—) from *Clostridium thermocellum.*

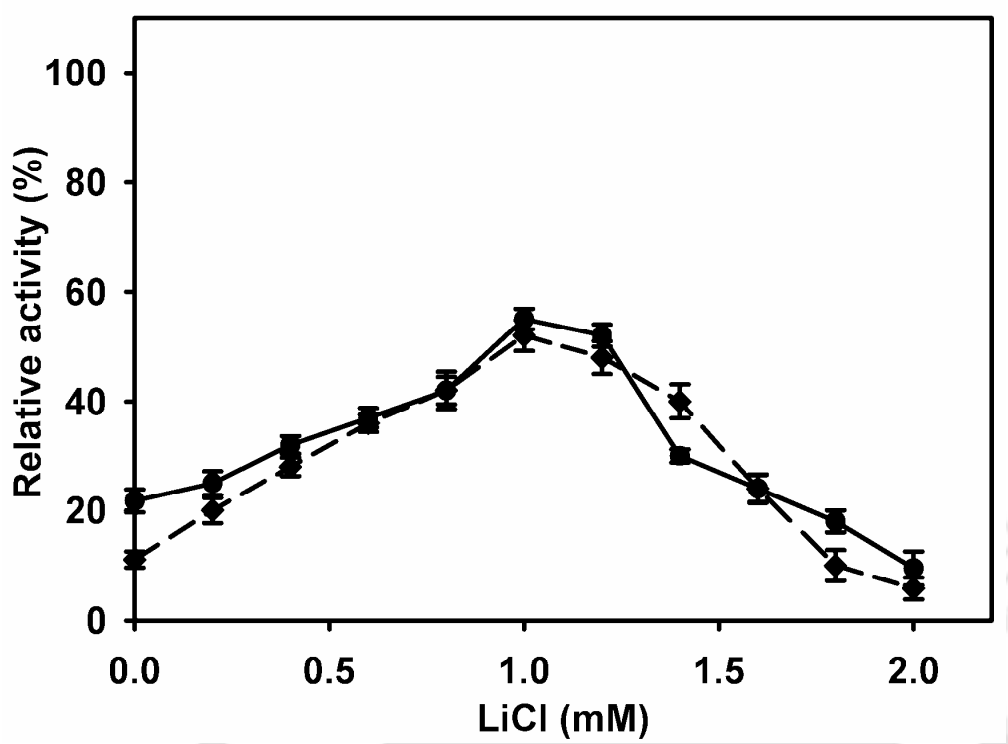


**Fig. 3.5I** Effect of LiCl on enzyme activity of PL1B-CBM35 (---) and PL1B (—) from *Clostridium thermocellum.*

### 3.3.8 Effect of other metal ions on activity of PL1B-CBM35 and PL1B in presence of $Ca^{2+}$ ions

Assay of both the enzymes was performed with equimolar concentration of different metal ions in presence of 0.6 mM $CaCl_2$. Sample containing only 0.6 mM $CaCl_2$ was considered as the control sample and its activity was taken as 100%. $MgCl_2$ and LiCl together with $CaCl_2$ increased the activity of both these enzymes 20% (22.2 U/mg) and 15% (21.3 U/mg), respectively (Fig. 3.6). Hence suggesting that these metal ions assists the amino acid side chain groups to build ionic interactions with the incoming substrate during catalysis, resulting in an enhanced catalytic efficiency. $MnCl_2$ and $NiSO_4$ reduced the activity of both the enzymes to around 50%. Whereas $CuCl_2$, $ZnSO_4$ and $CoCl_2$ significantly reduced 80% of the activity of PL1B-CBM35 and PL1B. It can be inferred from this experiment that

$MgCl_2$ or LiCl can be used as an additional additive to achieve enhanced activity of PL1B-CBM35 and PL1B along with the presence of $CaCl_2$ ions.

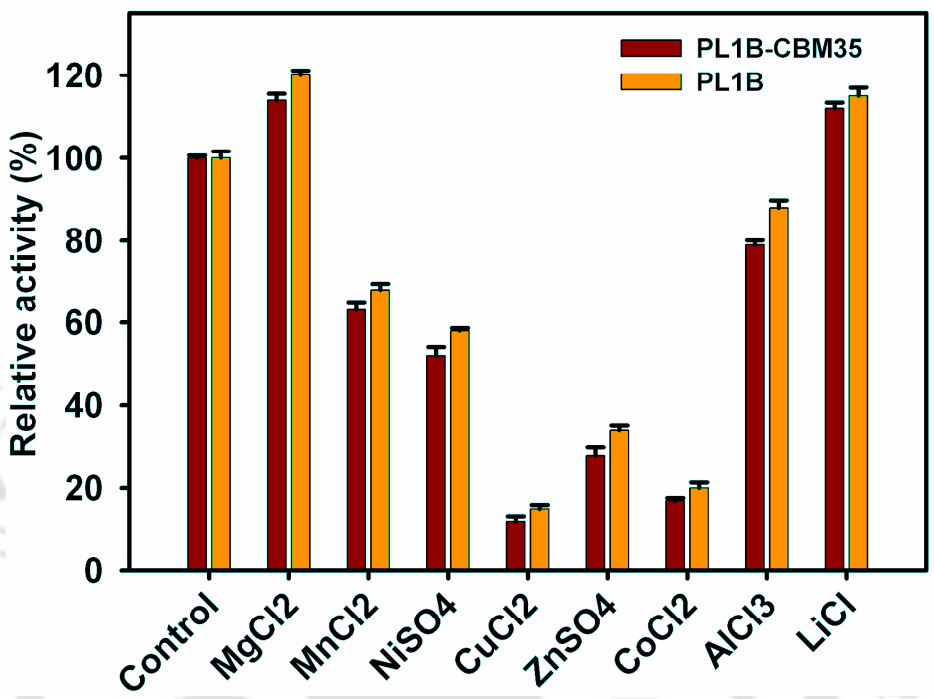


**Fig. 3.6** Effect of metal ions on activity of PL1B-CBM35 and PL1B in presence of equimolar $Ca^{2+}$ ion concentration.

### 3.3.9 Chelating effects of EGTA and EDTA on $CaCl_2$ from PL1B-CBM35 and PL1B

The activity of both the enzymes decreased to more than 90% in presence of 1.4 mM EGTA (Fig. 3.7A) as well as of 1.6 mM EDTA (Fig. 3.7B). The $Ca^{2+}$ ions were chelated by EGTA and EDTA and thus decreased the activity of both the enzymes. The extent of decrease in enzyme activity in the presence of EGTA and EDTA indicated that $Ca^{2+}$ ions are essential for their catalytic activity. It is a well known fact that EGTA specifically binds and chelates $Ca^{2+}$ ions in 1:1 molar ratio (Qin *et al*., 1999). But in this case it was found that the complete inhibition of activity of both the enzyme occurs only in presence of 1.5 mM EGTA or 1.8 mM EDTA. This clearly showed that to chelate 0.6 mM $CaCl_2$ approximately, 2-3 times more chelating

agent is required. As pectate lyase has strong affinity towards $Ca^{2+}$ ions, hence more $Ca^{2+}$ ions are present in the enzyme rather than the supplemented 0.6 mM $Ca^{2+}$ ions. These extra $Ca^{2+}$ ions the enzyme has taken up from any other source where it was available, this result also suggested that $Ca^{2+}$ ions have a strong affinity towards PL1B-CBM35 and PL1B. Again more amount of EDTA (1.8 mM) (Fig. 3.7B) in comparison with EGTA (1.5 mM) (Fig. 3.7A) was required to chelate the metal ions and to completely abolish the activity, which may be due to the presence other metal ions in the enzyme.

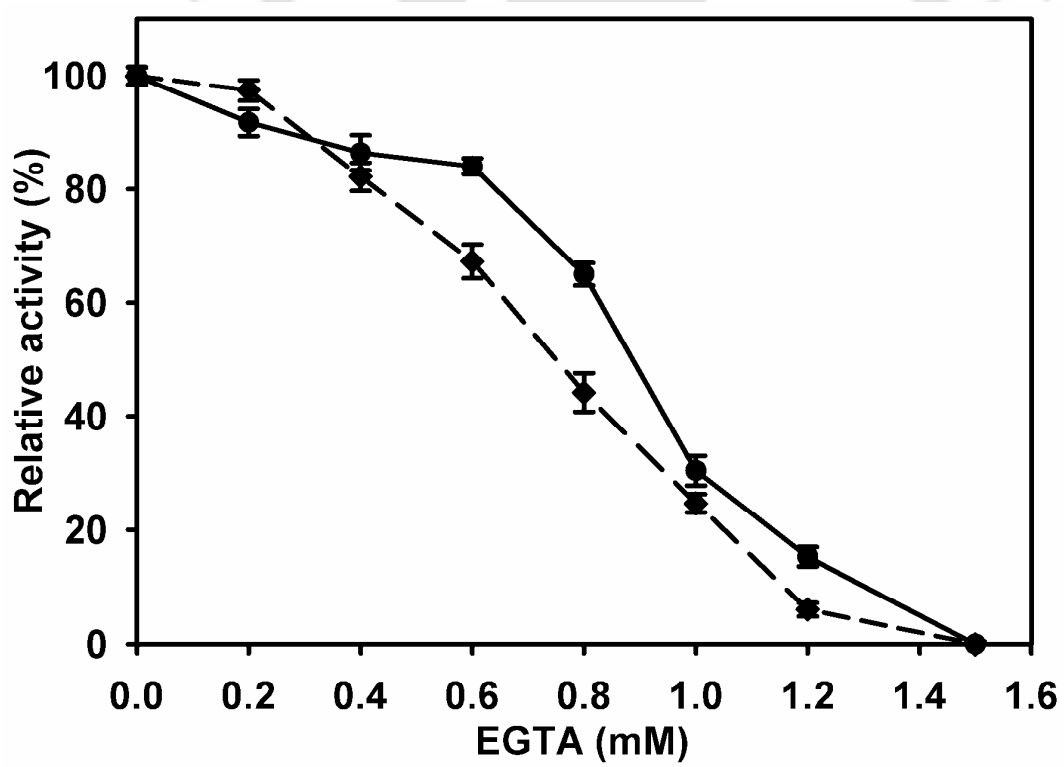


**Fig. 3.7A** Effect of EGTA on the activity of PL1B-CBM35 (---) and PL1B (—).

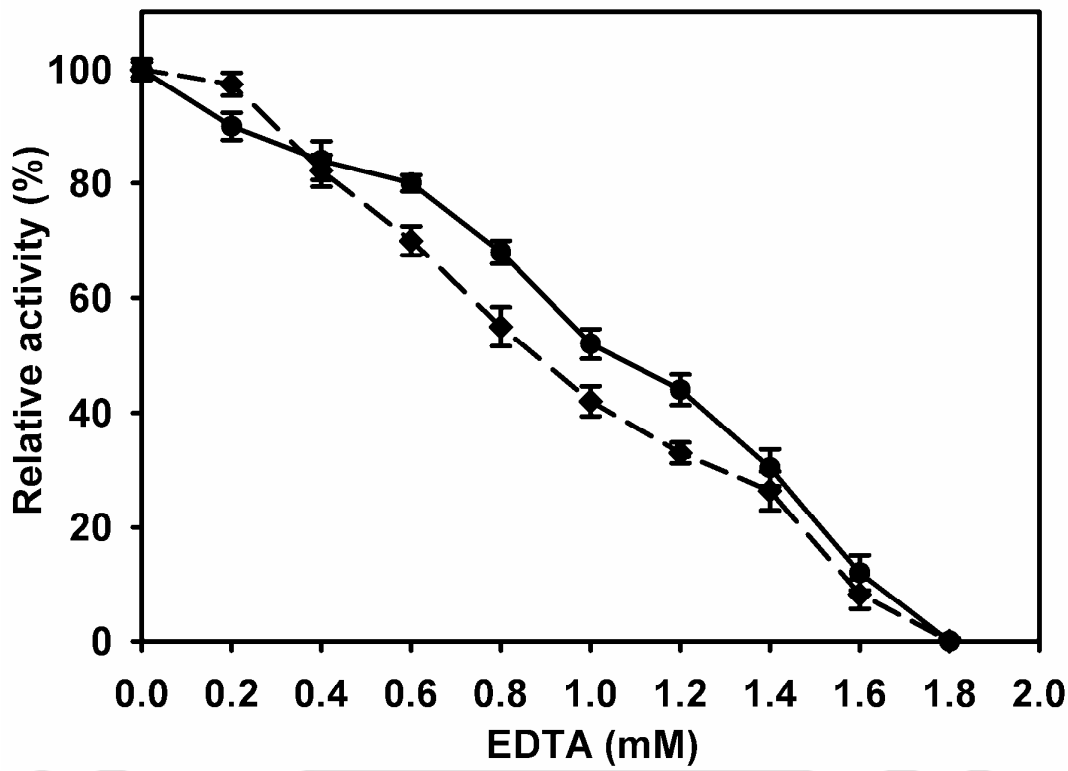


**Fig. 3.7B** Effect of EDTA on the activity of PL1B-CBM35 (---) and PL1B (—).

### 3.3.10 Analysis of the hydrolyzed products of recombinant PL1B by TLC

The products released by the enzymatic cleavage of PGA by PL1B and citrus pectin were determined after TLC analysis of the sample. The reactions were carried out under optimum conditions of pH and temperature for each individual enzyme as mentioned in Section 3.2.12. The samples from enzymatic reaction were collected at different time intervals of 0, 5, 10, 15, 20, 30, 45 and 60 min and separated through TLC. PL1B produced unsaturated di and tri-galacturonates from the beginning of the reaction and no higher size oligosaccharides were observed. The amount of unsaturated di- and tri-galacturonates increased with time and was highest at 60 min of the reaction (Fig. 3.8). The cleavage pattern of this enzyme suggested that it cleaves within the poly-galacturonan main chain of PGA and citrus pectin thus following an endo cleaving pattern. The recombinant PL1B from *Clostridium*

*thermocellum* cleaves the α-(1,4) glycosidic linkages in pectic polysaccharides by anti β-elimination mechanism resulting in Δ4,5 unsaturated galacturonates as the degradation product. Such endolytic cleavage pattern was previously reported for PelA from *Clostridium cellulovorans* (Tamaru *et al*., 2001). PelC from *B. subtilis* (Soriano *et al*., 2006), also an endo pectate lyase, showed a similar cleavage pattern producing mixtures of different degradation products, whereas PelX from *Erwinia chysanthemi* an exo-pectate lyase always produced a single degradation product either unsaturated di or tri-galacturonates (Shevchik *et al*., 1999). Hence, recombinant PL1B under investigation is conclusively an endo pectate lyase.

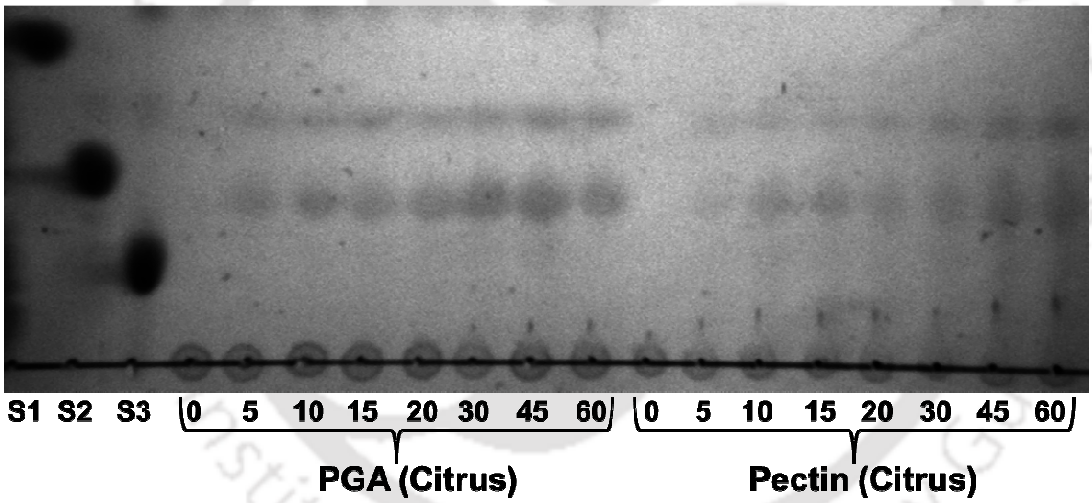


**Fig. 3.8** Thin layer chomatography (TLC) showing the enzymatic degradation products of PGA and citrus pectin (25% methyl-esterified). Chromatogram displaying hydrolysis by PL1B at 0, 5, 10, 15, 20, 30, 45 and 60 min. Standard oligosaccharides used were S1: D-galacturonic acid; S2: Di-galacturonic acid; S3: Tri-galacturonic acid.

### 3.3.11 Melting analysis of recombinant PL1B

The melting curve of PL1B displayed a single peak between 60°C and 74°C (Fig. 3.9). The presence of $Ca^{2+}$ ions (0.6 mM) caused significant change in the and the peak (shown as dotted lines) was shifted towards higher temperature protein-

melting profile of PL1B. The melting in presence of $Ca^{2+}$ ions started at 70°C and ended at 86°C (Fig. 3.9). This shifting of melting-curve peak suggested that $Ca^{2+}$ ions influence the melting because it imparts overall stability to the protein structure as also previously reported (Dvortsov *et al*., 2009). Therefore $Ca^{2+}$ ions are important for the activity and stability to PL1B structure.

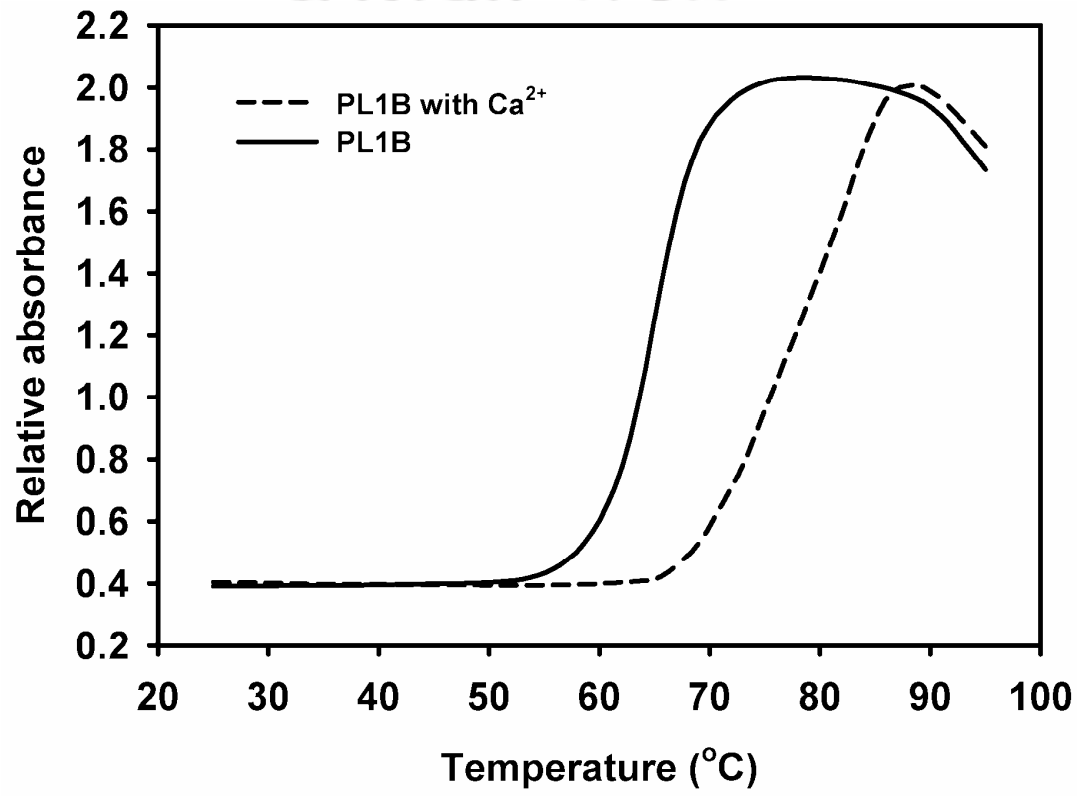


**Fig. 3.9** Protein-melting analysis displaying melting curve of PL1B (—) and melting curve of PL1B in presence of 0.6 mM $Ca^{2+}$ ions (- - -).

### 3.3.12 Effect of chaotropic agents on the structural stability of PL1B

The structural stability of PL1B at pH 8.6 and 25°C was evaluated by increasing the concentration of chaotropic agents (GuHCl or Urea) from 0.2 to 8 M. It was observed that with the increase in the concentration of GuHCl or Urea the fluorescence peak intensity of PL1B decreased. Along with the lowering of the peak intensity, the shift in peak towards the larger wavelength was observed, which is commonly known as red shift. PL1B treated with 6M GuHCl displayed a red shift of the fluorescence peak maxima from 322 nm to 334 nm, resulting in a shift of 12 nm (Fig. 3.10A). PL1B on treatment with 4M urea displayed a red shift from 331 nm to 340 nm, resulting in a shift of 9 nm (Fig. 3.10B). The lowering of the fluorescence intensity and peak shift occurred as the protein loses it structural organization in the presence of chaotropic agent. The buried tryptophan residues in PL1B got exposed due to the loss of non-covalent interactions which stabilize the tertiary structure and thus result in the shift of the fluorescence peak. Similar transition curves were reported for *Ct*CBM35 of β-Mannanase from *Clostridium thermocellum* (Ghosh *et al*., 2014). The loss of structural integrity can be understood from the two-state transition curve of PL1B in presence of varying concentrations of GuHCl or Urea (Fig. 3.11A). Low unfolded fraction of PL1B was obtained until 1M and 0.75M concentration of GuHCl and urea respectively (Fig. 3.11A). The unfolded fractions of PL1B increased till 6M of GuHCl or urea, and then reached the saturation phase leading to the final concentration of 8M. It was evident that PL1B was more stable in presence of GuHCl as compared to Urea (Fig. 3.11A). The apparent free energy of PL1B varied maintaining a linear relationship with the concentrations of chaotropic agents. A two-

step linearity was observed, one at a lower concentrations less than 1 M and another at higher concentrations from 2-6 M (Fig. 3.11B).

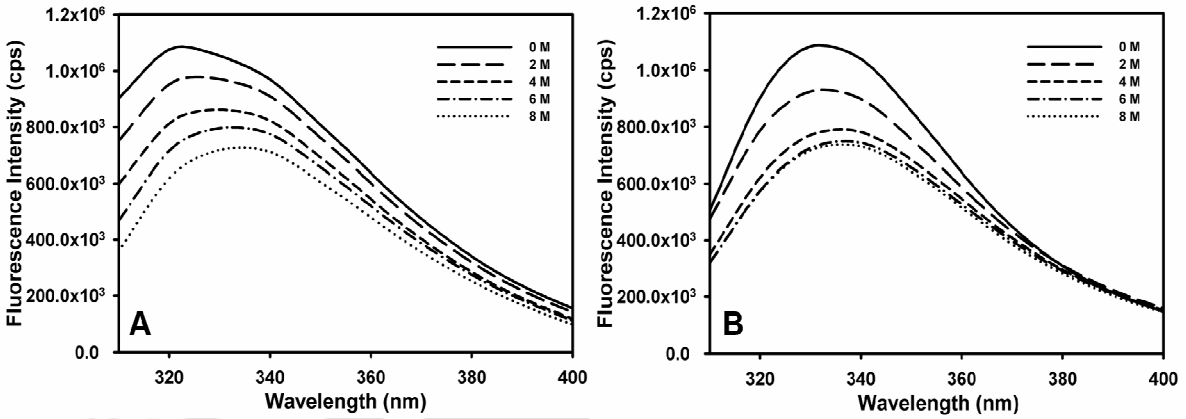


**Fig. 3.10** Tryptophan emission spectra of PL1B in presence of different concentration of chaotropic agents (A) Guanidine hydrochloride (GuHCl) and (B) Urea.

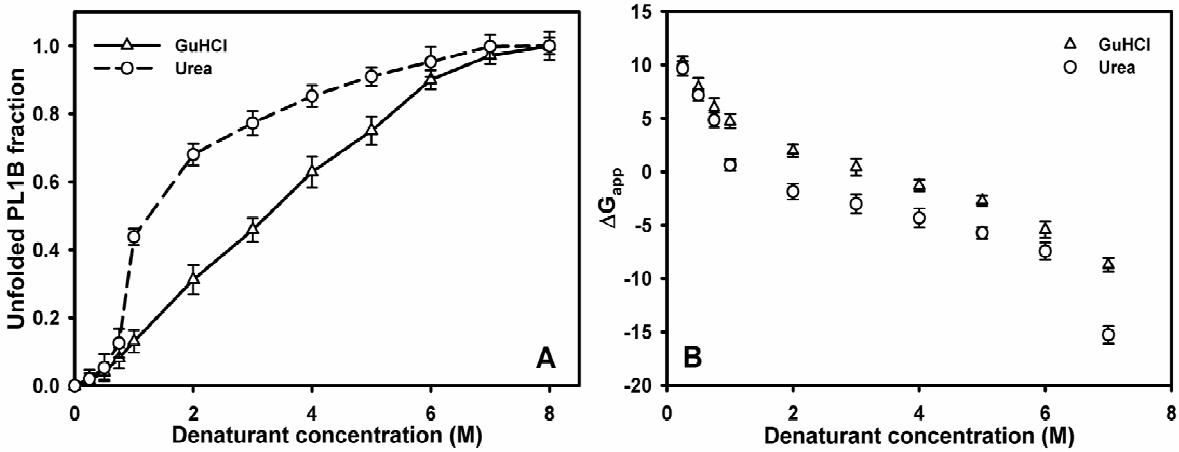


**Fig. 3.11** (A) Fractions of PL1B unfolded as a function of concentration of chaotropic agents, (B) Free energy ($\Delta G_{app}$) of different unfolded fractions of PL1B showing linear relationship with GuHCl and Urea concentration.

### 3.3.13 Binding analysis of CBMs to soluble polysaccharides

The binding analysis of CBM35 to polysaccharides was evaluated using affinity gel electrophoresis. Visual inspection revealed that there was no migration of CBM35 band in 0.2% (w/v) polysaccharide containing gels as compared to native gel devoid of any polysaccharides (Fig. 3.12). This experiment inferred that CBM35 from *Clostridium thermocellum* under investigation did not bind or may be binding very weakly to the polysaccharides used. Binding affinity is not a very sensitive technique hence the binding can be monitored through a more sensitive process in Isothermal titration calorimetry (ITC).

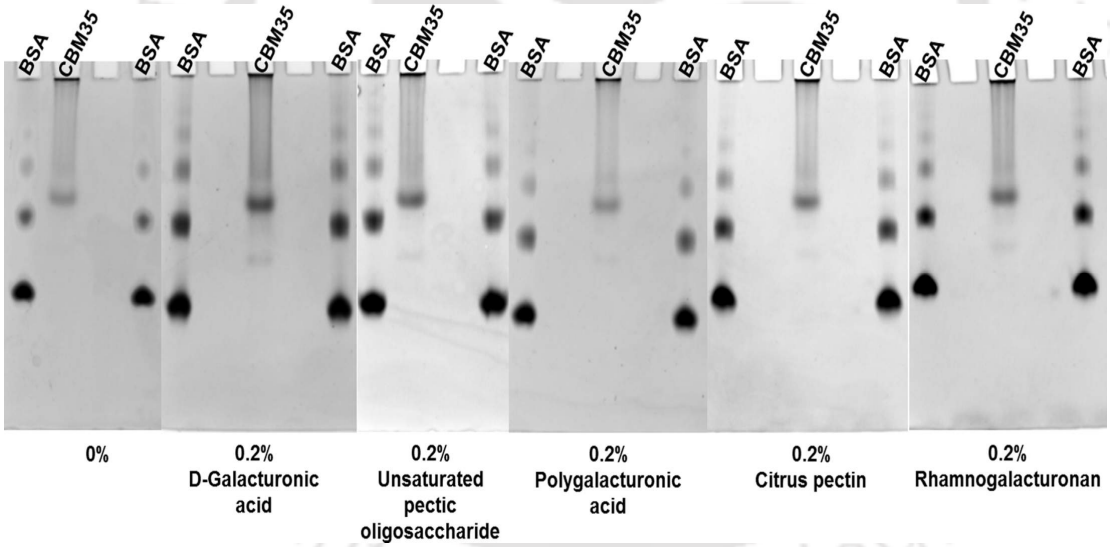


**Fig. 3.12** Affinity gel electrophoresis of CBM35 using Native-PAGE (7.5% gel) containing 0.2% (w/v) polysaccharides, where BSA was used as reference protein, gel marked as 0% do not contain any polysaccharide.

### 3.4 Conclusions

PL1B-CBM35 and PL1B showed maximum enzyme activity at optimum pH 9.6 and 9.8, respectively and both were active within the pH range of 8-10. The optimal temperature for both enzymes was 50ºC. PL1B-CBM35 and PL1B were stable over a pH range of 8-10. PL1B-CBM35 was stable in the temperature range of 30-50°C, whereas PL1B was stable in the range of 30-70°C. However PL1B-CBM35 over 60°C and PL1B over 70°C lost significantly the enzyme activity. Both the enzymes showed high activity towards pectic polysaccharides. PL1B-CBM35 and PL1B showed maximum activity 3.7 U/mg and 18.5 U/mg, respectively, with polygalacturonic acid (PGA). These enzymes also showed better activity towards 25% and 55% methyl-esterified citrus pectin than other pectate lyases. Generally, pectate lyase which is specific to non-methylated PGA, displays lower activity towards methylated pectin. But PL1B-CBM35 and PL1B even though displayed highest activity towards PGA also showed around 90-73% activity towards pectin. The kinetic parameters suggested that PL1B-CBM35 is less efficient than PL1B in degrading PGA and other pectic polysaccharides.

The enzyme activity of PL1B-CBM35 increased by nine-fold (0.41 U/mg to 3.70 U/mg) by 0.6 mM $Ca^{2+}$ or 1.2 mM $Mg^{2+}$ and of PL1B was increased four-fold (4.02 U/mg to 18.5 U/mg), by the same metal ions at same concentrations, implying that these ions are essential cofactors. Marginal increase in the activities of both enzymes was also observed with $Li^{+}$ and $Mn^{2+}$ ions. However, the enzyme activity was unaffected by lower concentrations of $Ni^{2+}$, $Cu^{2+}$, $Zn^{2+}$ and $Co^{2+}$ ions. The trivalent metal ion, $Al^{3+}$ also showed marginal increase in the activity. The addition metal ions 0.6 mM $Mg^{2+}$ or $Li^{+}$ in presence of 0.6 mM $Ca^{2+}$ ions also increased the

100% (3.7 U/mg) activity in PL1B-CBM35 by 14% (4.2 U/mg) and 12% (4.1 U/mg), respectively. The same metal ions of 0.6 mM of $Mg^{2+}$ or $Li^{+}$ ions to PL1B along with the presence of equimolar $Ca^{2+}$ ions in the reaction mixture increased the 100% (18.5 U/mg) activity of the enzyme by 20% (22.2 U/mg) and 15% (21.3 U/mg), respectively. 1.5 mM EGTA and 1.8 mM EDTA was required to chelate 0.6 mM $CaCl_2$ and completely abolish the activity of both the enzymes. Use of 2-3 times higher concentration of chelating agent suggested that $Ca^{2+}$ ions have a strong affinity towards both these enzymes. The TLC analysis of the hydrolysed products of PGA and citrus pectin by PL1B revealed that unsaturated di- and tri-galacturonate were the main sugars released. The accumulation of both these unsaturated products increased with time and was highest at 60 min of the reaction. The results of TLC analysis clearly suggested that PL1B followed an endolytic cleavage pattern towards its substrate and identified as an endo-pectate lyase. The protein-melting peak of PL1B shifted to higher temperature in the presence of $Ca^{2+}$ ions. This further corroborated the fact that $Ca^{2+}$ ions not only enhances activity but also impart thermal stability to the protein structure. The effect of chaotropic agents on PL1B was studied by change in tryptophan fluorescence intensity, which showed that the protein structure unfolds at 6M and 4M concentrations of GuHCl and Urea, respectively. Unfolded fraction of PL1B was less at a lower concentration of chaotropic agent and the apparent free energy change varied linearly with their varying concentrations. It was evident that the PL1B structure is stable and structural deformation occurs only at higher concentration of these chaotropic agents. CBM35 displayed no binding with any of the polysaccharides used in affinity gel electrophoresis.

### 3.5 References

Ahmad, F., Yadav, S., Taneja, S. (1992) Determining stability of protein from guanidinium chloride transition curve. Biochemical Journal, 287: 481–485.

Barras, F., Van Gigsegem, F., Chatterjee, A.K. (1994) Extracellular enzymes and pathogenesis of soft-rot *Erwinia*. Annual Review of Phytopathology, 32: 201–234.

Bayer, E.A., Kening, R., Lamed, R. (1983) Adherance of *Clostridium thermocellum* to cellulose. Journal of Bacteriology, 156: 818–827.

Branden, C., Tooze, J. (1991) In Introduction to Protein Structure, (2nd ed.), Garland publishing, Taylor and Francis Group, Ney York, NY.

Carpita, N.C., Gibeaut, D.M. (1993) Structural models of primary cell walls in flowering plants: consistency of molecular structure with the physical properties of the walls during growth. Plant Journal, 3: 1–30.

Chiliveri, S.R., Linga, V.R. (2014) A novel thermostable, alkaline pectate lyase from Bacillus tequilensis SV11 with potential in textile industry. Carbohydrate Polymers, 111: 264–72.

Cote, G.L., Leathers, T.D. (2005) A method for surveying and classifying *Leuconostoc sp*. Glucansucrases according to strain-dependent acceptor product patterns. Journal of Industrial Microbiology and Biotechnology, 32: 53–60.

Creighton, T.E. (1992) In Proteins: Structures and Molecular Properties, (2nd ed.), Freeman, W. H. & Company, Macmillan Higher Education, Ney York, NY.

Darvill, A.G., McNeil, M., Albersheim, P. (1978) Structure of plant cell walls VIII. A new pectic polysaccharide. Plant Physiology, 62: 418–422.

Davis, G., Henrissat, B. (1995) Structures and mechanisms of glycosyl hydrolases. Structure, 3: 853–859.

Dvortsov, I.A., Lunina, N.A., Chekanovskaya, L.A., Schwarz, W.H., Zverlov, V.V., Velikodvorskaya, G.A. (2009) Carbohydrate-binding properties of a separately folding protein module from beta-1,3-glucanase Lic16A of Clostridium thermocellum. Microbiology, 155: 2442–2449.

Ghosh, A., Verma, A.K., Gautam, S., Gupta, M.N., Goyal, A. (2014) Structure and functional investigation of ligand binding by a family 35 carbohydrate binding module (CtCBM35) of β-Mannanase of family 26 glycoside hydrolase from *Clostridium thermocellum*. Biochemistry (Moscow). 79(7): 672–86.

Gibbons, B. J., Roach, P. J., Hurley, T. D. (2002) Crystal Structure of the autocatalytic initiator of glycogen synthesis, glycogenin. Journal of Molecular Biology, 319: 463–477.

Hasegawa, S., Nagel, C. W. (1966) A New Pectic Acid Transeliminase produced exocellularly by a *Bacillus*. Journal of Food Science, 31: 838–845.

Hatada, Y., Kobayashi, T., Ito, S. (2001) Enzymatic properties of the highly thermophilic and alkaline pectate lyase Pel-4B from alkaliphilic *Bacillus sp*. strain P-4-N and the entire nucleotide and amino acid sequences. Extremophiles, 5: 127–133.

Herron, S.R., Scavetta, R.D., Garrett, M., Legner, M., Jurnak, F. (2003). Characterization and implications of $Ca^{2+}$ binding to pectate lyase. Journal of Biological Chemistry, 278: 12271–12277.

Hugouvieux-Cotte-Pattat, N., Condemine, G., Nasser, W., Reverchon. S., (1996). Regulation of pectinolysis in *Erwinia chrysanthemi*. Annual Review of Microbiology, 50: 213–257.

Kashyap, D.R., Vohra, P.K., Chopra, S., Tewari, R. (2001) Applications of pectinases in commercial sector: a review. Bioresource Technology, 77: 215–27.

Kluskens, L.D., van Alebeek, G.J., Voragen, A.G., de Vos, W.M., van der Oost, J. (2003) Molecular and biochemical characterization of the thermoactive family 1 pectate lyase from the hyperthermophilic bacterium *Thermotoga maritima*. Biochemical Journal, 370(Pt 2): 651–659.

Lamed, R., Setter, E., Bayer, E.A. (1983) Characterization of a cellulose-binding, cellulose-containing complex in *Clostridium thermocellum*. Journal of Bacteriology, 156: 828–836.

Linhardt, R.J., Galliher, P.M., Cooney, C.L. (1986) Polysaccharide lyases. Applied Biochemistry and Biotechnology, 12: 135–176.

Lojkwoska, E., Masclaux, C., Boccara, M., Robert-Baudouy, J., Hugouvieux-Cotte-Pattat, N. (1995) Characterization of *pelL* gene encoding a novel pectate lyase of *Erwinia chysanthemi* 3937. Molecular Microbiology, 16(6): 1183–1195.

McKie, V.A., Vincken, J-P, Voragen, A.G.J., Van Den Broek, L., Stimson, E., Gilbert, H.J. (2001) A new family of rhamnogalacturonan lyases contains an enzyme that binds to cellulose. Biochemical Journal, 355: 167–177.

Ochiai, A., Itoh, T., Maruyama, Y., Kawamata, A., Mikami, B., Hashimoto, W., Murata, K. (2007) A novel structural fold in polysaccharide lyases: *Bacillus*

*subtilis* family 11 rhamnogalacturonan lyase yesw with an eight-bladed β-propeller. Journal of Biological Chemistry, 282: 37134–37145.

Ogawa. A., Sawada, K., Saito, K., Hakamada, Y., Sumitomo, N., Hatada, Y., Kobayashi, T., Ito, S. (2000) A new high-alkaline and high-molecular-weight pectate lyase from a Bacillus isolate: enzymatic properties and cloning of the gene for the enzyme. Bioscience Biotechnology and Biochemistry, 64(6): 1133-1141.

Pages, S., Valette, O., Abdou, L., Belaich, A., Belaich, J.P. (2003) A rhamnogalacturonan lyase in the *Clostridium cellulolyticum* cellulosome. Journal of Bacteriology. 16: 4727–4733.

Pissavin, C., Robert-Baudouy, J., Hugouvieux-Cotte-Pattat, N. (1996) Regulation of pelZ, a gene of the pelBC cluster encoding a new pectate lyase in *Erwinia chrysanthemi* 3937. Journal of Bacteriology, 178: 7187–7196.

Pissavin, C., Robert-Baudouy, J., Hugouvieux-Cotte-Pattat, N. (1998) Biochemical characterization of the pectate lyase PelZ of *Erwinia chrysanthemi* 3937. Biochimica et Biophysica Acta, 1383: 188–196.

Qin, N., Olcese, R., Bransby, M., Lin, T. and Birnbaumer, L. (1999) $Ca^{2+}$-induced inhibition of the cardiac $Ca^{2+}$ channel depends on calmodulin. Proceedings of National Academy of Science (USA), 96: 2435–2438.

Rastogi G., Vishal's objective botany (1998). Meerut, India: Vishal Publishers.

Shevchik, V. E., Kester, H. C. M., Benen, J. A. E., Visser, J., Robert-Baudouy, J., Hugouvieux-Cotte-Pattat, N. (1999) Characterization of the exopolygalacturonate lyase PelX of *Erwinia chysanthemi* 3937. Journal of Bacteriology, 181: 1652–1663.

Shevchik, V. E., Robert-Baudouy, J., Hugouvieux-Cotte-Pattat, N. (1997) The pectate lyase PelI of *Erwinia chrysanthemi* belongs to a new family. Journal of Bacteriology, 179: 7321–7330.

Soriano, M., Blanco, A., Diaz, P., Pastor, F.I. (2000) An unusual pectate lyase from a *Bacillus sp*. with high activity on pectin: cloning and characterization. Microbiology. 146: 89–95.

Soriano, M., Diaz, P., Pastor, F.I. (2006) Pectate lyase C from *Bacillus subtilis:* a novel endo-cleaving enzyme with activity on highly methylated pectin. Microbiology. 152: 617–625.

Sukhumsiirchart, W., Kawanishi, S., Deesukon, W., Chansiri, K., Kawasaki, H., Sakamoto, T. (2009) Purification, characterization, and overexpression of thermophilic pectate lyase of *Bacillus* sp. RN1 isolated from a hot spring in Thailand. Biosciences Biotechnology Biochemistry, 73(2): 268–73.

Tamaru, Y., Doi, R.H. (2001) Pectate lyase A, an enzymatic subunit of the *Clostridium cellulovorans* cellulosome. Proceedings of National Academy of Science USA, 98: 4125–4129.

Tomme, P., Boraston, A., Kormos, J.M., Warren, R.A., Kilburn, D.G. (2000) Affinity electrophoresis for the identification and characterization of soluble sugar binding by carbohydrate-binding modules. Enzyme Microbial Technology, 27: 453–458.

White, G.W., Katona, T., Zodda, J.P. (1999) The Use of High-Performance Size Exclusion Chromatography (HPSEC) as a Molecular weight screening technique for polygalacturonic acid for use in pharmaceutical applications, Journal of Pharmaceutics and Biomedicine, 20: 905.

# Chapter 4

## Structure and substrate binding analysis of family 1 polysaccharide lyase (PL1B) catalytic module and associated family 35 carbohydrate binding module (CBM35) from *Clostridium thermocellum*

### 4.1 Introduction

Pectate lyase is plant cell wall degrading enzyme that causes plant tissue maceration by depolymerizing the pectic polysaccharides present within middle lamella. Pectate lyases from diverse origins like bacterial, fungal and plants share sequence similarities (Henrissat *et al*., 1996). These enzymes are commonly found is plant pathogens, causing soft rot disease in plant (Collmer *et al*., 1986; Barras *et al*., 1994). Among them the most widely studied organism is *Erwinia chrysanthemi*, in which pectate lyase exist in five major and two minor isoforms having profound sequence similarities (Barras *et al*., 1994; Lojkowska *et al*., 1995, Pissavin *et al*., 1996). Pectate lyases cleave the non or less methyl esterified pectic polysaccharides by β-elimination, producing an 4,5-unsaturated galacturonate residue leaving a reducing end (Linhardt *et al*., 1986). The crystal structure of pectate lyase C from *Erwinia chrysanthemi*, displayed a parallel β-helix fold (Yoder *et al*., 1993a). The

parallel β-helix folds into a stacked orientation forming a right handed cylinder. These networks of parallel β-helices are stabilized by interconnecting hydrogen bonds and other interacting side chain residues of the β-sheet (Yoder *et al*., 1993b). All the parallel β-helix found in pectate lyase C (Yoder *et al*., 1993a) and pectate lyase E (Lietzke *et al*., 1994) from *Erwinia chrysanthemi*, pectate lyase from *Bacillus subtilis* (Pickersgill *et al*., 1994) and Bsp165PelA from *Bacillus sp*. (Zheng *et al*., 2012) have a loop that protrudes out from one side of the structure. The loop sizes and their orientation vary in order to accommodate the substrate and thus forming the catalytic centre of the enzyme (Kita *et al*., 1996). Polysaccharide lyases are large group of carbohydrate active enzymes as listed at CAZy database (http://www.cazy.org/Polysaccharide-Lyases.html). Based on the sequence similarities of polysaccharide lyases they have been further sub-divided into 23 families, where pectate lyases are found in family 1, 2, 3, 9 and 10. Most of these enzymes are active under alkaline condition (Tardy *et al*., 1997) and have an absolute requirement of $Ca^{2+}$ ions for its activity (Yoder *et al*., 1995). It has been earlier shown that, there are two $Ca^{2+}$ ions associated with pectate lyases. One $Ca^{2+}$ ion remains associated with the enzyme irrespective of the presence of the substrate (Herron *et al*., 2003) and the second one facilitates the bridge formation between the substrate and enzyme (Scavetta *et al*., 1999).

Complex carbohydrate hydrolysing enzymes have a generic modular nature. Carbohydrate binding module (CBM) is one of these important modules, which remains associated with the catalytic module (Boraston *et al*., 2003; Boraston *et al*.,

2004). This association of CBM with the catalytic module increases its interaction with the substrate, thereby increasing the efficiency of the enzyme (Tomme *et al*., 1988; Hall *et al*., 1995). Moreover, CBMs are also involved in substrate targeting and disruption of insoluble crystalline plant polysaccharides (Cuyvers *et al*., 2012). In addition to their important role in plant cell wall degradation, CBMs have found new avenues in different biological applications. CBM has been used as a fusion tag in a vector system, because of its independent folding ability upon expression (Novy *et al*., 1997). Immobilized CBM has been used in affinity ligand binding of biomolecules (Johansson *et al*., 2006). Lignocellulose was efficiently degraded in presence of CBMs, which is beneficial for biofuel production (Ragauskas *et al*., 2006). Based on the sequence similarity, CBMs are grouped into 71 families as listed in CAZy database (http://www.cazy.org). Till date family 35 carbohydrate binding module contains 812, 9 and 45 bacterial, archaeal and eukaryotic proteins, respectively. Among them only 12 crystal structures have been determined (http://www.cazy.org/CBM35.html). The 3D structures of family 35 carbohydrate binding modules determined so far have a β-sandwich fold.

*Clostridium thermocellum* an anaerobic, thermophillic and carbohydrate degrading bacterium has a unique organization of multi-enzyme complexes known as cellulosome (Bayer *et al*., 1983). These cellulosomes together with the cohesin-dockerin interaction can host an array of catalytic and binding modules that can facilitate plant cell wall degradation (Lamed *et al*., 1983; Bayer *et al*., 2008). Till date cellulosomal pectate lyase A from *Clostridium cellulovorans* (Tamaru *et al*., 2001)

and three pectate lyases PL1A, PL1B and PL9 from *Clostridium thermocellum* (Chakraborty *et al*., 2015) have been characterized. Several CBM35s from *Clostridium thermocellum* have been characterized, among them two are Mannan specific *Ct*CBM35 (Cthe 0032) (Ghosh *et al*., 2013) and *Ct*CBM35 (Cthe 2811) (Ghosh *et al*., 2014). PelCBM35 associated with rhamnogalauronan acetyl esterase Rgae12A (Cthe_3141) showed specificity towards Δ4,5-Galacturonic acid (Montanier *et al*., 2009). It is observed that generally CBM displays ligand specificities towards same substrates which are hydrolysed by their associated catalytic module (Boraston *et al*., 2004). On contrary four CBM35 from *Clostridium thermocellum*, *Amycolatopsis orientalis*, *Cellvibrio japonicas* and an environmental isolate having profound sequence similarities exhibit divergent substrate specificities when compared to their respective appended catalytic modules (Montanier *et al*., 2009). The modular organization of the protein sequence ABN53381.1 from *C. thermocellum* displays an N-terminal catalytic module family 1 polysaccharide lyase (PL1B) and C-terminal family 35 carbohydrate binding module (CBM35) which has been mentioned previously in Chapter 1, Section 2.3.1. In the present study three dimensional structures of PL1B and CBM35 from *C. thermocellum* were constructed by homology modelling and the docking analysis of ligand was performed to ascertain the catalytic centre and key residues involved. The validation of secondary structure was done by CD analysis. The fluorescence study was performed to determine the structural integrity of the PL1B in presence of chaotropic agents.

## 4.2. Materials and Methods

### 4.2.1 Sequence alignment of PL1B and CBM35

The protein sequences of family 1 polysaccharide lyase (PL1B) and family 35 carbohydrate binding module (CBM35) were retrieved from NCBI database, with a GeneBank accession number ABN53381.1 (nucleotide accession number CP000568.1) and UniProt ID A3DHF2. Putative domain search in the query sequence was done by BLAST analysis with known PDB structures from X-ray or NMR data. The query sequence PL1B or CBM35 was aligned with known sequences and the presence of conserved and semi conserved residues were evaluated. Sequences were aligned by the ClustalW2 tool (Larkin *et al*., 2007) available on EMBL-EBI services page (http://www.ebi.ac.uk/Tools/msa/clustalw2/). The alignment file was then viewed for conserved residues by ESPript 3.0 (Robert *et al*., 2014).

### 4.2.2 Secondary structure prediction of PL1B and CBM35

The secondary structures of PL1B from its 353 amino acids and CBM35 from 124 amino acids sequence were determined by protein secondary structure prediction tools PsiPred (http://bioinf.cs.ucl.ac.uk/psipred/) and PDBSum (http://www.ebi.ac.uk/thornton-srv/databases/pdbsum/Generate.html). Both of these tools are available on the ExPASy SIB bioinformatics portal (http://www.expasy.org/proteomics).

### 4.2.3 Homology modeling of PL1B and CBM35

The three dimensional structure of PL1B and CBM35 was built by using Modeller 9v12 (http://salilab.org/modeller/). The comparative protein structure

modeling was done based on related known templates satisfying the spatial restraints (Eswar *et al*., 2006). Multiple template approach was followed, where the query template of PL1B and CBM35 was modeled on the basis of other closely related pectate lyases and other CBM35 sequences, respectively. PDB templates and sequences chosen for PL1B were, pectate lyase Bsp165PelA (3VMV_A) from *Bacillus sp.* N165 (Zheng *et al*., 2012), pectate lyase (3ZSC_A) from *Thermotoga maritime* (Kluskens *et al*., 2003), pectate lyase II (2QX3_A) from *Xanthomonus campestris* (Xiao *et al*., 2008) and pectate lyase C (1PLU_A) from *Erwinia chrysanthemi* (Yoder *et al*., 1995). PDB templates and sequence chosen for CBM35 modeling were rhamnogalauronan acetyl esterase (Rgae12A) associated CBM35 (2W1W_A) from *Clostridium thermocellum* (Montanier *et al*., 2009), exo-chitosanase (Csxa) associated CBM35 (2VZP_A) from *Amycolatopsis orientalis* (Montanier *et al*., 2009) and CBM35 (4QB1_A) from *Paenibacillus barcinonensis* (Sainz-Polo *et al*., 2014). The 3D model of PL1B and CBM35 was generated only after 100 GA runs, further loop refinement of the existing coordinates was achieved by using the loop model class in Modeller. The best modeled structure was chosen by evaluating the least global DOPE (discrete optimized protein energy) assessment score (Shen *et al*., 2006) and highest GA341 assessment score (John *et al*., 2003; Melo *et al*., 2002) of the models.

### 4.2.4 Refinement and quality assessment of modeled PL1B and CBM35

The best model with the least DOPE assessment score was energy minimized on the energy minimization server, YASARA (http://www.yasara.org/

minimizationserver.htm). On this server an extensive statistical analysis of protein structure is done based on the common structural feature and 3D coordinates with thousands of known structures present in PDB. Hence, the resulting energy function is known as knowledge based potential and has been incorporated into two new force fields (Krieger *et al*., 2009). The final energy minimized structures of PL1B and CBM35 were assessed on structure analysis and verification server (SAVES) available on the NHI-MBI Laboratory servers (http://nihserver.mbi.ucla.edu/SAVES/) of UCLA, USA.

### 4.2.5 Molecular dynamic simulation of modeled PL1B and CBM35 structure

The molecular dynamic (MD) simulation was performed by using widely accepted techniques with compatible force fields implemented in Gromacs 4.6.5 (Berendsen *et al*., 1995; Pronk *et al*., 2013). Protein forces were then calculated using GROMOS96 43a1 force field where PL1B and CBM35 were placed separately within single point charge (SPC) water model. After defining simulation box and solvent system (here water molecule) around the protein, charges on the protein molecule were neutralized by adding counter ions ($Na^+$). This step replaced same number of water molecule which was at least 3.00 Å from the protein surface. An equilibration for 500 ps in NVT ensemble (constant number of particles, volume and temperature) was carried out restraining the solute atoms. In the next step, the system was again equilibrated for 500 ps by NPT ensemble (constant number of particles, pressure and temperature) twice, once with restraints and then without restraints. Production run was performed for 5 ns with NPT ensemble adopting a 2 fs integration time. The

linear constraint solver (LINCS) algorithm (Hess *et al*., 1997) was employed to constrain the bonds associated with hydrogen atoms. Throughout the production run the modeled PL1B and CBM35 structures were analyzed as a time dependent function to ascertain its stability in the solvent system.

### 4.2.6 Docking analysis of modeled PL1B and CBM35

The active site residues of PL1B and binding residues of CBM35 were determined by docking the modeled structure with different ligands. Docking simulations were performed in AutoDock 4.2.1 (Morris *et al*., 2009), together with the viewer MGLTools 1.5.6 (http://mgltools.scripps.edu/). Ligands used in docking to PL1B and CBM35 were downloaded from PubChem (http://www.ncbi.nlm.nih.gov) in 3D SDF format were D-galacturonic acid (GAL) (CID 84740), unsaturated di-galacturonic acid (UnDiGAL) (CID 46173273), tri-galacturonic acid (TGA) (CID 3081397), de-esterified pectin (DEPEC) (CID 24892720), D-galacto methyl ester (GALME), amino-galacturonic acid (Amino-GAL) (CID 193487). The downloaded ligand structures were converted to PDB format by OpenBabel 2.3.2a (O'Boyle *et al*., 2011). Another ligands Δ4,5-galacturonic acid (Δ4,5GAL) was retrieved from ligand bound structure of CBM35 (2W47_A) from *Clostridium thermocellum* (Montanier *et al*., 2009). The D-galacturonic acid is naturally occurring uronic acid which is a major component of pectin and is a monomeric unit of polygalacturonic acid. It contains an aldehyde group at C1 and a carboxyl group at C6, which is partially methyl esterified. These galacturonic acid moieties are linked together by α-(1,4) bonds (O'Neill *et al*., 1990). However, Δ4,5-galacturonic acid is a hexouronic acid moiety with unsaturation

between the C4 and C5 carbon atom. Unsaturated di-galacturonic acid have two galacturonic acid residues linked together by α-(1,4) bond, and one of the galacturonic acid moiety has an unsaturation between the C4 and C5 position at the non-reducing end of the molecule. Tri-galacturonic acid has three galacturonic acid residues linked together by α-(1,4) bond. De-esterified pectin is made of repeated galacturonic acid moieties which are devoid of methyl esterification at the C5 position. Amino-galacturonic acid (2-amino-2-deoxy-D-galacturonic acid) is a deoxy D-galacturonic acid containing substitution of an amino group and it was isolated from different bacterial sources (Moreau *et al*., 1982; Yoshida *et al*., 1990). Individual ligands were prepared for docking by merging non-polar hydrogen atoms and assigning partial charges or Gasteiger charges which are automatically calculated by Autodock Tool 4.2.1. Finally the ligand was saved in PDBQT format after checking the correct torsion parameters and then used for docking. Similarly, the macromolecule PL1B and CBM35 was prepared for docking by following the same protocol used for the ligand and saved in PDBQT format. The grid box was then chosen in PL1B and CBM35 to correctly accommodate the ligand at the active site, such that it can rotate freely in the space provided. The X,Y and Z co-ordinates at the grid-centre for docking in PL1B were -10.005, 13.464 and 31.103, respectively, and for CBM35 the co-ordinates were -0.157, 13.323, 29.63 with 0.375Å grid point spacing for both macromolecules. The different conformations of the ligand within the Grid box was searched by Lamarckian Genetic Algorithm, with GA runs set at 30. All other parameters were set to default and the different conformations were generated. The

best conformation was selected after evaluating the binding energies of each conformation. Ligand in a particular conformation having the least binding energy (ΔG) was chosen and the protein-ligand complex was generated (Morris *et al*., 2009). The generated protein-ligand complexes were viewed in SPDB viewer (Guex *et al*., 1997) and PyMOL (http://www.PyMOL.org) to detect the polar and hydrophobic interactions.

### 4.2.7 Determination of secondary structure of PL1B and CBM35 by Circular Dichroism

PL1B and CBM35 were previously cloned and expressed as mentioned earlier in Chapter 2, Sections 2.3.3 and 2.3.4. The secondary structures of these proteins were determined by Circular Dichroism (CD) analysis. CD analyses of PL1B and CBM35 were carried out using 50 mM Tris-HCl buffer, pH 8.0. The far-UV CD spectrum was recorded on spectropolarimeter (Jasco Corporation, JASCO J-815), equipped with a peltier system for temperature control at 25°C using a sample cell with a path length of 0.1 cm. The CD spectrum was collected at a scanning rate of 50 nm/min and 1 nm bandwidth in the far UV region 190 to 250 nm with an average of six scans. The molar residual ellipticity (mre) was calculated from the ellipticity (θ) values at each wavelength (Kelly *et al*., 2005). The mre values of 190 to 240 nm were feed into the K2D3 server (http://k2d3.ogic.ca/) to estimate the percentage of different secondary structures present in PL1B and CBM35. CD data were compared with predicted secondary structure data to confirm the results.

## 4.3 Results and Discussion

### 4.3.1 Sequence analysis of PL1B and CBM35

BLAST analysis of amino acid sequence (GeneBank accession no. ABN53381.1) from *Clostridium thermocellum* ATCC 27405 revealed the presence of a putative catalytic module (PL1B) and a carbohydrate binding module (CBM35). The PL1B module belongs to superfamily 3 of pectate lyase, while CBM35 module belongs to superfamily CBM6-CBM35-CBM36.

The X-ray crystallographic structures having profound similarity with PL1B sequence were pectate lyase (Bsp165PelA) from *Bacillus sp*. N165 (Zheng *et al*., 2012), pectate lyase from *Thermotoga maritima* (Kluskens *et al*., 2003), pectate lyase II from *Xanthomonas campestris* (Xiao *et al*., 2008), pectate lyase C (Yoder *et al*., 1995) and pectate lyase A (Thomas *et al*., 2002) from *Erwinia chrysanthemi*, a thermosatble pectate lyase from *Bacillus sp*. TS-47 (Takao *et al*., 2001) and pectate lyase (BsPel) from *Bacillus subtilis* [10] (Table. 4.1). Multiple sequence alignment of PL1B with the above mentioned pectate lyase sequences revealed conserved and semi-conserved regions (Fig. 4.1). Other than that signature sequences like 'VWIDH' and 'VxxRxPxxRxGxxHxxxN' which are commonly found in pectate lyases (Hinton *et al*., 1989; Barras *et al*., 1994; Henrissat *et al*., 1996) are also present within the sequence of PL1B as 'IWIDH' and 'VKSRTPSYRGGTGHMFNN', respectively (Fig. 4.1).

**Table 4.1** BLAST analysis of PL1B.

| Organism | PDB ID | Identity (%) | Query coverage (%) | E-value | Total score |
|---|---|---|---|---|---|
| *Bacillus sp. N165* | 3VMV_A | 43 | 90 | 2e-63 | 206 |
| *Thermotoga maritima* | 3ZSC_A | 33 | 92 | 1e-31 | 122 |
| *Xanthomonas campestris* | 2QX3_A | 32 | 89 | 1e-31 | 121 |
| *Erwina chrysanthemi* | 1PLU_A | 32 | 93 | 2e-28 | 113 |
| *Bacillus sp. TS-47* | 1VBL_A | 35 | 44 | 3e-20 | 91.3 |
| *Bacillus subtilis* | 1GN8_A | 33 | 44 | 1e-17 | 84.3 |
| *Erwina chrysanthemi* | 1JRG_A | 30 | 62 | 4e-13 | 70.1 |

There are several CBM sequences which have similarity with the query CBM35 sequence (Table 4.2). These sequences were CBM35 from *Clostridium thermocellum* having PDB ID 2W1W_A and 2W47_A (Montainer *et al*., 2009), CBM35 from *Amycolatopsis orientalis* associated with exo-chitosanase (Csxa) (Montainer *et al*., 2009), CBM35 from *Paenibacillus barcinonensis* (Sainz-Polo *et al*., 2014) and CBM35 from *Cellvibrio japonicus* (Abf62) (Kellett *et al*., 1990). Multiple sequence alignment displayed conserved and semi-conserved regions within the sequence (Fig. 4.2), suggesting that CBM35 from *Clostridium thermocellum* in present study is a part of this CBM35 clan.

**Table 4.2** BLAST analysis of CBM35.

| Organism | PDB ID | Identity (%) | Query coverage (%) | E-Value | Total Score |
|---|---|---|---|---|---|
| *Clostridium thermocellum* | 2W47_A | 38 | 82 | 1e-16 | 72.8 |
| *Clostridium thermocellum* | 2W1W_A | 38 | 82 | 1e-16 | 72.8 |
| *Amycolatopsis orientalis* | 2VZP_A | 30 | 90 | 2e-12 | 61.2 |
| *Paenibacillus barcinonensis* | 4QB1_A | 35 | 83 | 8e-11 | 57.0 |
| *Cellvibrio japonicus* | 2W46_A | 34 | 99 | 2e-10 | 58.2 |

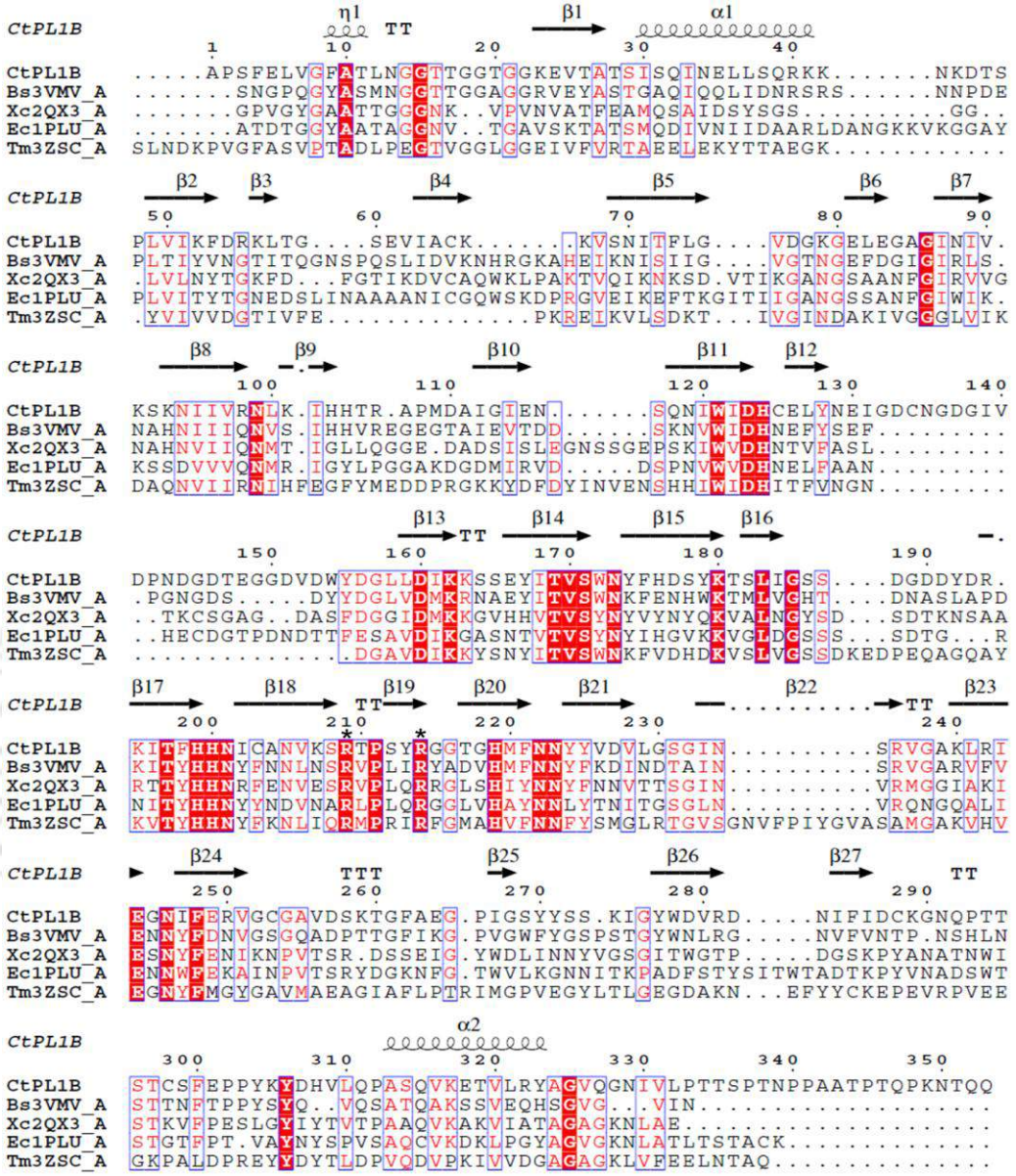


**Fig. 4.1.** Multiple sequence alignment of PL1B from *Clostridium thermocellum* with pectate lyases from *Bacillus subtilis* (Bs1GN8_A), *Bacillus sp.* TS-47 (Bs1VBL_A), *Bacillus sp.* 165 (Bs3VMV_A), *Erwinia chrysanthemi* (Ec1JRG_A and Ec1PLU_A), *Thermotoga maritima* (Tm3ZSC_A) and *Xanthomonas campestris* (Xc2QX3_A). The conserved residues are shown in black background and semi conserved residues are shown in box. The secondary structure components (helices-α, strands-β, turns-T, and $3_{10}$ helices-η) of PL1B are shown above the sequences. Conserved catalytic residues are marked as asterisks. The figure was developed by EsPript3.0 (http://espript.ibcp.fr/).

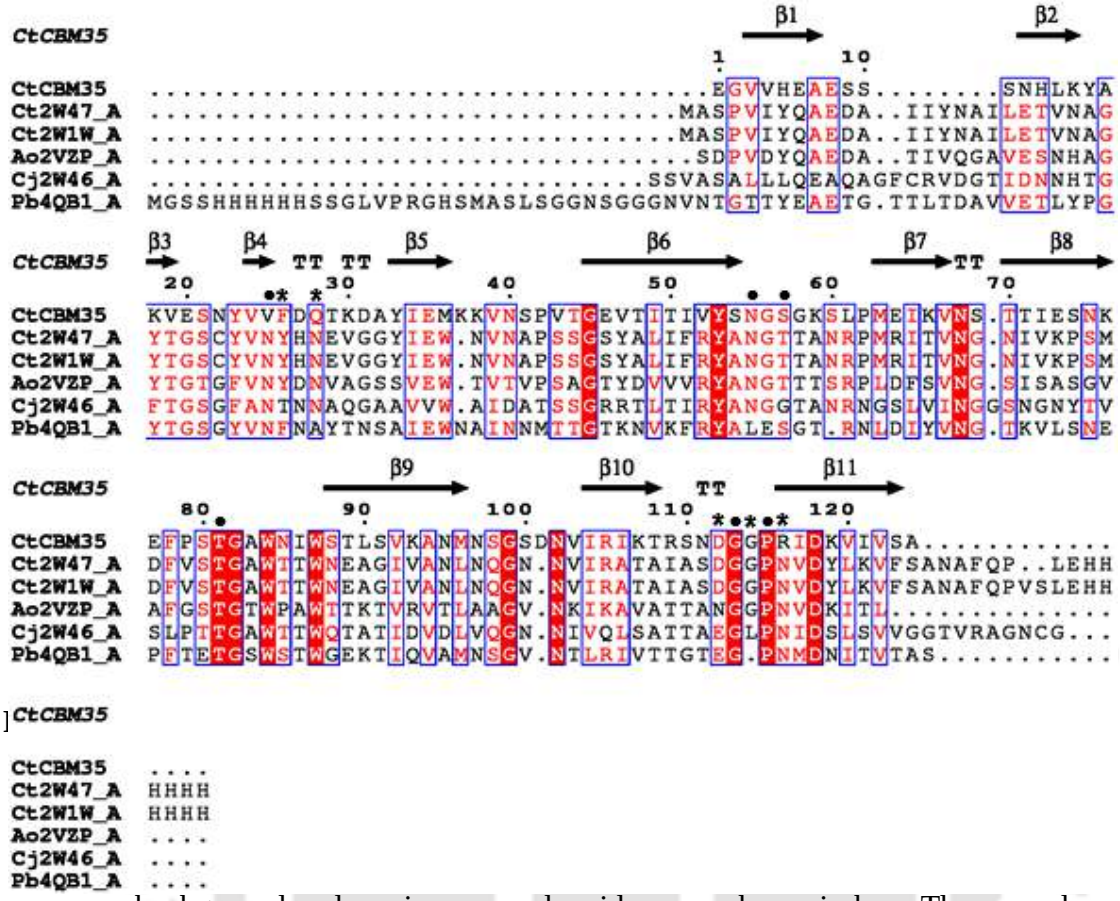


background and semi conserved residues are shown in box. The secondary structure components (strands-β and turns-T) of CBM35 are shown above the sequences. Residues showing polar interactions and hydrophobic interactions are marked in asterisks and dots respectively. The figure was developed by EsPript3.0 (http://espript.ibcp.fr/).

### 4.3.2 Secondary structure of PL1B and CBM35

The secondary structure of PL1B predicted by PsiPred showed the presence of 2 α-helices (<5%) at the N- and C-terminals, 27 β-strands (>35%) and 29 random coils (<60%) (Fig. 4.3) and (Table 4.3). The β-strands present throughout the structure form the parallel β-sheets, which are quite common in the structures of pectate lyase and evident from the previous characterizations (Yoder *et al*., 1993a; Lietzke *et al*., 1994; Pickersgill *et al*., 1994).

The predicted secondary structure of CBM35 showed the presence of 11 β-strands (<49.2%) and 19 random coils (<50.8%) (Fig. 4.4) and (Table 4.4). The abundance of β-strands throughout the structure forms the antiparallel β-sheets. Such structures are also common in previously characterized CBM35 (Montainer *et al*., 2009; Montanier *et al*., 2011; Sainz-Polo *et al*., 2014).

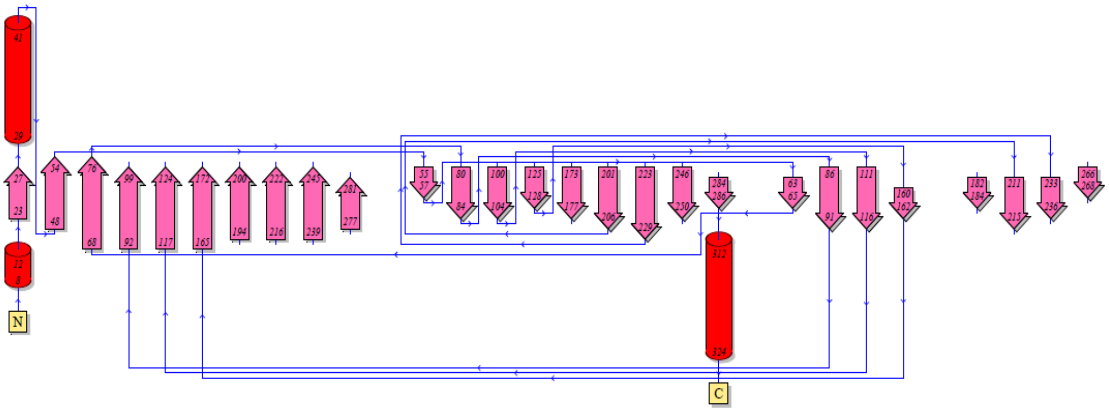


**Fig. 4.3.** Topology of modelled PL1B displaying the orientation of the secondary structures (thick arrows represent the β-strand and cylinders represent α-helix).

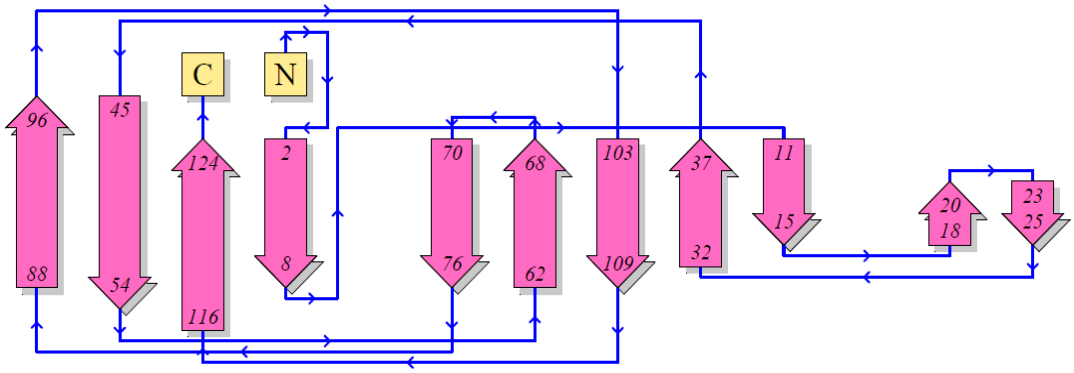


**Fig. 4.4.** Topology of modelled CBM35 displaying the orientation of the secondary structures (thick arrows represent the β-strands and thin arrowed connector represent loops).

### 4.3.3 Secondary structure analysis of PL1B and CBM35 by Circular Dichroism

The CD spectrum of PL1B and CBM35 was analyzed in the K2D3 server, where the dataset was compared with the available secondary structures of known proteins (Jeune *et al*., 2012). This revealed that PL1B contained only 2.06% α-helices (2 in number) 40.54% β-strands (27 in number), 57% random coils (29 in number) (Fig. 4.5) and CBM35 contained 2.02% α-helix, 47.3% β-strands (11 in number), 50.68% random coils (19 in number) (Fig. 4.6). These results were in accordance with the predicted values of secondary structure elements determined earlier (Table. 4.2 and 4.3). Later it was found that both the modeled PL1B (Fig. 4.7) and CBM35 (Fig. 4.11) structures are rich in β-strands and random coils as found in other pectate lyase C previously (Kamen *et al*., 2001) and characterized CBMs (Montainer *et al*., 2009).

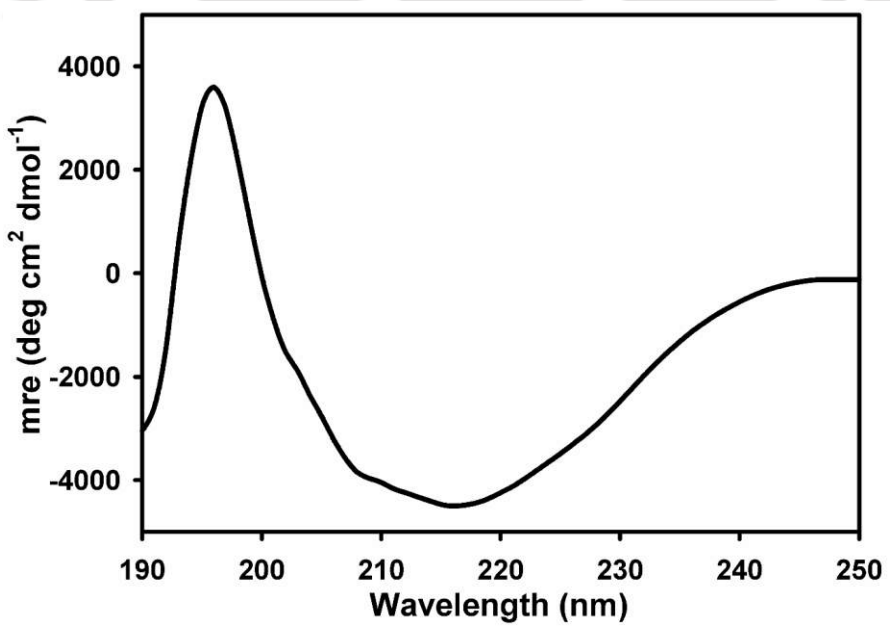


**Fig. 4.5.** Circular dichroism (CD) spectrum of PL1B for determining the secondary structure elements.

**Table 4.3** Secondary structure elements present in PL1B.

| Secondary structure element | PsiPred (%) | CD analysis (%) |
|---|---|---|
| α-helix | <5 | 2.06 |
| β-sheet | >35 | 40.54 |
| Random coil | <60 | 57.4 |

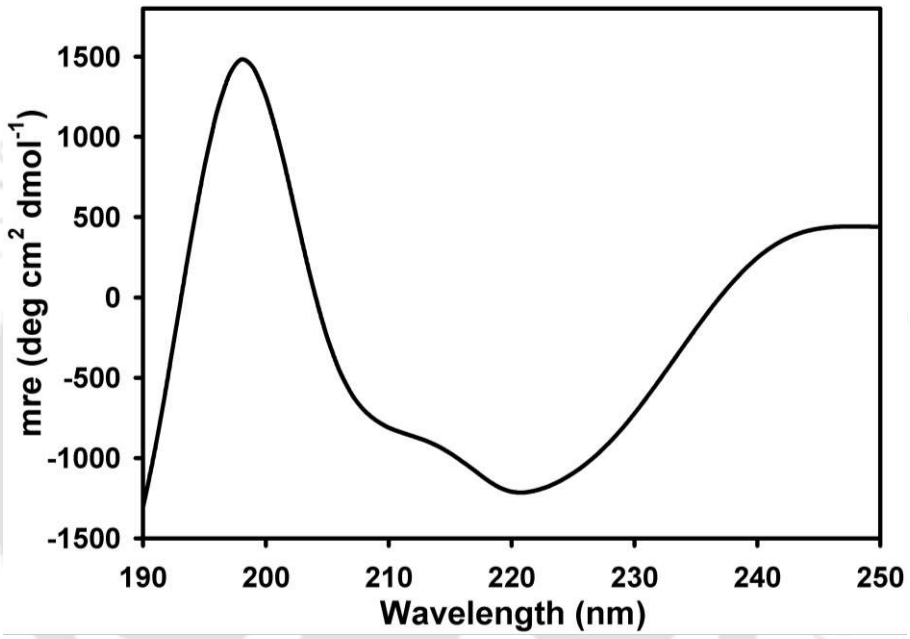


**Fig. 4.6.** Circular dichroism (CD) spectrum of CBM35 for determining the secondary structure elements.

**Table 4.4** Secondary structure elements present in CBM35.

| Secondary structure element | PsiPred (%) | CD analysis (%) |
|---|---|---|
| α-helix | 0 | 2.02 |
| β-sheet | <49.2 | 47.3 |
| Random coil | <50.8 | 50.68 |

### 4.3.4 Modeled structure and quality assessment of PL1B and CBM35

The modeled structure of PL1B represented the conventional parallel β-helix structure (Fig. 4.7A). The basic structural domains are parallel β-sheets, which fold into a right handed coiled structure. Three parallel β-sheets *viz.* S1, S2 and S3 are connected by random coils L1 (connecting S1 and S2), L2 (connecting S2 and S3) and L3 (connecting S3 and S1). This arrangement of S1, S2 and S3 β-sheets coils around the central core to form a final β-helix structure. The β-sheet S1 is composed of ten β-strands, while S2 and S3 are built from seven and nine β-strands, respectively. The L2 loop region contains an extended simple loop which is larger than that found in Bsp165PelA. The central core of the β-helix structure is made up of seven complete turns in the parallel β-sheets (Fig. 4.7A), as often found in other pectate lyase structures (Lietzke *et al*., 1994; Yoder *et al*., 1995a; Yoder *et al*., 1995b; Czerwinski *et al*., 2005; Xiao *et al*., 2008). The quality of the modeled structure after energy minimization was assessed on the Saves server. Ramachandran plot developed by Procheck displayed that 82.8% residues were in the favoured region, 14.7% and 1.8% residues were in additional and generously allowed region, respectively, and only 0.7% residues were in the disallowed region (Fig. 4.7B). In verify 3D the 1D-3D plot showed that 80% of amino acid present in modeled PL1B structure has an overall score of ≥ 0.2 (Fig. 4.7C). The catalytic core of PL1B was revealed after its superposition with Pectate lyase (Bsp165-PelA) from *Bacillus sp*. 165 (Zheng *et al*., 2012) with a RMS deviation value of 0.492 Å (Fig. 4.8). The binding cleft of PL1B was located at the same position as previously identified in Bsp165PelA. The binding

cleft PL1B is formed by parts of L2, L3 loops and S3 β-sheet, which is enough deep to accommodate the ligand. The superposition of structures showed that the key residues Asp151, Arg209, Arg236 and Tyr271 of PL1B perfectly aligns with the key residues of Bsp165PelA (Fig. 4.8).

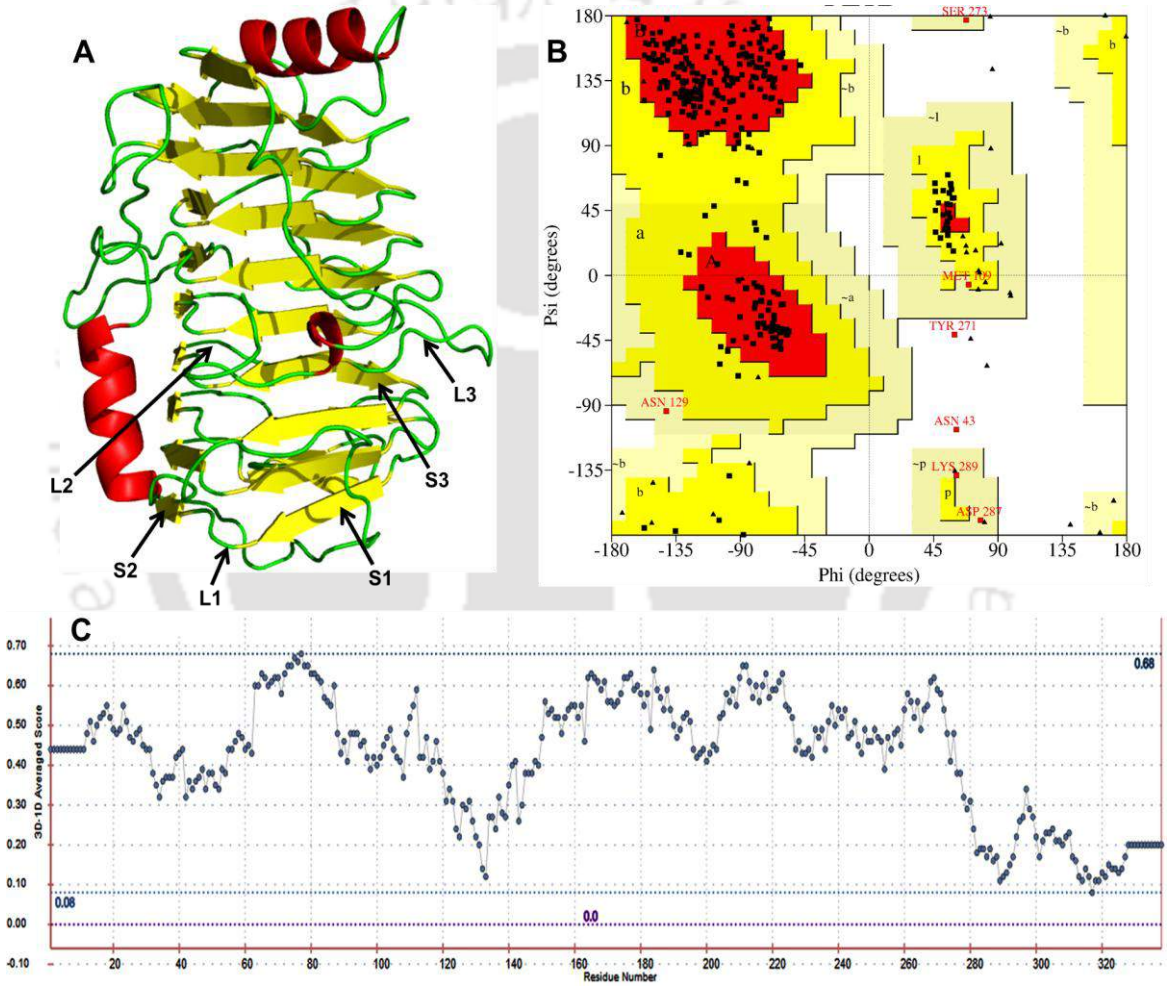


**Fig. 4.7.** (A) Cartoon representation of the modelled PL1B structure, displaying the parallel β-helix structure; where S1, S2, S3 are the parallel β-sheets made up of β-strands, and L1, L2 and L3 are loops interconnecting these β-sheets. Quality assessment of modelled PL1B structure by (B) Ramachandran plot and (C) Verify3D.

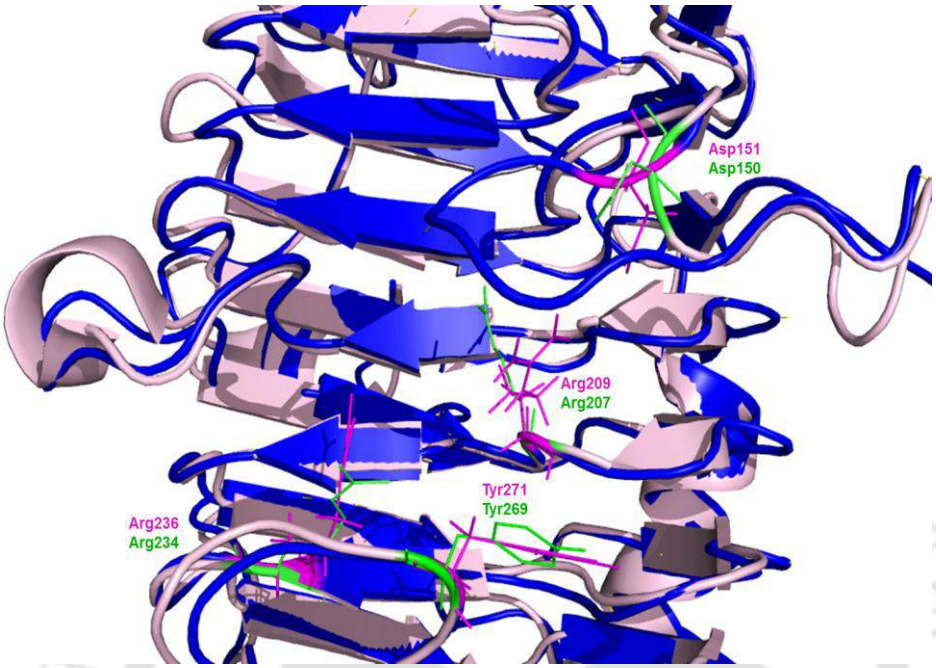


**Fig. 4.8.** Superposition of modelled PL1B (shown in blue) structure with Bsp165PelA (shown in light-pink) from *Bacillus sp*., showing the binding cleft. Some residues from the binding cleft of PL1B are marked in magenta and those from Bsp165PelA are marked in green.

The modeled CBM35 noncatalytic module of 124 amino acid residues from *Clostridium thermocellum* displayed a jelly roll type β-sandwich fold as also reported earlier for four different CBMs *viz*. Rhe-CBM35 (Rgae12A), Pel-CBM35 (Pel10), Chi-CBM35 (CsxA), and Xyl-CBM35 (CjXyn10B) (Montanier *et al*., 2009). β-Sandwich fold has also been reported for Cellulosomal CBM from *C. thermocellum* (Montanier *et al*., 2011), Glucuronoxylanase Xyn30D associated CBM35 from *Paenibacillus barcinonensis* (Sainz-Polo *et al*., 2014) and β-mannanase associated *Ct*CBM35 from *C. thermocellum* (Ghosh *et al*., 2014). The structure contained two antiparallel sheets S1 and S2, made of 4 and 5 antiparallel β-strand, respectively. These two antiparallel sheets are connected by loops L1 and L2, to build the jelly roll β-sandwich structure (Fig. 4.9A). Energy minimized structure of CBM35 was verified

for correct torsion angles, where Ramachandran plot showed 92.7% residues in favoured region and 7.3% in additionally allowed region (Fig. 4.9B). In verify 3D the 1D-3D plot showed that 70% of amino acid present in modeled CBM35 structure has an overall score of ≥ 0.2 (Fig. 4.9C).

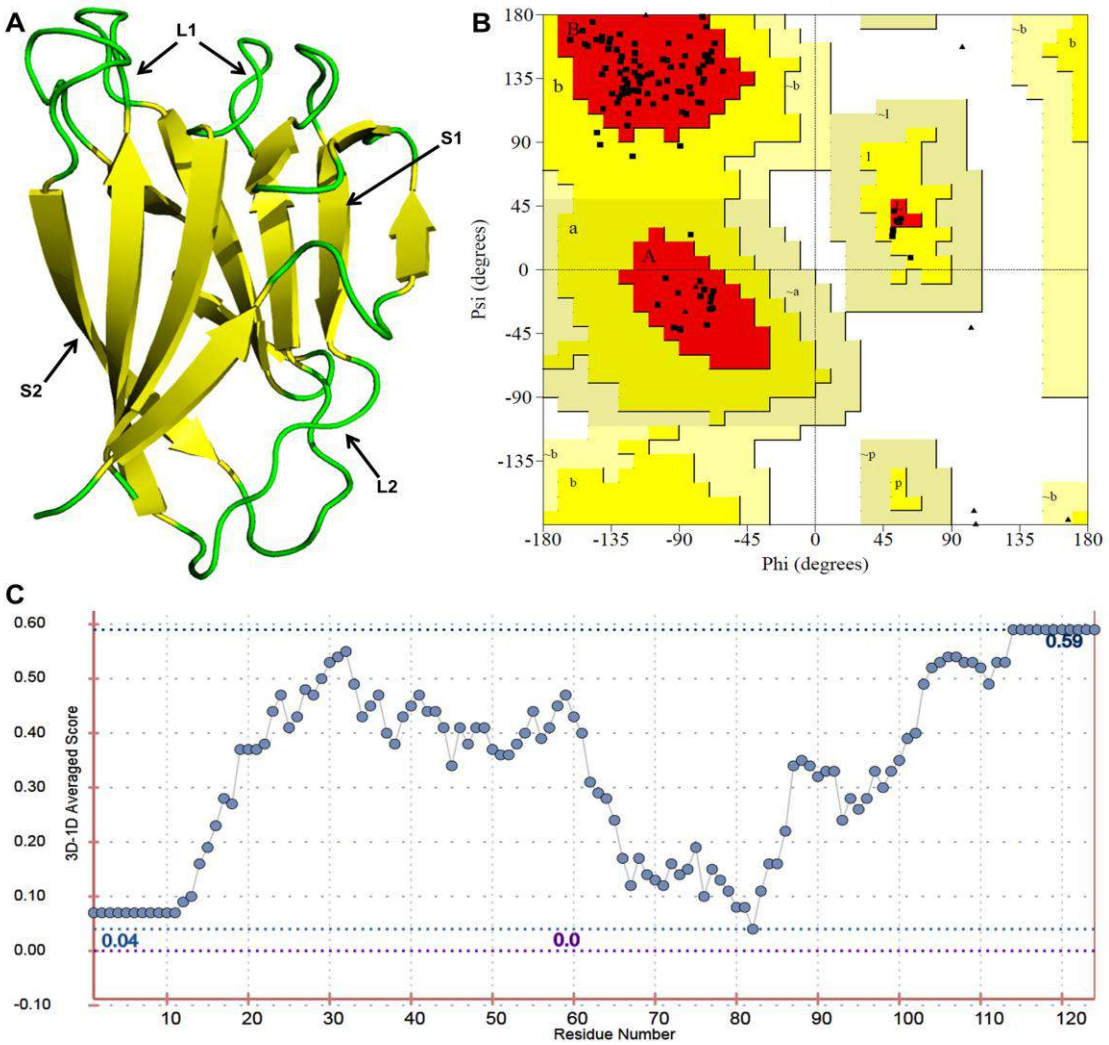


**Fig. 4.9.** (A) Cartoon representation of the modelled CBM35 structure, displaying the jellyroll type β-sandwich structure; where S1and S2 are the antiparallel β-sheets made up of β-strands, and L1 and L2 are loops interconnecting these β-sheets. Quality assessment of modelled CBM35 structure by (B) Ramachandran plot and (C) Verify3D.

The binding center of CBM35 was revealed when the modeled structure was aligned with another *Clostridium thermocellum* CBM35 (PDB ID: 2W1W_A) (Montainer *et al*., 2009) with a RMS deviation of 0.505Å (Fig. 4.10). The substrate binding cleft in CBM35 is located in the L1 region of the β-sandwich structure, where the residues from loop L1 and sheets S1, S2 participated during substrate binding. Superposition of both the structures showed that the key residues Phe26, Gln28, Asp112, Gly114 and Arg116 of CBM35 are involved in substrate binding and which perfectly aligns with the major residues of CBM35 (PDB ID: 2W1W_A) (Fig. 4.10).

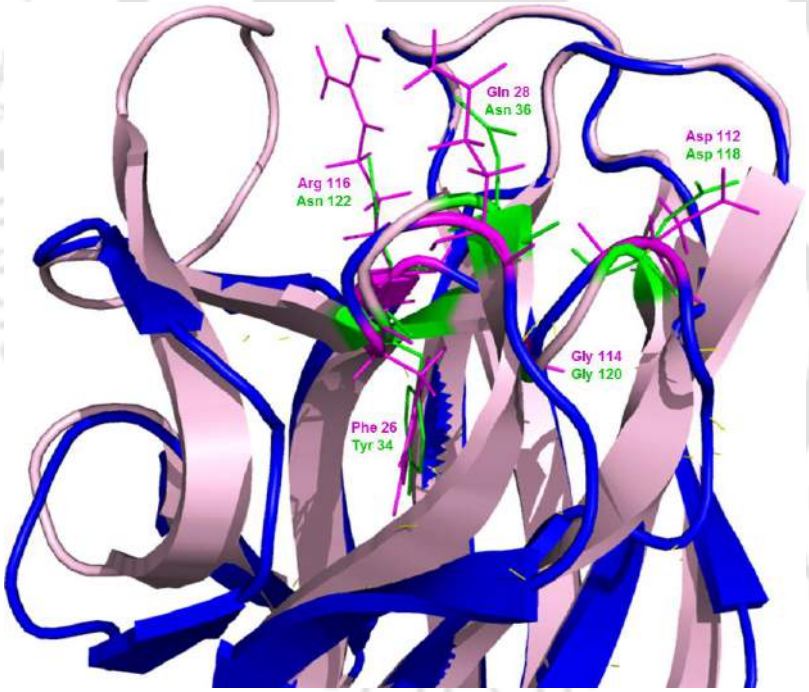


**Fig. 4.10.** Superposition of modelled structure of CBM35 (shown in blue) with CBM35 (2W1W_A) (shown in light-pink) from *Clostridium thermocellum* showing the binding cleft. Some residues from the binding cleft of CBM35 are marked in magenta and those from CBM35 (2W1W_A) are marked in green.

### 4.3.5 Molecular dynamics simulation of modeled PL1B and CBM35

Molecular dynamics simulation on modeled PL1B and CBM35 was performed for elucidating the overall structural stability and closeness of the secondary structures over a span of 5 ns. The results showed that significant changes in PL1B structure in the initial 1.75 ns of simulation, whereas after 2 ns the fluctuations reduced and the overall deflection was less than 0.4 Å (Fig. 4.11A). This suggested that the modeled PL1B structure has a stable conformation. The difference in RMS deviation value between the energy minimized modeled structure of PL1B and the final structure developed after MD simulation was only 0.532 Å.

CBM35 simulation results showed that the CBM35 structure stabilizes after 0.3 ns, with no major fluctuations and the overall deflection was 0.3Å (Fig. 4.11B). The modeled CBM35 showed a stable configuration. Its structure is much smaller than PL1B therefore a rapid stabilization was observed. RMS deviation value between the energy minimized modeled structure of PL1B and the final structure developed after MD simulation was only 0.328 Å. Considering the results obtained after MD simulation it could be concluded that the modeled PL1B and CBM35 structures are stable and compact and was used for docking studies.

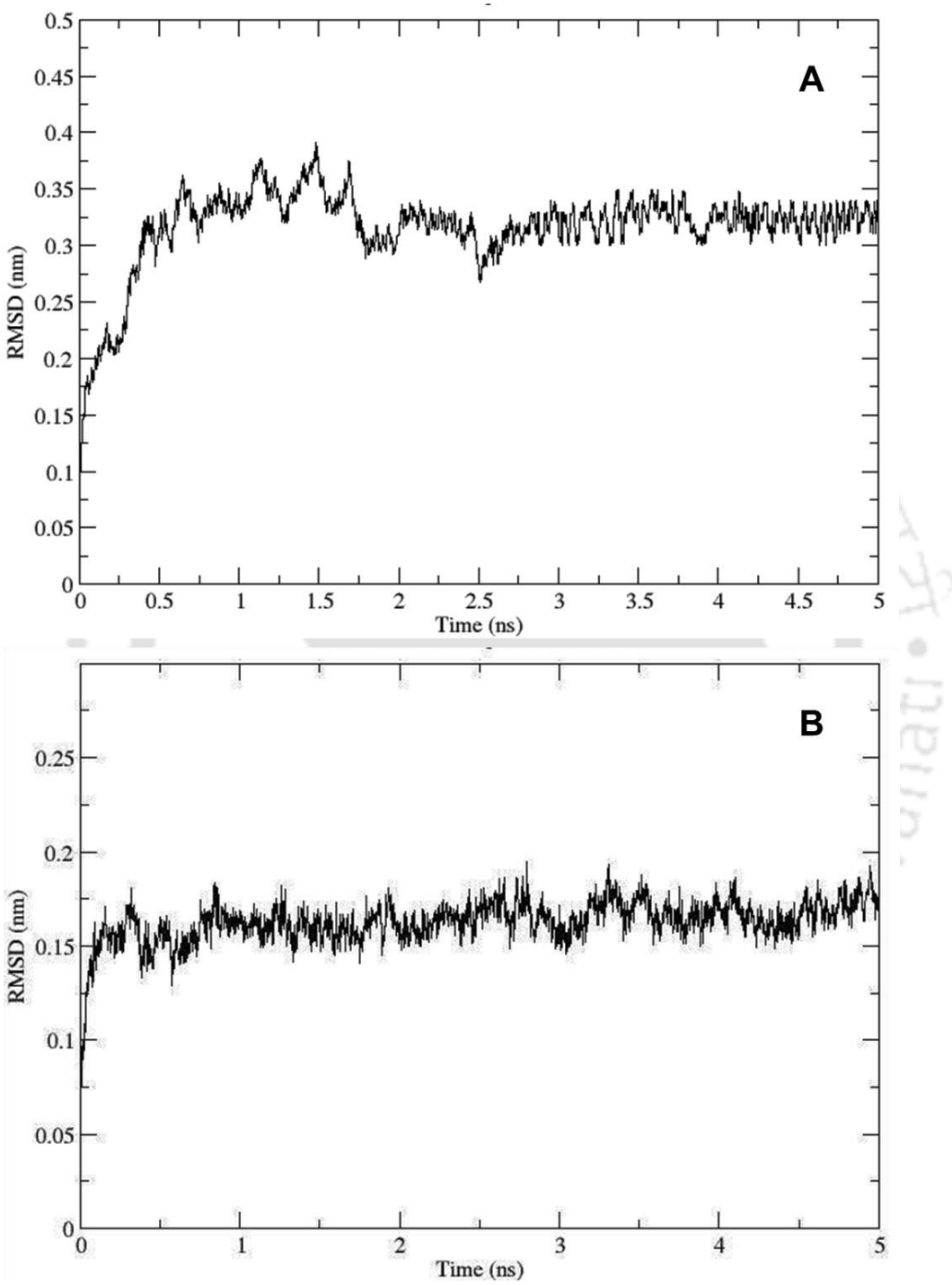


**Fig. 4.11.** Molecular dynamic (MD) simulation of modelled (A) PL1B and (B) CBM35 structure showed that the structure remained almost remains stable during the entire process of simulation.

### 4.3.6 Docking analysis and ligand binding interaction of PL1B and CBM35

The docking analysis of PL1B with different ligands showed best binding affinity with tri-galacturonic acid (TGA) and the complex had the least binding energy of -6.99 Kcal/mol (Table 4.5). Interaction of PL1B with all the docked ligands and their respective binding energies are listed in Table 4.5. In the PL1B-TGA complex structure, TGA was located within the catalytic cleft formed by the extended loop of L2, parts of L3 loop and S3 β-sheet of the central core (Fig. 4.12A and B). Similar binding groove was found in the structure of pectate lyase (Bsp165-PelA) from *Bacillus sp*. (Zheng *et al*., 2012) having 43% sequence similarity with PL1B. The residues involved in polar interaction with TGA are Asp151, Arg209, Asn234, Arg236, Tyr271 and Ser272, showing interaction with the oxygen atoms in and around galacturonate moiety (Fig. 4.12C). In Bsp165-PelA from *Bacillus sp*. the interacting residues at the catalytic center were Thr121, Asp150, Lys177, Arg207 and Tyr269 (Zheng *et al*., 2012). Similarly, in PelC from *Erwinia chrysanthemi* the residues involved were Asp131, Asp170, Lys190, Arg218 and Tyr268 (Herron *et al*., 2003). Comparing the residues of PL1B involved in the catalysis it was evident that Asp 151 and Arg209 was involved in polar interactions with all the ligands, having the least distance as compared with other residues. Similarly, in PL1B-UnDiGAL complex the same residues of PL1B were found interacting with the oxygen atoms in and around the galacturonate moiety of UnDiGAL, Asp 151 and Arg209 showed the nearest polar interaction (Fig. 4.12D). In all the other complexes almost similar residues of PL1B were found to interact with the ligand, Asp 151 and Arg209 was

found to be the nearest polar contact (Table 4.5). A close insight into the sequence alignment revealed that Arg209 in PL1B is conserved and it corresponds to Arg207 in Bsp165-PelA, Arg218 in PelC, Arg207 in pectate lyase II from *Xanthomonas campestris* (Xiao *et al*., 2008) and Arg197 in pectate lyase from *Thermotoga maritima* (Kluskens *et al*., 2003). Owing to the polar interaction and position of Asp 151 and Arg209 in PL1B it is clear that the residue Asp 151 is involved in proton donation and Arg 209 is involved in proton abstraction during the catalysis by β-elimination mechanism. In the β-elimination mechanism of polysaccharide lyases the polygalacturonan chain is cleaved to produce a Δ4,5 unsaturated residues at the non-reducing end (Linhardt *et al*., 1986; Davis *et al*., 1995).

**Table 4.5.** Amino acid residues of PL1B showing polar and residues within 4Å of around the ligand at docking site, hydrophobic residues are underlined.

| Ligand | Binding Energy (kcal/mol) | Polar Interactions | Residues within 4Å |
|---|---|---|---|
| De-esterified pectin (DEPEC) | -2.75 | Arg209, Gly150, Asp151, Arg214, Ser272, Asp257, Tyr271 | Asp257, Thr260, Arg236, Ser273, Ser186, Gly150, Lys259, Ser258 |
| D-Galacto methyl ester (GALME) | -3.42 | Ser212, Arg236, Arg214, Arg209 | Asn234, Ser186, Asp151, Leu183, Tyr271, Tyr270, Ser212 |
| Amino-galacturonic acid (Amino-GAL) | -4.74 | Arg236, Arg214, Ser272, Ser212, Arg209 | Tyr271, Ser186, Asp151, Gly150, Leu183 |
| D-Galacturonic acid (GAL) | -4.59 | Ser212, Arg209, Gly150 | Leu183, Arg236, Tyr271, Asp151 |
| Unsaturated Di-Galacturonic acid (UnDiGAL) | -5.34 | Asn234, Ser212, Ser272, Arg214, Arg209 | Leu183, Tyr271, Tyr179, Asp151, Gly150, Arg236 |
| Tri-Galacturonic acid (TGA) | -6.99 | Asp151, Arg236, Asn234, Tyr271, Ser272, Arg209 | Glu148, Gly149, Gly150, Tyr179, Leu183, Arg214, Ser212, Ser272, Tyr270, Lys259, Ser258, Asp257 |

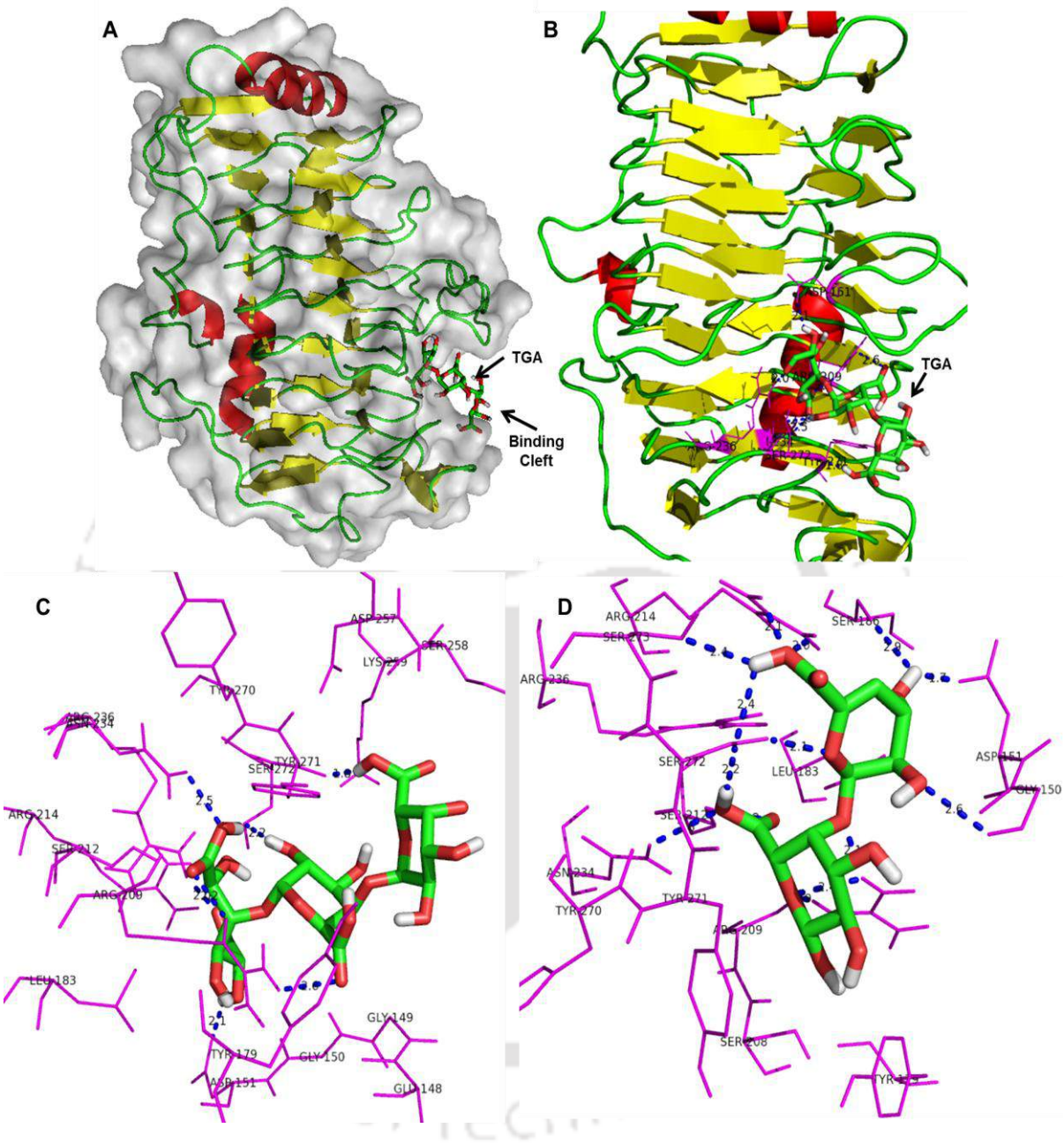


**Fig. 4.12.** (A) Surface view of the active site cleft of PL1B with TGA docked at the site (B) amino acid residues of PL1B interacting with TGA. The figure was generated in Pymol. 3D representation of the ligand (C) TGA and (D) Unsaturated di-galacturonic acid interacting with the active side amino acid residues of PL1B. (- - -) represents the hydrogen bond and the residues marked in magenta are within 4Å radius forming hydrophobic interaction with the ligand.

The docking analysis of CBM35 with different ligands elucidated that it has a strong affinity towards Galacturonic acid (GAL) (Fig. 4.13A&B). The binding energy obtained after interaction of CBM35 with GAL and Δ4,5-GAL was -3.34 Kcal/mol and -2.7 Kcal/mol, respectively (Table 4.6). This inferred that CBM35 has strong affinity towards GAL rather than Δ4,5-GAL. Hence, CBM35 behaved more like Xyl-CBM35 from *Cellvibrio japonicus* (Montanier *et al*., 2009) and Chi-CBM35 from *Amycolatopsis orientalis* (Montanier *et al*., 2009) which also showed more affinity towards GAL. Such diversity in CBM35 towards substrate binding is common due to the change in location of the binding site residues, which has been well established and reported earlier (Montanier *et al*., 2009). The residues of CBM35 making polar interaction with GAL (Fig. 4.13C) and Δ4,5-GAL (Fig. 4.13D) were Phe26, Gln28, Asp112, Gly114 and Arg116, which interacted with the oxygen atom in and around the galacturonate moiety. It was observed that the binding energy drastically decreased upon docking with unsaturated di-galacturonic acid (UnDiGAL) and no binding was observed with tri-galacturonic acid (TGA), suggesting that CBM35 has no affinity for polygalacturonan.

**Table 4.6.** Amino acid residues of CBM35 showing polar and residues within 4Å of around the ligand at docking site, hydrophobic residues are underlined.

| Ligand | Binding Energy (kcal/mol) | Polar Interactions | Residues within 4Å |
|---|---|---|---|
| Unsaturated Di-galacturonic acid (UnDiGAL) | -0.84 | Phe26, Gln28, Asp112, Gly114, Arg116 | Val25, Asp27, Thr29, Asn55, Ser57, Lys59, Leu61, Trp84, Gly113, Pro115 |
| Δ4,5-Galacturonic acid (Δ4,5GAL) | -2.7 | Phe26, Gln28, Asp112, Gly114, Arg 116 | Val25, Asp27, Thr29, Asn55, Ser57, Lys59, Leu61, Trp84, Gly113, Pro115 |
| D-Galacturonic acid (GAL) | -3.34 | Phe26, Gln28, Asp112, Gly114, Arg116 | Val25, Asp27, Thr29, Trp 84, Gly113, Pro115 |

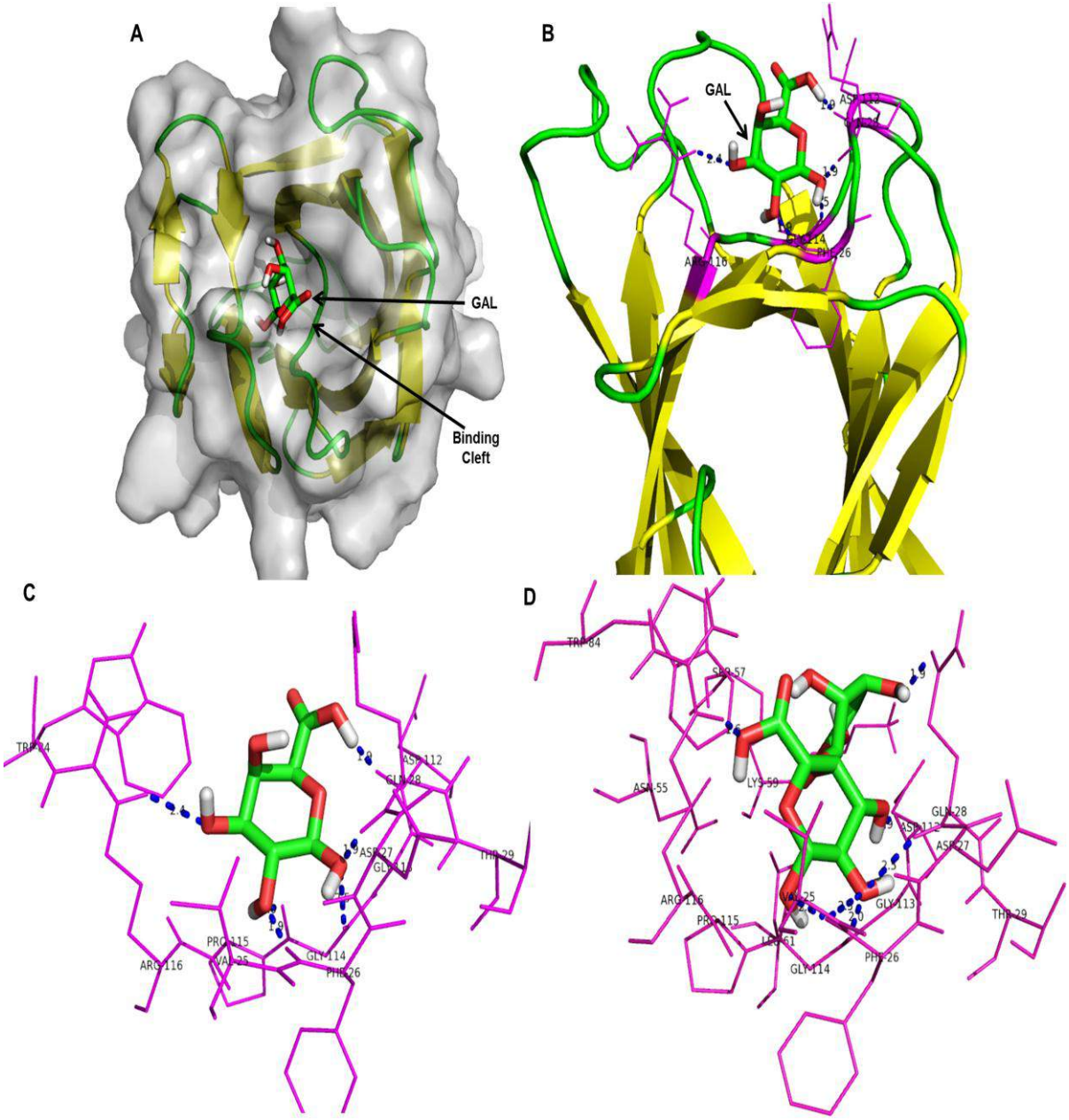


**Fig. 4.13.** (A) Surface view of the active site cleft of CBM35 with GAL docked at the site (B) amino acid residues of CBM35 interacting with GAL. The figure was generated in Pymol. 3D representation of the ligand (C) GAL and (D) Δ4,5-GAL interacting with the active side amino acid residues of CBM35. (- - -) represents the hydrogen bond and the residues marked in magenta are within 4Å radius forming hydrophobic interaction with the ligand.

## 4.4 Conclusions

The 3-dimensional structures of endo-pectate lyase (PL1B) of family 1 polysaccharide lyase and family 35 carbohydrate binding module (CBM35) from *Clostridium thermocellum*, were generated by comparative modelling. The secondary structures of PL1B and CBM35 predicted from their amino acid sequence showed that PL1B is composed of <5% α-helices, >35% β-sheets and <60% random coils and CBM35 of <49.2% β-sheets and <50.8% random coils. The predicted secondary structures were verified by CD analyses, where PL1B displayed presence of 2 α-helices (2.06%), 23 β-sheets (40.54%) and 26 random coils (57.4%) and CBM35 contained α-helix (2.02%), 11 β-strands (47.3%) and 19 random coils (50.68%). The 3-D structural model of PL1B and CBM35 was predicted by multiple template based homology modelling. The PL1B model showed a right handed parallel β-helix structure, where three parallel β-sheets are linked by loops. However, CBM35 displayed the jelly-roll type β-sandwich fold where the two β-sheets are connected by loops. Conclusively, both PL1B and CBM35 structures were rich in β-sheets and loops. The quality of predicted structure was assessed by Ramachandran plot, where in the PL1B and CBM35 structures, 82.8% and 92.7% amino acid residues, respectively, were found in the most favoured region. Molecular dynamic simulation for 5 ns was carried out to understand the stability and compactness of both the predicted models. The results showed significant changes in PL1B structure in the initial 1.75 ns of simulation, whereas after 2 ns the fluctuations reduced and the overall deflection was less than 0.4 Å. MD results of CBM35 displayed that the

changes in the structure are very less and the structure is stabilized after 0.3 ns with deflection less than 0.3 Å. The significant difference in time for the structures to stabilize was due to the presence of 353 aa residues in PL1B as compared to 124 aa residues in CBM35. PL1B showed highest affinity towards tri-galacturonic acid (TGA) with a binding energy of -6.99 Kcal/mol. The key of PL1B residues involved during catalysis were Asp151, Arg209, Asn234, Arg236, Tyr271 and Ser272. Asp151 and Arg209 at the catalytic site were found to be responsible for proton donation and abstraction during β-elimination. CBM35 displayed highest affinity towards D-galacturonic acid and no affinity for polygalacturonan. The binding energy of CBM35 with D-galacturonic acid was -3.34 Kcal/mol. The residues of CBM35 involved in substrate binding were Phe26, Gln28, Asp112, Gly114 and Arg116.

**4.5 References**

Barras, F., van Gigsegem, F., Chatterjee, A.K. (1994) Extracellular enzymes and pathogenesis of soft-rot *Erwinia*. Annual Review in Phytopathology, 32: 201–234.

Bayer, E.A., Kening, R., Lamed, R. (1983) Adherance of *Clostridium thermocellum* to cellulose. Journal of Bacteriology, 156: 818–827.

Bayer, E.A., Lamed, R., White, B.A., Flint, H.J. (2008) From cellulosomes to cellulosomics. The Chemical Record, 8: 364–377.

Berendsen, H.J.C., van der Spoel, D., van Drunen, R. (1995) GROMACS: A message-passing parallel molecular dynamics implementation. Computational Physics Communications, 91(1-3): 43–56.

Boraston A.B., Bolam D.N., Gilbert H.J., Davies G.J. (2004) Carbohydrate-binding modules: Fine-tuning polysaccharide recognition. Biochemical Journal, 382: 769–781.

Boraston A.B., Kwan E., Chiu P., Warren R.A., Kilburn D.G. (2003) Recognition and hydrolysis of noncrystalline cellulose. Journal of Biological Chemistry, 278: 6120–6127.

Chakraborty, S., Fernandes, V.O., Dias, F.M.V., Prates, J.A.M., Ferreira, L.M.A., Fontes, C.M.G.A., Goyal, A., Centeno, M.S.J. (2015) Role of pectinolytic enzymes identified in *Clostridium thermocellum* Cellulosome. PLoS ONE, 10(2): e0116787. doi:10.1371/journal.pone.0116787.

Collmer, A., Keen, N.T. (1986) The role of pectic enzymes in plant pathogenesis. Annual Review in Phytopathology, 24: 383–409.

Cuyvers, S., Dornez, E., Delcour, J.A., Courtin, C.M. (2012) Occurrence and functional significance of secondary carbohydrate binding sites in glycoside hydrolases. Critical Review Biotechnology, 32: 93–107.

Czerwinski, E.W., Midoro-Horiuti, T., White, M.A., Brooks, E.G., Goldblum, R.M. (2005) Crystal structure of Jun a 1, the major cedar pollen allergen from *Juniperus ashei*, reveals a parallel beta-helical core. Journal of Biological Chemistry, 280: 3740–3746.

Davis G., Henrissat B. (1995) Structures and mechanisms of glycosyl hydrolases. Structure, 3: 853–859.

Eswar, N., Marti-Renom, M.A., Webb, B., Madhusudhan, M.S., Eramian, D., Shen, M., Pieper, U., Sali. A. (2006) Comparative Protein Structure Modeling With MODELLER. Current Protocols in Bioinformatics, 15: 5.6.1–5.6.30.

Ghosh A., Luís A.S., Brás J.L.A., Pathaw N., Chrungoo N.K. (2013) Deciphering ligand specificity of a *Clostridium thermocellum* family 35 Carbohydrate binding module (*Ct*CBM35) for gluco- and galacto- substituted mannans and its calcium induced stability. PLoS ONE, 8(12): e80415. doi:10.1371/journal.pone.0080415

Ghosh, A., Verma, A.K., Luis, A.S., Bras, J.L.A., Fontes, C.M., Goyal, A. (2014) Mannan specific family 35 carbohydrate-binding module (*Ct*CBM35) of

*Clostridium thermocellum*: structure analysis and ligand binding. Biologia, 69(10): 1271–1282.

Guex, N., Peitsch, M.C. (1997) SWISS-MODEL and the Swiss-PdbViewer: An environment for comparative protein modeling. Electrophoresis, 18: 2714–2723.

Hall, J., Black, G.W., Ferreira, L.M., Millward-Sadler, S.J., Ali, B.R., Hazlewood, G.P., Gilbert. H.J. (1995) The noncatalytic cellulose-binding domain of a novel cellulase from *Pseudomonas fluorescens subsp*. cellulosa is important for the efficient hydrolysis of Avicel. Biochemical Journal, 309: 749–756.

Henrissat, B., Heffron, S.E., Yoder, M.D., Lietzke, S.E., Jurnak, F. (1996) Functional implication of structure-based sequence alignment of proteins in the extracellular pectate lyase superfamily. Plant Physiology, 107: 963–976.

Herron, S.R., Scavetta, R.D., Garrett, M., Legner, M., Jurnak, F. (2003) Characterization and implications of $Ca^{2+}$ binding to pectate lyase C. Journal of Biological Chemistry, 278: 12271–12277.

Hess, B., Bekker, H., Berendsen, H.J.C., Fraaije, J.G.M. (1997) LINCS: A linear constraint solver for molecular simulations. Journal of Computational Chemistry, 18(12): 1463–1472.

Hinton, J.C.D., Sidebotham, J.M., Gill, D.R., Salmond, G.P.C. (1989) Extracellular and periplasmatic isoenzymes of pectate lyase from Erwinia caratovora subspecies carotovora belong to different gene families. Molecular Microbiology, 3: 1785-1795.

Jeune, C.L., Navarro, M.A.A., Iratxeta, C.P. (2012) Prediction of protein secondary structure from circular dichroism using theoretically derived spectra. Proteins: Structure Function and Bioinformatics, 80: 374–381.

Johansson, R., Gunnarsson, L.C., Ohlin, M., Ohlson, S. (2006) Thermostable carbohydrate-binding modules in affinity chromatography. Journal of Molecular Recognition, 19: 275–281.

John, B., Sali, A. (2003) Comparative protein structure modeling by iterative alignment, model building and model assessment. Nucleic Acids Research, 31: 3982–3992.

Kamen, D.E., Woody, R.W. (2001) A partially folded intermediate conformation is induced in pectate lyase C by the addition of 8-anilino-1-naphthalenesulfonate (ANS). Protein Science, 10: 2123–2130.

Kellett, L.E., Poole, D.M., Ferreira, L.M., Durrant, A.J., Hazlewood, G.P., Gilbert, H.J. (1990) Xylanase B and an arabinofuranosidase from Pseudomonas fluorescens subsp. cellulosa contain identical cellulose-binding domains and are encoded by adjacent genes. Biochemical Journal, 272: 369–376.

Kelly, S.M., Jess, T.J., Price N.C. (2005) How to study proteins by circular dichroism (Review). Biochimica et Biophysica Acta, 1751: 119–139.

Kita, N., Boyd, C.M., Garrett, M.R., Jurnak, F., Keen, N.T. (1996) Differential effect of site directed mutations in pelC on pectate lyase activity, plant tissue maceration, and elicitor activity. Journal of Biological Chemistry, 271: 26529–26535.

Kluskens, L.D., van Alebeek, G.W.M., Voragen, A.G.J., De Vos W.M., Van Der Oost, J. (2003) Molecular and biochemical characterization of the thermoactive family 1 pectate lyase from the hyperthermophilic bacterium *Thermotoga maritima*. Biochemical Journal, 370: 651–659.

Krieger, E., Joo, K., Lee, J., Raman, S., Thompson, J., Tyka, M., Baker, D., Karplus, K. (2009) Improving physical realism, stereochemistry, and side-chain accuracy in homology modeling: Four approaches that performed well in CASP8. Proteins, 77: 114–122.

Lamed, R., Setter, E., Bayer, E.A. (1983) Characterization of a cellulose-binding, cellulose-containing complex in *Clostridium thermocellum*. Journal of Bacteriology, 156: 828–836.

Larkin M.A., Blackshields G, Brown N.P., Chenna R, McGettigan P.A., McWilliam H, Valentin F, Wallace I.M., Wilm A, Lopez R, Thompson J.D., Gibson T.J., Higgins D.G. (2007) Clustal W and Clustal X version 2.0. Bioinformatics, 23: 2947–2948.

Lietzke, S. E., Keen, N. T., Yoder, M. D., Jurnak, F. (1994) The three-dimensional structure of pectate lyase E, a plant virulence factor from *Erwinia citrysanthemi*. Plant Physiology, 106: 849–862.

Linhardt, R.J., Galliher, P.M., Cooney, C.L. (1986) Polysaccharide lyases. Applied Biochemistry and Biotechnology, 12: 135–176.

Lojkowska, E., Masclaux, C., Boccara, M., Robert-Baudouy, J., Hugouvieux-Cotte-Pattat, N. (1995) Characterization of the pelL gene encoding a novel pectate lyase of *Erwinia chrysanthemi* 3937. Molecular Microbiology, 16: 1183–1195.

Melo, F., Sanchez, R., Sali, A. (2002) Statistical potentials for fold assessment. Protein Science, 11: 430–448.

Montanier, C., van Bueren, A.L., Dumona, C., Flint, J.E., Correia, M.A., Prates, J.A., Firbank, S.J., Lewis, R.J., Grondin, G.G., Ghinet, M.G., Gloster, T.M., Herve, C., Knox, J.P., Talbot, B.G., Turkenburg, J.P., Kerovuo, J., Brzezinski, R., Fontes, C.M.G.A., Davies, G.J., Boraston, A.B., Gilbert, H.J. (2009) Evidence that family 35 carbohydrate binding modules display conserved specificity but divergent function. Proceedings of National Academy of Science (USA), 106: 9, 3065–3070.

Montanier, C.Y., Correia, M.A.S., Flint, J.E., Zhu, Y., Basle, A., McKee, L.S., Prates, Jose A.M., Polizzi, S.J., Coutinho, P.M., Lewis, R.J., Henrissat, B., Fontes, C.M.G.A., Gilbert, H.J. (2011) Novel, noncatalytic carbohydrate-binding module displays specificity for galactose-containing polysaccharides through calcium-mediated oligomerization. Journal of Biological Chemistry, 286(25): 22499–22509.

Moreau M., Chaby R., Szabo L. (1982) Isolation of a trisaccharide containing 2-amino-2-deoxy-D-galacturonic acid from the Bordetella pertussis endotoxin. Journal of Bacteriology, 150(1): 27–35.

Morris, G. M., Huey, R., Lindstrom, W., Sanner, M. F., Belew, R. K., Goodsell, D. S., Olson, A. J. (2009) Autodock4 and AutoDockTools4: automated docking with selective receptor flexiblity. Journal of Computational Chemistry, 16: 2785–91.

Novy R., Yaeger K., Monsma S., McCormick M., Berg J. (1997) Cellulose binding domain expression vectors for the rapid, low cost purification of CBD-fusion proteins. FASEB Journal, 11: A1151–A1151.

O'Boyle, N. M., Banck, M., James, C. A., Morley, C., Vandermeersch, T., Hutchison, G. R. (2011) Open Babel: An open chemical toolbox. Journal of Cheminformatics, 3: 33.

O'Neill M., Albersheim P., Darvill A. (1990) The pectic polysaccharides of primary cell walls; In Methods in Plant Biochemistry; Academic Press: London, Vol. 2, pp. 415–441.

Pickersgill R., Jenkins J., Harris G., Nasser W., Robert-Baudouy J. (1994) The structure of Bacillus subtilis pectate lyase in complex with calcium. Nature Structural Biology, 1: 717-723.

Pissavin, C., Robert-Baudouy, J., Hugouvieux-Cotte-Pattat, N. J. (1996) Regulation of pelZ, a gene of the pelB-pelC cluster encoding a new pectate lyase of *Erwinia chrysanthemi*. Bacteriology, 3937(178): 7187–7196.

Pronk, S., Pall, S., Schulz, R., Larsson, P., Bjelkmar, R., Apostolov, R., Shirts, M.R., Smith, J.C., Kasson, P.M., van der Spoel, D., Hess, B., Lindahl, E. (2013) GROMACS 4.5: a high-throughput and highly parallel open source molecular simulation toolkit. Bioinformatics, 29(7): 845–854.

Ragauskas, A.J., Williams, C.K., Davison, B.H., Britovsek, G., Cairney, J., Eckert, C.A., Frederick Jr., W.J., Hallett, J.P., Leak, D.J., Liotta, C.L., Mielenz, J.R., Murphy, R., Templer, R., Tschaplinski T. (2006) The path forward for biofuels and biomaterials. Science, 311: 484–489.

Robert, X., Gouet, P. (2014) Deciphering key features in protein structures with the new ENDscript server. Nucleic Acids Research, 42(W1): W320–W324.

Sainz-Polo, M.A., Valenzuela, S.V., Gonzalez, B., Pastor, F.I., Sanz-Aparicio, J. (2014) Structural analysis of glucuronoxylan-specific Xyn30D and its attached CBM35 domain Gives Insights into the Role of Modularity in Specificity, Journal of Biological Chemistry, 289(45): 31088–31101.

Scavetta, R.D., Herron, S.R., Hotchkiss, A.T., Kita, N., Keen, N.T., Benen, J.A., Kester, H.C., Visser, J., Jurnak, F. (1999) Structure of a plant cell wall fragment complexed to pectate lyase C. Plant cell, 11: 1081–1092.

Shen, M.Y., Sali, A. (2006) Statistical potential for assessment and prediction of protein structures. Protein Science, 15: 2507–2524.

Takao, M.; Nakaniwa, T.; Yoshikawa, K.; Terashita, T.; Sakai. T. (2001) Molecular cloning, DNA sequence, and expression of the gene encoding for thermostable pectate lyase of thermophilic *Bacillus sp.* TS 47. Bioscience Biotechnology and Biochemistry, 65: 322–329.

Tamaru, Y., Doi, R.H. (2001) Pectate lyase A, an enzymatic subunit of the *Clostridium cellulovorans* cellulosome. Proceedings of National Academy of Science (USA), 98: 4125–4129.

Tardy, F., Nasser, W., Robert-Baudouy, J., Hugouvieux-Cotte-Pattat, N. (1997) Comparative analysis of the five major *Erwinia chrysanthemi* pectate lyases: enzyme characteristics and potential inhibitors. Journal of Bacteriology, 179: 2503– 2511.

Thomas, L.M., Doan, C.N., Oliver, R.L., Yoder, M.D. (2002) Structure of pectate lyase A: comparison to other isoforms. Acta Crystallography, D58: 1008–1015.

Tomme, P., van Tilbeurgh, H., Pettersson G., van Damme J., Vandekerckhove J., Knowles, J., Teeri, T., Claeyssens, M. (1988) Studies of the cellulolytic system of *Trichoderma reesei* QM9414. Analysis of domain function in two cellobio hydrolases by limited proteolysis. European Journal of Biochemistry, 170: 575–581.

Xiao, Z., Bergeron, H., Grosse, S., Beauchemin, M., Garron, M.L., Shaya, D., Sulea, T., Cygler, M., Lau, P.C. (2008) Improvement of the thermostability and activity of a pectate lyase by single amino acid substitutions, using a strategy based on melting-temperature-guided sequence alignment. Applied Environmental Microbiology, 74: 1183–1189.

Yoder, M. D., Keen, N. T., Jurnak, F. (1993a) New domain motif: structure of pectate lyase C, a secreted plant virulence factor. Science, 260: 1503–1507.

Yoder, M.D., Jurnak, F. (1995b) The refined three-dimensional structure of pectate lyase C from *Erwinia chrysanthemi* at 2.2 Angstrom resolution (implications for an enzymatic mechanism). Plant Physiology, 107: 349–364.

Yoder, M.D., Jurnak, F. (1995b) Protein motifs. 3. The parallel beta helix and other coiled folds. FASEB Journal, 9: 335–342.

Yoder, M.D., Lietzke, S.E., Jurnak, F. (1993b) Unusual structural features in the parallel β-helix in pectate lyases. Structure, 1: 241–251.

Yoshida K., Ohtomo T., Suganuma M. (1990) Isolation of a serologically different compact-colony-forming active substance from strains of *Staphylococcus aureus*. Microbiology and Immunology, 34(10): 801–808.

Zheng, Y., Huang, C.H., Liu, W., Ko, T.P., Xue, Y., Zhou, C., Guo, R.T., Ma. Y. (2012) Crystal structure and substrate-binding mode of a novel pectate lyase from alkaliphilic *Bacillus sp*. N16-5. Biochemical and Biophysical Research Communications, 420: 269–274.

# Chapter 5

## Immobilization of recombinant family 1 polysaccharide lyase (PL1B) on magnetic nanoparticles for bioscouring of cotton fabric

### 5.1 Introduction

Pectins are polymeric compounds found in the middle lamella of plant cell walls, which are α-1,4 linked galacturonan chains. The constituents of these polysaccharides are homogalacturonan, rhamnogalacturonan-I and rhamnogalacturonan-II (Ridley *et al*., 2001). Pectin accounts for 0.5-4% of the total plant material, which is extracted as a highly viscous and soluble material from fruits (Kashyap *et al*., 2001). Pectin degrading enzymes act on the substrate by hydrolysis and lysis. In the lysis mechanism the α-1,4 glycosidic bond in the pectic polysaccharide chain is cleaved by a β-transelimination mechanism to produce a 4,5 unsaturated galacturonide residue at the non-reducing end (Sakai *et al*., 1993). Pectate lyase can cleave pectic acid (polygalacturonic acid) or low methylated pectins. *Erwinia chrysanthemi* is known to cause soft rot in plant and five major isozymes of pectin degrading enzymes have been identified from the same (Tardy *et al*., 1997).

Bacterial thermostable pectate lyases were characterized from *Bacillus subtillis* (Soriano *et al*., 2006), *Clostridium cellovorans* (Tamaru *et al*., 2001) which may be efficiently used in various industrial processes. Pectinases have immense application in processes like fruit juice clarification, vaccum infusion for removal of citrus peels, bioscouring of cotton fabric, degumming of plant fibers, paper and pulp making, citrus oil extraction and wine production (Jayani *et al*., 2005).

Immobilization of pectinases has always been proved to be a better mode of increasing the efficiency and thermostability of these enzymes. Commercial pectinase immobilized on ion exchange resin particles were further used for mash treatment of vegetables in order to recover more juice during puree production (Demir *et al*., 2001). Covalent immobilization of pectinase facilitated on silica coated iron oxide nanoparticles was reported to improve its activity and stability (Lei *et al*., 2007). Magnetic nanoparticles negatively charged with docusate sodium salt were used for immobilization of pectinase, where large amount of enzyme was successfully immobilized on the support (Bahrami *et al*., 2013). Pectinase from *Bacillus licheniformis* was immobilized on microporous resin coated with chitosan that efficiently reduced the cationic demand and pitch deposit on whitewater (Liu *et al*., 2012). Hence this immobilized pectinase was successfully used for treatment of whitewater in paper manufacturing industries. Pectate lyase from *Bacillus megaterium* immobilized on hydroxyapatite nanoparticles showed improved activity, stability and half-life at 90ºC (Mukhopadhyay *et al*., 2012). Bioscouring of cotton fabric is an ecofriendly technique where removal of non-cellulosic substances improves the wetability of the fabric (Li *et al*., 1998). It not only prevents the fabric damage but

also protects the environment from corrosive compounds like caustic soda generally used in chemical bioscouring process (O'Neill *et al*., 1999).

A catalytic domain of *Clostridium thermocellum* ATCC 27405 in family 1 polysaccharide lyase of the CAZY database (http://www.cazy.org/PL1_bacteria.html) showed sequence similarity with pectate lyase domain of *Bacillus sp*. (Zheng *et al*., 2012), *Thermotoga maritima*, *Xanthomonas campestris* and *Erwina chrysanthemi* (Xiao *et al*., 2008). In the present study the 353 aa long catalytic module PL1B from *Clostridium thermocellum*, which was cloned and expressed earlier as mentioned in Chapter 2, Section 2.3.3 and 2.3.4, was immobilized on synthesized MNPs and used for bioscouring of cotton fabric.

## 5.2 Materials and Methods

### 5.2.1 Recombinant PL1B

The recombinant PL1B (GeneBank accession number ABN53381.1) from *Clostridium thermocellum* ATCC 27405 belonging to family 1 polysaccharide lyase (PL1B) of CAZy database (http://www.cazy.org/PL1_bacteria.html) was expressed and purified by immobilized metal ion affinity chromatography as described in Chapter 2, Section 2.2.15 and used for further study.

### 5.2.2 Synthesis of $Fe_3O_4$ nanoparticles

Super paramagnetic iron oxide nanoparticles were synthesized by chemical co-precipitation from the mixture of Ferric salts. In this process $Fe_3O_4$ magnetic nanoparticles (MNPs) were synthesized from a mixture of $FeCl_3.6H_2O$ and $FeCl_2.4H_2O$ salts in the molar ratio 1:2. MNPs were formed between pH 8 and 14 under vigorous stirring with drop-wise addition of 0.1M $NH_4OH$ solution, pH of the solution was constantly monitored during the process (Huang *et al*., 2003). The precipitation of MNPs was indicated by color change of the solution to dark-black. The reaction was carried out under inert atmosphere using nitrogen gas in order to prevent the oxidation of MNPs. After the precipitation of MNPs, its repeated washing with deionized water facilitated the lowering of pH from 12 to 7. To obtain chloride free particles, the precipitate was twice washed with deionized and distilled water, and later on with ethanol, to remove the water present on the surface of MNPs. Synthesized MNPs were finally dried in a lyophilizer (Christ, Alpha 1-2 LD Freeze Dryer) to obtain the fine powder.

### 5.2.3 Size and shape analysis of synthesized MNPs

$Fe_3O_4$ MNPs were subjected to powder X-ray diffraction (XRD) for analysis of their structural features. The particle size was quantitatively evaluated from the XRD data using the Debye-Scherrer equation (Patterson *et al*., 1939), which is a relationship between peak broadening and particle size.

$$D= k\lambda/(\beta.\cos\theta)$$

Where, k is Sherrer constant (0.89), λ is the X-ray wavelength (0.15406 nm), β is the peak width of half-maxima, and θ is the Bragg diffraction angle [19]. Further, confirmation of the structural properties of the MNPs was carried out by Transmission electron microscope (JEOL, JEM 2100). High resolution images of MNPs were taken by high resolution transmission electron microscope (HRTEM) and selected area electron diffraction (SAED). The samples for TEM analysis were prepared after uniform dispersion of MNPs by a 2 min sonication cycle. Dispersed MNPs were placed in a drop of acetone on a copper grid and the samples were further dried in a desiccator before imaging.

### 5.2.4 Immobilization of PL1B to MNPs

Water soluble carbodiimide (EDC hydrochloride / EDC) activates the hydroxyl group and couples the amino group of enzyme with MNPs (Mehta *et al*., 1997; Koneracka *et al*., 2006). The purified PL1B was buffer exchanged with 50 mM Tris-HCl buffer, pH 7.4 containing 100 mM NaCl and concentrated using Amicon ultra centrifugal filter (Merck Millipore) and used for immobilization. 10-100 mg MNPs was suspended in 1 ml 50 mM phosphate buffer, pH 7.4 containing 100 mM NaCl. 0.5 ml of EDC solution (20 mg/ml in 50 mM phosphate buffer, pH 7.4, 100 mM NaCl) was added to the MNPs and sonicated in a bath sonicator for 20 min at

4°C. This process facilitated the carbodiimide activation of hydroxyl groups on MNP's and further sonication helped in monodispersion. After the carbodiimide activation of MNPs, 0.5 ml (2 mg/ml) enzyme (PL1B) was added and sonicated at 4°C for 45 min. This process replaced the bound carbodiimide on MNPs and linked the amino groups of PL1B to MNPs as also reported earlier by Kouassi *et al*., 2005. Excess and unbound PL1B was removed by repeated washing in 50 mM Tris-HCl buffer pH 7.4 containing 100 mM NaCl for three times, and finally PL1B immobilized MNPs were recovered by the help of a magnet. Presence of NaCl in the solution hinders the aggregation of the nanoparticles especially under alkaline condition (Kondo *et al*., 1997). The concentration of unbound protein in the supernatant left after removal of MNPs was determined by measuring the absorbance at 280 nm ($A_{280}$), using the extinction coefficient of PL1B as 44725 $M^{-1}cm^{-1}$. The percentage of bound enzyme was calculated from the following formula:

$$E_{Bound}\ (\%) = [(C_{in} - C_{su}) / C_{in}] \times 100$$

Where, $C_{in}$ and $C_{su}$ is the concentration (mg/ml) of enzyme initially taken and left in supernatant, respectively.

### 5.2.5 Analysis of immobilized PL1B-MNP

Immobilization of PL1B on MNPs was confirmed by analyzing the bare MNPs and immobilized PL1B-MNP by Field emission scanning electron microscopy (FESEM) (Zeiss, Sigma) under nanoscale magnification. Chemical characterization as well as elemental analysis of the samples was done by Energy dispersive X-ray spectroscopy (EDX) (LEO, 1430vp), where an X-ray beam knocks out an electron from the outer electron shell of an element, which is emitted as another X-ray. The presence of a particular element was determined by the difference in energy between

the incident and emitted electrons (Goldstein *et al*., 2003). The samples for FESEM and EDX analysis were prepared from lyophilized MNPs and immobilized PL1B-MNP uniformly dispersed on carbon tape attached stubs. Individual KBr pellets of 1 mm thickness were prepared with MNPs, PL1B and immobilized PL1B-MNP which were analyzed by FT-IR spectroscope (Perkin-Elmer, Spectrum Two). Change in magnetization of MNPs at different stages of immobilization process was determined by Vibrating sample magnetometer (VSM) (Lakeshore, 4710 series) under a magnetic field of 18,000 Oersted (Oe), by analyzing the dried at 25°C.

### 5.2.6 Assay of PL1B and immobilized PL1B-MNP

The activity of PL1B and immobilized PL1B-MNP was determined using 0.1% (w/v) Polygalacturonic acid (PGA) and Citrus pectin as substrate. A reaction volume of 1 ml contained 50 mM Tris-HCl buffer pH 8.6, 0.6 mM $CaCl_2$, 10 µl immobilized PL1B (1.4 mg/ml). The reaction mixture of PL1B and immobilized PL1B-MNP was incubated at 50ºC for 5 min. After the reaction was stopped by incubating on ice for 10 min, immobilized PL1B-MNP was removed by a magnet and the un-hydrolyzed polysaccharides were removed by centrifugation at 10,000 rpm. Absorbance at 235 nm ($A_{235}$) of the supernatant was measured by UV-visible spectrophotometer (Varian, Cary 100 Bio) to determine the amount of 4,5-unsaturated oligogalactouronates produced (Tamaru *et al*., 2001). One unit of enzyme activity is defined as the amount of enzyme that liberates 1 µmol of unsaturated oligogalacturonates per minute under the above reaction conditions. The molar extinction coefficient of 4,600 $M^{-1}$ $cm^{-1}$ was used for 4,5-unsaturated oligogalacturonates (Hasegawa *et al*., 1966). The reaction condition for PL1B assay was same as followed for the immobilized PL1B-MNP where no magnetic separation

was required for recovery of the enzyme. It was observed that 1 mg of PL1B bound to 70 mg of MNPs.

### 5.2.7 Thermal stability of immobilized PL1B-MNP

Thermal stability of free and immobilized PL1B-MNP was determined by incubating 10 µl (1.4 mg/ml) of each in 100 µl of 50 mM Tris-HCl buffer pH 8.6 at different temperatures ranging from 30ºC to 100ºC for 30 min. To determine the retention of activity by immobilized PL1B-MNP and PL1B, they were incubated at a particular temperature over a time period of 15 min to 4 h. After incubation the enzymes were assayed with 0.1% (w/v) PGA following the procedure as mentioned earlier in Section 5.2.6.

### 5.2.8 Operational stability of immobilized PL1B-MNP

In order to determine the operational stability of immobilized PL1B-MNP 10 µl (1.4 mg/ml), it was assayed using 0.1% (w/v) PGA in 1 ml reaction mixture containing 50 mM Tris-HCl buffer, pH 8.6 and 0.6 mM $CaCl_2$ at 50°C for 5 min. Immobilized PL1B-MNP was removed by a magnet and the absorbance at 235 nm ($A_{235}$) was measured to estimate the unsaturated oligogalacturonate concentration, following the protocol as mentioned earlier. After each cycle immobilized PL1B-MNP was thoroughly washed with 50 mM Tris-HCl buffer pH 7.4 containing 100 mM NaCl to remove the bound substrate. The next reaction cycle was setup by following the above mentioned protocol, and was followed for 8 consecutive cycles.

### 5.2.9 Bioscouring of cotton fabric

Coarse cotton fabric of 2.5x6.5 cm dimension and weighing 1.0 g each was used for bioscouring. The fabric was pretreated by thoroughly washing with hot water and treating with 1 mg/ml α-amylase to remove waxes and sizing material from the

surface of the fabric (Morozova *et al*., 2006). The pretreated fabrics were then soaked in 10 ml of 50 mM Tris-HCl buffer pH 8.6 containing 0.6 mM $CaCl_2$. This cotton fabric was again treated with varying concentrations (0.05 to 0.5 mg/ml) of PL1B or immobilized PL1B-MNP. The reactions were incubated at 50°C under constant shaking at 220 rpm. The increase in the wetability of the treated fabric was determined by the time taken to absorb water on its surface, with reference to the control sample (cotton fabric without pretreatment or pectinase treatment). The removal of pectin from the fabric was visualized after dyeing it with Ruthenium Red dye at 50ºC for 30 min (Morozova *et al*., 2006).

## 5.3. Results and Discussion

### 5.3.1 Characterization of synthesized MNPs

The X-ray diffraction (XRD) pattern of $Fe_3O_4$ MNPs showed series of characteristic peaks at 2.96(220), 2.52(311), 2.09(400), 1.71(422), 1.61(511), 1.47(440) and 1.27(533) (Fig. 5.1) which indicated the cubic spinel phase of $Fe_3O_4$. The crystal size calculated from the XRD data using the Debye-Scherrer equation was found to be 20±5 nm in size. TEM image analysis of $Fe_3O_4$ MNPs (Fig. 5.2A) revealed that their shapes were not strictly spherical, but it could be approximated to sphere. HRTEM (Fig. 5.2B) and selected area electron diffraction (SAED) analysis (Fig. 5.3) confirmed the formation of highly crystalline $Fe_3O_4$ nanoparticles.

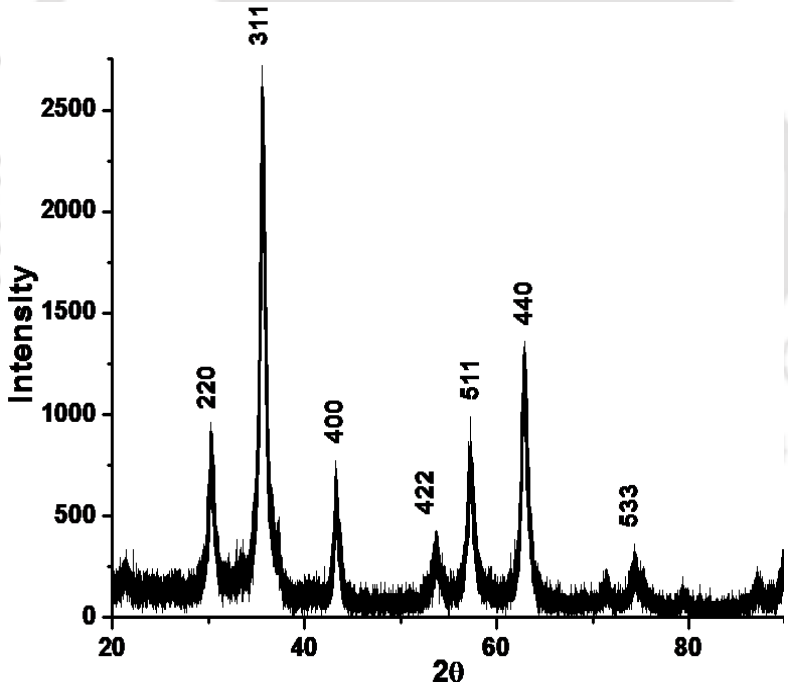


**Fig. 5.1** XRD analysis of synthesized $Fe_3O_4$ magnetic nanoparticles (MNPs), showing characteristics peaks from where their size was calculated.

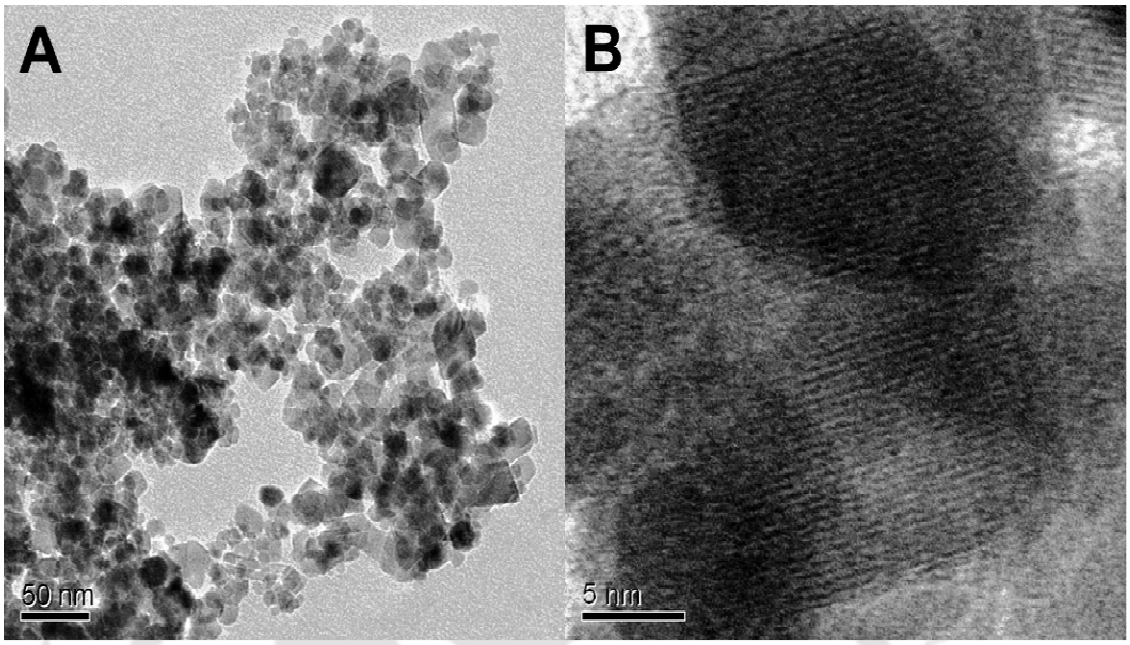


**Fig. 5.2** TEM images of synthesized MNPs (A) Normal and (B) High Resolution TEM showing that they are not perfectly spherical

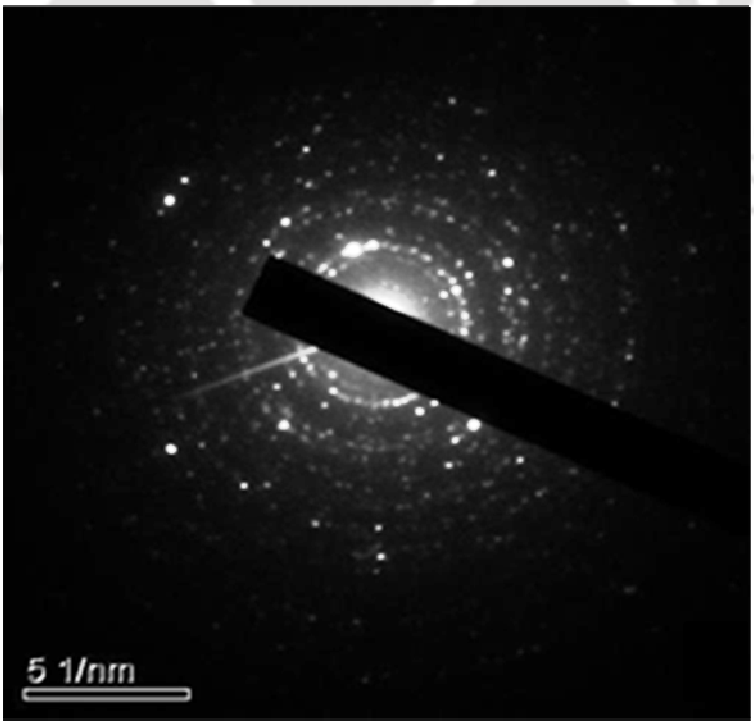


**Fig. 5.3** SAED analysis of synthesized MNPs showing their highly crystalline nature.

### 5.3.2 Binding efficiency of PL1B with MNPs

The immobilization of PL1B was carried out after activation of hydroxyl groups on the surface of MNPs by carbodiimide, as per the scheme shown in Fig. 5.4A. A fixed concentration (1 mg/ml) of the enzyme was used, with varying concentration of MNPs. The amount of enzyme bound to MNPs was calculated by determining the concentration of unbound PL1B remaining in the supernatant after immobilization. It was observed that at 50 mg/ml concentration of MNPs the binding efficiency of PL1B was 97%, whereas at 70 mg/ml and above concentration of MNPs the binding efficiency was 100% (Fig. 5.4B)

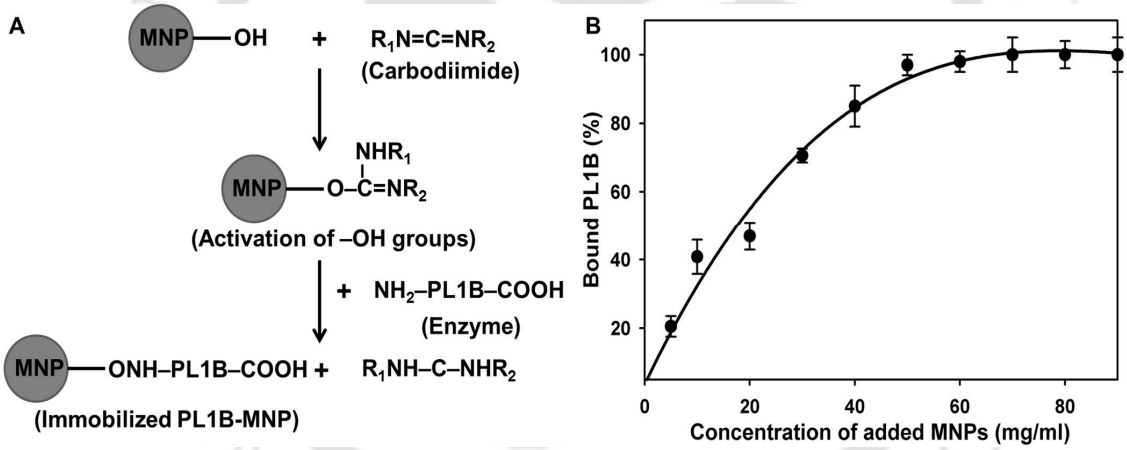


**Fig. 5.4** (A) Schematic representation of immobilization of PL1B on MNPs by activation method; (B) Binding efficiency of PL1B (1 mg/ml), with varying concentration of MNPs.

### 5.3.3 Confirmation of binding of PL1B with MNPs

#### 5.3.3.1 FESEM analysis of immobilization

FESEM images of bare MNPs and PL1B bound MNPs confirmed the binding of PL1B to MNPs. The bare MNPs were uniformly dispersed and distinctly visible (Fig. 5.5A), whereas the PL1B bound MNPs were found to be covered by a layer

encapsulating the entire particle (Fig. 5.5B). Though some aggregates were visible due to the large surface area to volume ratio and high surface energy of immobilized PL1B-MNP as also reported earlier by Honga *et al*., 2008. The surface energy increased during the drying of bare and enzyme bound MNPs.

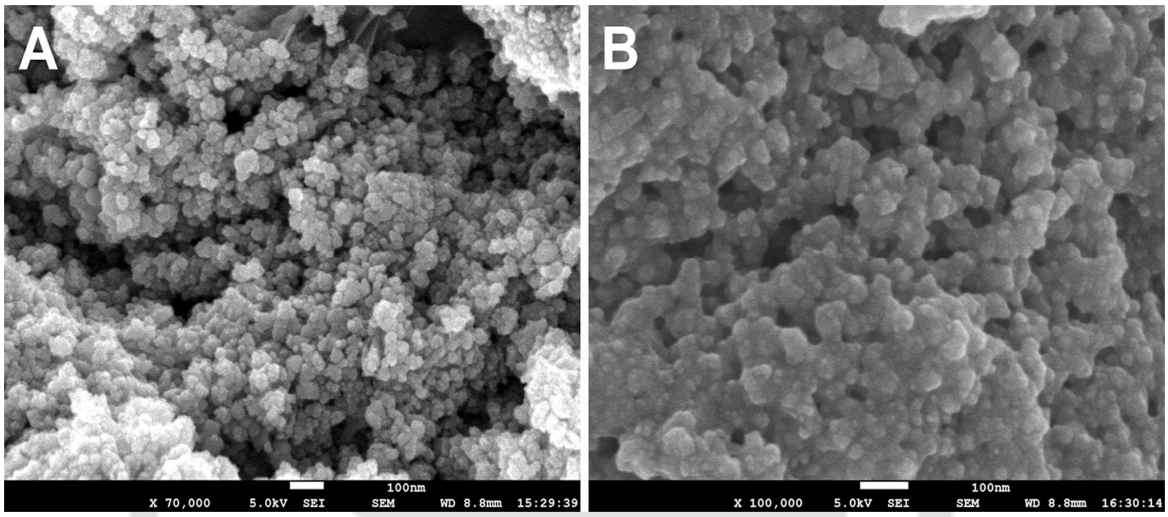


**Fig. 5.5** FESEM images of (A) bare MNPs and (B) immobilized PL1B-MNP.

**5.3.3.2 FT-IR analysis for confirming immobilization of PL1B**

Binding of PL1B to MNPs was further confirmed by FT-IR analysis of the sample. Bare MNPs displayed a peak at 561 $cm^{-1}$ (Fig. 5.6A) which is due to the Fe–O bond, and the peak at 3452 $cm^{-1}$ (Fig. 5.6A) was due to O–H stretching of the hydroxyl groups on the surface of bare MNPs, which resulted from the absorbed water as also reported by Honga *et al*., 2008. The peak at 1635 $cm^{-1}$ (Fig. 5.6A) was assigned to N–H bending from amino group as they were absorbed during formation of MNPs by chemical co-precipitation process using $NH_4OH$, as also reported earlier (Huang *et al*., 2003). The peak size at 3452 $cm^{-1}$ for O–H stretching obtained in the bare MNPs (Fig. 5.6A) significantly reduced after the immobilization of PL1B (Fig. 5.6C), which clearly suggested that the binding was accomplished via hydroxyl

groups of MNPs and the amino groups of PL1B. This can also be understood from the scheme presented in Fig. 5.4A. The characteristic peak of PL1B at 1558 $cm^{-1}$ (Fig. 5.6B) appeared in the immobilized MNPs (Fig. 5.6C), due to C–C stretching in aromatic species which was from the aromatic amino acid residues of PL1B. Another characteristic peak at 1069 $cm^{-1}$ (Fig. 5.6B) appeared after immobilization (Fig. 5.6C) from the C–N stretching in aliphatic amines present in the amino acid side chains of PL1B. Hence, the presence of PL1B is obvious in the sample, thus confirming the binding of PL1B to MNPs after immobilization.

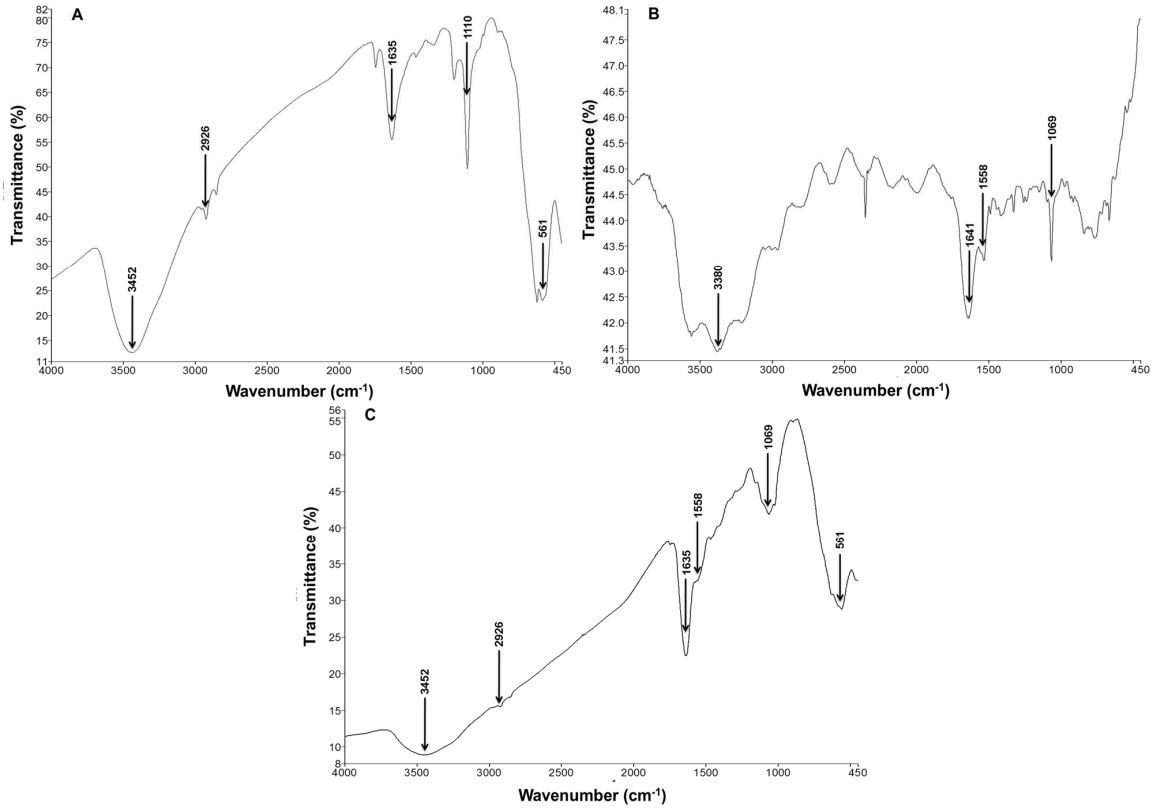


**Fig. 5.6** FT-IR analysis of (A) bare MNPs, (B) PL1B, (C) immobilized PL1B-MNP confirming the binding of PL1B to MNPs.

### 5.3.3.3 EDX analysis of immobilized PL1B-MNP

EDX analysis of immobilized PL1B-MNP showed the presence of significant elements which were incorporated only after successful immobilization. The EDX spectrum of immobilized PL1B-MNP showed presence of Iron (Fe) and Oxygen (O) in a percent atomic weight of 8.44 and 20.03, respectively which suggested the presence of MNPs (Fig. 5.7). On the other hand the percentage atomic weight of elements like Carbon (C), Sulphur (S), Calcium (Ca) and Chloride (Cl) were 14.6, 1.57, 0.35 and 51.68 percent, respectively (Fig. 7). This showed that presence of carbon and sulphur was due to carbon backbone and di-sulphide bonds from PL1B. As PL1B unlike other pectate lyases is a calcium dependent protein, hence it has a strong affinity towards calcium ion; hence, the presence of calcium was justified. Chloride in the EDX spectra is from the $CaCl_2$ and NaCl, which were used to stabilize the protein during purification.

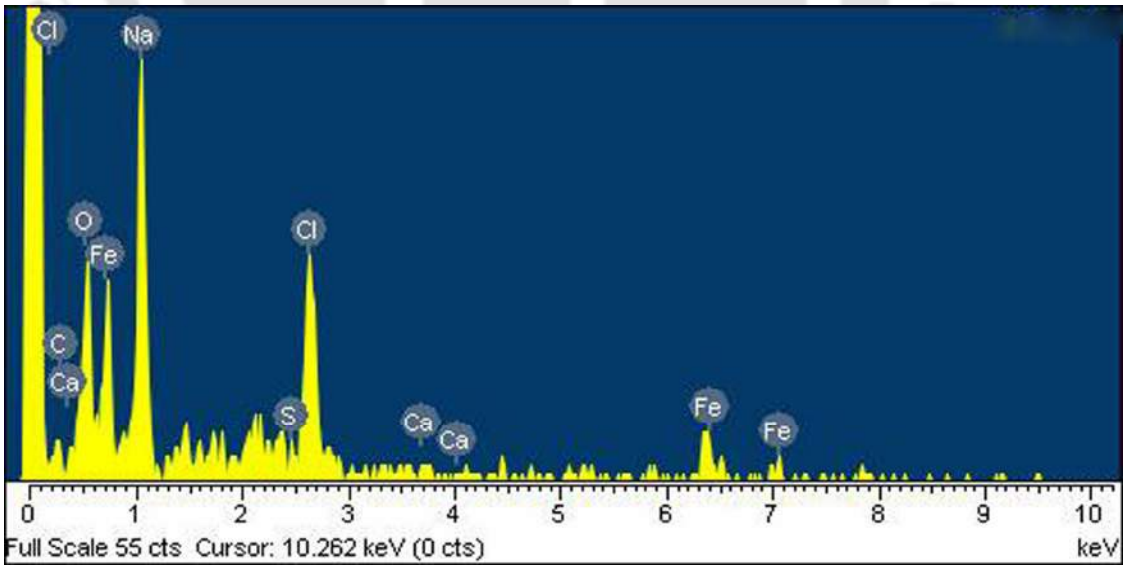


**Fig. 5.7** EDX spectra of immobilized PL1B-MNP showing the presence of different elements, thus confirming the presence of elements which were not present in bare MNPs.

### 5.3.4 Determination of magnetic properties of immobilized PL1B-MNPs

VSM analysis showing the plot of magnetic field vs magnetic moment, suggested that the synthesized MNPs has a saturation magnetization (*M*s) of 52 emu/gm (Fig. 5.8a). This was less than that of bulk magnetite ($Fe_3O_4$) having an *M*s of 92 emu/gm as reported earlier (Zaitsev *et al*., 1999). This decrease in *M*s was due to the large reduction in size of synthesized MNPs which significantly reduced the magnetic moment in a specified magnetic field (Chen *et al*., 2000). On the contrary due to the large surface area to volume ratio of MNPs the magnetic particles on the surface always had a disordered spin, as a result the *M*s decreased significantly (Batlle *et al*., 2000). *M*s was found to reduce further to 36 emu/gm (Fig. 5.8b) and 17 emu/gm (Fig. 5.8c) after activation of MNPs by EDC and immobilization of PL1B, respectively. This reduction in magnetization of the immobilized MNPs was due to the presence of PL1B, which encapsulated the MNPs thus quenching the magnetic moment. Again a large amount of PL1B was attached to a single MNP resulting in a decrease of *M*s by 65% of the synthesized MNPs. The quenching of the magnetic moment also occured due to the exchange of electrons between protein and atoms present on the surface of MNPs as observed earlier by Vanleeuwen *et al*., 1994.

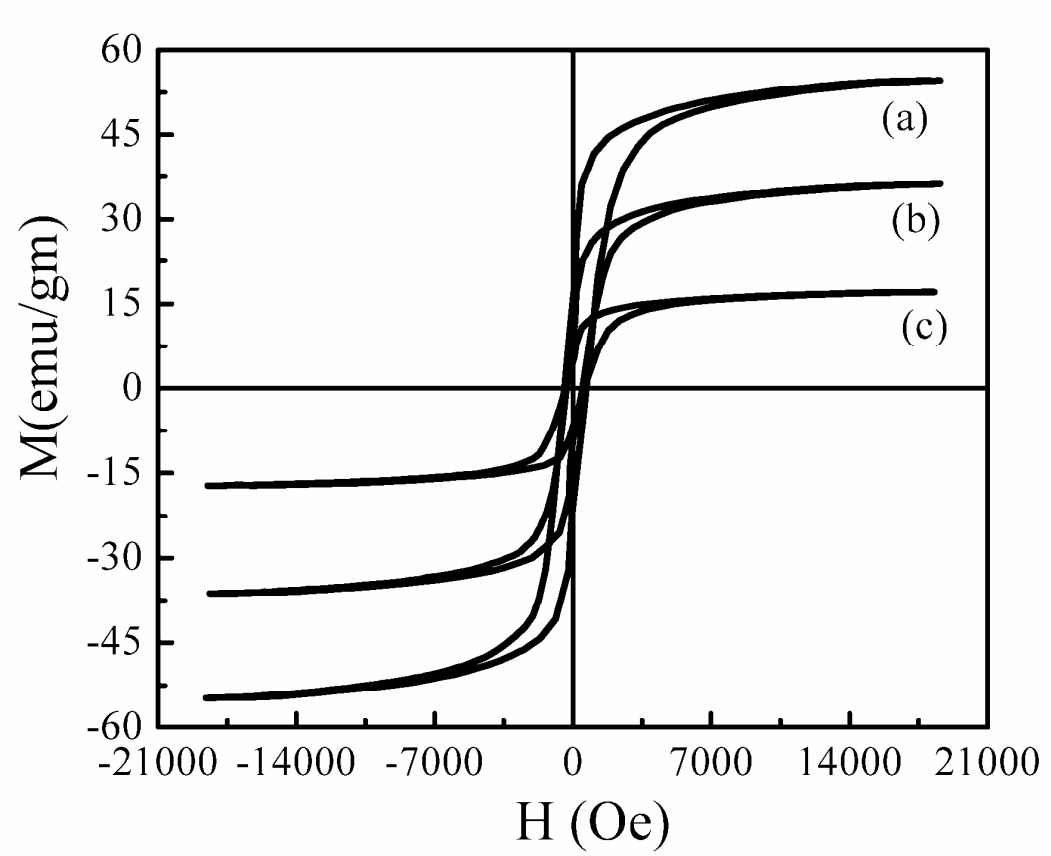


**Fig. 5.8** VSM analysis to determine the magnetic properties of (a) bare MNPs, (b) MNPs activated by EDC and (c) immobilized PL1B-MNP.

### 5.3.5 Enzyme activity of immobilized PL1B-MNP

The optimized reaction conditions for PL1B were pH 9.8 and temperature of 50°C as mentioned in Chapter 3, Sections 3.3.2 and 3.3.3. It was observed that there is a loss in the magnetization of synthesized MNPs at high alkaline pH. Therefore, the reactions of PL1B and immobilized PL1B-MNP were carried out at a lower pH of 8.6 at 50°C. At pH 8.6, PL1B retained 96.5% of its maximum activity at pH 9.8. PL1B showed 17.8 and 16.2 U/mg specific activity, whereas immobilized PL1B-MNP showed slightly higher specific activity of 20.3 and 18.2 U/mg with PGA and Citrus pectin, respectively. The immobilized PL1B-MNP displayed 14.3% and 12.3%

increased specific activity on PGA and Citrus pectin, respectively, as compared with PL1B (Table 5.1).

**Table 5.1** Specific activity of PL1B and immobilized PL1B-MNP towards 0.1% (w/v) pectic substrates.

| | Free PL1B (U/mg) | Immobilized PL1B-MNP (U/mg) | Increase in activity (%) |
|---|---|---|---|
| **Polygalacturonic acid** | 17.8 ±0.38 | 20.3 ±0.15 | 14.3 |
| **Citrus Pectin** | 16.2 ±0.11 | 18.2 ±0.29 | 12.3 |

### 5.3.6 Operational stability of immobilized PL1B-MNP

Operational stability of enzymes is a very important aspect from commercial point of view. Free enzymes are difficult to recover and are lost most of the time. Hence, immobilized enzymes are preferred owing to their easy recovery from the reaction mixture and reuse. Immobilized PL1B-MNP could be easily recovered after each reaction with the help of a magnet within 60s. The recovered enzyme was used in the next set of reaction after washing with 50 mM Tris-HCl buffer pH 7.4. 70% of the initial activity was retained by immobilized PL1B-MNP till 5$^{th}$ cycle of use, after that there was an abrupt fall in the activity (Fig. 5.10A). The activity was lost due to leakage of enzyme from the MNP surface. Immobilized PL1B-MNP proved to be more potent than free PL1B as it can be easily separated by aid of a magnet and reused several times, hence making any industrial process much more economic.

### 5.3.7 Thermal stability of PL1B and immobilized PL1B-MNP

Thermal stability of PL1B and immobilized PL1B-MNP was determined at temperatures varying from 30 to 100°C. The residual activity of PL1B and immobilized PL1B-MNP was 3% and 96%, respectively at 80°C and retained 2.7% and 40% activity, respectively at 90°C. Hence, 32 and 14 fold enhanced stability was observed at 80°C and 90°C for immobilized PL1B-MNP as compared with PL1B (Fig. 5.10B). Immobilized PL1B-MNP retained 50% of its initial activity at 50°C (Fig. 5.10C), 60°C (Fig. 5.10D), 70°C (Fig. 5.10E) and 80°C (Fig. 5.10F) till 3.7 h, 3.5 h, 3 h and 1.9 h of incubation, respectively. Hence immobilized PL1B-MNP can be used at higher temperature for industrial bioprocesses. Such enhanced stability was reported for hydroxyapetite immobilized pectate lyase from *Bacillus megaterium* showing 60 fold enhanced stability at 90°C for 4 h (Mukhopadhyay *et al*., 2012).

A possible explanation for the enhanced activity and thermostability of PL1B-MNP can be due to enzyme rigidification after the immobilization. There are large numbers of hydroxyl groups available on the surface of MNPs, which after activation by carbodiimide can bind the enzyme and this leads to the tight packing of the enzyme molecules providing less space for their movement. Hence, the immobilization of PL1B produced a strong structural rigidification of enzyme thus resisting any distortion of the structure. The enzyme without any structural distortion displayed enhanced structural stability and activity. While in case of the free enzyme due to unavailability of such structural rigidification it is prone to distorted structure mainly at higher temperature. The enzyme rigidification due to immobilization has been previously reported by Mateo *et al*., 2007 and Rodrigues *et al*., 2013.

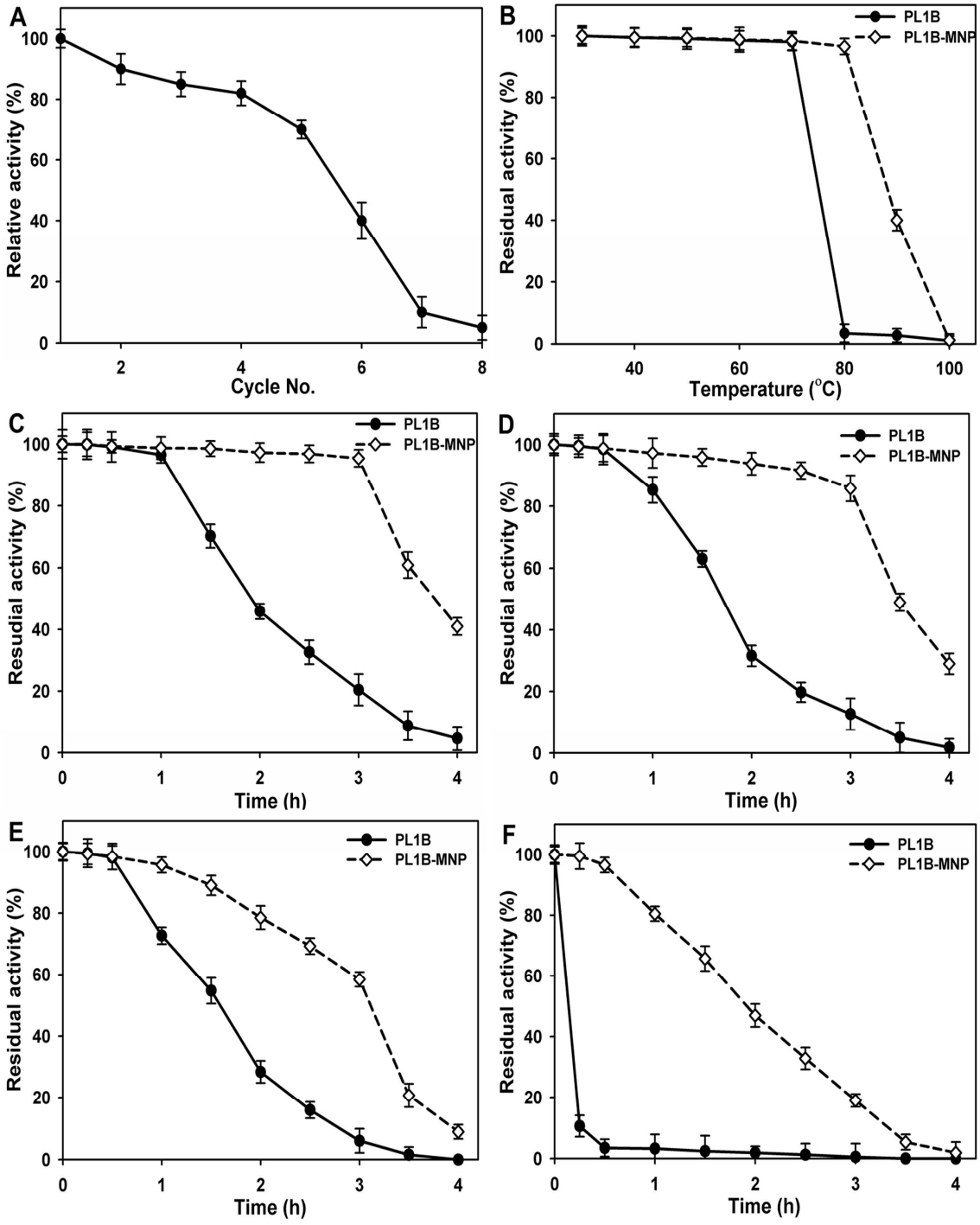


**Fig. 5.10** (A) Operational stability of immobilized PL1B-MNP, showing efficient reuse for 5 continuous cycles of reaction; (B) Thermal stability of immobilized PL1B-MNP over PL1B, showing an improved stability at 80°C and 90°C; Retention of activity by immobilized PL1B-MNP over PL1B at (C) 50°C, (D) 60°C, (E) 70°C and (F) 80°C, where 100% activity refers to 20.3 U/mg for immobilized PL1B-MNP and 17.8 U/mg for PL1B.

### 5.3.8 Bioscouring of cotton fabric

Hot water and α–amylase pretreatment of the coarse cotton fabric facilitated the removal of sizing materials present on the fabric. The pretreated cotton fabric was then subjected to bioscouring process by PL1B and immobilized PL1B-MNP. Removal of pectin was determined by comparing the water absorbing capacity of the treated and untreated fabric. The untreated coarse cotton fabric used as control absorbed 50 µl water droplet on its surface in 21 min. The fabric treated with 0.5 mg/ml of immobilized PL1B-MNP absorbed 50 µl water droplet on its surface in just 15 sec, whereas fabric treated with 0.5 mg/ml of PL1B absorbed the same droplet in 3 min (Fig. 5.11A). This result demonstrated that the coarse cotton fabric after treatment with immobilized PL1B-MNP has acquired a higher wettability. It has been shown earlier that cotton fabric after treatment with acidic or alkaline pectinase acquires enhanced wettability (Tzanov *et al*., 2001). Immobilized PL1B-MNP proved to be more efficient in pectin removal than PL1B, which may be due to its improved activity and specificity towards pectic substrates. Throughout the period of treatment the immobilized PL1B remain attached to the surface of the cotton fabric as can be seen in Fig. 5.11B, tube 2. The removal of pectin from the surface of cotton fabric was further confirmed after dyeing the treated fabric with Ruthenium red dye. Positively charged molecule of the dye interacted with the negatively charged carboxylic groups of pectin, imparting dark colour to the fabric that indicates the presence of pectin (Morozova *et al*., 2006). Immobilized PL1B-MNP treated fabric displayed lightest colour as compared to the untreated and PL1B treated fabric (Fig. 5.12). This was due to the effective removal of pectin by immobilized PL1B, due to which the dye did not bind to the surface of the fabric, thus imparting a light colour.

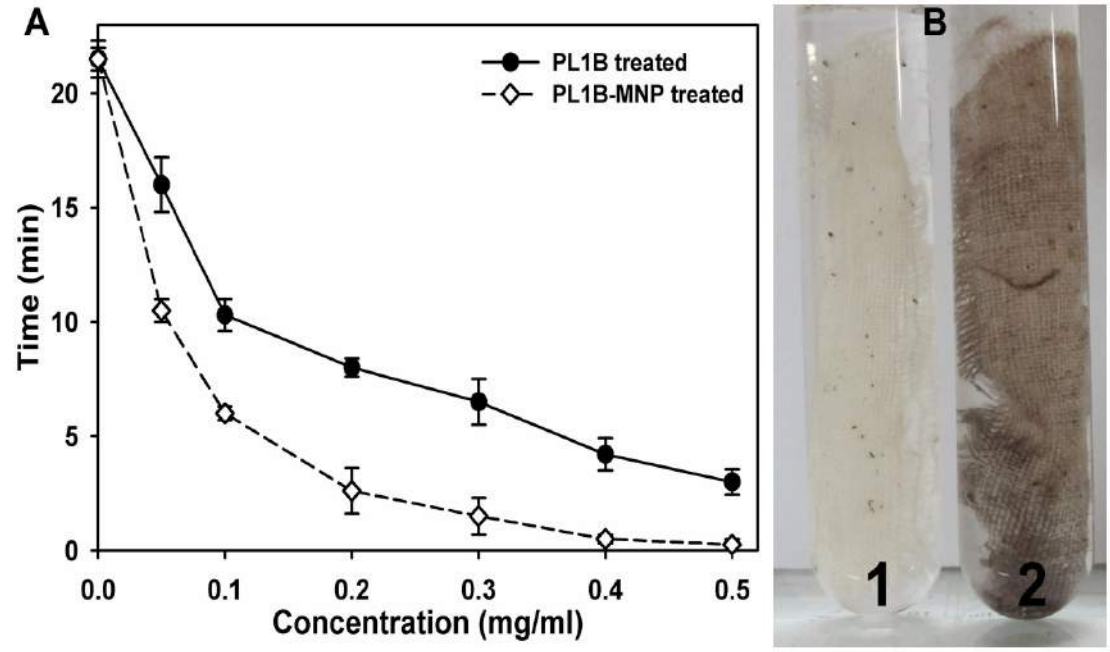


**Fig. 5.11** (A) Increase in wettability of treated cotton fabric upon treatment by varying concentration of PL1B and immobilized PL1B-MNP, (B) bioscouring process of cotton fabric by PL1B (1) and immobilized PL1B-MNP (2).

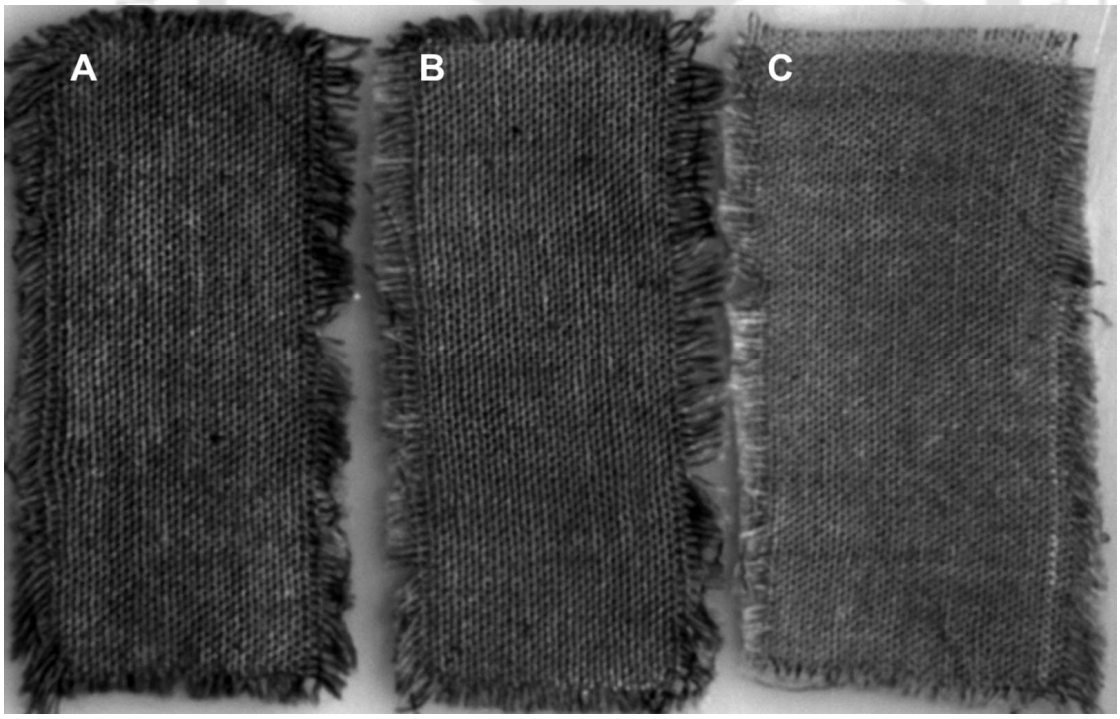


**Fig. 5.12** Visualization of extent of pectin removal from (A) untreated, (B) PL1B treated and (C) immobilized PL1B-MNP treated cotton fabric showing variation in colour intensity, after dyeing with Ruthenium red dye.

## 5.4 Conclusions

The superparamagnetic nanoparticles (MNPs) were successfully synthesized by chemical coprecipitation from mixture of $FeCl_3.6H_2O$ and $FeCl_2.4H_2O$ salts in the molar ratio 1:2. The X-ray diffraction (XRD) analysis of synthesized MNPs showed series of characteristic peaks at 2.96(220), 2.52(311), 2.09(400), 1.71(422), 1.61(511), 1.47(440) and 1.27(533) which indicated the cubic spinel phase and an average size 20±5 nm. HRTEM analysis displayed that MNPs were not perfectly spherical and SAED analysis confirmed the formation of highly crystalline nanoparticles. A simple protocol for activation and immobilization of recombinant PL1B from *Clostridium thermocellum* on MNPs was developed. MNPs were activated in the presence of EDC hydrochloride (carbodiimide), which facilitated the direct binding of the protein to MNPs. It was observed that at 50 mg/ml concentration of MNPs the binding efficiency of PL1B was 97%, whereas at 70 mg/ml and above concentration of MNPs the binding efficiency was always 100%. The binding of PL1B to MNPs was confirmed by FT-IR spectroscopy studies, where the peak at 1628 $cm^{-1}$ due to N-H bending in bare MNPs was significantly shortened after immobilization of PL1B. This result suggested that the binding was accomplished via the reaction between the amino group on $Fe_3O_4$ nanoparticles and the carboxyl group of the protein after being activated by carbodiimide. The characteristic peak of PL1B at 1418 $cm^{-1}$ due to the C-C stretching in aromatic residues appeared in PL1B immobilized MNPs (PL1B-MNP), suggested the presence of aromatic amino acid residues from PL1B. EDX analysis of immobilized PL1B-MNP showed the presence of Carbon (C), Sulphur (S), Calcium (Ca) and Chloride (Cl) beside Iron (Fe) and Oxygen (O). The presence of carbon and sulphur in the sample suggested that these elements were from the carbon

backbone and di-sulphide bonds of PL1B. Saturation magnetization (*M*s) of activated MNPs and immobilized PL1B-MNP were 36 emu/gm and 17 emu/gm, respectively. The reduction in Ms resulted due to encapsulation of MNP by PL1B attached to its surface. Immobilized PL1B-MNP showed slightly higher specific activity of 20.3 and 18.2 U/mg compared to PL1B of 17.8 and 16.2 U/mg with PGA and citrus pectin, respectively. The immobilized PL1B-MNP could be easily recovered from the reaction mixture with the help of a magnet and reused till 5 cycles, retaining 70% of initial activity at the completion of 5 cycles. The immobilized PL1B-MNP showed enhanced thermostablilty at 80° and 90°C as compared to PL1B which only showed thermostability till 70°C. The improved thermostability and reusability of immobilized PL1B-MNP makes it a good candidate for use in various industrial processes involving high temperature. After bioscouring of coarse cotton fabric with PL1B the water absorbing time was decreased to 3 min as compared to untreated fabric, which was further reduced to 15 sec only after treatment of the fabric with immobilized PL1B-MNP. Hence efficient pectin removal and improved wettability was displayed by immobilized PL1B-MNP during bioscouring of cotton fabrics. Therefore, this alkaline pectinase upon immobilization can find new avenues in textile industries, providing an economic and environment friendly method as an alternative to chemical bioscouring process. To our knowledge this is the first attempt of bioscouring of cotton fabric by immobilized pectinase.

## 5.5 References

Bahrami, A., Hejazi, P. (2013) Electrostatic immobilization of pectinase on negatively charged AOT-$Fe_3O_4$ nanoparticles. Journal of Molecular Catalysis B: Enzymatic. 93: 1–7.

Batlle, X., Obradors, X., Medarde, M., Carvajal, J.R., Pernet, M., Regi, M.V. (1993) Surface spin canting in $BaFe_{12}O_9$ fine particles. Journal of Magnetism and Magnetic Material, 124: 228–238.

Chen, D.H., Wu, S.H. (2000) Synthesis of nickel nanoparticles in water-in-oil microemulsions. Chemistry of Material, 12: 1354–1360.

Demir, N., Acar, J., Sarioglu, K., Mutlu, M. (2001) The use of commercial pectinase in fruit juice industry. Part 3: Immobilized pectinase for mash treatment. Journal of Food Engineering, 47: 275–280.

Goldstein, J.I., Newbury, D.E., Echlin, P., Joy, D.C., Lyman, C.E., Lifshin, E., Sawyer, L., Michael, J.R. (2003) X-Ray Spectral Measurement: EDS and WDS. Scanning Electron Microscopy and X-Ray Microanalysis, 3rd edition, (eds. James A.M) pp: 297–353. Kluwer Academic/Plenum Publishers, New York.

Hasegawa, S., Nagel C.W. (1966) A new pectic acid transeliminase produced exocelluarly by a *Bacillus*. Journal of Food Science, 31: 838–845.

Hong R.Y., Ren, Z.Q., Han, Y.P., Li, H.Z., Ding, J., Zheng, Y. (2006) Preparation, characterization and application of bilayer surfactant stabilized ferro fluids. Powder Technology, 170: 1–11.

Honga, R.Y., Lia, J.H., Lib, H.Z., Dingc, J., Zhengd, Y., Weie, D.G. (2008) Synthesis of $Fe_3O_4$ nanoparticles without inert gas protection used as precursors of

magnetic fluids. Journal of Magnetism and Magnetic Material, 320: 1605–1614.

Huang S.H., Liao M.H., Chen D.H. (2003) Direct binding and characterization of lipase onto magnetic nanoparticles. Biotechnology Progress, 19: 1095–1100.

Jayani, R.S., Saxena, S., Gupta, R. (2005) Microbial pectinolytic enzymes: A review. Process Biochemistry, 40: 2931–2944.

Kashyap, D.R., Vohra, P.K., Chopra, S., Tewari, R. (2001) Applications of pectinases in the commercial sector: a review. Bioresource Technology, 77: 215–227.

Kondo, A., Fukuda, H. (1997) Preparation of thermo-sensitive magnetic hydrogel microspheres and application to enzyme immobilization. Journal of Fermentation and Bioengineering, 84: 337–341.

Koneracka, M., Kopcansky, P., Timko, M., Ramchand, C.N., Saiyed, Z.M., Trevan, M., de Sequeira, A., 2006. Immobilization of enzymes on magnetic particles, in: Guisan, J.M. (Ed.), Methods in Biotechnology: Immobilization of enzymes and cells. Humana Press Inc., Totowa, NJ, 2nd Edition, pp. 217–228.

Kouassi, G.K., Irudayaraj, J., McCarty, G., 2005. Examination of Cholesterol oxidase attachment to magnetic nanoparticles J. Nanobiotechnology. 3(1), 1–9.

Lei, Z., Bi, S., Hu, B., Yang, H. (2007) Combined magnetic and chemical covalent immobilization of pectinase on composites membranes improves stability and activity. Food Chemistry, 105: 889–896.

Li, Y., Hardin, I.R. (1998) Enzymatic scouring of cotton - surfactants, agitation, and selection of enzymes. Textile Chemist and Colorist, 30(9): 23–29.

Liu, K., Zhao, G., He, B., Chen, L., Huang, L. (2012) Immobilization of pectinase and lipase on macroporous resin coated with chitosan for treatment of whitewater from papermaking. Bioresource Technology, 123: 616–619.

Mateo, C., Palomo, J.M., Fernandez-Lorente, G., Guisan, J.M., Fernandez-Lafuente, R., 2007. Improvement of enzyme activity, stability and selectivity via immobilization techniques. Enzyme Microb. Technol. 40, 1451–1463.

Mehta, R.V., Upadhyay, R.V., Charles S.W., Ramchand C.N., 1997. Direct binding of protein to magnetic particles. Biotechnol. Tech., 11(7), 493–496.

Morais, P.C., Silva, S.W., Soler, M.A.G., Buske, N. (2001) Raman spectroscopy in magnetic fluids. Biomolecular Engineering, 17: 41–49.

Morozova, V.V., Semenova, M.V., Salanovich T.N., Okunev O.N., Koshelev A.V., Bubnova T.V., Krichevskii G.E., Timatkov A.G., Barysheva N.V., Sinitsyn A.P. (2006) Application of neutral-alkaline pectate lyases to cotton fabric boil off. Applied Biochemistry and Microbiology, 42(6): 603-608.

Mukhopadhyay, A., Dasgupta, A.K., Chattopadhyay, D., Chakrabarti, K. (2012) Improvement of thermostability and activity of pectate lyase in presence of hydroxyapatite nanoparticles. Bioresource Technology, 116: 348–354.

O'Neill, C., Hawkes, F.R., Hawkes, D.L., Lourenco N.D., Pinheiro H.M., Delee W. (1999) Colour in textile effluents sources, measurement, discharge consents and simulation: a review. Journal of Chemical Technology & Biotechnology, 74: 1009–1018.

Patterson, A.L. (1939) The Scherrer formula for X-ray particle size determination. Physics Reports, 56: 978.

Ridley, B.L., O'Neill, M.A., Mohnen, D. (2001) Pectins: structure, biosynthesis, and oligogalacturonide-related signaling, Phytochemistry, 57: 929–967.

Rodrigues, R.C., Ortiz, C., Berenguer-Murcia, A., Torres, R., Fernandez-Lafuente, R., 2013. Modifying enzyme activity and selectivity by immobilization. Chem. Soc. Rev. 42(15), 6290–6307.

Sakai, T., Sakamotojo, T., Hallaert, J., Vandamme, E.J. (1993) Pectin, pectinase and protopectinase: production properties and applications. Advance Applied Microbiology, 39: 213–294.

Soriano, M., Diaz, P., Javier Pastor, F.I. (2006) Pectate lyase C from Bacillus subtilis: a novel endo-cleaving enzyme with activity on highly methylated pectin. Microbiology, 152: 617–625.

Sun, J., Zhou, S., Hou, P., Yang, Y., Weng, J., Li, X., Li, M. (2007) Synthesis and characterization of biocompatible $Fe_3O_4$ nanoparticles. Journal of Biomedical Material Research A, 80A: 333–341.

Tamaru, Y., Doi, R.H. (2001) Pectate lyase A, an enzymatic subunit of the *Clostridium cellulovorans* cellulosome. Proceedings of National Academy of Science (USA), 98(7): 4125–4129.

Tardy, F., Nasser, W., Robert-Baudouy, J., Hugouvieux-Cotte- Pattat, N. (1997). Comparative analysis of the five major *Erwinia chrysanthemi* pectate lyases: enzyme characteristics and potential inhibitors. Journal of Bacteriology, 179: 2503–2511.

Tzanov, T., Calafell, M., Guebitz, G.M., Cavaco-Paulo, A. (2001) Bio-preparation of cotton fabrics. Enzyme Microbial Technology, 29: 357–362.

Vanleeuwen, D.A., Vanruitenbeek, J.M., Dejongh, L.J., Ceriotti, A., Pacchioni, G., Haberlen, O.D., Rosch, N. (1994) Quenching of magnetic-moments by ligand-metal interactions in nanosized magnetic metal-clusters. Physics Review Letters, 73: 1432–1435.

Xiao, Z., Bergeron, H., Grosse, S., Beauchemin, M., Garron, M.L., Shaya, D., Sulea, T., Cygler, M., Lau, P.C.K. (2008) Improvement of the thermostability and activity of a pectate lyase by single amino acid substitutions, using a strategy based on melting-temperature-guided sequence alignment. Applied and Environmental Microbiology, 74(4): 1183–1189.

Zaitsev, V.S., Filimonov, D.S., Presnyakov, I.A., Gambino, R.J., Chu, B. (1999) Physical and chemical properties of magnetite and magnetite-polymer nanoparticles and their colloidal dispersions. Journal of Colloid and Interface Science 212: 49–57.

Zheng, Y., Huang, C.H., Liu, W., Ko, T.P., Xue, Y., Zhou, C., Guo, R.T., Ma, Y. (2012) Crystal structure and substrate-binding mode of a novel pectate lyase from alkaliphilic *Bacillus sp*. N16-5. Biochemical and Biophysical Research Communications, 420: 269–274.

# Chapter 6

## Production of pectic oligosaccharides from extracted sweet lemon peels pectin by recombinant pectate lyase (PL1B), their characterization and effect on colon cancer cells

### 6.1 Introduction

Food industries during their manufacturing process produce a lot of waste which has been a serious worldwide issue. Hence complete utilization of these wastes is necessary to develop a sustainable environment. Citrus peels form 60 to 65% of the total waste after processing of citrus fruits at industry (McCready *et al*., 1954). This citrus peel which is considered as waste is rich in pectin, from where the commercial pectin is extracted (Cruess *et al*., 1958). Pectins are widely used in food industry as a gelling and stabilizing agent, in jam, jelly, milk products and candy production (May, 1990). Pectin was also used as emulsifier during vegetable oil extraction (Leroux *et al*., 2003). The pectin backbone is mainly composed of four structural domains namely Homogalacturonan (HG), Rhamnogalacturonan I (RGI), Rhamnogalacturonan II (RGII), and Xylogalacturonan (XGA) (Mohen, 2008). HG the 'smooth' region of

pectin contains the repeated units of α-1,4-linked galacturonic acid (GalA) residues, which are often methylated or acetylated at the C-5 carbon (Zhan *et al*., 1998). While RGI and RGII are the 'hairy' regions of pectin containing alternate units of rhamnose (Rha) and GalA residues, with complex branched side chains (O'Neill *et al*., 1990; O'Neill *et al*., 2004). It was reported earlier that citrus peels, apple pomace and sugar beet form a good source for pectin (Kar *et al*., 1999). Pectin and pectic polysaccharides has several health benefits like activation of complementary system and initiation of tumor necrosis factor alpha production from human monocytes (Yamada *et al*., 1994; Samuelsen *et al*., 1995), reduction of total and low density lipoprotein (LDL) cholesterol in serum (Brown *et al*., 1999), activation of peritoneal macrophages (Iacomini *et al*., 2005), spleen cell proliferation (Zhao *et al*., 2006), inhibition of hyaluronidase and histamine release from isolated rat peritoneal mast cells, thus showing anti-allergic properties (Sawabe *et al*., 1992). Pectin and pectic oligosaccharides were reported as an effective inhibitor against proliferation and metastasis, induction of apoptosis in cancer cells thus decreasing the chance of tumor incidence (Platt *et al*., 1992; Pienta *et al*., 1995; Olano-Martin *et al*., 2003; Jackson *et al*., 2007). Other beneficial effects of these molecules are inhibition in signal transduction of fibroblast growth factor (Liu *et al*., 2001; Liu *et al*., 2002). Citrus pectin can block the lipopolysaccharide (LPS) signaling pathway during macrophage activation thus can be an important agent in cancer chemoprevention and anti-inflammation (Chen *et al*., 2006). Looking at the mentioned earlier reports it is undoubted fact that pectin and pectic oligosaccharides have found immense importance as functional food (Manderson *et al*., 2005). Production of pectic oligosaccharides by enzymatic cleavage of pectin is a conventional and reliable

technique for specific oligosaccharide production without the formation of other undesirable by-products (Leitao *et al*., 1995; Cabrera *et al*., 2005; Zykwinska *et al*., 2008).

In the present study the pectin from waste peels of sweet lemon (*Citrus limetta*) was extracted. The extracted pectin (EP) was characterized for degree of methyl-esterification. Isolated pectin was enzymatically degraded by recombinant endo-pectate lyase (PL1B) from *Clostridium thermocellum* (Chakraborty *et al*., 2015) to produce the corresponding pectic oligosaccharides. Oligosaccharides produced from commercial polygalacturonic acid (PGA), Citrus pectin (25% methyl-esterification) (CP25) and extracted pectin (EP) upon enzymatic cleavage by PL1B were characterized and purified separately by gel filtration. The purified pectic oligosaccharides from the above mentioned three different sources were used for studying their effects on colon cancer cells (HT-29).

## 6.2 Materials and Methods

### 6.2.1 Materials

Sweet lemon peels were collected from a fruit shop. Polygalacturonic acid (PGA), citrus pectin (25% methyl-esterified) (CP25) and cell culture medium RPMI-1640, Thiazolyl Blue Tetrazolium Bromide powder (MTT) were procured from Sigma-Aldrich Pvt. Ltd. Endo-pectate lyase (PL1B) from *Clostridium thermocellum* ATCC 27405 was cloned from genomic DNA as described in Chapter 2, Section 2.3.3 and 2.3.4 (Chakraborty *et al*., 2015). Silica coated aluminum TLC plates were purchased from Merck, Germany. Colon cancer cell line (HT-29) was procured from National Center for Cell Science (NCCS), Pune, India. Bio-Gel P-2 matrix was purchased from Bio-Rad. Fetal Bovine Serum (FBS) was procured from Gibco (Invitrogen).

### 6.2.2 Extraction of pectin from citrus peel

Sweet lemon (*Citrus limetta*) peels were shredded into small pieces, dried and were further grinded in a grinder to obtain fine granules. Extraction of pectin was carried out in 1M citric acid at pH 2 (Srivastava *et al*., 2011). 200 g of grinded citrus peel was mixed in 1 litre of the above mentioned solution and heated in a microware (LG, MG608AP) at 1350 watt power for 15 min. The solution was cooled to 25°C and filtered through filter cloth and then by Whatman filter (No. 1). 66 g of filtrate was removed and the filtered solution was treated with 95% ethanol to aggregate the jelly pectin. The aggregated pectin was removed from the solution by centrifugation at 10,000 rpm for 20 min. Clear solution was decanted and jelly pectin was collected as pellet. The extracted jelly pectin was freeze dried overnight using a lyophilizer (Christ, Alpha 1-2 LD Freeze Dryer).

Percent yield of extracted pectin was calculated by using the formula,

$$Y\ (\%) = \frac{DP}{(P_{Init} - F_{Remov})} \times 100 \qquad (1)$$

Where, Y (%) is percent yield of extracted pectin, DP total amount of extracted dried pectin in g, $P_{Init}$ grinded citrus peels initially used and $F_{Remov}$ filtrate removed in g.

### 6.2.3 Determination of degree of methylation in extracted pectin

The percentage of degree of methylation (DM) in extracted pectin was determined by NMR spectroscopy. 1% (w/v) of extracted pectin (EP) in 2 ml $D_2O$ was prepared and $^1H$ NMR spectrum was recorded on 600 MHz NMR spectrometer (Bruker, Avance III HD). The peaks in the NMR spectrum were assigned to the different hydrogen atoms present in the galacturonate moiety of pectin. The DM of extracted pectin was calculated from the NMR spectrum using the formula as mentioned below (Rosenbhom *et al*., 2008).

$$DM\ (\%) = \frac{(I_{COOCH3} + I_{H1}) - I_{COOH}}{(I_{COOCH3} + I_{H1}) + I_{COOH}} \times 100 \qquad (2)$$

Where $I_{COOCH3}$ is integral value of H-5 adjacent to esters and $I_{COOH}$ is integral value of H-5 adjacent to carboxylates. Due to the overlapping of signals of H-1 and H-5 esters, only the combined integral values for H-1 and H-5 ester ($I_{COOCH3} + I_{H1}$) can be determined (Rosenbhom *et al*., 2008).

### 6.2.4 Activity of PL1B on extracted pectin

The activity of endo pectate lyase PL1B from *Clostridium thermocellum* was determined under the optimized reaction condition as mentioned earlier in Chapter 3, Section 3.3.1. 0.1% (w/v) extracted pectin (EP) was used in a 1 ml reaction volume. The unsaturated oligogalacturonates produced upon enzymatic cleavage was analyzed

on a spectrophotometer (Varian, Cary 100) by measuring absorbance at 235 nm ($A_{235}$). 1 unit of enzyme was defined as the amount of enzyme required to produce 1 µmol of Δ-4,5-unsaturated oligogalacturonate per min, where the molar extinction coefficient of these unsaturated products being 4,600 $M^{-1}cm^{-1}$ at $A_{235}$ (Hasegawa *et al*., 1966).

The oligosaccharides produced from EP upon enzymatic cleavage by pectate lyase PL1B were identified by thin layer chromatography. 1% (w/v) EP was used as substrate and the reactions were carried out under optimized conditions of 50 mM Glycine-NaOH buffer (pH 9.8), 50°C and 0.6 mM $CaCl_2$ for varying time period from 0 min to 24 h. After completion of reaction 1 µl of the reaction sample was loaded on TLC plate and run using a mobile phase containing butan-1-ol/water/acetic acid in the ratio of 5:3:2 (Lojkwoska *et al*., 1995). The spots were visualized after staining with a solution containing 0.5% (w/v) α-naphthol and 5% (v/v) sulphuric acid in ethanol (Cote *et al*., 2005) and heating the TLC plate at 95°C for 10 min. Standard oligogalacturonides like D-galacturonic acid (S1), di-galacturonic acid (S2) and tri-galacturonic acid (S3) were used as molecular mass markers.

### 6.2.5 ESI-Mass Spectrometric analysis of PL1B degraded products

PL1B degraded products from three substrates polygalacturonic acid (PGA), citrus pectin (25% methyl-esterified) (CP25) and extracted pectin (EP) were analyzed by Electronspray ionization (ESI) mass spectrometer (Waters, Q-Tof Premier) in MS and tandem MS mode. Reaction of PL1B was carried out separately with PGA, CP25 and EP following the reaction conditions mentioned in Section 6.2.4 for 24 h. Reaction samples of 1 ml was treated with equal volume of ethanol and centrifuged at 10,000 g for 15 min to precipitate unhydrolyzed polysaccharides. The supernatant after centrifugation was collected and dried at 80°C in hot air oven to remove the ethanol

completely. Dried samples containing the pectic oligosaccharides were diluted in 1:1 (v/v) ratio by methanol and used 20 µl for analysis. The MS and tandem MS analysis was carried out in the negative ion mode, where the parameters for MS analysis were collision energy 5 eV, ionization energy 1 eV, capillary voltage 3 eV, desolvation temperature 250°C, source temperature 80°C and flow rate 10 µl/sec. While for tandem MS analysis a nanospray ionization source was used where voltage was 3 eV, collision energy 20 eV and Argon was used as collision gas.

### 6.2.6 Purification of pectic oligosaccharides

The reaction of PL1B with 3% (w/v) PGA or citrus pectin (25% methyl esterified, CP25) or extracted pectin (EP) were set up under optimized condition as mentioned earlier in Section 6.2.4 for 24 h. The samples after reaction were processed as mentioned in Section 6.2.5 before purification. Pectic oligosaccharides were purified by size exclusion chromatography using Bio-Gel P2 matrix, using degassed deionized water as the mobile phase. The column was run on a FPLC (Akta Purifier 100, GE healthcare) at a flow rate of 0.2 ml/min. The purified unsaturated pectic oligosaccharides from the column were detected by UV detector at $A_{235}$ and 1 ml fractions were collected using fraction collector. The fraction of each peak maxima of the chromatogram were run on TLC plates (as mentioned in Section 6.2.4) to identify the purified oligosaccharides. Purified pectic oligosaccharides after identification were mixed together, freeze dried and stored at -20°C for further use.

### 6.2.7 Treatment of colon cancer cells (HT-29) by pectic oligosaccharides

Colon cancer cells (HT-29) were grown on RPMI 1640 medium containing 10% FBS at 37°C and in presence of 5% $CO_2$. MTT assay (Mosmann, 1983) was carried out in 96 well culture plates, where 10,000-12,000 (counted by

Haemocytometer after staining with Trypan blue) cells were seeded per well. The plates were incubated overnight at 37°C and 5% $CO_2$ for proper attachment of cells. HT-29 cells were treated with varying concentration (0.05–0.5 mg/ml) of pectic oligosaccharides from the three different substrate source mentioned above, for a period of 3, 6, 12 and 24 h. The medium of cells after pectic oligosaccharide treatment was removed and 100 µl of MTT was added from 5 mg/ml stock and further incubated at 37°C for 2-3 h. During this period the yellow Tetrazole in MTT is reduced to purple Formazan in the living cells (Mosmann, 1983). MTT was removed and 100 µl DMSO was added to the cells to dissolve the insoluble purple Formazan. Immediately the absorbance at 570 nm ($A_{570}$) was measured on Elisa plate reader (Tecan, Infinite M200, Durham, NC, USA), with a reference wavelength of 690 nm ($A_{690}$). The final absorbance values were calculated after subtracting 690 nm reference read from the 570 nm absorbance read. Cell viability was determined by using the formula as mentioned below,

$$\text{Cell viability (\%)} = \frac{(A_{\text{Cont}} - A_{\text{Tret}})}{A_{\text{Cont}}} \times 100 \qquad (3)$$

Where $A_{\text{Cont}}$ is absorbance of control cells and $A_{\text{Tret}}$ is absorbance of treated cells. Considering maximum inhibition being 100%, subtracting the percent of cell viability from this value provided the actual percent inhibition of HT-29 cells in presence of purified pectic oligosaccharides from three different substrate sources.

## 6.3 Results and Discussion

### 6.3.1 Pectin extraction from sweet lemon peels

Pectin was extracted from 200 g dried and grinded peels from sweet lemon by acid extraction after microwave heating. 60 g of filtrate was removed after filtration of extraction solution, 45 g extracted jelly pectin was precipitated by ethanol and collected as pellet after centrifugation. After lyophilization of this jelly pectin finally 17 g of dried powdered pectin was recovered (Table 1). Using the equation mentioned in Section 6.2.1 the yield of EP was found to be around 12%. Previous studies have showed that pectin extracted from sweet lemon (*C. limetta*) at optimized pH 1.5 gave an yield of 16.7% (Aina *et al*., 2012). Another study showed that after statistical analysis and optimization of all parameters extraction of pectin from *Citrus limon* at pH 3.2 enhanced the yield to 32.4% (Kanmani *et al*., 2014). Extraction of pectin using microwave heating required lesser time and resulted in higher yield as compared with water based extraction (Fishman *et al*., 2003). Pectin extraction by microwave heating has higher anhydrogalacturonate content, degree of methylation and increased viscosity (Fishman *et al*., 2000). The microwave heating during pectin extraction creates high pressure within the material. This modifies the physical properties of the tissue, disrupts cell structures and develops increased porosity. This facilitates easy entry of the extraction fluid to easily enter the material and thus resulting in an effective extraction process (Srivastava *et al*., 2011).

**Table 1.** Pectin extraction from sweet lemon peels.

| Stages of extraction | Weight (g) | Recovery (%) |
|---|---|---|
| Grinded citrus peel initially taken | 200 | - |
| Filtrate removed after extraction | 60 | 30 |
| Jelly pectin after extraction | 45 | 22.5 |
| Final dried pectin | 17 | 8.5 |

### 6.3.2 Determination of degree of methyl-esterification in extracted pectin

The $^{1}H$ NMR spectrum (Fig. 6.1A) of EP was determined by dissolving the dried sample in $D_2O$. The H-5 proton (Fig. 6.1B) adjacent to the carboxylate group in the galacturonate moiety of pectin is found at 4 ppm with an integral value of 0.21 (Fig. 6.1A), while the H-5 proton (Fig. 6.1B) adjacent to the ester group is found at 4.2 ppm with an integral value of 1.86 (Fig. 6.1A). The H-4 proton (Fig. 6.1B) of galacturonate moiety was identified at 3.8 ppm (Fig. 6.1A). Some residual water molecule was found at 3.7 ppm which was not removed from pectin even after complete drying of the sample. H-3 and H-2 protons (Fig. 6.1B) were identified at 3 ppm and 2.9 ppm respectively, as very large peaks each being two adjacent peaks without a baseline separation (Fig. 6.1A). The calculated percent degree of methyl-esterification (DM) from equation 2 of Section 6.2.3 was found to be 77%. It has been previously reported that pectin extracted from by microwave heating of Orange peels had a degree of methyl-esterification around 91-73% (Fishman *et al*., 2000), whereas pectin extracted from lime peels was 72% (Fishman *et al*., 2006). Another study showed that pectin extracted from grape peels showed only 12% methyl-esterification (Khan *et al*., 2014). Hence EP from sweet lemon showed comparable degree of methyl-esterification in its structure usually found in pectin from peels of citrus fruits.

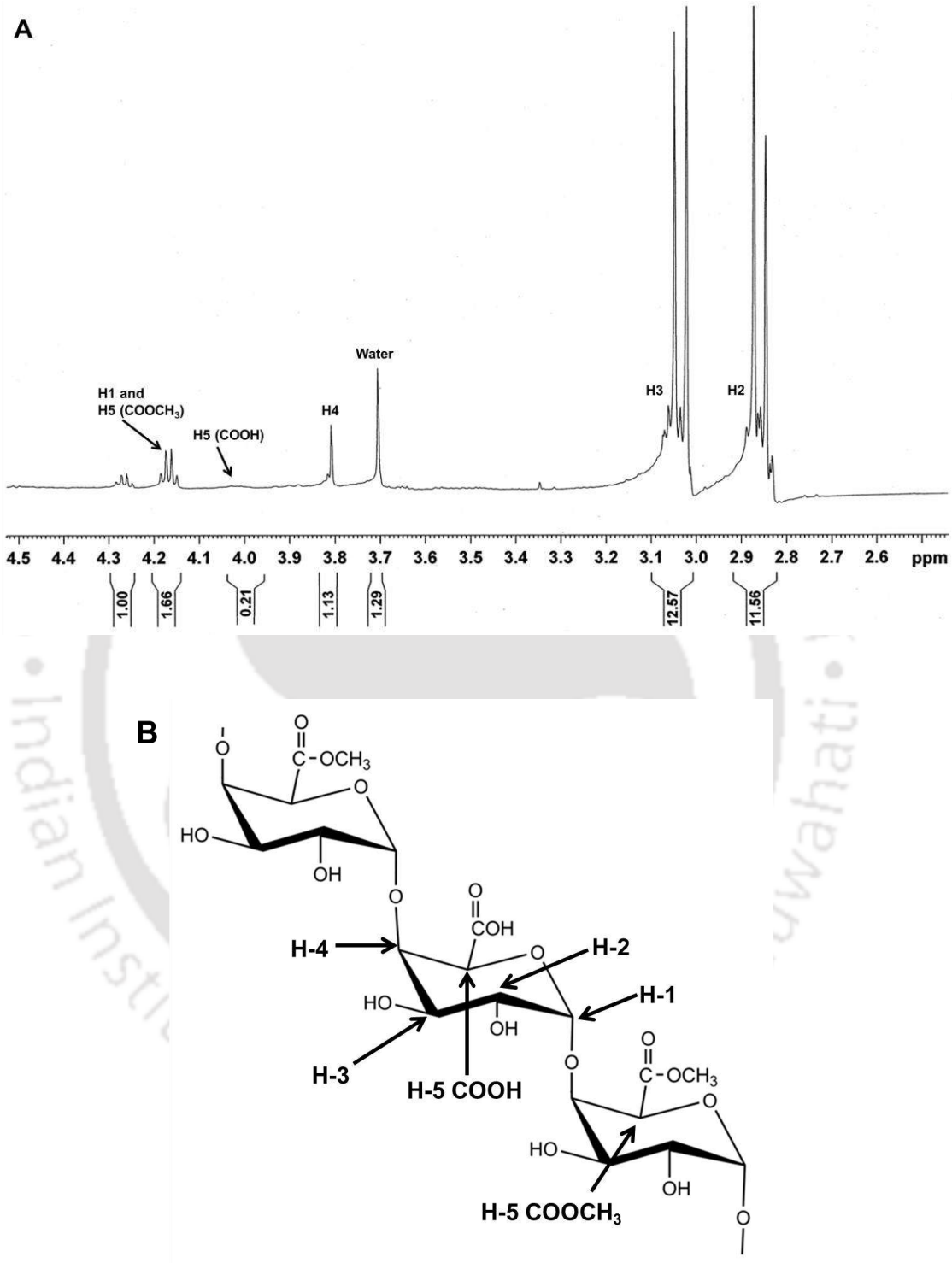


**Fig. 6.1** (A) $H^1$ NMR spectra of extracted pectin (EP) from sweet lemon peels with integral values of each hydrogen atom, (B) showing different positions of hydrogen atoms in galacturonate moiety in pectin

### 6.3.3 PL1B activity on extracted pectin and TLC analysis of degradation products

PL1B under optimized conditions showed 11.1±0.35 U/mg specific activity on EP. Previously in Chapter 3, Section 3.3.1 it was found that PL1B showed highest activity of 18.5±0.23 U/mg towards PGA (non-methylated pectin) and subsequent decrease in activity occurred with highly methyl-esterified pectin. PL1B exhibited 13.50±0.17 U/mg and 5.92±0.10 U/mg specific activity with 55% methyl-esterified and 85% methyl-esterified pectin, respectively. Hence the specific activity of PL1B towards EP (77% methyl-esterified) is quite comparable with previous results. Pectate lyases are usually specific towards PGA and show no or very less activity towards methylated pectin, but in case of PL1B it exhibited around 60% activity towards extracted pectin with 77% methyl-esterification. Pectate lyase PelZ from *Erwinia chrysanthemi* which has more specificity towards PGA, showed only 10% activity with 75% methyl-esterified pectin considering activity with PGA as 100%. While pectate lyase PelA from *Bacillus sp*. BP-23 (Soriano *et al*., 2000) and PelC from *Bacillus subtilis* (Soriano *et al*., 2006) showed 97% and 90% activity, respectively on 89% methyl-esterified pectin.

Time dependent TLC analysis of the degraded products released after treatment of EP by PL1B showed that unsaturated di-galacturonate was the major product (Fig. 6.2). At 0 min the presence of unsaturated mono-galacturonate (anhydrogalacturonate) was observed, which was produced during the extraction by microwave heating. It has been reported earlier that pectin extraction by microwave heating produces higher amount of anhydrogalacturonate (Fishman *et al*., 2000). Unsaturated di-galacturonate production gradually increased with time and its maximum accumulation occurred at

24 h. Although anhydrogalacturonate was initially present in the reaction, but as the reaction time progresses there was minute increase in its concentration, which occurred due to the cleavage of EP by PL1B. TLC analysis of PL1B degradation products from PGA and CP25 has been presented earlier in Chapter 3, Section 3.3.8. These results revealed that unsaturated di-galacturonate was the major products produced after enzymatic degradation.

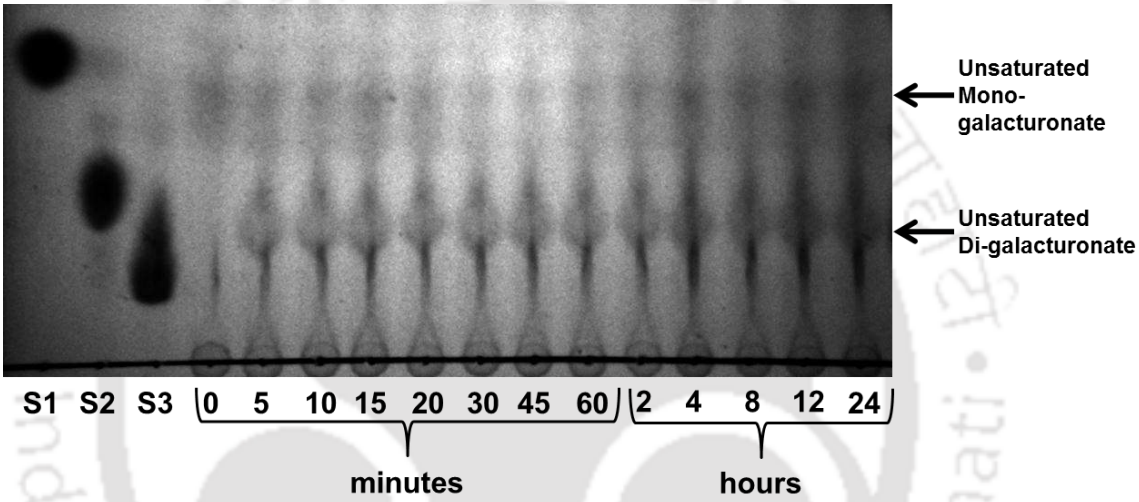


**Fig. 6.2** Thin layer chomatography showing the degraded products released from extracted pectin from sweet lemon peels treated with PL1B. Where standard oligosaccharides used as molecular size markers are S1: D-galacturonic acid; S2: Di-galacturonic acid; S3: Tri-galacturonic acid

### 6.3.4 ESI mass spectrometric (ESI-MS) analysis of PL1B degraded products

PL1B degraded products from three different substrates source *viz*. PGA, CP25 and EP was subjected to MS and tandem MS analysis. The MS spectra of PGA degraded products showed the presence of three peaks at (*m/z* 175), (*m/z* 351) and (*m/z* 527) corresponding to unsaturated mono-galacturonate (Δ-4,5-GalA), di-galacturonate (Δ-4,5-di-GalA) and tri-galacturonate (Δ-4,5-tri-GalA), respectively (Fig. 6.3A and 6.4A). The MS spectra also inferred that abundance of unsaturated di-galacturonate was higher than mono- or tri-galacturonate. During tandem MS the peaks at *m/z* 351 and *m/z* 527 were further ionized separately to learn its composition. The peak at *m/z*

351 after ionization displayed a large peak at *m/z* 175 and a smaller peak at *m/z* 351 (Fig. 6.4B), which signifies that unsaturated di-galacturonate (Δ-4,5-di-GalA) is composed of two mono-galactouronates (Δ-4,5-GalA). Similarly ionization of *m/z* 527 peak produced three peaks at *m/z* 175, *m/z* 351 and relatively smaller peak at *m/z* 527 (Fig. 6.4C). This signifies that tri-galacturonate (Δ-4,5-tri-GalA) is composed of mono-galacturonate (Δ-4,5-GalA) and di-galacturonate (Δ-4,5-di-GalA). Both MS and tandem MS analysis of PGA degraded products suggested that unsaturated di- and tri-galacturonate were the major products produced after enzymatic cleavage by PL1B.

Similar results were obtained with PL1B degraded products released from CP25, where the three corresponding peaks for unsaturated mono-galacturonate (Δ-4,5-GalA), di-galacturonate (Δ-4,5-di-GalA) and tri-galacturonate (Δ-4,5-tri-GalA) were identified at (*m/z* 175), (*m/z* 351) and (*m/z* 528), respectively (Fig. 6.3A and 6.5A). In this case unsaturated di-galacturonate and tri-galacturonate were the major products. Moreover, it was clearly seen that the peak at *m/z* 528 corresponding to unsaturated tri-galacturonate was significantly larger suggesting its higher abundance than unsaturated mono- and di-galacturonate. Ionization during tandem MS of the peaks at *m/z* 351 (Fig. 6.5B) and *m/z* 528 (Fig. 6.5C), produced their corresponding mono and di-saccharide units, confirming their structural composition.

MS analysis of PL1B degraded products from EP showed a single major peak at *m/z* 383 (Fig. 6.3B and 6.6A). This peak corresponds to unsaturated methyl-esterified di-galacturonate (Δ-4,5-di-GalMe). Ionization during tandem MS of the peak at *m/z* 383 displayed a large peak at m/z 191 and a smaller peak at *m/z* 383 (Fig. 6.6B). The peak at *m/z* 191 corresponds to unsaturated methyl-esterified mono-galacturonate (Δ-4,5-GalMe). These results revealed that methylated di-galacturonate is composed of

two units of methylated mono-galacturonate. EP from sweet lemon contains 77% methyl-esterification as mentioned in Section 6.3.2, thus the PL1B degraded products obtained were methylated species. The results obtained after analysis of PL1B degradation products from PGA, CP25 and EP were in accordance to the results obtained earlier by Ralet *et al*., 2009 and Munoz *et al*., 2012. Where a detail ESI-MS analysis of pectic oligosaccharides was perform to study the structural composition of pectin. The m/z values for methylated mono-galacturonate (Δ-4,5-GalMe) and methylated di-galacturonate (Δ-4,5-di-GalMe) was reported as 193 and 385, respectively (Ralet *et al*., 2009). While the m/z values for unsaturated mono-galacturonate (Δ-4,5-GalA), di-galacturonate (Δ-4,5-di-GalA) and tri-galacturonate (Δ-4,5-tri-GalA) was reported as 175, 351 and 527, respectively (Munoz *et al*., 2012).

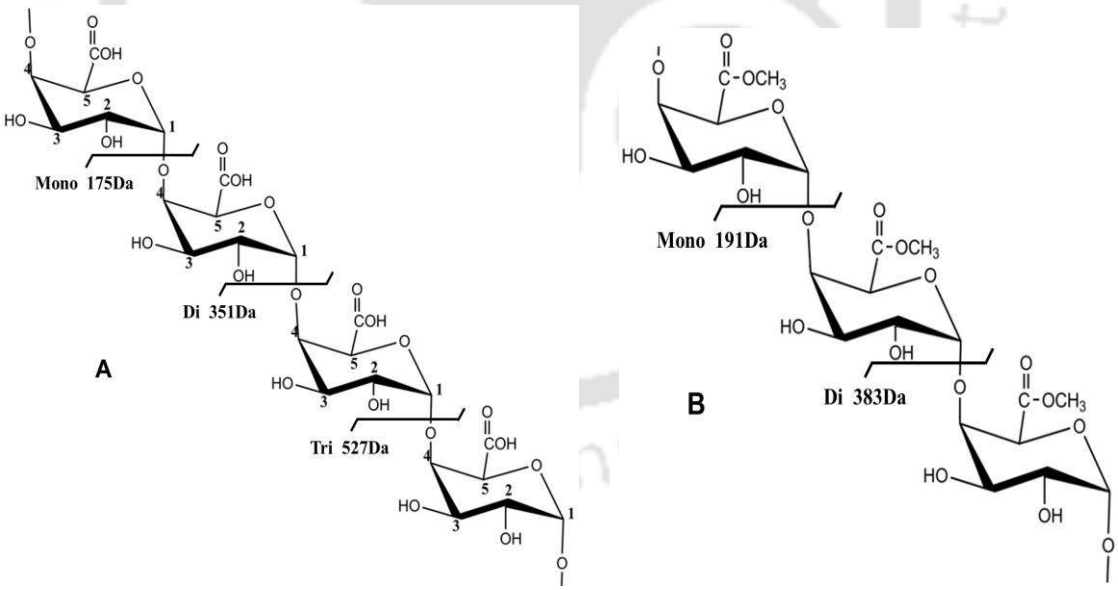


**Fig. 6.3** Schematic representation of PL1B cleavage sites on (A) PGA and CP25 producing unsaturated di- (mass 351) and tri-galacturonate (mass 527), corresponding monosaccharide is unsaturated mon-galacturonate (mass 175); (B) EP producing unsaturated methyl-esterified di-galacturonate (mass 383), the corresponding monosaccharide being unsaturated methyl-esterified mono-galacturonate (mass 191).

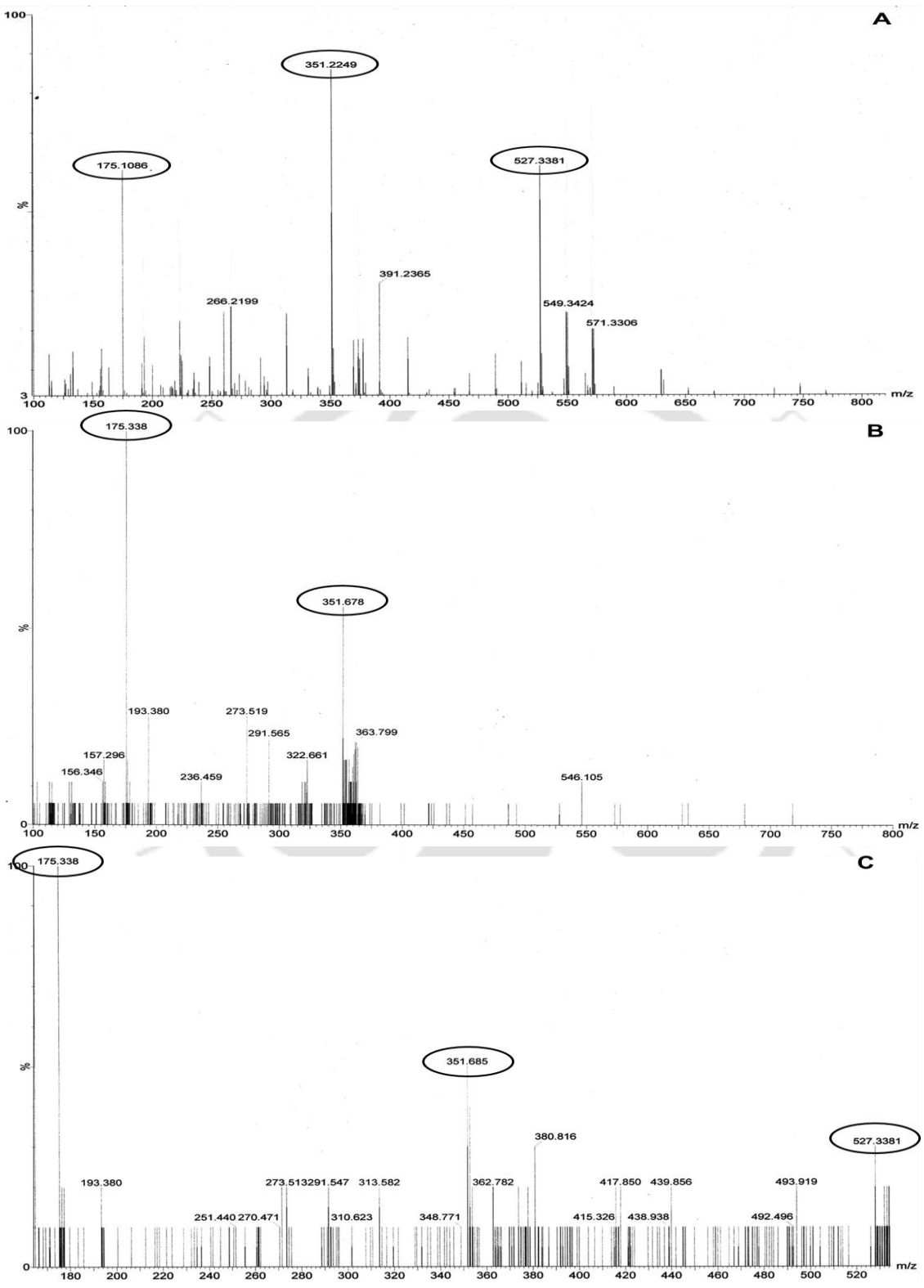


**Fig. 6.4** ESI-Mass spectrometric analysis of PL1B degraded products released from PGA (A) MS analysis showing three distinct peaks at *m/z* 175 ppm, 351 ppm and 527 ppm; tandem MS analysis of peak at (B) *m/z* 351 ppm and (C) *m/z* 527 ppm.

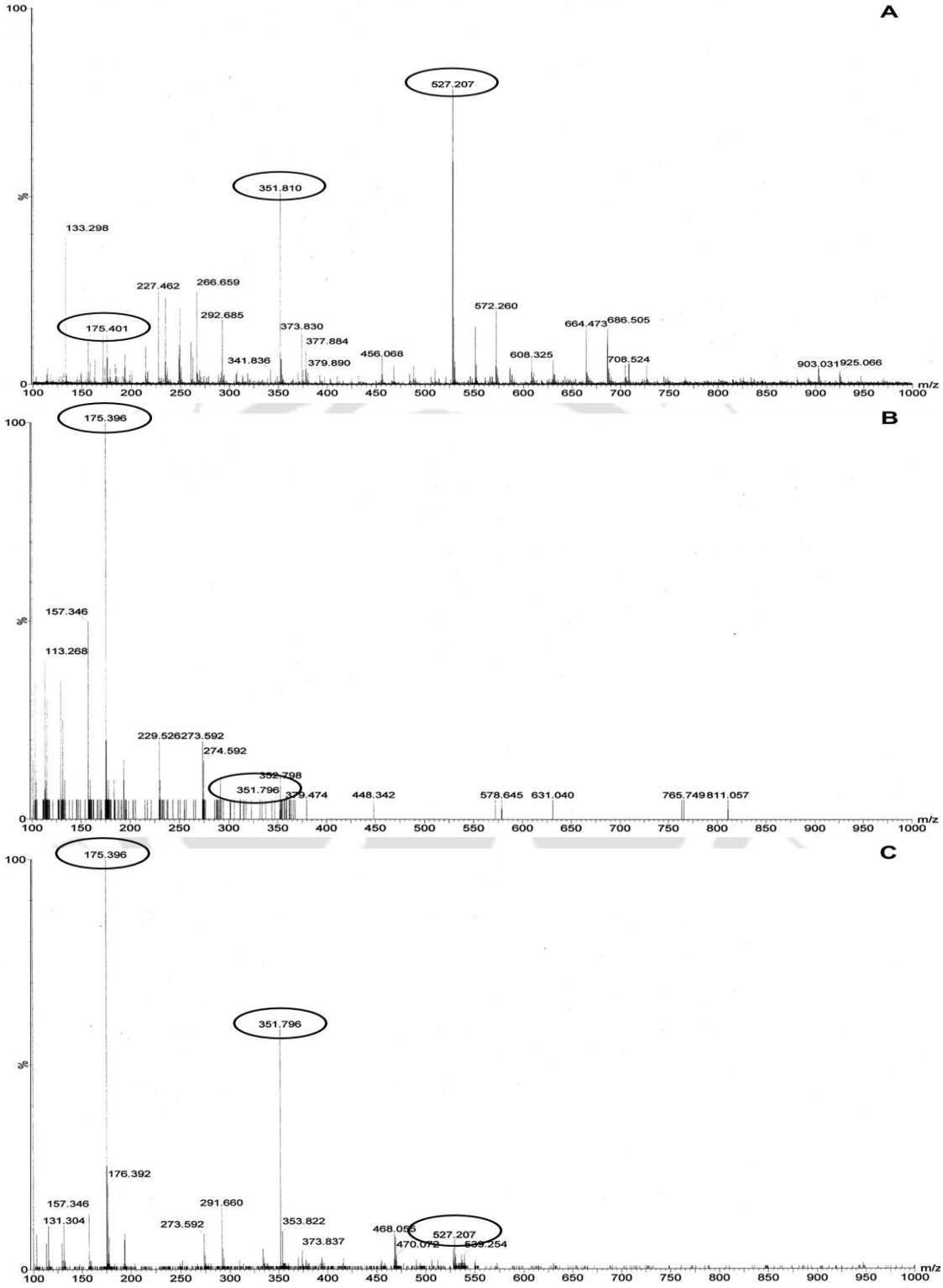


**Fig. 6.5** ESI-Mass spectrometric analysis of PL1B degraded products released from Citrus pectin (25% methyl-esterified) (CP25) (A) MS analysis showing three distinct peaks at *m/z* 175 ppm, 351 ppm and 527 ppm; tandem MS analysis of peak at (B) *m/z* 351 ppm and (C) *m/z* 527 ppm.

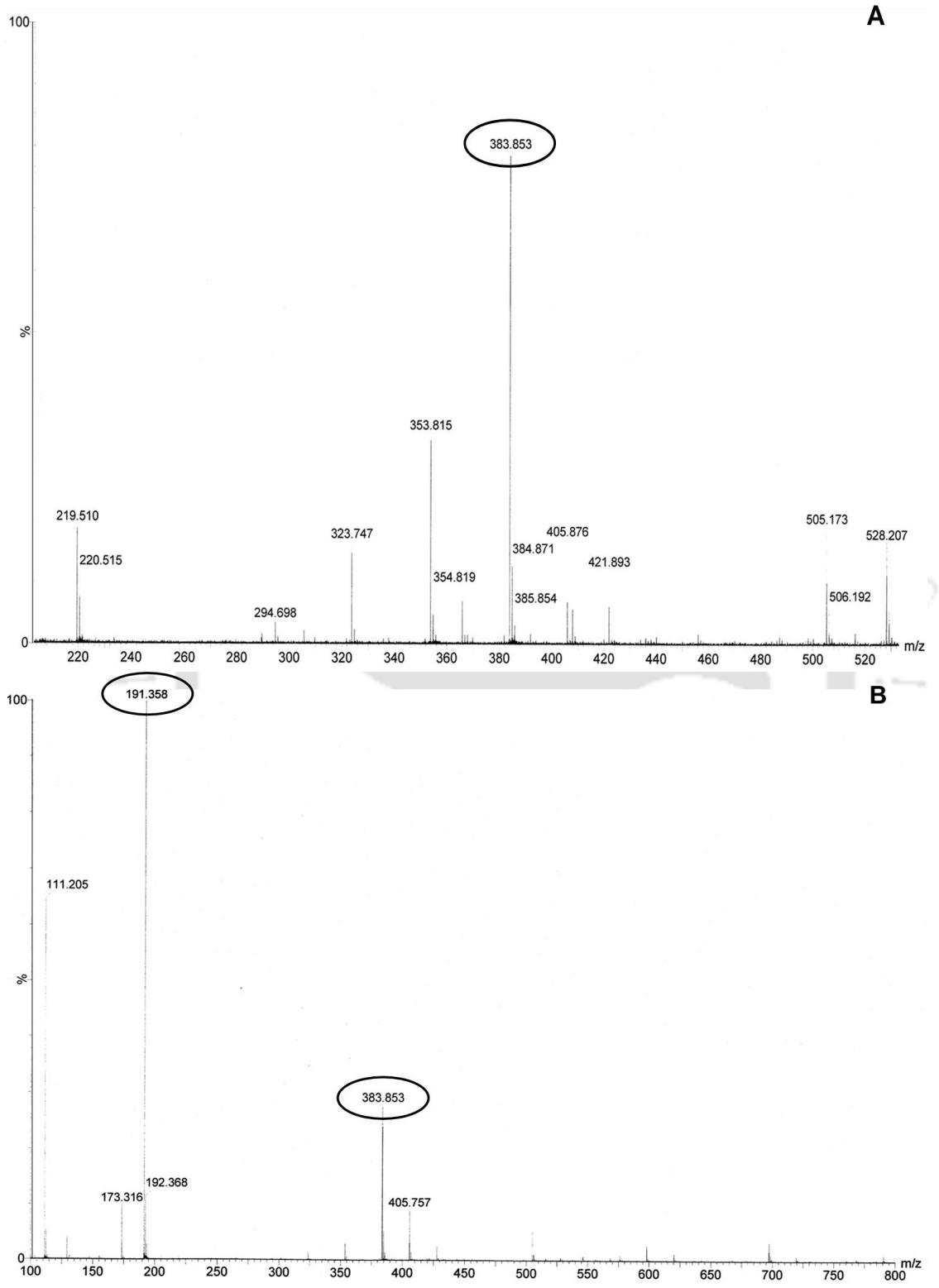


**Fig. 6.6** ESI-Mass spectrometric analysis of PL1B degraded products released from extracted pectin (EP) from sweet lemon peel (A) MS analysis showing single peak at *m/z* 383 ppm; (B) tandem MS analysis of peak at *m/z* 383 ppm.

### 6.3.5 Purification of pectic oligosaccharides

Pectic oligosaccharides obtained after PL1B degradation of PGA, CP25 and EP was purified by size exclusion chromatography using Bio-Gel P2 matrix. The purified oligosaccharides were detected at ($A_{235}$) and subsequently collected as 1 ml fraction by the fraction collector. Oligosaccharides purification from PGA developed a chromatogram where two distinct peaks at 77 and 93 ml (Fig. 6.7A) were found corresponding to unsaturated tri-galactouronate and di-galacturonate respectively, as confirmed by TLC analysis of the peak maxima (Fig. 6.7B). Two small peaks at 47 and 51 ml occurred due to the presence of some un-hydrolyzed polysaccharides present after reaction (Fig. 6.7A). TLC analysis of purified oligosaccharides showed that the concentration of unsaturated di-galactuonate was more as compared with tri-galactuonate.

The purification of pectic oligosaccharides released from CP25 resulted in two distinct peaks at 68 and 93 ml (Fig. 6.8A) belonging to unsaturated tri-galactouronate and di-galacturonate respectively, as confirmed by TLC analysis of the peak maxima (Fig. 6.8B). The un-hydrolyzed polysaccharide was also present which eluted at around 41 ml (Fig. 6.8A). The TLC analysis of purified oligosaccharides indicated that the unsaturated tri-galacturonate concentration was more than di-galactuonate.

The chromatogram for purification of pectic oligosaccharides from EP displayed a single peak at 63 ml (Fig. 6.9A) that corresponded to unsaturated methyl-esterified di-galacturonate as confirmed by TLC analysis (Fig. 6.9B). The unhydrolyzed polysaccharide was eluted at 45 ml (Fig. 6.9A). The purified oligosaccharides after each set of purification were collected, mixed and freeze dried.

Total dry weight of pectic oligosaccharides recovered after purification from PGA, CP25 and EP from sweet lemon was 6, 4.8 and 3.2 mg, respectively.

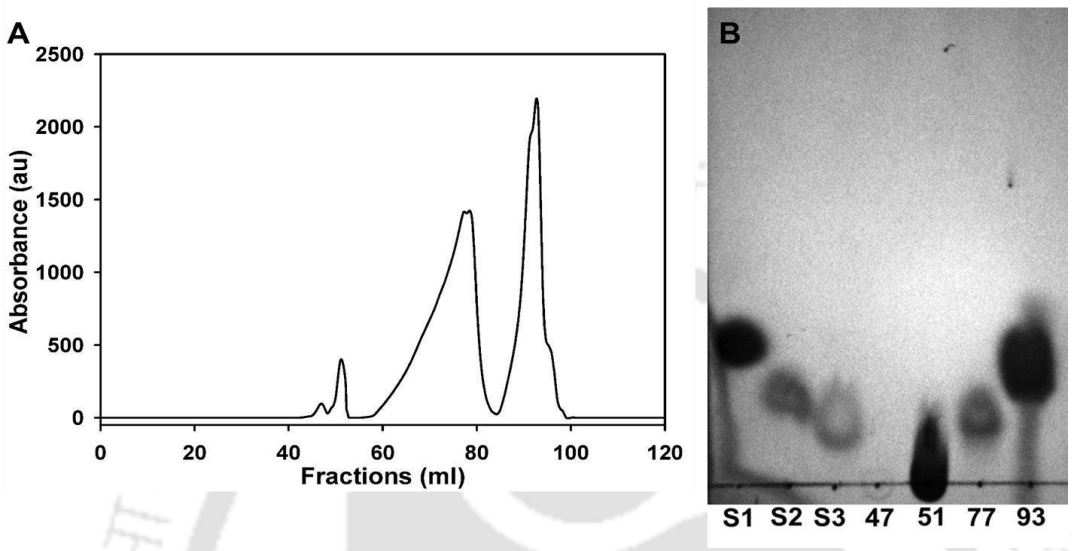


**Fig. 6.7** (A) Chromatogram showing purification of pectic oligosaccharides after PL1B degradation of PGA, (B) Thin layer chromatography showing the recovered pectic oligosaccharide after purification, where standard oligosaccharides used as size markers are S1: D-galacturonic acid; S2: Di-galacturonic acid; S3: Tri-galacturonic acid.

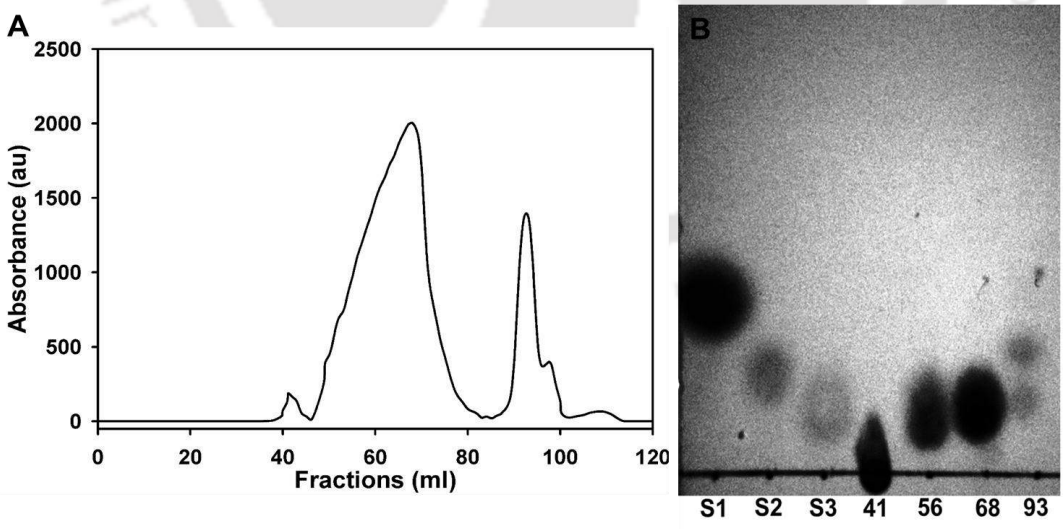


**Fig. 6.8** (A) Chromatogram showing purification of pectic oligosaccharides after PL1B degradation of CP25, (B) Thin layer chromatography showing the recovered pectic oligosaccharide after purification, where standard oligosaccharides used as size markers are S1: D-galacturonic acid; S2: Di-galacturonic acid; S3: Tri-galacturonic acid.

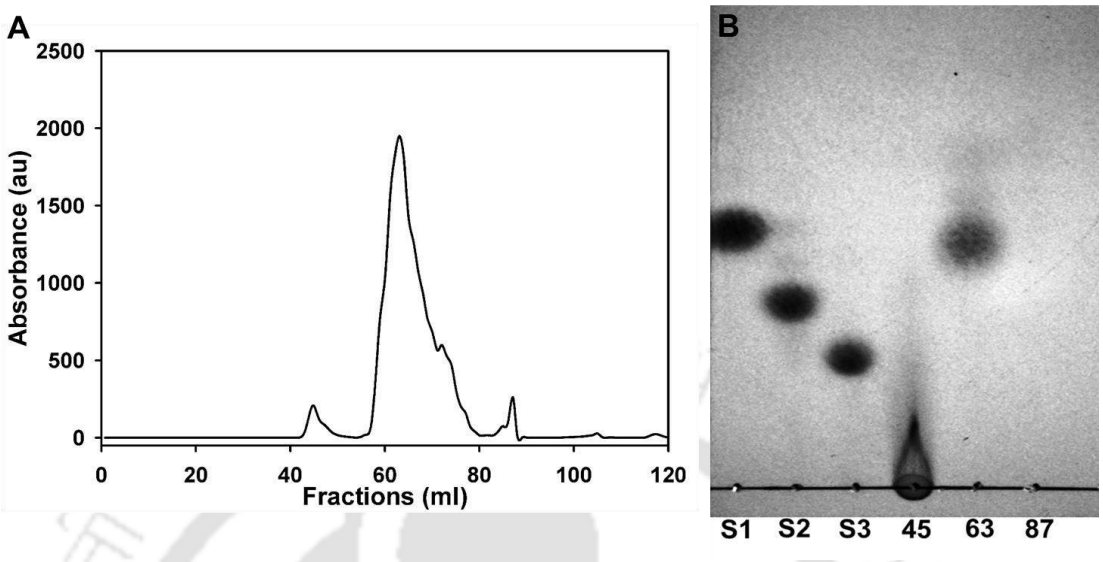


**Fig. 6.9** (A) Chromatogram showing purification of pectic oligosaccharides after PL1B degradation of EP, (B) Thin layer chromatography showing the recovered pectic oligosaccharide after purification, where standard oligosaccharides used as size markers are S1: D-galacturonic acid; S2: Di-galacturonic acid; S3: Tri-galacturonic acid.

### 6.3.6 Treatment of Colon cancer cells (HT-29) with pectic oligosaccharides

Colon cancer cells (HT-29) were treated with varying concentration (0.05 – 0.5 mg/ml) of purified pectic oligosaccharides from three different substrate sources *viz.* PGA, CP25 and EP for discrete time periods of 3, 6, 12 and 24 h. The dose and time dependent effect of pectic oligosaccharides on HT-29 cells was observed. Cells were incubated with varying concentration of pectic oligosaccharides as mentioned above and maximum inhibition was observed with 0.5 mg/ml pectic oligosaccharides after 24 h treatment. HT-29 cells when treated with 0.5 mg/ml pectic oligosaccharide from PGA, Citrus pectin (25% methyl-esterified) and extracted pectin for 24 h showed percent cell viability of 47% (Fig. 6.10), 39% (Fig. 6.12) and 23% (Fig. 6.14), respectively. Hence an overall inhibition of HT-29 cell growth was 53%, 61% and 77% in presence of pectic oligosaccharides from PGA, CP25 and EP respectively. A

significant change in cell morphology was observed where disintegrated cell membrane are clearly visible after treatment of HT-29 cells for 3, 6, 12 and 24 h with 0.5 mg/ml of purified pectic oligosaccharides from PGA (Fig. 6.11), CP25 (Fig. 6.13) and EP (Fig. 6.15). Effect of these pectic oligosaccharides was negligible during initial treatment period of 3 and 6 h, while substantial effects were observed at 12 and 24 h. It has been reported earlier that human colon carcinoma cells HuCC and HT-29 when treated with methyl-esterified citrus pectin inhibited cell proliferation by 57 to 70% at a concentration of 1 to 2 mg/ml (Bergman *et al*., 2010). Another study showed that proliferation of human colon cancer cells Colo 205 were inhibited by 50% when treated with 0.65 mg/ml of citrus pectin (Huang *et al*., 2012). Comparing the effect of citrus pectin on various colon cancer cells it can be inferred that pectic oligosaccharides under this investigation showed significant inhibition of cancer cells and can be used for cancer prevention.

Galectin 3 (Gal3) is a conserved evolutionary protein found in all species ranging from lower invertebrates to mammals. Mammalian lectin Gal3 has a C-terminal carbohydrate recognition domain (CRD) connected to a tail like N-terminal domain made of proline-glycine-alanine-tyrosine repeat motif (Barondes *et al*., 1994a; Barondes *et al*., 1994b). CRD can effectively recognize β-galactoside residues and found to bind lactose, galactose, polylactosamine, and n-acetyllactosamine (Seetharaman *et al*., 1998; Sorme *et al*., 2005; Collins *et al*., 2007). Gal3 actively participate in cancer progression and metastasis, it can be activated by glucoconjugates like laminin or fibronectin (Kuwabara *et al*., 1996). Once activated Gal3 mediates self-aggregation of cells, thus allowing detachment of primary tumor cells and progression of secondary tumor (Nangia-Makker *et al*., 2000). Sometime these detached primary

cells enters into the blood stream and remain as aggregates for prolong period of time while migrating to other parts of the body (Inohara *et al*., 1995). The galactouronic moiety of pectin can successfully bind to carbohydrate recognition domain of Gal3 and hinders its activation, thus inhibiting cell migration and metastatic spread (Inohara *et al*., 1994). Hence pectic oligosaccharides under study when treated with HT-29 cells might have interacted with the Gal3 and resulted in reduced cell viability. Numerous reports have demonstrated that colon cancer cells produce various galectins, but mainly Gal3 (Hittelet *et al*., 2003; Bidon-Wagner *et al*., 2004; Greco *et al*., 2004). Pectin being a large molecule it is difficult for it to permeate through the lining of alimentary canal and get absorb into the blood stream. While these pectic oligosaccharides produced by enzymatic cleavage of pectate lyase PL1B being small molecules can easily infuse through the lining and enter the blood stream. Although the production of these oligosaccharides by enzymatic degradation is little expensive, but the enhanced bioavailability achieved due to their smaller size makes them an effective functional food to prevent cancer.

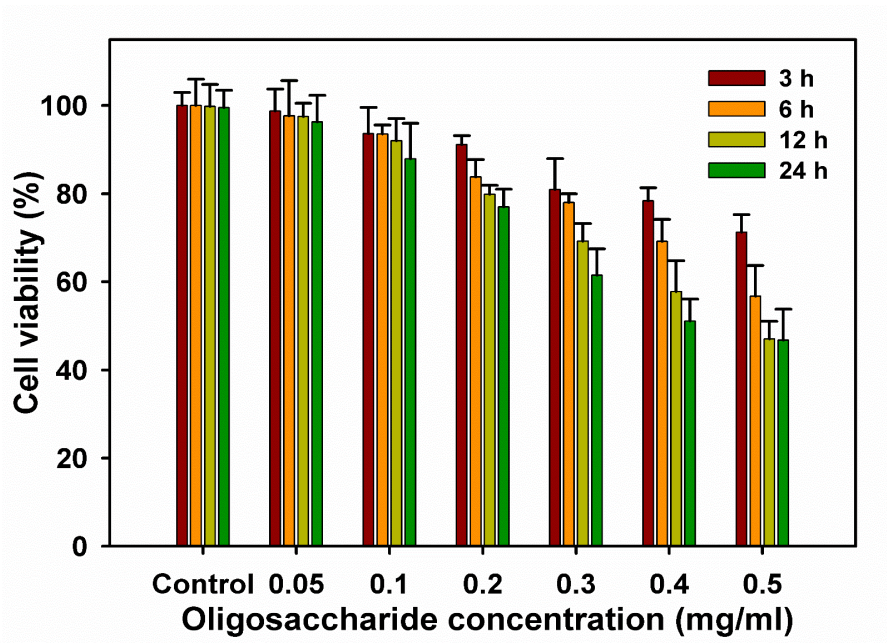


**Fig. 6.10** Percent cell viability after treatment of HT-29 cells for 3, 6, 12, 24 h by varying concentration (0.1-0.5 mg/ml) of purified pectic oligosaccharides from PGA. All the experiments are performed in triplicate and repeated thrice, standard error calculated from the mean of these three experiments.

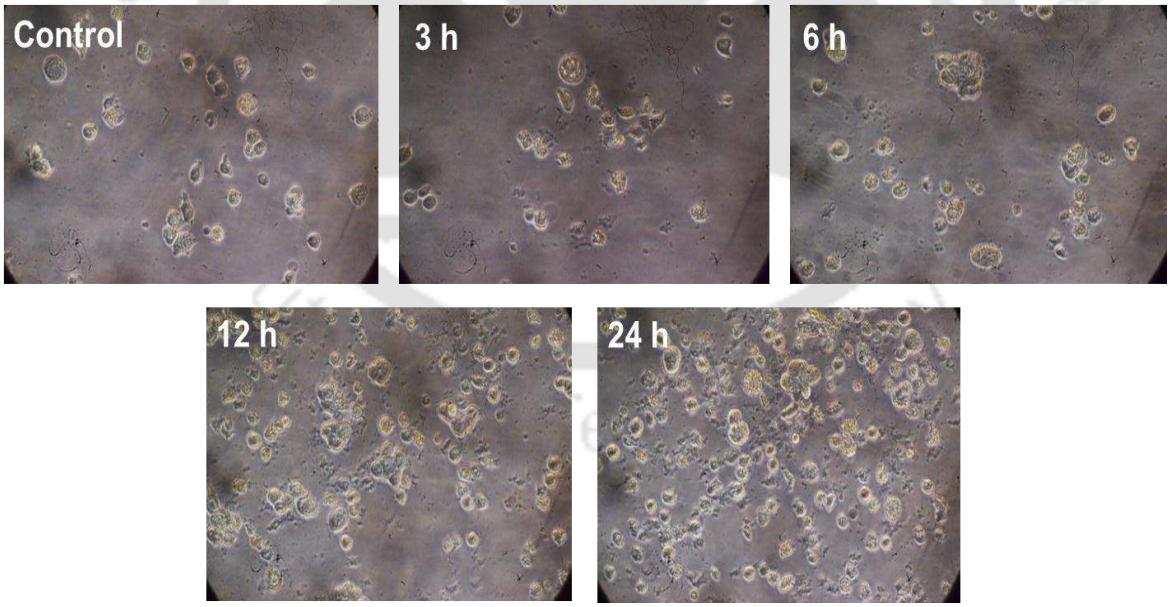


**Fig. 6.11** Changes in cell morphology of HT-29 cells after treatment with 0.5 mg/ml of purified pectic oligosaccharides from PGA.

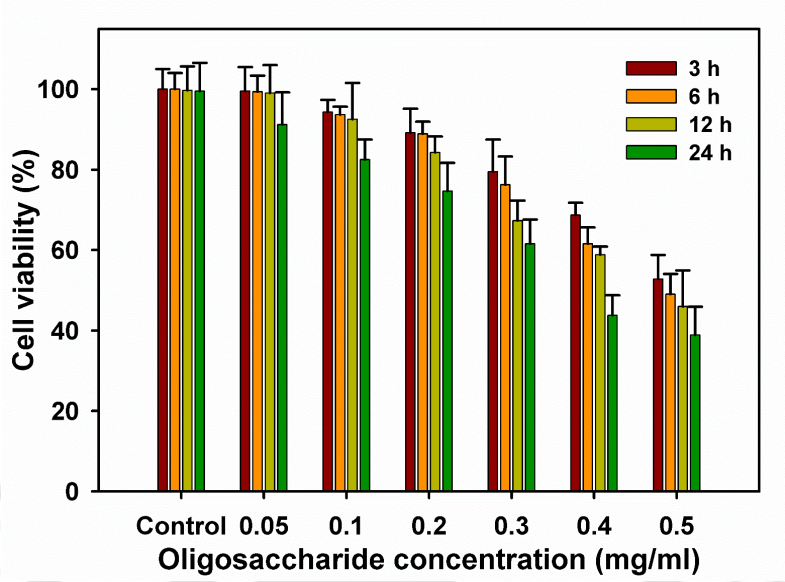


**Fig. 6.12** Percent cell viability after treatment of HT-29 cells for 3, 6, 12, 24 h by varying concentration (0.1-0.5 mg/ml) of purified pectic oligosaccharides from CP25. All the experiments are performed in triplicate and repeated thrice, standard error calculated from the mean of these three experiments.

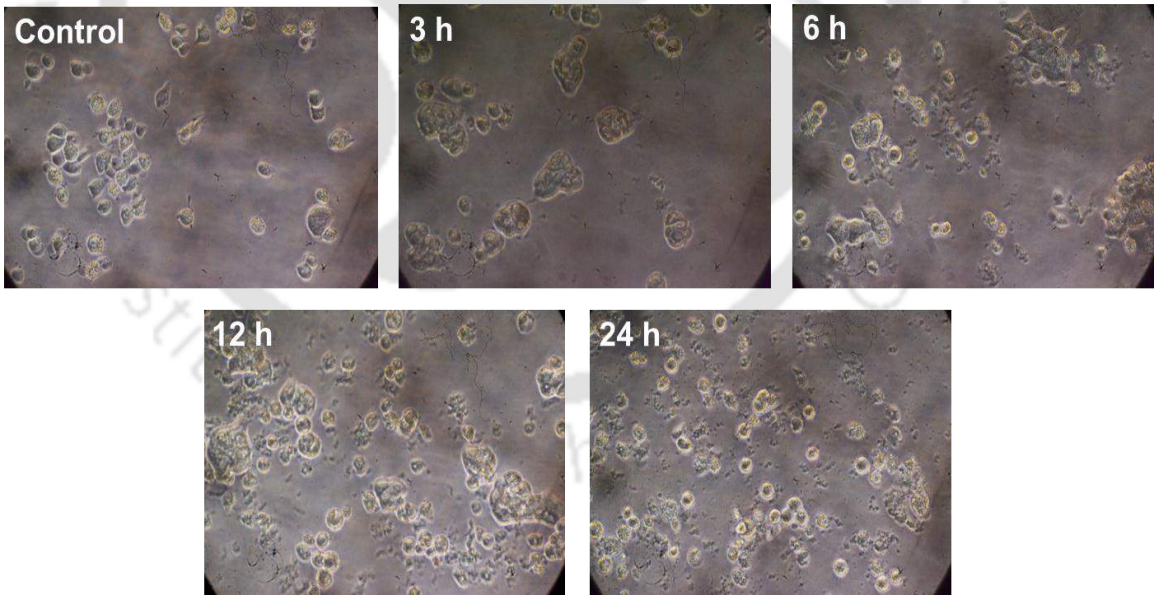


**Fig. 6.13** Changes in cell morphology of HT-29 cells after treatment with 0.5 mg/ml of purified pectic oligosaccharides from CP25.

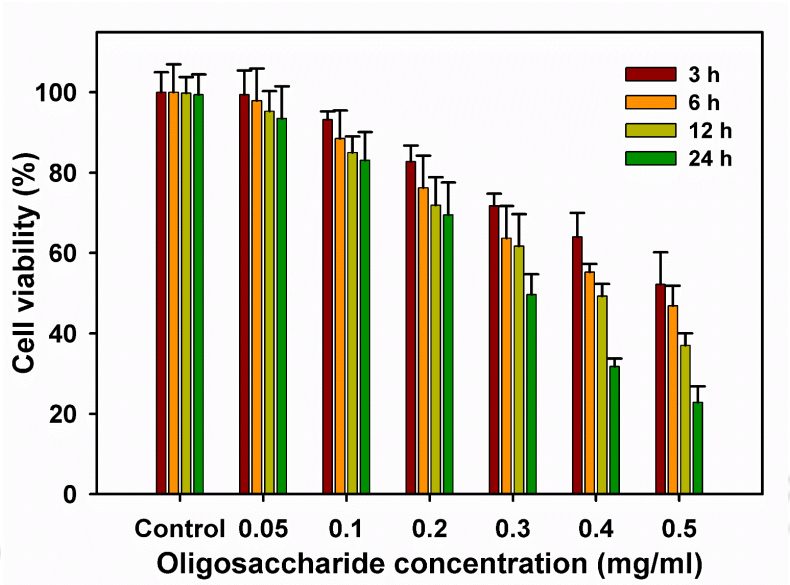


**Fig. 6.14** Percent cell viability after treatment of HT-29 cells for 3, 6, 12, 24 h by varying concentration (0.1-0.5 mg/ml) of purified pectic oligosaccharides from EP. All the experiments are performed in triplicate and repeated thrice, standard error calculated from the mean of these three experiments.

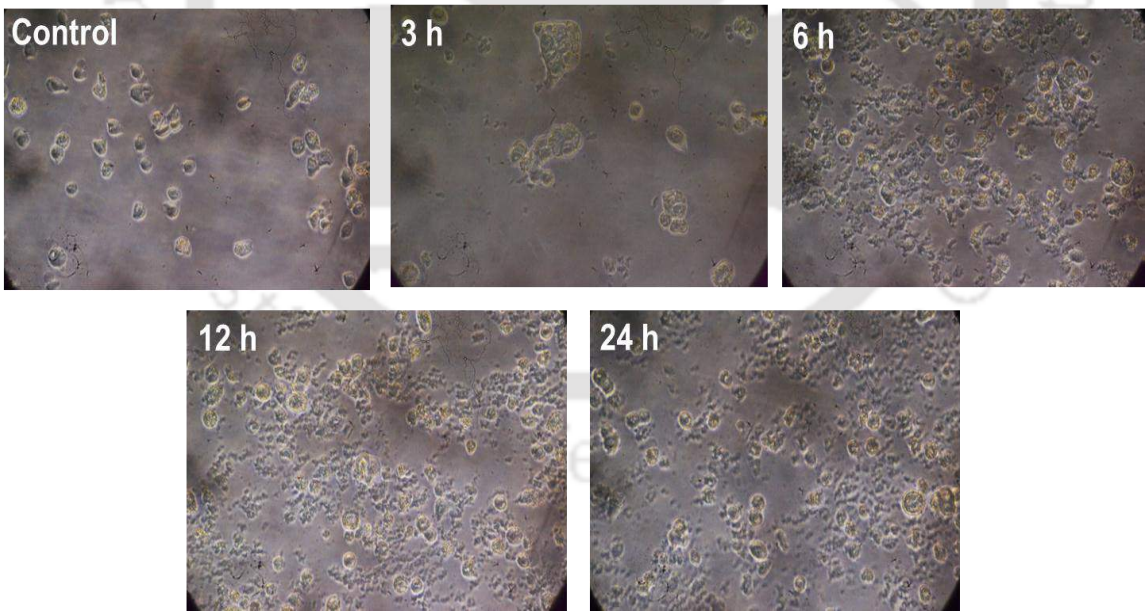


**Fig. 6.15** Changes in cell morphology of HT-29 cells after treatment with 0.5 mg/ml of purified pectic oligosaccharides from EP.

## 6.4 Conclusions

Pectin was extracted from waste citrus peels of *Citrus limetta* (Sweet lemon) by treating with acid and microwave heating, resulting in 12% yield. The structure of natural extracted pectin (EP) was characterized by NMR spectroscopy and was found to contain 77% methyl-esterification in the polysaccharide chain. Enzymatic treatment of the EP by recombinant pectate lyase PL1B produced unsaturated di-galacturonate as the major product, as confirmed by TLC analysis. PL1B degraded products released from commercial PGA and CP25 analysed by tandem mass spectroscopy showed molecular mass of 175 Da, 351 Da and 527 Da for unsaturated mono-, di- and tri-galacturonate, respectively. Whereas the PL1B degraded products from EP were methylated unsaturated mono- and di-galacturonate displaying molecular mass of 191 Da and 383 Da, respectively. These oligosaccharides were then purified and separated by gel filtration using Bio-Gel P2 matrix, analysed by TLC and then mixed and lyophilized. The effect of these purified pectic oligosaccharides was studied on colon cancer cell lines (HT-29) for 3, 6, 12, 24 h. The population of viable cells present after the treatment was measured by MTT assay and the cell viability is measured by the colorimetric changes. The results showed 53%, 61% and 77% inhibition in the growth of HT-29 cells after treatment for 24 h with 0.5 mg/ml of oligosaccharides, produced after enzymatic reaction of PL1B with PGA, CP25 and EP, respectively. Light microscopic images of 0.5 mg/ml oligosaccharides treated HT-29 cells showed disintegrated cell membrane as compared to the untreated cells. A close insight into the HT-29 cells inhibition pattern revealed that higher methyl-esterified oligosaccharides show relatively higher inhibition of the cell growth as compared with less methyl-esterified oligosaccharides. Pectin being large polymeric compound is

difficult to get absorbed by the alimentary canal hence enzymatic degradation facilitates the production of smaller oligosaccharides which gets easily absorbed by the alimentary canal. Hence, the pectic oligosaccharides can be produced from citrus peels by recombinant endo pectate lyase PL1B from *Clostridium thermocellum* on a large scale. The citrus peel which is generally considered as waste can serve as source for a potent healthcare commodity.

## 6.5 References

Aina, V.O., Barau, M.M., Mamman, O.A., Zakari, A., Haruna, H., Umar, M.S.H., Abba, Y.B. 2012 Extraction and characterization of pectin from peels of lemon (*Citrus limon*), grape fruit (*Citrus paradisi*) and sweet orange (*Citrus sinensis*). British Journal of Pharmacology and Toxicology, 3(6): 259–262.

Barondes, S. H., Castronovo, V., Cooper, D. N. W., Cummings, R. D., Drickamer, K., Feizi, T., Gitt, M. A., Hirabayashi, J., Hughes, C., Kasai, K., Leffler, H., Lui, F. T., Lotan, R., Mercurio, A. M., Monsigny, M., Pillai, S., Poirer, F., Raz, A., Rigby, P. W. J., Rini, J. M., Wang, J. L. (1994a) Galectins - a family of animal β-galactoside-binding lectins. Cell, 76: 597–598.

Barondes, S. H., Cooper, D. N. W., Gitt, M. A., Leffler, H. (1994b) Galectins-structure and function of a large family of animal lectins. Journal of Biology Chemistry, 269: 20807–20810.

Bergman, M., Djaldetti, M., Salman, H., Bessler, H. (2010) Effect of citrus pectin on malignant cell proliferation. Biomedicine & Pharmacotherapy, 64: 44–47.

Bidon-Wagner, N., Pennec, L.J.P. (2004) Human galectin-8 isoforms and cancer. Glycoconjugate Journal, 19: 557–63.

Brown, L., Rosner, B., Willett, W.W., Sacks, F.M. (1999) Cholesterol-lowering effects of dietary fiber: A meta-analysis. The American Journal of Clinical Nutrition, 69: 30–42.

Cabrera, J.C., van Cutsem, P. (2005) Preparation of chitooligosaccharides with degree of polymerization higher than 6 by acid or enzymatic degradation of chitosan. Biochemical Engineering Journal, 25: 165–172.

Chen, C.H., Sheu, M.T., Chen, T.F., Wang, Y.C., Hou, W.C., Liu, D.Z., Chung, T.C., Liang, Y.C. (2006) Suppression of endotoxin-induced proinflammatory responses by citrus pectin through blocking LPS signaling pathways. Biochemical Pharmacology, 72: 1001–1009.

Collins, P., Hidari, K. I. P. J., Blanchard, H. (2007) Slow diffusion of lactose out of galectin-3 crystals monitored by X-ray crystallography: possible implications for ligand-exchange protocols. Acta Crystallographica, D63: 415–419.

Cote, G.L., Leathers, T.D. (2005) A method for surveying and classifying *Leuconostoc sp*. Glucansucrases according to strain-dependent acceptor product patterns. Journal of Industrial Microbiology Biotechnology, 32: 53–60.

Cruess, W.V. (1958) Commercial fruit and vegetable products, 4th ed. McGraw Hill book company, Inc. New York, U.S.A

Fishman, M.L., Chau, H.K, Hoagland, P., Ayyad, K. (2000) Characterization of pectin, flash-extracted from orange albedo by microwave heating, under pressure. Carbohydrate Research, 323: 126–138.

Fishman, M.L., Chau, H.K., Hoagland, P.D., Hotchkiss, A.T. (2006) Microwave-assisted extraction of lime pectin. Food Hydrocolloids, 20: 1170–1177.

Fishman, M.L., Walker, P.N., Chau, H.K., Hotchkiss, A.T. (2003) Flash extraction of pectin from orange albedo by steam injection. Biomacromolecules, 4(4): 880–889.

Greco, C., Vona, R., Cosimelli, M., Matarrese, P., Straface, E., Scordati, P., Giannarelli, D., Casale, V., Assisi, D., Mottolese, M., Moles, A., Malorni, W. (2004) Cell surface overexpression of galectin-3 and the presence of its ligand

90k in the blood plasma as determinants in colon neoplastic lesions. Glycobiology, 14: 783–792.

Hasegawa, S., Nagel, C.W. (1966) A New Pectic Acid Transeliminase produced exocellularly by a *Bacillus.* Journal of Food Science, 31: 838–845.

Hittelet, A., Legendre, H., Nag, N., Bronckart, Y., Pector, J.C., Salmon, I., Yeaton, P., Gabius, H.J., Kiss, R., Camby, I. (2003) Upregulation of galectins-1 and -3 in human colon cancer and their role in regulating cell migration. International Journal of Cancer, 103: 370–379.

Huang, P.H., Fu, L.C., Huang, C.S., Wang, Y.T., Wua, M.C. (2012) The uptake of oligogalacturonide and its effect on growth inhibition, lactate dehydrogenase activity and galactin-3 release of human cancer cells. Food Chemistry, 132: 1987–1995.

Iacomini, M., Serrato, R. V., Sassaki, G. L., Lopes, L., Buchi, D. F., Gorin, P. A. J. (2005) Isolation and partial characterization of a pectic polysaccharide from the fruit pulp of *Spondias cytherea* and its effect on peritoneal macrophage activation. Fitoterapia, 76: 676–683.

Inohara, H., Raz, A. (1994) Effects of natural complex carbohydrate (citrus pectin) on murine melanoma cell properties related to galectin-3 functions. Glycoconjugate Journal, 11: 527–532.

Inohara, H., Raz, A. (1995) Functional evidence that cell-surface galectin-3 mediates homotypic cell-adhesion. Cancer Research, 55: 3267–3271.

Jackson, C.L., Dreaden, T.M., Theobald, L.K., Tran, N.M., Beal, T.L., Eid, M., Gao, M.Y., Shirley, R.B., Stoffel, M.T., Kumar, M.V., Mohnen, D. (2007) Pectin

induces apoptosis in human prostate cancer cells: Correlation of apoptotic function with pectin structure. Glycobiology, 17: 805–819.

Kanmani, P., Dhivya, E., Aravind, J., Kumaresan, K. (2014) Extraction and analysis of pectin from citrus peels: augmenting the yield from *Citrus limon* using statistical experimental design. Iranica Journal of Energy and Environment, 5 (3): 303-312.

Kar, F., Arslan, N. (1999) Characterization of orange peel pectin and effect of sugars, L-ascorbic acid, ammonium persulfate, salts on viscosity of orange peel pectin solutions. Carbohydrate Polymers, 40: 285–291.

Khan, A.A., Butt, M.S., Randhawa, M.A., Karim, R., Sultan, M.T., Ahmed, W. (2014) Extraction and characterization of pectin from grapefruit (*Duncan cultivar*) and its utilization as gelling agent. International Food Research Journal, 21(6): 2195–2199.

Kuwabara, I., Liu, F.T. (1996) Galectin-3 promotes adhesion of human neutrophils to laminin. Journal of Immunology, 156: 3939–3944.

Leitao, M.C.A., Alarcao Silva, M.L., Januario, M.I.N., Azinheira, H.G. (1995) Galacturonic acid in pectic substances of sunflower head residues: quantitative determination by HPLC. Carbohydrate Polymers, 26: 165–169.

Leroux, J., Langendorff, V., Schick, G., Vaishnav, V., Mazoyer, J. (2003) Emulsion stabilizing properties of pectin. Food Hydrocolloids, 17(4): 455–462.

Liu, Y., Ahmad, H., Luo, Y., Gardiner, D.T., Gunasekera, R.S., McKeehan, W.L., Patil, B.S. (2001) Citrus pectin: characterization and inhibitory effect on fibroblast growth factor-receptor interaction. Journal of Agricultural and Food Chemistry, 49: 3051–3057.

Liu, Y., Ahmad, H., Luo, Y., Gardiner, D.T., Gunasekera, R.S., McKeehan, W.L., Patil, B.S. (2002) Influence of harvest time on citrus pectin and its in vitro inhibition of fibroblast growth factor signal transduction. Journal of the Science of Food and Agriculture, 82: 469–477.

Lojkwoska, E., Masclaux, C., Boccara, M., Robert-Baudouy, J., Hugouvieux-Cotte-Pattat, N. (1995) Characterization of pelL gene encoding a novel pectate lyase of *Erwinia chysanthemi* 3937. Molecular Microbiology, 16(6): 1183–1195.

Manderson, K., Pinart, M., Tuohy, K.M., Grace, W.E., Hotchkiss, A.T., Widmer, W., Yadhav, M.P., Gibson, G.R., Rastall, R.A. (2005) In vitro determination of the prebiotic properties of oligosaccharides derived from an orange juice manufacture by-product stream. Applied Environmental Microbiology, 71(12): 8383–8389.

May, C.D. (1990) Industrial pectins: Sources, production and applications. Carbohydrate Polymers, 12(1): 79-99.

McCready, R. M, Owens, H. S. (1952) Pectin: A product of citrus waste. Economic Botany, 8: 29.

Mohnen, D., Bar-Peled, M., Somerville, C. (2008) Biosynthesis of plant cell walls. biomass recalcitrance, Chapter 5 (eds. Himmel, M.), pp. 94-187. Blackwell Publishing, Oxford.

Mosmann, T. (1983) Rapid colorimetric assay for cellular growth and survival: application to proliferation and cytotoxicity assays. Journal of Immunological Methods, 65(1-2): 55–63.

Munoz, A.L., Gutierrez, G.R., Senent, F.R., Bolanos, J.F. (2012) Production, characterization and isolation of neutral and pectic oligosaccharides with low

molecular weights from olive by-products thermally treated. Food Hydrocolloids, 28: 92–104.

Nangia-Makker, P., Honjo, Y., Sarvis, R., Akahani, S., Hogan, V., Pienta, K.J., Raz, A. (2000) Galectin-3 induces endothelial cell morphogenesis and angiogenesis. American Journal of Pathology, 156: 899–909.

O'Neill, M., Albersheim P, Darvill, A. (1990) The pectic polysaccharides of primary cell walls. In: Methods in Plant Biochemistry, Vol. 2. (eds. Dey D.M.), pp: 415-441. Academic Press, London.

O'Neill, M.A., Ishii, T., Albersheim, P., Darvill, A.G. (2004) Rhamnogalacturonan II: structure and function of a borate cross-linked cell wall pectic polysaccharide. Annual Review of Plant Biology, 55: 109-139.

Pienta, K. J., Naik, H., Akhtar, A., Yamazaki, K., Replogle, T. S., Lehr, J., Donat, T.L., Tait, L., Hogan, V., Raz, A. (1995) Inhibition of spontaneous metastasis in a rat prostate cancer model by oral administration of modified citrus pectin. Journal of the National Cancer Institute, 87: 348–353.

Platt, D., Raz, A. (1992) Modulation of the lung colonization of B16–F1 melanoma cells by citrus pectin. Journal of the National Cancer Institute, 84: 438–442.

Ralet, M.C., Lerouge, P., Quemener, B. (2009) Mass spectrometry for pectin structure analysis. Carbohydrate Research 344: 1798–1807.

Rosenbohm, C., Lundt, I., Christensen, T.M.I.E., Young, N.W.G. (2003) Chemically methylated and reduced pectins: preparation, characterisation by $^{1}$H NMR spectroscopy, enzymatic degradation, and gelling properties. Carbohydrate Research, 338: 637–649.

Samuelsen, A. B., Paulsen, B. S., Wold, J. K., Otsuka, H., Yamada, H., Espevik, T. (1995) Isolation and partial characterization of biologically active polysaccharides from Plantago major L. Phytotherapy Research, 9: 211–218.

Sawabe, Y., Nakagomi, K., Iwagami, S., Suzuki, S., Nakazawa, H. (1992) Inhibitory effects of pectic substances on activated hyaluronidase and histamine release from mast cells. Biochimica et Biophysica Acta, 1137: 274–278.

Seetharaman, J., Kanigsberg, A., Slaaby, R., Leffler, H., Barondes, S. H., Rini, J. M. (1998) X-ray crystal structure of the human galectin-3 carbohydrate recognition domain at 2.1-Å resolution. Journal of Biological Chemistry, 273: 13047–13052

Soriano, M., Blanco, A., Diaz, P., Pastor, F.I.J. (2000) An unusual pectate lyase from a *Bacillus sp*. with high activity on pectin: cloning and characterization. Microbiology, 146: 89–95.

Soriano, M., Diaz, P., Pastor, F.I. (2006) Pectate lyase C from *Bacillus subtilis*: a novel endo-cleaving enzyme with activity on highly methylated pectin. Microbiology, 152: 617–625.

Sorme, P., Arnoux, P., Kahl-Knutsson, B., Leffler, H., Rini, J.M., Nilsson, L.J. (2005) Structural and thermodynamic studies on cation-II interactions in lectin-ligand complexes: high affinity galectin-3 inhibitors through fine-tuning of an arginine-arene interaction. Journal of American Chemical Society, 127: 1737–1743.

Srivastava, P., Malviya. R. (2011) Source of pectin extraction, and its application in pharmaceutical industry. Indian journal of natural product and resources, 2(1): 10-18.

Yamada, H, (1994) Pectic polysaccharides from Chinese herbs: Structure and biological activity. Carbohydrate Polymers, 25: 269–276.

Zhan, D., Janssen, P., Mort, A.J. (1998) Scarcity or complete lack of single rhamnose residues interspersed within the homogalacturonan regions of citrus pectin. Carbohydrate Research, 308: 373-380.

Zhao, Z., Li, J., Wu, X., Dai, H., Gao, X., Liu, M., Tu, P. (2006) Structures and immunological activities of two pectic polysaccharides from the fruits of *Ziziphus jujuba* Mill. cv. jinsixiaozao Hort. Food Research International, 39: 917–923.

Zykwinska, A., Boiffard, M.H., Kontkanen, H., Buchert, J., Thibault, J.F., Bonnin, E. (2008) Extraction of green labeled pectins and pectic oligosaccharides from plant byproducts. Journal of Agricultural Food Chemistry, 56: 8926–8935.

## FUTURE PROSPECTS

The characterized enzyme PL1B displayed activity towards pectic polysaccharides. Owing to this fact, PL1B can be used in various industrial processes involving degradation of pectic polysaccharides *viz*. clarification of fruit juice, improvement of colour and stability of wine, degumming of plant fibers, extraction of citrus oil, etc.

The thermostability of PL1B makes it a good candidate for use in high temperature industrial operations. PL1B an endo pectate lyase can be used as a cocktail with other pectinolytic enzyme like pectin metylesterase and rhamnogalacturonan lyase for complete degradation of complex pectin.

Pectin is the first layer of defense in plant cell wall hence, PL1B pretreatment of hemicellulosic biomass can provide improved yields of biofuel.

Immobilization of PL1B on suitable matrix for development of immobilized packed bed reactors can be useful for efficient reuse of the enzyme with enhanced thermostability and activity. This will also help in large scale production of pectic oligosaccharides from pectin extracted from cheaper sources like waste citrus peels.

Pectic oligosaccharides has been identified as a potent inhibitor for colon cancer cells, hence it can be further used for targeted delivery to specific cancer cells by ligand-receptor interaction. This will increase the bioavailability of the pectic oligosaccharides and show improved inhibitory response towards cancer cell growth.

**Journal Publications**

1. **Soumyadeep Chakraborty**, Vania O. Fernandes, Fernando M.V. Dias, Jose A.M. Prates, Luis M.A. Ferreira, Carlos M.G.A. Fontes, Arun Goyal and Maria S.J. Centeno (**2015**) Role of pectinolytic enzymes identified in *Clostridium thermocellum* cellulosome. **Plos One**, e0116787.
2. **Soumyadeep Chakraborty**, Kedar Sharma, Joyeeta Mukherjee, Munishwar N. Gupta and Arun Goyal (**2015**) Structure, substrate binding analysis and stability studies of endo-pectate lyase (PL1B) of family 1 polysaccharide lyase from *Clostridium thermocellum*. **Protein and Peptide Letters,** 22(6): 557 – 568.
3. **Soumyadeep Chakraborty**, T. Jagan Mohan Rao and Arun Goyal (**2015**) Immobilization of recombinant family 1 polysaccharide lyase (PL1B) from *Clostridium thermocellum* ATCC 27405 and its application in bioscouring of cotton fabric. **(Under review)**
4. **Soumyadeep Chakraborty**, Aruna Rani and Arun Goyal (**2015**) From waste to health care product: Colon cancer cells inhibited by pectic oligosaccharide produced from citrus peels by recombinant endo-pectate lyase (PL1B). **(Under review)**

**Conferences/Symposia/Meetings**

1. **Soumyadeep Chakraborty**, Aruna Rani and Arun Goyal **(2015)** Waste to health care: role of pectic oligosaccharide produced upon enzymatic cleavage of endo-pectate lyase PL1B on Colon cancer cells, Carbohydrate bioengineering meeting (CBM11), May 2015, Aalto University, Espoo, Finland.
2. **Soumyadeep Chakraborty,** T. Jagan Mohan Rao and Arun Goyal (**2013**) Immobilization of recombinant endo pectate lyase of family 1 Polysaccharide lyase (PL1B) from *Clostridium thermocellum* and its application in bioscouring of cotton fabric. International conference on advances in biotechnology and bioinformatics (ICABB 2013), November 2013, D.Y. Patil University, Pune.
3. **Soumyadeep Chakraborty**, Carlos M.G.A. Fontes and Arun Goyal (**2013**) Structural in-sight of thermostable endo pectate lyase (PL1B) from *Clostridium thermocellum*. 42nd National seminar in crystallography and international workshop on application of x-ray diffraction for drug discovery (NSC42), November 2013, JNU, New Delhi. (Oral presentation)
4. **Soumyadeep Chakraborty** and Arun Goyal (**2013**) Pectic substrate degrading family 1 Polysaccharide Lyase (*Ct*PL1-CBM35) and its truncated derivative (*Ct*PL1) from *Clostridium thermocellum*. 10th Carbohydrate bioengineering meeting (CBM10), May 2013, Prague, Czech Republic.
5. **Soumyadeep Chakraborty** and Arun Goyal (**2012**) Biochemical characterization of family 1 Polysaccharide Lyase (CtPL1-CBM35) and its truncated derivative CtPL1 from *Clostridium thermocellum* showing activity towards pectic substrates. 81st Meeting of The Society of Biological Chemists (SBC 2012), November 2012, Kolkata.
6. **Soumyadeep Chakraborty** and Arun Goyal (**2012**) Cloning and expression of family 1 polysaccharide lyase (*Ct*PL1) and family 35 carbohydrate binding module (*Ct*CBM35) from *Clostridium thermocellum* having specificity towards pectic substrates. IFIB-2012, International Forum on Industrial Bioprocesses (IFIBiop), October 2012, Taipei, Taiwan.
7. **Soumyadeep Chakraborty** and Arun Goyal (**2011**) Determining possible 3-dimensional structure of family 1 polysaccharide lyase (*Ct*PL1) and family 35 carbohydrate binding module (*Ct*CBM35) from *Clostridum thermocellum* using bioinformatics tools. International Conference on New Horizons in Biotechnology (NHBT 2011), BRSI Annual meeting, November 2011, NIST, Trivandrum.
8. **Soumyadeep Chakraborty** and Arun Goyal (**2011**) Cloning of family 1 polysaccharide lyase (*Ct*PL1) and family 35 carbohydrate binding module (*Ct*CBM35) from *Clostridum thermocellum* for biochemical studies and characterization. CARBO XXVI, Association of Carbohydrate Chemists and Technologists (ACCTI), November 2011, IICB, Kolkata.
9. Rishikesh Shukla, Seema Patel, Damini Kothari, **Soumyadeep Chakraborty**, Debashish Das and Arun Goyal (**2010**) Combined effect of pH and dissolved oxygen on dextran production from a mutant of soil isolate. 51st Annual Conference, Association of Microbiologists India (AMI), December 2010, BIT Mesra, Rachi.

# VITAE

*The author was born on November 11, 1985 in the city of Kolkata, (West Bengal). He passed the Secondary Examination conducted by West Bengal Board of Secondary Education (10th Class), West Bengal in 2002 and Higher Secondary Examination conducted by West Bengal Council of Higher Secondary Education (12th Class), West Bengal in 2004. He completed B.Tech. (Biotechnology) from Bengal College of Engineering & Technology, Durgapur affiliated to West Bengal University of Technology, Kolkata (West Bengal) in July, 2008. He completed M.Tech. (Biotechnology) from Heritage Institute of Technology, Kolkata, affiliated to West Bengal University of Technology, Kolkata (West Bengal) in July, 2010.*

*Mr. Soumyadeep Chakraborty joined the Ph.D. program in July, 2010 at Department of Biosciences and Bioengineering, Indian Institute of Technology Guwahati, Guwahati 781 039, Assam, India. He successfully completed the course work with 9/10 CPI. He received Institute Fellowship (IIT Guwahati) from Aug 2010 to Jul 2014, under the scheme run by the Ministry of Human Resource and Development (MHRD), New Delhi. From August 2014 onwards he received fellowship as from a DBT sponsored project in Department of Biosciences & Bioengineering under Prof. Arun Goyal. He delivered the open (PhD Synopsis) Seminar on February 03, 2015 and presented his thesis work before the Doctoral Committee and his performance was satisfactory. He submitted the PhD thesis in March 2015. Presently, he is continuing under same DBT project at the Department.*